



Natural Environment Research Council  
Institute of Geological Sciences

# Mineral Reconnaissance Programme Report



This report relates to work carried out by the Institute of Geological Sciences on behalf of the Department of Industry. The information contained herein must not be published without reference to the Director, Institute of Geological Sciences

D. Ostle  
Programme Manager  
Institute of Geological Sciences  
Keyworth,  
Nottingham NG12 5GG

No. 40

**Stratabound barium-zinc  
mineralisation in Dalradian schist  
near Aberfeldy, Scotland: Final  
report**

---

INSTITUTE OF GEOLOGICAL SCIENCES

Natural Environment Research Council

Mineral Reconnaissance Programme

Report No. 40

**Stratabound barium-zinc  
mineralisation in Dalradian schist  
near Aberfeldy, Scotland: Final  
report**

*Geology and geochemistry*

J. S. Coats, PhD

C. G. Smith, PhD

M. J. Gallagher, PhD, MIMM

F. May, PhD

W. J. McCourt, BSc

*Geophysics*

M. E. Parker, BA

*Mineralogy*

N. J. Fortey, PhD

## Mineral Reconnaissance Programme Reports

- 1 The concealed granite roof in south-west Cornwall
- 2 Geochemical and geophysical investigations around Garras Mine, near Truro, Cornwall
- 3 Molybdenite mineralisation in Precambrian rocks near Lairg, Scotland
- 4 Investigation of copper mineralisation at Vidlin, Shetland
- 5 Preliminary mineral reconnaissance of Central Wales
- 6 Report on geophysical surveys at Struy, Inverness-shire
- 7 Investigation of tungsten and other mineralisation associated with the Skiddaw Granite near Carrock Mine, Cumbria
- 8 Investigation of stratiform sulphide mineralisation in parts of central Perthshire
- 9 Investigation of disseminated copper mineralisation near Kilmelford, Argyllshire, Scotland
- 10 Geophysical surveys around Talnotry mine, Kirkcudbrightshire, Scotland
- 11 A study of the space form of the Cornubian granite batholith and its application to detailed gravity surveys in Cornwall
- 12 Mineral investigations in the Teign Valley, Devon. Part 1—Barytes
- 13 Investigation of stratiform sulphide mineralisation at McPhun's Cairn, Argyllshire
- 14 Mineral investigations at Woodhall and Longlands in north Cumbria
- 15 Investigation of stratiform sulphide mineralisation at Meall Mor, South Knapdale, Argyll
- 16 Report on geophysical and geological surveys at Blackmount, Argyllshire
- 17 Lead, zinc and copper mineralisation in basal Carboniferous rocks at Westwater, south Scotland
- 18 A mineral reconnaissance survey of the Doon-Glenkens area, south-west Scotland
- 19 A reconnaissance geochemical drainage survey of the Criffel-Dalbeattie granodiorite complex and its environs
- 20 Geophysical field techniques for mineral exploration
- 21 A geochemical drainage survey of the Fleet granitic complex and its environs
- 22 Geochemical and geophysical investigations north-west of Llanrwst, North Wales
- 23 Disseminated sulphide mineralisation at Garbh Achadh, Argyllshire, Scotland
- 24 Geophysical investigations along parts of the Dent and Augill Faults
- 25 Mineral investigations near Bodmin, Cornwall. Part 1—Airborne and ground geophysical surveys
- 26 Stratabound barium-zinc mineralisation in Dalradian schist near Aberfeldy, Scotland: Preliminary report
- 27 Airborne geophysical survey of part of Anglesey, North Wales
- 28 A mineral reconnaissance survey of the Abington-Biggarr-Moffat area, south-central Scotland
- 29 Mineral exploration in the Harlech Dome, North Wales
- 30 Porphyry style copper mineralisation at Black Stockarton Moor, south-west Scotland
- 31 Geophysical investigations in the Closehouse-Lunedale area
- 32 Investigations at Polyphant, near Launceston, Cornwall
- 33 Mineral investigations at Carrock Fell, Cumbria. Part 1—Geophysical survey
- 34 Results of a gravity survey of the south-west margin of Dartmoor, Devon
- 35 Geophysical investigation of chromite-bearing ultrabasic rocks in the Baltasound-Hagdale area, Unst, Shetland Islands
- 36 An appraisal of the VLF ground resistivity technique as an aid to mineral exploration
- 37 Compilation of stratabound mineralisation in the Scottish Caledonides
- 38 Geophysical evidence for a concealed eastern extension of the Tanygrisiau microgranite and its possible relationship to mineralisation
- 39 Copper-bearing intrusive rocks at Cairngarroch Bay, south-west Scotland
- 40 Stratabound barium-zinc mineralisation in Dalradian schist near Aberfeldy, Scotland: Final report

The Institute of Geological Sciences was formed by the incorporation of the Geological Survey of Great Britain and the Geological Museum with Overseas Geological Surveys and is a constituent body of the Natural Environment Research Council

### *Bibliographical reference*

Coats, J. S., Smith, C. G. and others. 1981. Stratabound barium-zinc mineralisation in Dalradian schist near Aberfeldy, Scotland: Final report *Mineral Reconnaissance Programme Rep. Inst. Geol. Sci.*, No. 40

Printed in England for the Institute of Geological Sciences by Ashford Press Ltd

## CONTENTS

### Summary 1

### Introduction 1

### Location and general geology 1

#### Geochemistry 1

- Regional drainage survey 1
- Detailed drainage surveys 11
- Litho-geochemistry 13

#### VLF mapping 17

- Introduction 17
- Outline of the VLF-EM method 17
- Filtering VLF-EM data 19
- Survey methods 19
- Results and interpretation 19
- Conclusions 19

#### Mineralogy 22

- Introduction 22
- Barium feldspars 24
- Cymrite 25
- Micas 25
- Chlorite and clay minerals 27
- Carbonates 27
- Baryte 27
- Iron sulphides 27
- Sphalerite 29
- Galena 29
- Copper minerals 30
- Magnetite 30
- Rutile 30
- Other minerals 30

#### Petrography 30

- Ben Eagach Schist 30
- Ben Lawers Schist 32
- Metabasites 32

#### Characteristics of the mineralised zone: general 33

##### Characteristics of the mineralised zone:

###### Creag an Fhithich district 33

- Geology 33
- Geochemistry 34
- VLF mapping 36

##### Characteristics of the mineralised zone:

###### Ben Eagach to Farragon Hill 36

- Geology 36
- Geochemistry 41
- VLF mapping 42

##### Characteristics of the mineralised zone:

###### Creagan Loch to Meall Tairneachan 42

- Geology 42
- Geochemistry 43
- VLF mapping 45

#### Discussion and conclusions 45

- Genesis of mineralisation 45
- Economic significance 55

#### Acknowledgments 56

#### References 56

#### Appendices

- I Borehole logs and supplementary notes 58
- II Geochemical analyses of borehole cores 85

### III Summary of petrographic data 97

### IV Geochemical analysis of deep overburden samples 111

### V Beneficiation studies on baryte samples 113

## FIGURES

- 1 General geological environment of the Aberfeldy and other stratabound mineral deposits in the Scottish Highlands: based on Johnstone and Gallagher (1980) 2
- 2 General geology of the area of mineralisation north of Aberfeldy, showing location of boreholes 3
- 3 Geological map of the area of mineralisation north of Aberfeldy *in pocket*
- 4 Barium in (a) regional stream sediment samples and (b) regional panned concentrate samples 7
- 5 Zinc in (a) regional stream sediment samples and (b) regional panned concentrate samples 8
- 6 Lead in (a) regional stream sediment samples and (b) regional panned concentrate samples 9
- 7 (a) Manganese in regional stream sediment samples (b) Scores on Factor 1 (Mineralisation) 10
- 8 Dispersion of barium, lead and zinc downstream of one section of the mineralised zone 12
- 9 Cumulative frequency distribution of barium in drill core samples 14
- 10 Cumulative frequency distribution of titanium in drill core samples 16
- 11 Sketch of magnetic fields around a conductor in a VLF field 18
- 12 Sketch of magnetic vectors around the conductor in Fig. 11 18
- 13 Sketch map showing area of VLF-EM survey near Aberfeldy and position of profile Fig 14 and survey areas Figs. 19, 25 and 30 20
- 14 Interpretation of VLF-EM profile across the Ben Eagach Schist, east side of Farragon Hill (see Fig. 13) 21
- 15 Interpretation map of VLF-EM survey of the area of mineralisation north of Aberfeldy *in pocket*
- 16 Plot of barium content against specific gravity for samples of borehole core from the mineralised zone near Aberfeldy 23
- 17 Geology of the Creag an Fhithich area *in pocket*
- 18 Geology, mineralisation and geochemical traverse in till, north of Creag an Fhithich 35
- 19 VLF-EM map of area north of Creag an Fhithich. (a) contour map of Fraser-filtered data, (b) profile along line ABC and its geophysical interpretation compared against the geological section in Fig. 20 37
- 20 Section through boreholes 5 and 7, north of Creag an Fhithich, located on Figs. 17 and 18 38
- 21 Section through borehole 8, north-east of Creag an Fhithich; located on Figs. 17 and 18 39
- 22 Section through borehole 6, north-west of Creag an Fhithich, and borehole 4, south-west of Ben Eagach; located on Figs. 17, 18 and 23 40
- 23 Geological map of the mineralised area south-west of Ben Eagach; located by BH 4 on Fig. 2 *in pocket*
- 24 Geology of the area between Creagan Loch and Frenich Burn *in pocket*

- 25 Fraser-filtered VLF real component data over the area of French Burn headwater; located on Fig. 13 46
- 26 Geology, mineralisation and barium distribution in overburden, upper French Burn (above) and the area north of Creagan Loch (below); A-B is a common boundary 47
- 27 Section through BH 3, north of Creagan Loch; located on Figs. 24 and 26 48
- 28 Section through boreholes 1 and 11, upper French Burn, and borehole 2, Creag an Chanaich; located on Figs. 24 and 29 49
- 29 Geology of the area between Creag an Chanaich and Meall Tairneachan; located by boreholes 2, 9 and 10 on Fig. 2 *in pocket*
- 30 Real component profiles (a), Fraser-filtered real component data (b), and outline geology and geophysical interpretation (c) for part of the area between Creag an Chanaich and Meall Tairneachan located on Fig. 13; the diagonally striped ornament on Fig. 30c represents the geophysically inferred suboutcrop of the Ben Lawers Schist 50
- 31 Geology, mineralisation and barium distribution in overburden, between Creag an Chanaich and Meall Tairneachan; zinc and lead anomalies in overburden are shown where not coincident with barium anomalies 51
- 32 Section through borehole 9, Creag an Chanaich; located on Fig. 29 52
- 33 Section through boreholes 10 and 10A, north of Meall Tairneachan; located on Fig. 29 53

## TABLES

- 1 Formations of Middle Dalradian (Easdale and Islay Subgroups) in Aberfeldy area. 4
- 2 Summary statistics for regional drainage survey of the Tay-Tummel area. 5
- 3 Comparison of median metal values – Tay-Tummel and Central Argyll areas. 5
- 4 Factor loadings for regional drainage samples from the Aberfeldy area. 6
- 5 Average partial analyses of the major components of the mineralised zone. 15
- 6 Comparison of gravity anomalies resulting from baryte bodies and overburden variations. 17
- 7 Resistivities of rocks in Aberfeldy survey area. 19
- 8 High resistivity zones worthy of investigation. 22
- 9 Minerals identified in the Ben Eagach Schist mineralised zone. 22
- 10 Electron microprobe analyses of celsian and hyalophane. 24
- 11 Electron microprobe analyses of barian muscovite. 25
- 12 Modal analyses of thin sections of baryte-rich rocks from Boreholes 1, 2, 4 and 5. 26
- 13 Semi-quantitative estimates of major elements in calcite from Borehole 4, 21.20 m. 27
- 14 Partial analyses of baryte concentrates by XRF. 28
- 15 Electron microprobe analyses of sphalerite. 28
- 16 Electron microprobe analyses of galena. 29

## SUMMARY

The discovery and preliminary assessment of stratabound barium-zinc mineralisation in Dalradian metamorphic rocks near Aberfeldy (outlined in MRP Report No. 26) resulted from co-ordinated geological, geochemical, geophysical and mineralogical studies, full details of which are presented here. The presence of an extensive zone of mineralisation in the area was recognised initially by a geochemical drainage survey and reconnaissance geological mapping. Subsequently, more detailed mapping and drainage sampling were supplemented by VLF-EM geophysical surveys, overburden and rock sampling, and shallow drilling. The VLF-EM technique successfully delineated resistive rocks within the generally conductive graphitic schists and proved a valuable mapping aid in areas of poor exposure.

The mineralised zone is defined by the presence of bedded baryte, sulphide concentrations, quartz-celsian rock and micaceous schists in which the muscovite is barium-rich. It varies in thickness from about 60 m to 110 m and extends, at least intermittently, over 7 km of strike and through a vertical interval of 370 m. Individual baryte bands are 2.3–15.5 m thick and may extend along strike for up to 1.8 km. The greatest sulphide concentration is in carbonate rock assaying 8.5% Zn and 3.6% Pb over 4.3 m. Other unusual constituents of the mineralised zone are the barium silicates hyalophane and cymrite and the chromian muscovite fuchsite.

It is concluded that the mineralisation is of synsedimentary origin, involving the introduction of metal-rich hydrothermal brine into an euxinic basin.

## INTRODUCTION

The Mineral Reconnaissance Programme has as its primary objective the identification of areas of promise for the discovery of economic metalliferous deposits, in which mining companies would conduct further investigations if they considered them to be justified. It has an additional remit to undertake research to develop and optimise methods of mineral investigation. To meet the first objective, a preliminary report on the discovery of stratabound barium-zinc mineralisation near Aberfeldy (Coats, Smith and others, 1978) was published, although much of the analytical data had not then been processed.

This report is intended to complement and enlarge on the preliminary report and, though the bulk of its substance is new data in appendix form (detailed bore logs, geochemical analyses, and mineralogical studies), some overlap with the preliminary report is unavoidable. Concurrently with the publication of this report, supplementary geophysical and geochemical maps have been placed on open file and are available respectively from the Heads of Applied Geophysics Unit (Princes Gate Office) and Metalliferous Minerals and Applied Geochemistry Unit (Keyworth Office).

The Aberfeldy barium-zinc deposit is almost certainly the major non-energy mineral discovery in Scotland in the present century. In view of its potential economic significance, scientific aspects of the IGS results were presented at the Institution of Mining and Metallurgy's Symposium on 'Mineralisation in Northern Britain', held at Strathclyde University in May 1979 (Coats, Smith and others, 1980; Parker, 1980). The deposit is characterised by a suite of unusual barium minerals, including celsian and barian muscovite, which are under detailed investigation.

The successful application of VLF-EM mapping in an unusual geophysical environment in which resistive targets are located in conductive host-rocks (Parker, 1980); the delineation of sub-surface baryte ore by deep overburden sampling (Coats, Smith and others, 1980), and the development of a rapid technique for determining barium in uncrushed samples (Grout and Gallagher, 1980), represent significant advances in research on exploration methods. A short review of these methods is given by Gallagher and Smith (in preparation).

## LOCATION AND GENERAL GEOLOGY

Straths Tay and Tummel lie in the northern part of Perth and Kinross District, about 100 km north-west of Edinburgh. The site of the investigation is the watershed between these glaciated troughs, the ENE trend of the ridge reflecting the strike of the underlying rocks. The ridge has a stepped profile culminating in a dissected steep-sided summit-ridge with a number of distinct tops — Meall Tairneachan, Farragon Hill (780 m), Ben Eagach, and Meall a'Charra. At its western end the ridge is separated from the higher Rannoch-Lyon watershed by a narrow valley marking the NE-trending Loch Tay Fault.

The area is situated in the southern part of the Scottish Highlands (one-inch Geological Sheet 55) in rocks making up part of the Dalradian Supergroup (Harris and Pitcher, 1975), a succession comprising up to 25 km of marine metasedimentary and metavolcanic rocks which accumulated over a 300 Ma period between the late Precambrian and Cambro-Ordovician, and which were subjected to polyphase metamorphism and deformation during the Caledonian Orogeny (Figs. 1–3). The stratigraphically controlled baryte and base metal concentrations to the north of Aberfeldy occur at or close to the top of the Ben Eagach Schist, one of the formations of the Middle Dalradian Easdale Subgroup (Table 1). A more detailed account of the geology may be found in Coats, Smith and others (1978, 1980).

## GEOCHEMISTRY

### REGIONAL DRAINAGE SURVEY

Stream sediment sampling was undertaken in 1975 with the aims of completing the coverage of the Middle Dalradian

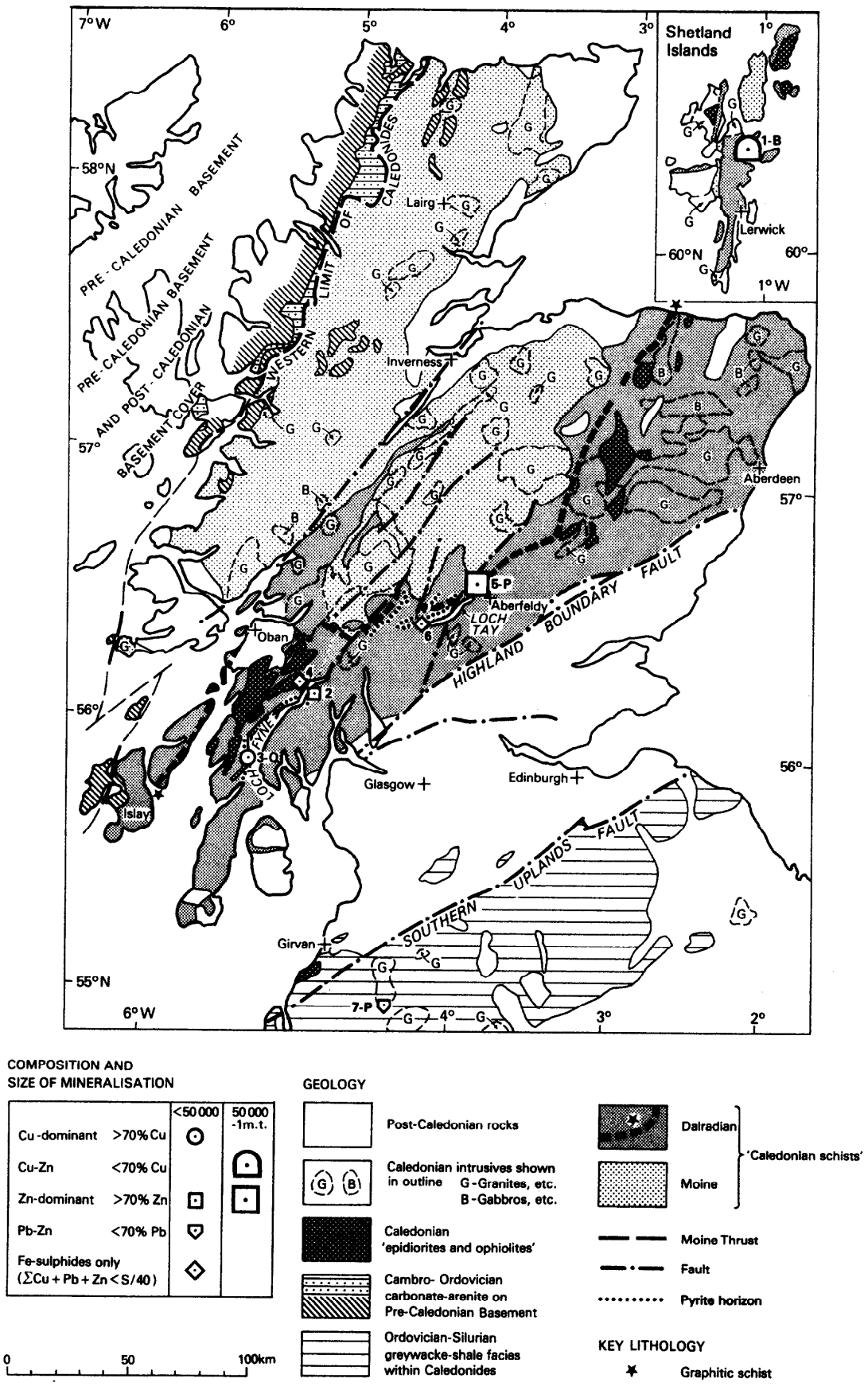


Fig 1 General geological environment of the Aberfeldy and other stratabound mineral deposits in the Scottish Highlands: based on Johnstone and Gallagher (1980)



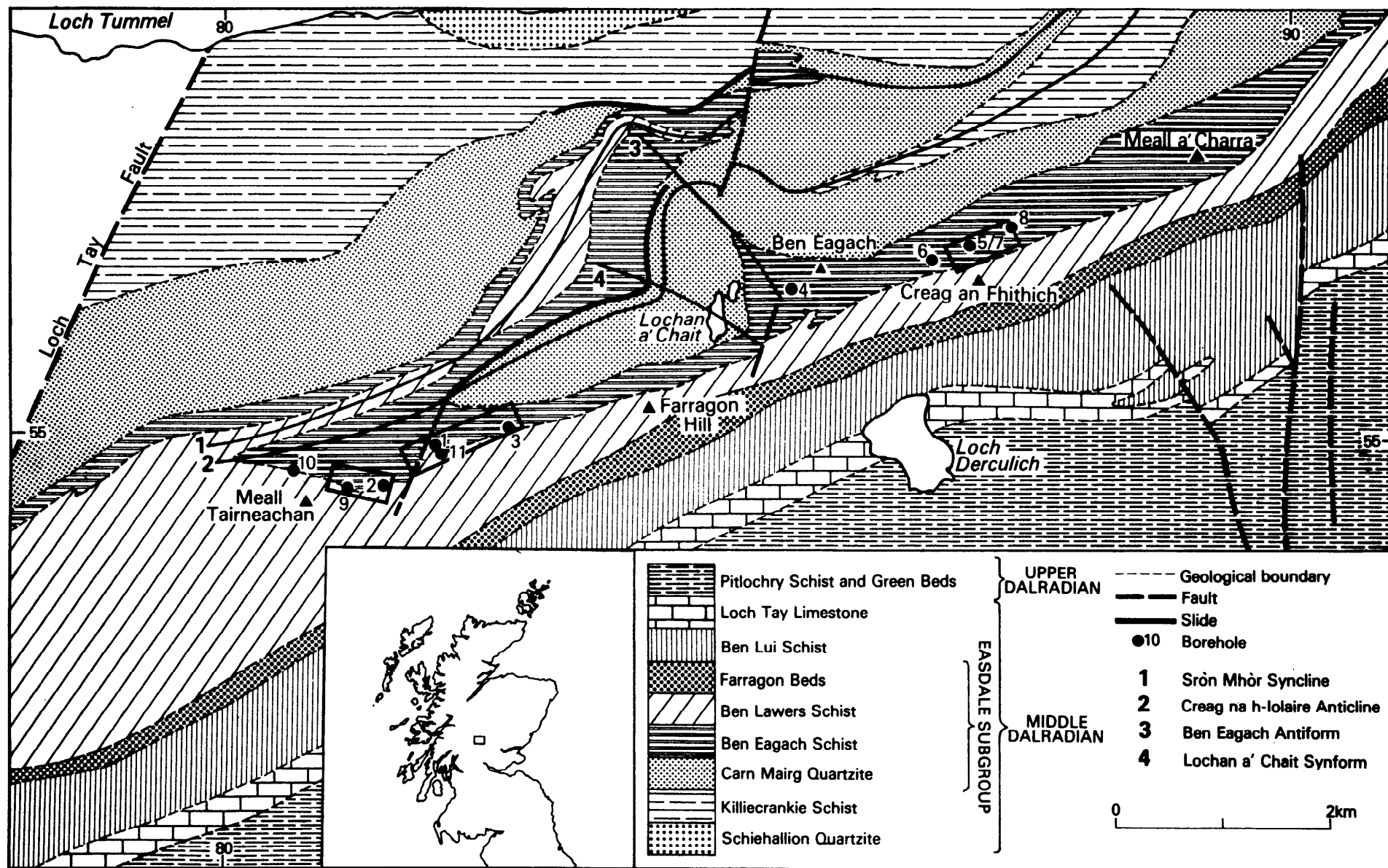


Fig 2 General geology of the area of mineralisation north of Aberfeldy, showing location of boreholes (modified from Coats, Smith and others, 1978)

**Table 1** Formations of the Middle Dalradian (Easdale and Islay Subgroups) in the Aberfeldy area

Formation	Lithology
Easdale Subgroup	
1. Farragon Beds (youngest)	Hornblendic and epidotic schists, quartzite and mica-schist.
2. Ben Lawers Schist	Calcareous mica-schist, commonly hornblendic and garnetiferous and with thin bands of calcareous quartzite and metabasic sheets; pyritic horizon in upper part.
3. Ben Eagach Schist	Graphitic schist, mica-schist and quartzite with thin bands of dark limestone; some thin metabasic sheets; <i>mineralised zone in upper part.</i>
4. Carn Mairg Quartzite	Thick beds of pebbly quartzite, commonly graded and separated by thin bands of graphitic schist.
Islay Subgroup	
5. Killiecrankie Schist	Micaceous schist, locally graphitic, with abundant layers of quartzite and hornblende-schist.

outcrop between Ben Lawers (sampled in 1973/4) and Blair Atholl (sampled in 1974/5), and tracing the extension of stratabound pyrite mineralisation in the Ben Lawers Schist, known to contain minor copper in the Loch Tay area to the west (Smith and others, 1977). An average sampling density of about 1 sample per 1.5 km<sup>2</sup> was used, samples being of closer interval in the upland areas and more sparse in the east and south where the lack of water in the streams, and extensive drift cover, make collection more difficult.

#### Methods

A sample of the active sediment in the stream course was collected and wet sieved through 2000 and 150 μm aperture nylon sieves using a minimum quantity of water. The 150–2000 μm fraction was panned on site to produce a heavy mineral concentrate. The <150 μm fraction, after drying and grinding to about 50 μm, was analysed for Cu, Pb, Zn and Ag by atomic absorption spectrophotometry; for U by delayed neutron activation, and for Be, B, V, Cr, Mn, Fe, Co, Ni, Y, Zr, Nb, Mo, Sn and Ba by semi-automated photographic emission spectrometry (Tait and Coats, 1976). Half of the heavy mineral concentrate was retained for reference, the other half being ground and analysed by X-ray fluorescence for Ce, Ba, Sb, Sn, Pb, Zn, Cu, Ca, Ni, Fe, Mn and Ti (Leake and Aucott, 1973).

#### Results

All results of the chemical analyses are available for inspection at the IGS Keyworth Office and the summary statistics of the elements are tabulated in Table 2. Comparison of the median values with those from other regional drainage surveys, for example Central Argyll (Tandy, Coats and Michie, in prep.) which covers Middle Dalradian rocks of similar age and lithologies, shows that

most elements are at background levels for the Middle Dalradian, with only Ca, Fe and Mn in panned concentrate samples having much higher median values (Table 3).

#### Interpretation

Cumulative frequency diagrams were used to identify anomalous populations using the methods of Lepeltier (1969) and also to provide class intervals for the preparation of greyscale maps. Most of the elements show a fairly close approximation to a lognormal population. Those elements which show a marked break of slope in the cumulative frequency curve, indicating the presence of an anomalously high population, were Pb<sub>c</sub>, Zn<sub>c</sub>, Mn<sub>c</sub>, Ba<sub>c</sub>, Ba<sub>p</sub>, Pb<sub>p</sub>, Zn<sub>p</sub>, U<sub>c</sub>, B<sub>c</sub>, Ce<sub>p</sub>, Cu<sub>p</sub>, Ni<sub>p</sub>, and Fe<sub>p</sub>.

Strong inter-element relationships are also present and these were displayed using a factor analysis model. The first five factors extracted by the method were found to be geologically significant and account for 59% of the total variation. The factor loadings are given in Table 4. As some of the elements do not approximate to either normal or lognormal distributions, this violates one of the basic premises of the method and even if the data are 'standardised' to unit variance the presence of two populations invalidates its use to some extent. However the factors are geologically meaningful and the spatial distribution of the elements indicates that the same underlying geochemical and geological controls are influencing the elements grouped in these factors. The factor analysis model is therefore robust enough to allow for some violation of its basic premises.

The group of elements in the first factor, Ba-Zn-Pb-Mn-U, include most of those that show a highly anomalous population and are related to the mineralisation. The individual sample scores on this factor can be used to provide an overall picture of the mineralisation combining

**Table 2** Summary statistics for regional drainage survey of the Tay-Tummel area

Element	Arithmetic		Geometric		Median	Minimum	Maximum
	Mean	Deviation	Mean	Deviation			
Cu <sub>c</sub>	17.7	10.9	15.4	1.74	15	5	65
Pb <sub>c</sub>	37.3	34.9	32.3	1.58	30	10	390
Zn <sub>c</sub>	169.7	209.7	123	2.04	110	30	1340
U <sub>c</sub>	3.5	1.8	3.2	1.48	2.8	1.0	18.2
Be <sub>c</sub>	1.4	0.6	1.3	1.4	1	0	4
B <sub>c</sub>	58.6	49.1	46.8	2.00	45	2	392
V <sub>c</sub>	123.2	46.6	117	1.41	114	46	334
Cr <sub>c</sub>	73.1	24.8	69	1.32	70	35	220
Mn <sub>c</sub>	3660	5098	2344	2.24	2000	441	39075
Fe <sub>c</sub> (%)	4.68	1.35	4.57	1.32	4.5	1.89	9.47
Co <sub>c</sub>	28.3	12.9	25.7	1.51	26	8	106
Ni <sub>c</sub>	39.8	29.3	34.7	1.66	33	10	324
Y <sub>c</sub>	34.2	9.0	33.1	1.29	32	19	78
Zr <sub>c</sub>	1017	534	891	1.70	900	286	3027
Nb <sub>c</sub>	21.8	4.9	21.4	1.26	21	8	38
Mo <sub>c</sub>	0.3	0.6	1.0	1.2	0	0	3
Sn <sub>c</sub>	0.6	3.1	1.1	1.7	0	0	30
Ba <sub>c</sub>	694	738	525	2.04	510	12	7010
Ce <sub>p</sub>	39.1	22.4	33.1	2.0	35	0	128
Ba <sub>p</sub>	2262	14640	110	4.9	90	0	149154
Sb <sub>p</sub>	2.6	2.7	2.1	2.2	1	0	12
Sn <sub>p</sub>	6.4	42.1	1.5	2.8	0	0	469
Pb <sub>p</sub>	14.7	46.7	3.5	4.5	2	0	419
Zn <sub>p</sub>	83.8	43.7	77.6	1.48	75	29	457
Cu <sub>p</sub>	19.8	17.8	14.4	2.34	16	0	152
Ca <sub>p</sub> (%)	3.01	1.24	2.69	1.62	3.01	0.64	9.19
Ni <sub>p</sub>	17.8	12.6	15.5	1.32	15	5	129
Fe <sub>p</sub> (%)	13.07	5.24	11.75	1.62	13.0	3.07	28.60
Mn <sub>p</sub> (%)	0.53	0.30	0.44	2.00	0.47	0.06	1.27
Ti <sub>p</sub> (%)	1.49	1.19	1.17	1.91	1.1	0.25	7.47

Subscript c = stream sediment  
p = panned concentrate

All values in ppm except where indicated

Number of samples (n) = 193 for the stream sediments  
= 179 for the panned concentrates

**Table 3** Comparison of median metal values – Tay-Tummel and Central Argyll areas.

	Stream Sediments					Panned Concentrates											
	Cu	Pb	Zn	U	Ni	Ce	Ba	Sb	Sn	Pb	Zn	Cu	Ca	Ni	Fe	Mn	Ti
Tay-Tummel	12	30	110	2.8	33	35	90	1.4	0	2	76	16	3.0	15	13.	0.5	1.1
C. Argyll	20	43	160	2.0	35	40	139	2.5	1	20	100	19	2.0	34	7.9	0.09	2.2

**Table 4** Factor loadings for regional drainage samples from the Aberfeldy area

Factor Loading	I	II	III	IV	V
0.9	Zn <sub>c</sub>		Sn <sub>p</sub>		Mn <sub>p</sub> Fe <sub>p</sub>
0.8	Pb <sub>c</sub>	Cr <sub>c</sub>	Sn <sub>c</sub>	Y <sub>c</sub>	
0.7	Mn <sub>c</sub>	Ni <sub>c</sub> Fe <sub>c</sub> V <sub>c</sub>			Ti <sub>p</sub> Ca <sub>p</sub>
	Ba <sub>c</sub>	Co <sub>c</sub>	Pb <sub>p</sub>		
0.6	Ba <sub>p</sub>	Cu <sub>c</sub>		Nb <sub>c</sub> Zr <sub>c</sub>	
	Zn <sub>p</sub>				Zn <sub>p</sub>
0.5					
0.4	U <sub>c</sub>			Be <sub>c</sub> B <sub>c</sub> Mo <sub>c</sub>	
0.3	Co <sub>c</sub> Pb <sub>p</sub>				
0					
-0.3					
-0.4					Ba <sub>p</sub>
-0.5		Zr <sub>c</sub>			

Subscript p = panned concentrate  
c = stream sediment

Variables with factor loadings between +0.3 and -0.3 are not shown.

all these elements (Fig. 7b) and to give an order of priority for future work. The three samples in the headwaters of Frenich Burn which drains the ridge east of Meall Tairneachen have the highest factor scores (>4.0) and several samples downstream have significant values. The other group of samples having anomalous values are those from streams draining north from Creag an Fhithich into Middleton Burn, and south from Ben Eagach into Loch Derculich. There are also isolated anomalous samples, one north of Meall Tairneachen and another west of the B846 draining into Allt Kynachan.

The distribution of each element associated with the mineralisation is now considered separately, the class intervals of the 'dot maps' (Figs. 4-7) being chosen at the 75, 90 and 97.5 percentile levels to facilitate comparison.

Whilst the levels of lead in the stream sediment samples are not high, reaching a maximum of 390 ppm, the highest values group to the south and east of Ben Eagach and in the headwaters of Frenich Burn (Fig. 6a). There is a fairly long dispersion train down this burn and a WSW-ENE trending zone of values greater than 40 ppm running from Allt Coire Pheiginn (NN 763 504) to near Pitlochry (NN 910 589). Lead in panned concentrate samples shows a much more sharply defined distribution, only Frenich Burn being strongly anomalous (Fig. 6b). The streams draining south from Meall Tairneachen are slightly anomalous but the picture is complicated by the presence of samples with greater than 10 ppm Sn, indicating metal contamination near to a line of grouse butts. This is

confirmed by the absence of anomalies in the accompanying stream sediment samples which are less affected by heavy metallic impurities.

Zinc shows a similar pattern (Fig. 5a) to lead in the stream sediments (as shown by the high correlation coefficient  $r = 0.58$ ) but with less of a spread to the south of Meall Tairneachen. This confirms the view that the latter area is contaminated by metallic lead. In the panned concentrates (Fig. 5b) zinc is only highly anomalous in Frenich Burn, where a sample 3 km downstream is still greater than the 97.5 percentile level (180 ppm). The lack of anomalies in the other streams may indicate that the zinc mineralisation is very localised. The group of samples in the Allt Kynachan to the north west of the area (upstream of NN 778 572) contains zinc greater than the 75% percentile level, probably due to zinc enrichment in rocks of Lower Dalradian age. Zinc in panned concentrates is also associated with Mn, Fe, Ti and Ca as shown by factor V and spatially related to epidiorites in the Upper Dalradian.

Barium in the stream sediment samples (Fig. 4a) is at a high level in the headwaters of the Frenich Burn and the streams draining south and east from Ben Eagach. There is a fairly wide spread of those samples above the threshold of 1100 ppm. In the panned concentrates (Fig. 4b) barium reaches a peak of 15% and the cumulative frequency diagram shows a marked break in the population at 300 ppm. There is far less scatter than in the previous diagram and the mineralisation is clearly defined as running between Meall Tairneachen and Creag an Fhithich, the major anomalies lying to the north of the watershed but with some dispersion to the south and downstream to the north.

Manganese in the stream sediments (Fig. 7a) shows a similar pattern to the other elements associated with the mineralisation and Frenich Burn is strongly anomalous. The manganese is probably present as an oxide coating on the sediment grains. The close association with lead, zinc and barium might indicate the effect of scavenging of these elements by the precipitated manganese oxide, but the anomalies of lead, zinc and barium in the heavy mineral concentrates show that this scavenging is not the only cause of the stream sediment anomalies. The correlation of manganese with Pb, Zn and Ba was not suspected before the factor analysis was performed and carbonate rocks containing high manganese levels (for example, CZR3927 with 5.8% Mn) were subsequently found. Manganese in panned concentrates shows no correlation with the mineralisation and the dominant control is the occurrence with Fe, Ti and Ca in metabasic rocks.

Uranium in the stream sediments has a moderate loading on the first factor and the high values >7 ppm are found in Frenich Burn and those draining south from Ben Eagach into Loch Derculich. Black schists are known to show enrichment in uranium and the comparable environment of the stratiform Kuroko deposits of Japan also contains significant uranium anomalies (Lambert and Sato, 1974).

The following brief summary of the spatial distribution and geological interpretation of the other elements indicates the regional geochemical pattern. Elements with strong loadings on the second factor are Cr, Ni, Fe, V, Co and Cu, all in stream sediments. These are related to the 'Green Beds' and the epidiorites in the Upper Dalradian. Their levels of concentration are comparable with those determined in rock samples of the 'Green Beds' by Kamp (1970). Two of the elements, Cu and Ni, show moderately enriched levels in streams draining the Farragon Beds and the Ben Lawers Schist, a similar pattern to that shown further

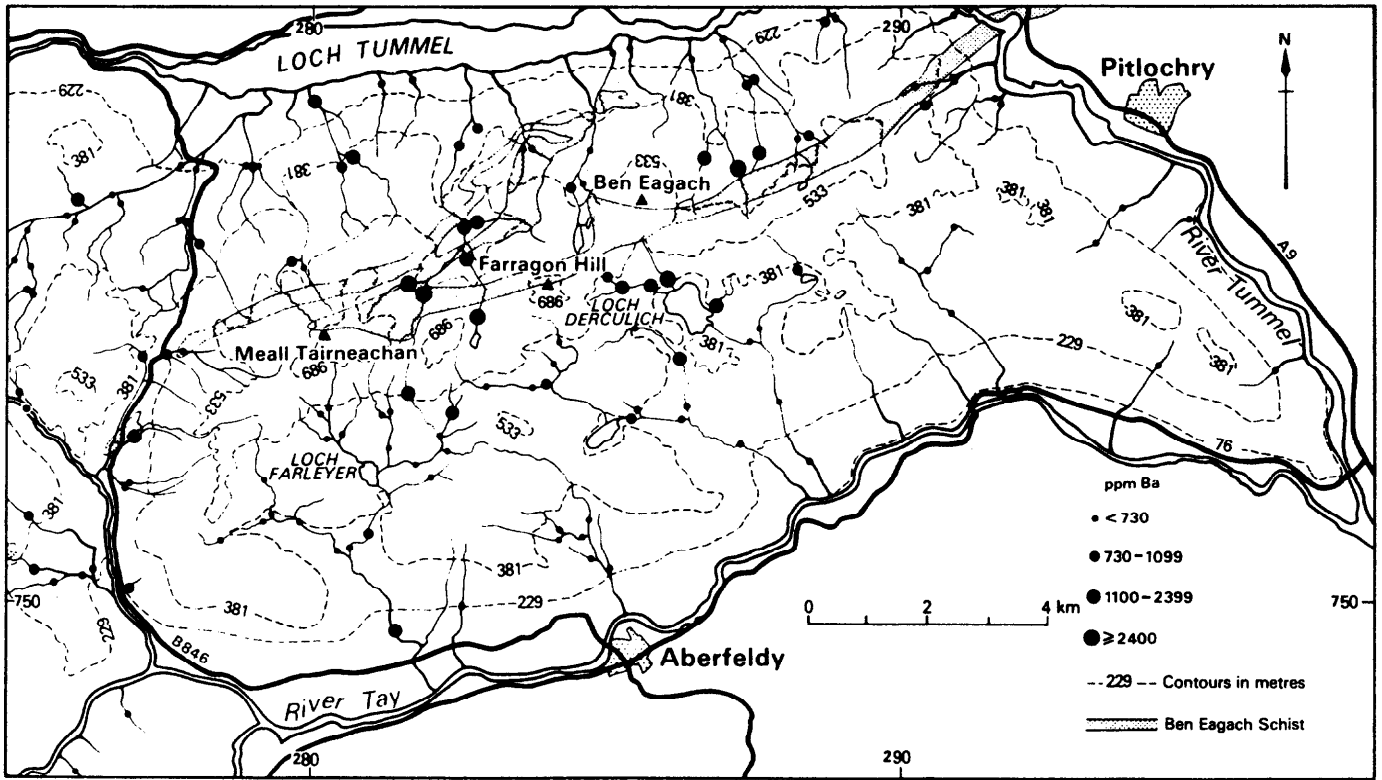


Fig 4a Barium in regional stream sediment samples

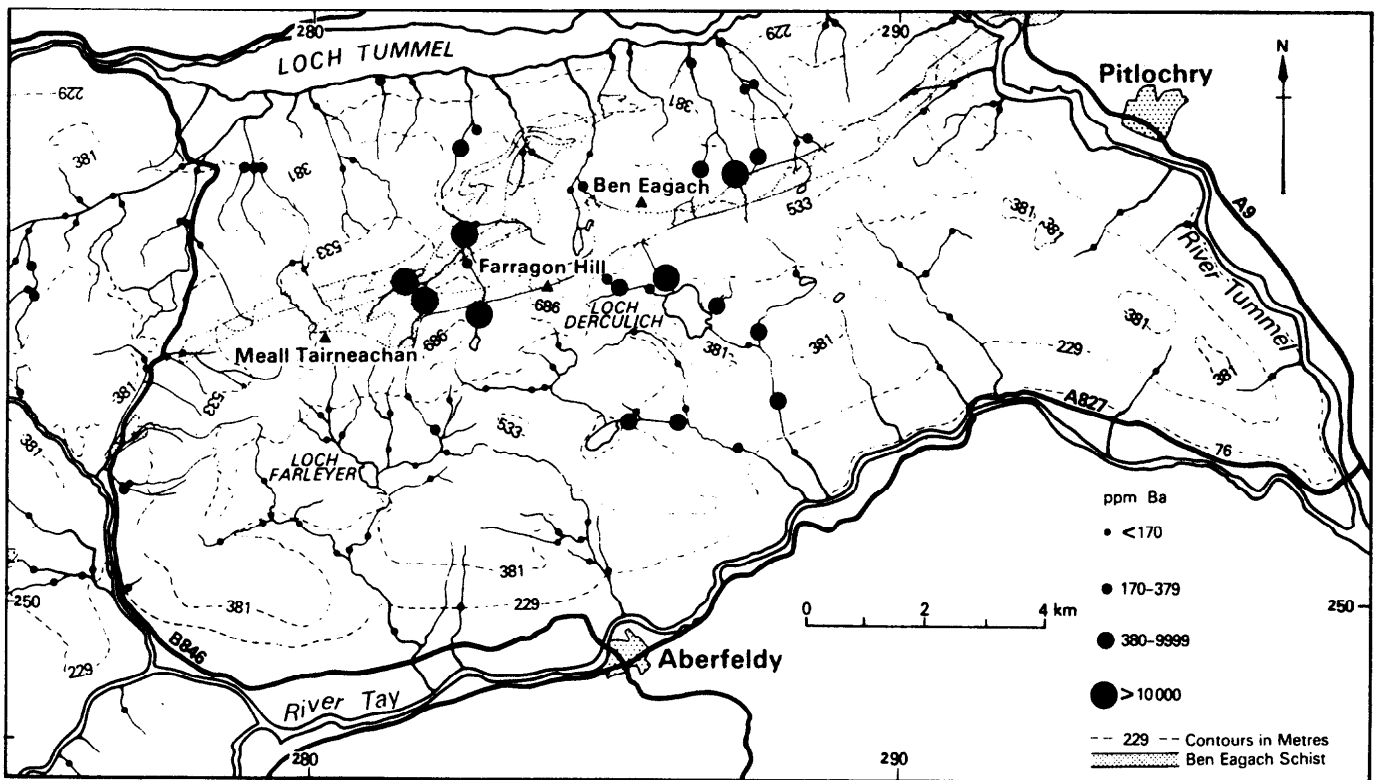


Fig 4b Barium in regional panned concentrate samples

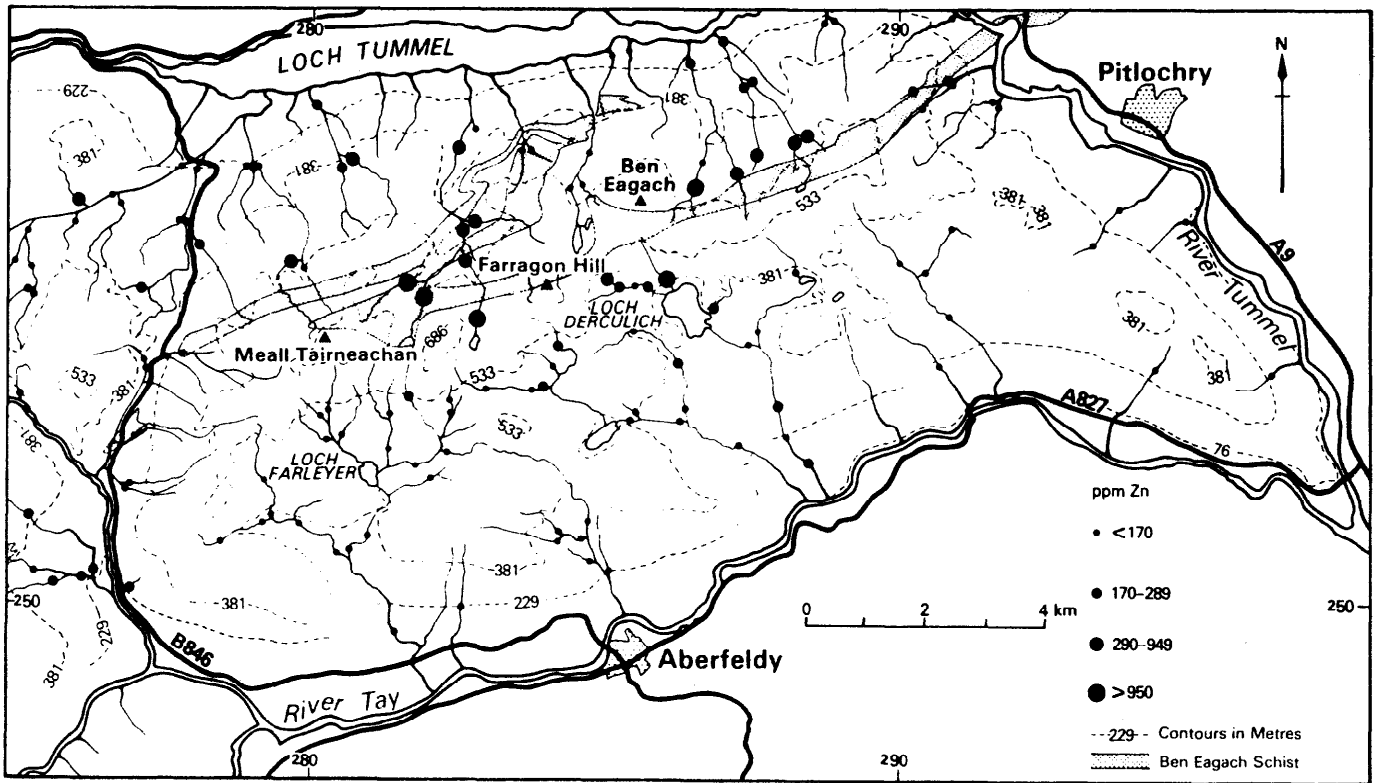


Fig 5a Zinc in regional stream sediment samples

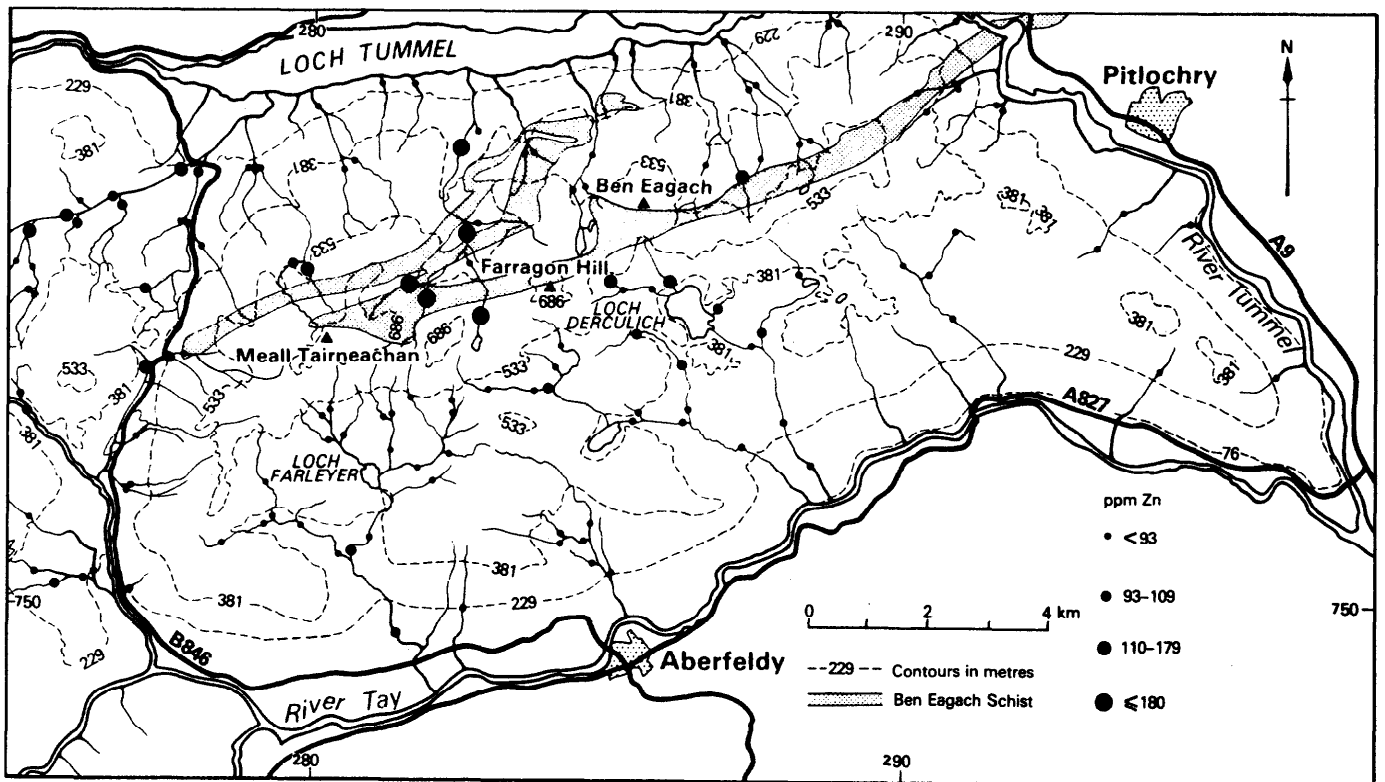


Fig 5b Zinc in regional panned concentrate samples

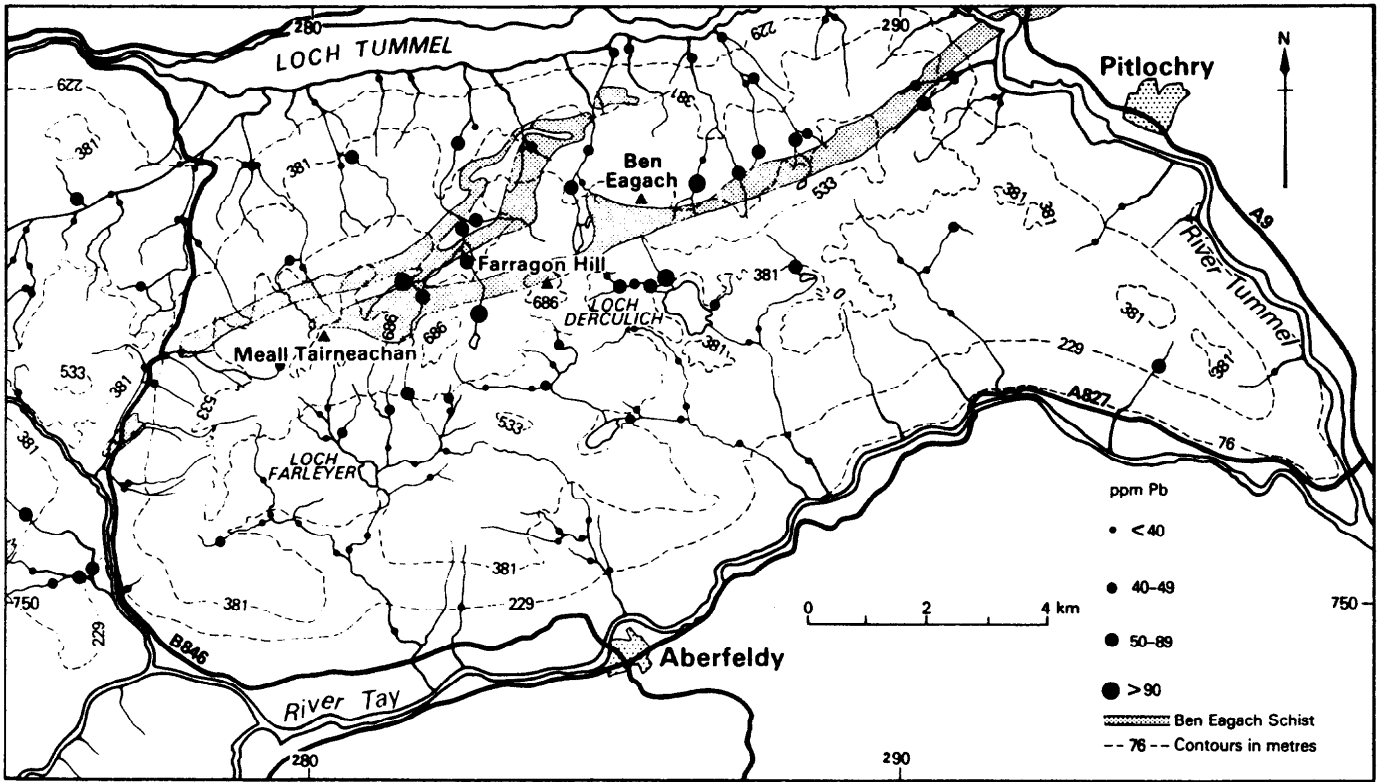


Fig 6a Lead in regional stream sediment samples

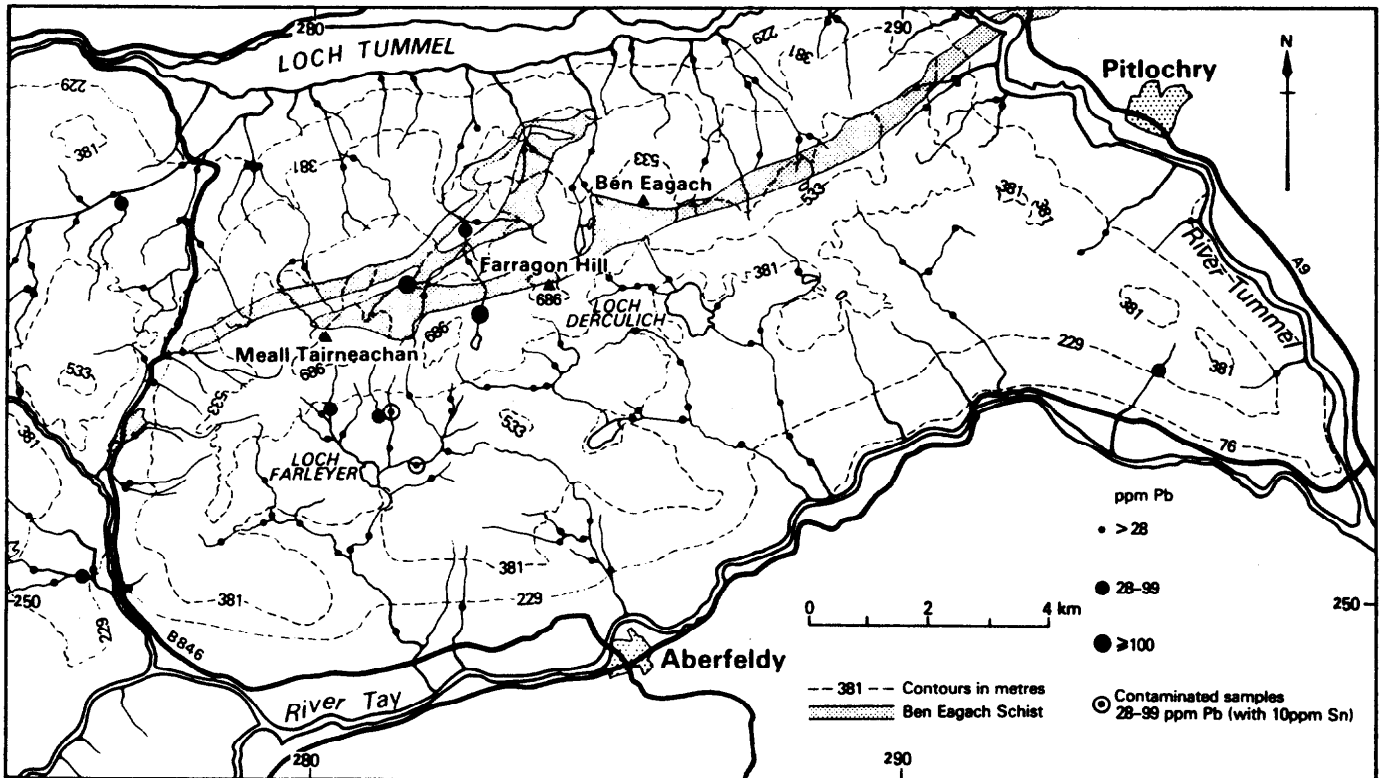


Fig 6b Lead in regional panned concentrate samples

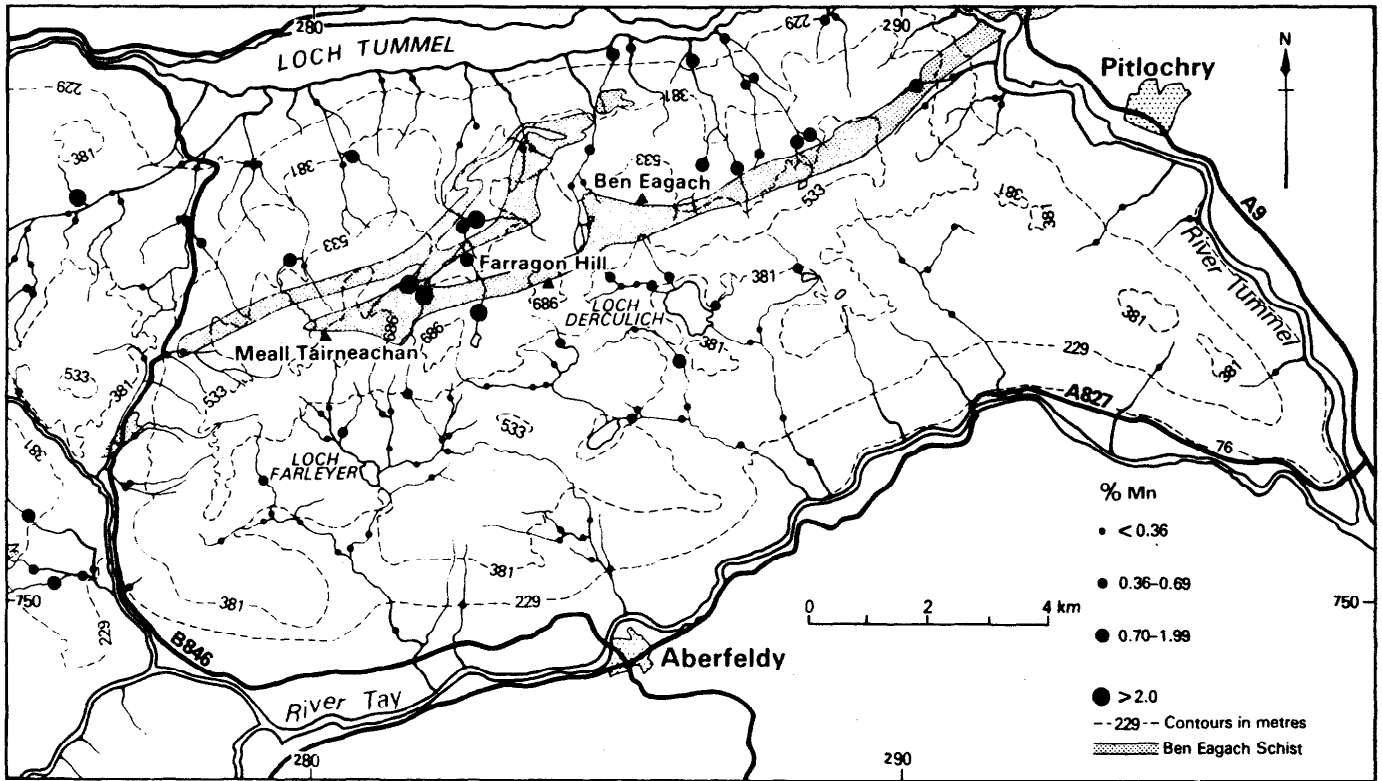


Fig 7a Manganese in regional stream sediment samples

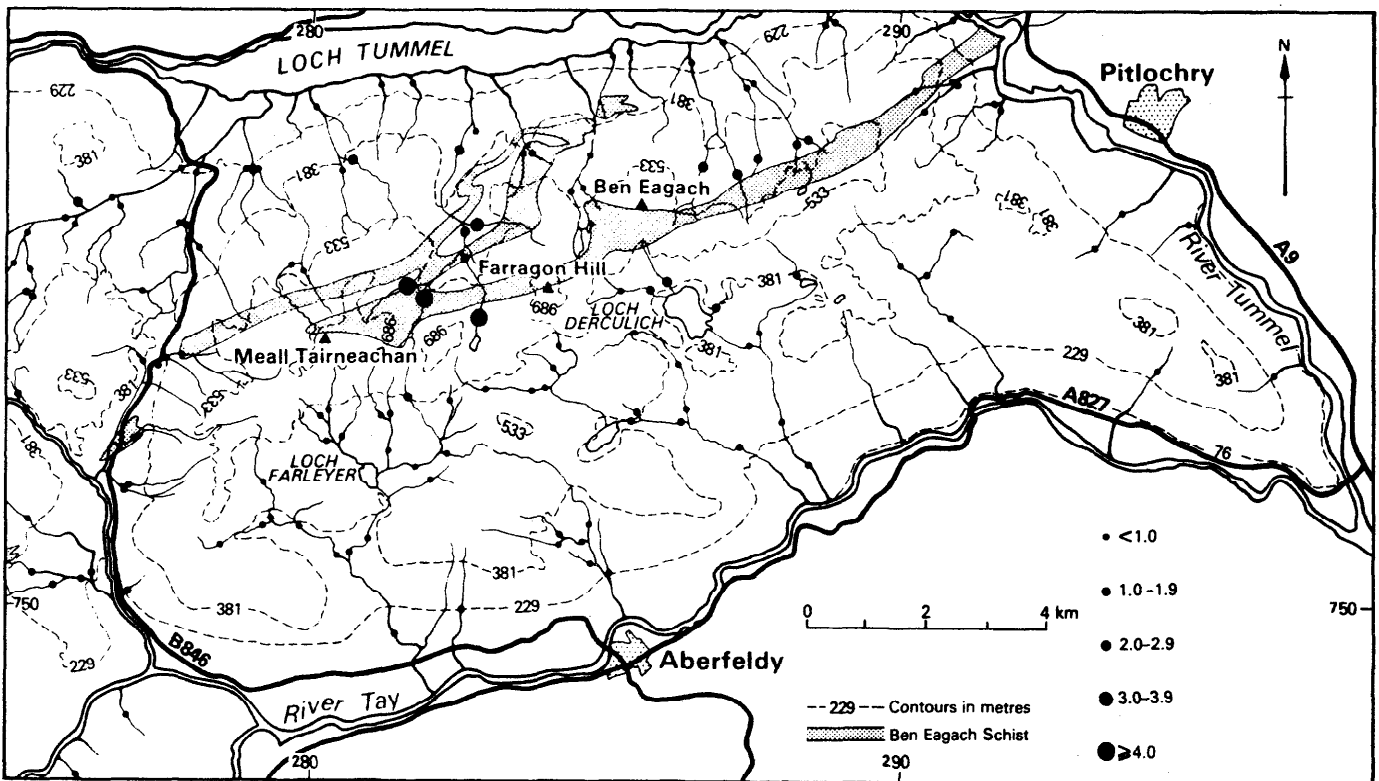


Fig 7b Scores on Factor 1 (Mineralisation)



west in the Ben Lawers area (Coats, in preparation). Most of the elements identified by factor II occur at levels below the median over the Carn Maig Quartzite and Killiecrankie Schist. Iron in the stream sediments is also relatively high in Frenich Burn and this may be related to the local enrichment of pyrite in the Ben Eagach mineralised zone, which, on weathering, produced a high iron oxide content in the sediment.

The third factor is clearly related to contamination. Mineralogical examination of samples with high tin and lead from elsewhere in the Highlands shows that minute grains of metal are present in the heavy mineral concentrate. Other elements may be present such as copper or zinc but the metal association Sn–Pb is the best indicator of contamination and is probably derived from the solder used in tin cans, and from lead shot. Contamination in the streams draining south from Meall Tairneachan has already been mentioned.

The fourth factor Y-Nb-Zr-Be-B-Mo is spatially related to the outcrop of the Lower Dalradian in the Allt Kynachan (upstream of NN 778 572) and possibly in the Fincastle area (north of Loch Tummel). This grouping of elements, which is believed to be characteristic of the Lower Dalradian, is probably related to the well-sorted, shallow-water, marine nature of the sediments deposited in a shelf sea environment. These sediments contrast with those of poorly-sorted, deep water character which predominate in the Upper Dalradian.

The fifth factor has high loadings of Mn, Fe, Ti and Zn, which occur in the heavy mineral concentrate, predominantly in magnetite and related spinels. The association of calcium may indicate that hornblende is also present. Spatially they are related to the epidiorites and the meta-basic rocks at the Loch Tay Limestone horizon, which may explain the linkage with calcium rather than hornblende.

Copper in the heavy mineral concentrates is not strongly correlated with any factor and does not show a consistent relationship with any lithology, except for being generally higher over the Ben Lawers Schist and possibly over the 'Pyrite Zone' within that formation (Smith and others, 1977). This is also the pattern further west, north of Loch Tay, where the Ben Lawers Schist shows an erratic enrichment in chalcopyrite (Coats, in preparation).

#### Summary

The geochemical drainage survey outlined a source of anomalously high levels of Pb, Zn, Ba and Mn, extending over a length of 7 km along the central part of the ridge north of Aberfeldy. It also showed that the strongest anomalies were to the north of the watershed in the Frenich and Middleton Burns. The one anomalous stream draining into Loch Derculich drains the only section of the mineralised zone situated to the south of the main ridge; but the dispersion to the south of the watershed is otherwise believed to be due to glacial transport of mineralised material from the north. The much longer dispersion to the north is caused by recent fluvial and earlier fluvio-glacial transport. Because the pyritic mineralisation in the Ben Lawers Schist lies almost entirely in stream catchments draining south into the River Tay, this is clearly not the source of the baryte, lead and zinc mineralisation.

#### DETAILED DRAINAGE SURVEYS

The regional survey outlined a WSW–ENE trending zone with anomalously high levels of barium, zinc and lead which is related to the outcrop of the Ben Eagach Schist. Detailed follow-up drainage sampling employed the same methods but samples were collected at 200 m intervals upstream of the anomalous sites with the aim of more closely defining the source. The stream sediment samples were analysed for Cu, Pb, Zn, Ag, Mn, Fe, Co, Ni, Ba and U and the panned concentrates for Ce, Ba, Sb, Sn, Pb, Zn, Cu, Ca, Ni, Fe, Mn and Ti (the subscripts c for stream sediment and p for panned concentrate are used throughout). The full analytical results are not presented here. They are available for inspection at the IGS, Keyworth Office and only a brief summary of the conclusions is presented here.

The elements of interest, with the greatest peak to threshold ratio, were  $Ba_p > Zn_c > Ba_c > Pb_c > Zn_p > Pb_p$ , this order generally reflecting the persistence of downstream dispersion. The latter varies from greater than 3 km, for the first two elements, to less than 200 m for lead in concentrates (Fig. 8). Barium in the concentrates is clearly one of the best indicators for the detection of the mineralisation because of its greatest contrast and length of the dispersion train. However the 150–2000  $\mu\text{m}$  fraction of the sediment does have a more variable content of barium and the downstream decline in concentration is not regular. Variation in panning efficiency is not the cause of this irregularity because individual sites have reproducible barium contents in the panned fraction, even at different times and with different operators. The zinc content of the  $<150 \mu\text{m}$  fraction of the stream sediments is a more reliable widespread indicator of the mineralisation and still has a dispersion in excess of 3 km.

In detail, barium in the panned concentrates is found at levels greater than 10% for half a kilometre below outcrops of the baryte-rock in Frenich Burn and is still above the threshold value 3 km downstream (Fig. 8). Discrete sources of baryte mineralisation were indicated to be present in the following streams; the three principal headwaters of Frenich Burn which drain the western sector of the mineralised zone between BHs 3 and 10; the stream that drains the south face of Ben Eagach and enters Loch Derculich, and the two tributaries of Middleton Burn which drain the eastern sector between BHs 6 and 8. Baryte-rock occurs in the mineralised zone and the outcrops in the catchments of these streams and is not indicated to be present in the catchments of the other streams which were sampled in detail. The stream valley draining the north-east face of Meall Tairneachan between BH 9 and 10, whilst crossing no outcropping baryte-rock, does exhibit a barium anomaly in the deep overburden samples, indicating that baryte-rock sub-outcrops. Allt Coirein a'Chinn, downstream of BH 8, shows a similar pattern and, whilst no baryte-rock was intersected in that borehole, baryte was identified in a heavy mineral concentrate prepared from the basal overburden. As a general rule, barium values do not show a sharp cut-off upstream of the mineralised zone but reduce gradually because of the presence of mineralised boulders and finer material transported southwards and uphill by ice movement.

Barium in the fine fraction of the stream sediments shows a similar pattern but a smoother decline away from the source (Fig. 8), indicating a more even distribution within the stream sediment. It also has a wider distribution of low level anomalies of between 1200 and 2400 ppm Ba. For example, it is present at these levels in Allt Tarruinchon (at NN 798 557) NW of Meall Tairneachan, and in the

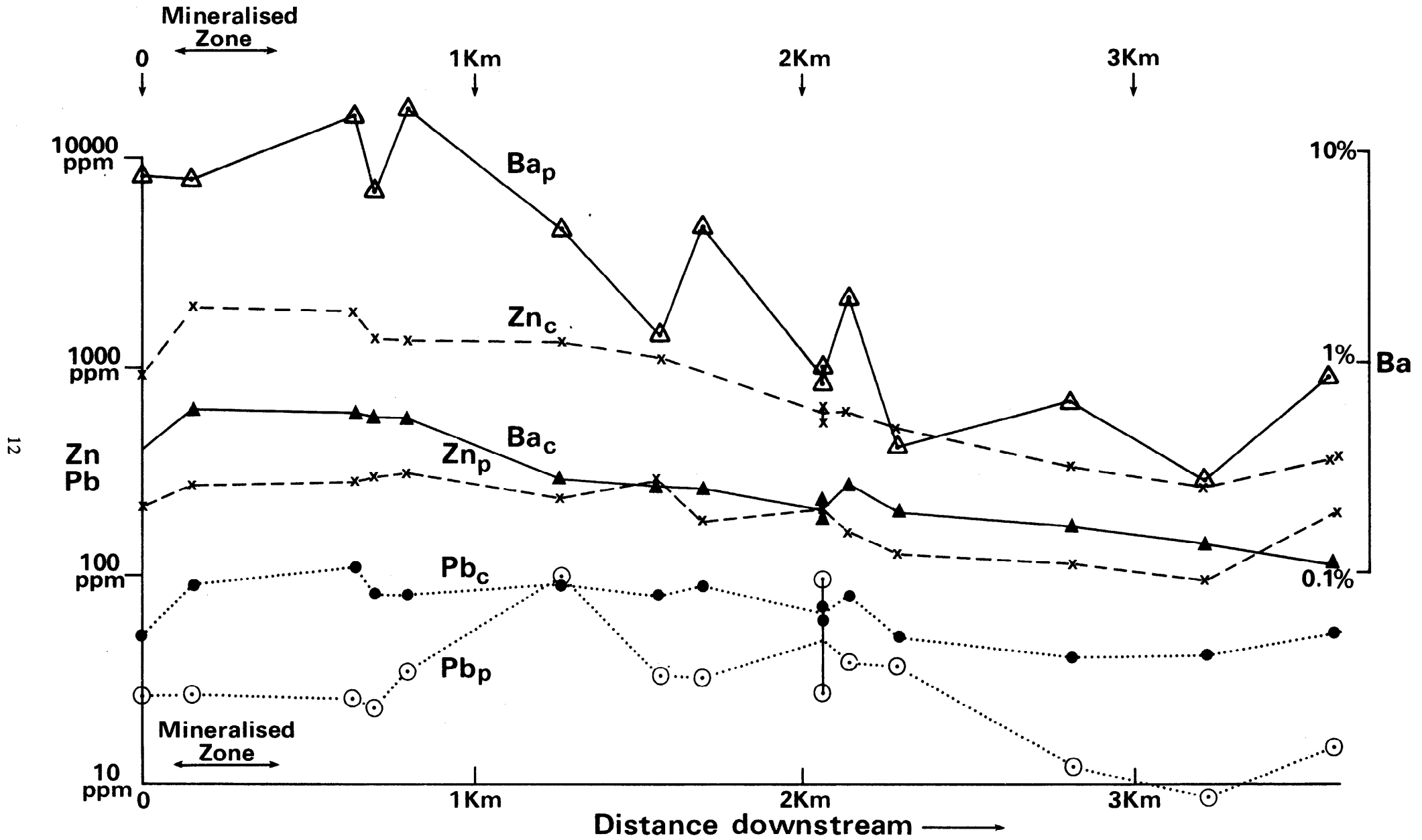


Fig. 8: Dispersion of barium, lead and zinc downstream of one section of the mineralised zone

unnamed stream to the east (NN 806 575) draining Creagan Dubh and Doire Leathan. Barium mineralisation may be present in the former stream catchment because of one isolated value of 3200 ppm Ba at NN 7979 5402.

This wider distribution indicates that the Ben Eagach Schist is enriched in barium over a larger area than the mapped extent of the mineralised zone and that the barium is present in a silicate phase, such as celsian or barian mica, which is not concentrated in the panning method. Strong anomalies, greater than 6000 ppm Ba, are located only immediately below the outcrops near BHs 1 and 3.

Zinc is similarly enriched in the sediments from all the streams cutting the Ben Eagach Schist Formation over a wide area from Meall Tairneachan to Meall a'Charra. It shows a sharp peak downstream of the mineralised zone and a nearly perfect exponential decline with distance which, together with its good reproducibility at each site, makes it probably the most useful element for both reconnaissance and follow-up investigations. Zinc in panned concentrates has a more localised distribution, indicating that sphalerite fairly rapidly breaks down and the zinc enters the fine fraction. Perhaps because several low level, dispersed sources of sphalerite in the Ben Eagach Schist are present in Frenich Burn the dispersion, up to 2.5 km, is longer in this stream than elsewhere.

The distribution of lead in the panned concentrates is a precise indicator of lead mineralisation; for example, in the stream below the outcrop at BH 3, lead concentration falls to background levels of less than 60 ppm within 200 m. Anomalies in the concentrates therefore indicate very local sources of lead. A fairly large anomaly of 335 ppm Pb in Frenich Burn at NN 81675532, and at the next site downstream, occurs in an area of poor exposure though traces of galena are present in graphitic schist and galena-bearing quartzite float assayed 0.37% Pb. This part of the Ben Eagach Schist outcrop was not covered by the geochemical overburden sampling and is worthy of further investigation, especially as it occurs close to the Ben Lawers Schist and the geophysical work indicates some non-conductive zones in the schist. Lead in the stream sediment samples shows a similar limited dispersion. Frenich Burn is again exceptional, confirming the concentrate anomaly.

In summary, the distribution of zinc and barium in the stream sediments is considered to be the best guide to the location of similar mineralised areas to Ben Eagach. These elements have a wider distribution within the Ben Eagach Schist than the visibly mineralised rocks, and they also exhibit the greatest downstream dispersion. The barium content of the panned concentrates is also a good guide to mineralisation, with a large contrast between the peak values and the threshold, but its distribution in the coarse fraction of the sediment between different sample sites is erratic and there is not a regular downstream fall in concentration. Lead, especially in the concentrates, has a limited dispersion and is probably the most precise guide to the source of the mineralisation. It also has the added advantage that galena, like baryte, can be readily identified in the field. Barium, zinc and lead mineralisation is shown, by the detailed drainage survey, to be present in a zone at the upper contact of the Ben Eagach Schist Formation over a distance of 7 km from Meall Tairneachan to Creagan Fhithich. Large barium anomalies indicative of outcropping baryte are confined to three sections: the western section in the headwaters of Frenich Burn, the central section near Ben Eagach and the eastern section near Creagan Fhithich. The Ben Eagach Schist Formation in the Aberfeldy area also shows a more widespread but lower level of enrichment of zinc and barium.

## LITHOGEOCHEMISTRY

The mineralised zone which occurs at the stratigraphic top of the Ben Eagach Schist is characterised by its anomalous barium content. Rocks of predominantly metasedimentary aspect, including calcareous mica-schist, muscovite-schist and graphitic mica-schist have levels of barium which separate them distinctly from the normal metasediments that make up the Ben Eagach Schist and the succeeding Ben Lawers Schist Formation. A close inspection of the distribution of barium in the rocks of the mineralised zone is therefore warranted.

The majority of the rocks sampled by the eleven boreholes form part of the mineralised zone. The cumulative frequency distribution (Fig. 9) reflects this, with 90% of the samples having  $>0.1\%$  Ba. This value should be compared with the background or normal levels of barium in sedimentary rocks of 546 ppm Ba in shales and 316 ppm Ba in sandstones (Wedepohl, 1969). Several features can be deduced from the frequency distribution. Firstly, there is a sharp inflection at 25% Ba and an absence of samples with 20–30% Ba indicating that the samples of baryte-rock with above 30% Ba form a separate population. Close inspection of the samples with just over 30% Ba shows that these core lengths consist of baryte-rock interbanded with another distinct lithology and that most of the baryte-rocks group around 51.0% Ba, the arithmetic mean (standard deviation = 4.3% Ba). Baryte-rock has, therefore, at the scale of sampling employed, a distinct composition and this point is also brought out by the multivariate methods described below.

Another population break occurs at 5% Ba and the population between 5 and 25% Ba consists predominantly of quartz-celsian rock. Some muscovite schists with hyalophane occur in this group at the lower end, for example CYD 517 with 7.0% Ba (A\*II, T\*VII), but these are exceptional. Below 5% Ba there is a single lognormal population which runs from 0.07 to 4% Ba. The samples of this 'mineralised schist' population have varied lithologies and the levels of barium do not show a simple relation to the gross mineralogy. Higher levels of barium tend to be confined to muscovite-schist, which is often dolomitic and occasionally carries celsian, but rocks with 0.3–0.4% Ba can consist of a number of lithologies such as calc schist or graphitic mica-schist.

The inflection point at 0.07% Ba (Fig. 9) is the statistical divide between the mineralised schist population and the background population but there is some overlap and a level of 0.15% Ba is taken as the cut-off level of the barium mineralisation. Thus some samples (about 15%) below this level will be part of the mineralised schist population but nearly all (85%) of the background population will be below the cut off. The median of this background population is 700 ppm which agrees reasonably well considering the small number of samples (24), with the average level of barium in shales of 546 ppm (Wedepohl, 1969). Occasional samples within the mineralised zone belong to this background population; for example, quartzites such as CYD 665 (A II, T X), or limestones such as CYD 594 (A II, T IX); but the dominant lithologies of this population are metabasites, calcareous mica-schists belonging to the Ben Lawers Schist Formation, and graphitic mica-schists belonging to the Ben Eagach Schist Formation. Comparison of the lithological logs with the barium contents (Appendix I and II) shows that the chemical definition of the mineralised zone does not agree exactly with the lithostratigraphic definition. For example, in BH 7 (A II, T VII) the lithostratigraphic boundary of the Ben Lawers Schist is taken at the bottom of sample CYD 555, the last

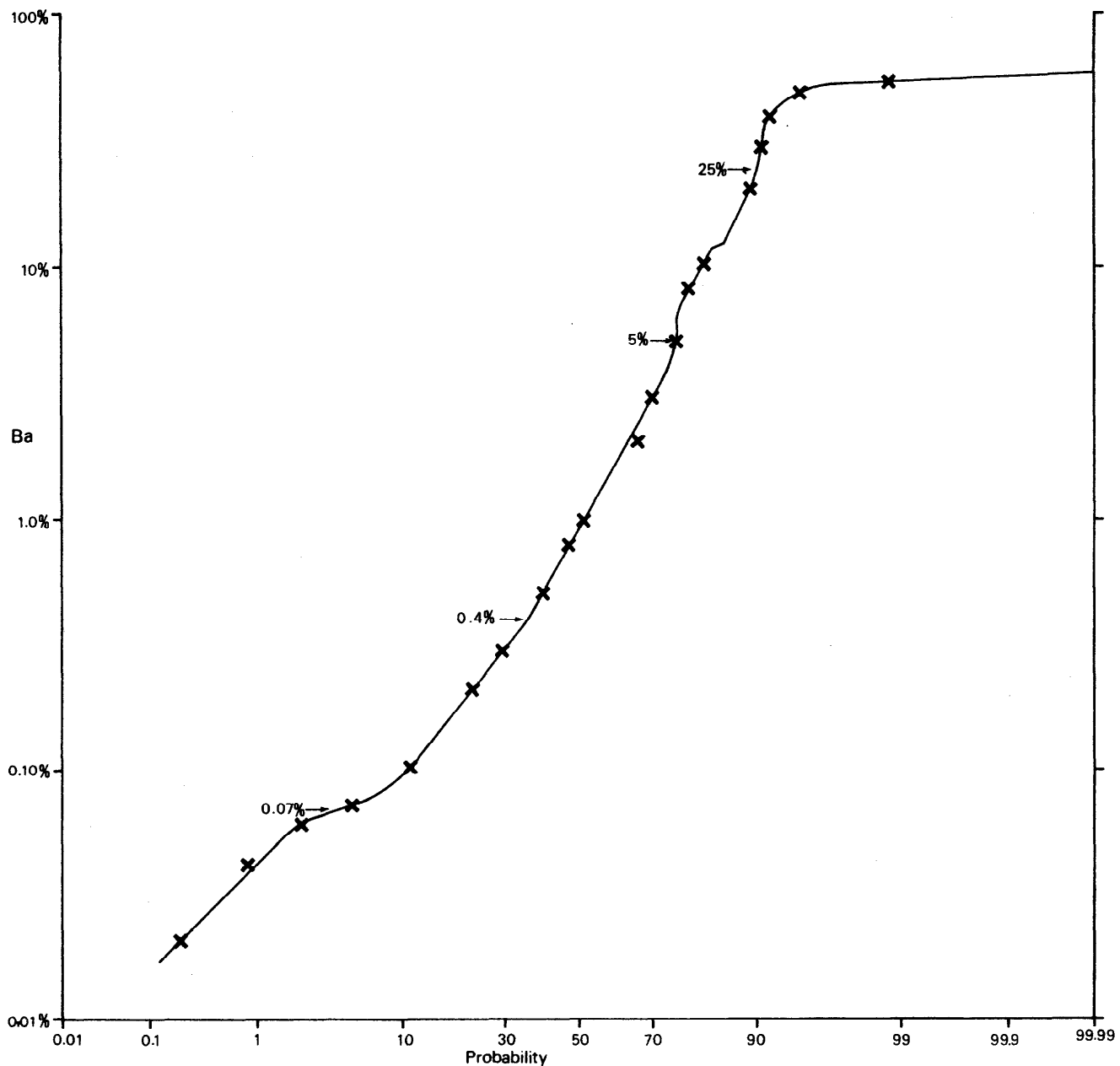


Fig 9 Cumulative frequency distribution of barium in drill core samples

graphitic mica-schist, whereas barium continued at  $>0.15\%$  until sample CYD 558, another 6.17m. Below this sample in the Ben Lawers Schist, barium levels are uniformly low, ranging from 0.04 to 0.10% Ba. Similar barium concentrations are characteristic of the Ben Eagach graphitic schist outside the mineralised zone. The barium mineralisation therefore only coincides approximately with lithostratigraphic boundaries. The calc schist, encountered in BH 11 (A II, T XI) and lithologically indistinguishable from Ben Lawers Schist, is on the other hand clearly differentiated on the grounds of barium content, with levels of between 0.2 and 3.6% Ba (except for one sample CYD 774 of dolomitic quartzite with 0.13% Ba).

Conclusions that can be drawn from the barium frequency distribution are as follows:—

- Baryte-rock forms a distinct population
- Quartz-celsian rock is similarly distinct but there is some gradation to muscovite-hyalophane-schist
- Barium mineralisation at lower levels shows a single population of between 0.07% and 4% Ba and it is suggested that this is the result of a single geochemical process, perhaps relating to the incorporation of barium into clay minerals

- The weaker barium mineralisation is not confined to particular lithologies but barium falls to background levels within a few metres of lithostratigraphic boundaries such as that between the Ben Eagach Schist and Ben Lawers Schist.

Twenty-two elements were determined on samples from BHs 1–5 and nearly complete analyses are available, lacking only  $\text{Na}_2\text{O}$ ,  $\text{H}_2\text{O}$ , and  $\text{CO}_2$  of the routinely determined oxides (A II, T I–V). Fuller conclusions can therefore be drawn from these analyses than from those of samples from BHs 6–11, the cores from which were only analysed for eleven elements (A II, T VI–XI).

Most of the major elements except sulphur show an antipathetic relationship to barium and this is partly the effect of adding to a constant sum (Chayes, 1960) so that bivariate data plots are relatively uninformative. Trivariate plots are more helpful, for example that of Ba,  $\text{Al}_2\text{O}_3$  and  $\text{SiO}_2$  which shows that the samples plot into three main groups: (i) Baryte-rocks along the Ba- $\text{SiO}_2$  side near the Ba apex, (ii) Quartz-celsian rocks in a group clustered along the theoretical celsian- $\text{SiO}_2$  join, and (iii) a group on or just above the  $\text{Al}_2\text{O}_3$ - $\text{SiO}_2$  side and clustering about the average  $\text{Al}_2\text{O}_3/\text{SiO}_2$  ratio (21:79) of shales (Wedepohl,

Table 5 Average partial analyses of the major components of the mineralised zone

	Baryte-rock	Mineralised mica-schist	Quartz-celsian-rock	Carbonate-rock
%				
SiO <sub>2</sub>	6.2	52.8	48.6	18.7
Al <sub>2</sub> O <sub>3</sub>	0.028	15.2	8.7	1.36
Fe <sub>2</sub> O <sub>3</sub> *	0.83	6.75	3.66	8.53
MgO	0.59	4.20	2.68	5.99
CaO	1.50	6.15	3.75	16.42
K <sub>2</sub> O	0.04	5.35	3.20	0.14
MnO	0.006	0.53	0.16	0.83
S <sup>†</sup>	12.5	0.93	2.6	12.9
BaO	57.1	0.98	16.1	8.0
SrO	0.54	0.018	0.11	0.24
ppm				
Cu	40	56	55	188
Pb	1130	750	970	21200
Zn	2350	3060	3130	56500
Ag	4	2	3	31
Number of Analyses	36	24	21	16

\*Total iron as Fe<sub>2</sub>O<sub>3</sub> †total sulphur as S

Elements determined by X-ray fluorescence except for Cu, Pb, Zn and Ag (by atomic absorption spectrophotometry) on core samples from boreholes 1–5 (see Fig. 1).

Analysts – D.J. Bland and M.E. Stuart

1969). There is a clear divide running from the SiO<sub>2</sub> apex between these latter two groups which indicates that there is a limiting Ba/Al ratio below which barium is present in mica and above which barium is dominantly in celsian or hyalophane. Intermediate samples are rare, indicating that there is a difference in conditions of formation between quartz-celsian rock and the mineralised schists.

Cluster analysis (a mathematical method of discerning natural groupings of the sample analyses) was used to provide information on the mean composition of the different rock types within the mineralised zone and also to decide if the lithological groupings coincided with the major element chemical classification. Four clusters of samples were chosen (Table 5) on the basis of stable grouping of samples

of similar lithologies. More clusters than this did not significantly increase the percentage of variance explained and fragmented certain lithologies to produce single number groups. With a lower number of clusters, heterogeneous groups are produced and there is a large variance within each group. The most stable cluster is that of baryte-rock which consists predominantly of baryte and lesser amounts of quartz and carbonate and, as expected has high Ba, S and Sr values. Another stable grouping consists predominantly of mineralised mica-schist (boreholes 1–5 sampled only the mineralised zone) with high concentrations of K, Si, Al and Mg and relatively low S, Ba and Sr reflecting the high pelite content. The other two groups are less stable and tend to fragment if the number of groups is increased.

The third group, with high values of Ca, Mg, Fe, Mn, S, Pb and Zn, and low K and Al, includes samples CYD 30–35 and 70–75 which have the highest carbonate and sulphide contents. The fourth group consists predominantly of quartz-celsian rock with high levels of Si, Al and Ba. The baryte and quartz-celsian rock groups confirm the conclusions reached from the barium frequency distribution. Relative to average black shale (Vine and Tourtelot, 1970), the mineralised mica-schist is strongly enriched by factors of 20–40 in manganese, barium, lead, zinc and silver and slightly enriched, by factors of 2–4, in iron, magnesium, calcium and potassium.

Another statistical method of studying the variation of the chemistry of the mineralised zone is factor analysis which brings out the underlying factors which may control the interelement variation. Four factors explain 84% of the variation of the 22 elements determined on the core from the first five boreholes (A II, T I–V). The first factor has high positive loadings (loading >0.3) of Al, K, Rb, Si, Zr, Nb, Y, U, Ti and Fe and strong negative loadings (<-0.3) of Sr, Ba and S. This is clearly related to the antipathetic variation of pelitic sedimentary material and baryte. Factor two has high loadings of Sb, Pb, Zn, Ag, S and Fe and describes the variation of sulphides. The inclusion of iron in this factor shows that pyrite has a sympathetic relationship to the base metal sulphides. The third factor has strong negative loadings of Mg, Ca, Fe, Mn and Cu coupled with moderate to low positive loadings of Ba (0.44) and Sr (0.22). It clearly expresses the variation of carbonate and its relatively antipathetic relationship with baryte. The strong correlation ( $r=0.553$ ) between Mn and Ca is evidence that Mn is to a large extent present in carbonate (as confirmed by the high Mn content of calcite from BH 4, Table 13) along with some Fe. The presence of copper in this factor is unusual and if the number of factors is increased copper becomes dominant in factor five accompanied by iron, reflecting the variation of pyrite and chalcopyrite. Factor four has strong loadings of Ni and Ti and as will be explained later probably reflects the influx of basic volcanic material into the basin.

The Ni–Ti factor is also exhibited by the samples from boreholes 6–11 and cluster analysis of the 367 samples from these boreholes produces groups similar to those shown by the earlier samples. However, because of the

smaller number of elements, only Ba, Ca, Fe, Mn and Ti of the majors being determined (A II, T VI–XI), several sample groups are combined. For example, quartz-celsian rock is combined with the other high-barium group of baryte-rock. Five clusters are significant and these can be summarised as follows: I – high Ba (baryte-rock and quartz-celsian rock), II – high Pb, Zn, Ag (samples with high base metal sulphides), III – low Ba, Pb, Zn and Ag (background schists), IV – high Ba, Pb and Zn (a small group of three samples with barium and base metals) V – high Ni, Ti, Fe and Ca (metabasic rocks). The last cluster included all those that had been recognised as basic or metabasic rocks such as amphibolites, epidiorites and lamprophyres and also a group of samples not obviously igneous in character. Discriminant analysis, using the easily recognisable metabasic rocks as a training group, produces a clear separation between these metabasic and other rocks with the discriminant function (the mathematical function that separates the two groups) based mainly on Ti and with lesser contributions from Ni, Fe and Ca. A similar conclusion can be reached from the cumulative frequency distribution of titanium (Fig. 10). Three populations can be distinguished: I 0.05–0.3% Ti (28% of the sample population), II 0.3–0.7% Ti (67% of population), and III >0.7% Ti (5% of population). There are no samples between 0.6 and 0.7% Ti and thus little overlap between the upper two populations. The level of 0.7% Ti is significant in that normal sedimentary rocks do not exceed 0.72% Ti (equivalent to 1.2% TiO<sub>2</sub>, Wedepohl, 1969) and the range of normal shales (247 samples) is 0.42–1.13% TiO<sub>2</sub>. Samples with greater than 0.7% Ti include all the undoubted basic rocks such as lamprophyre, amphibolite and epidiorite which have fairly low barium contents (the lamprophyres are slightly higher) accompanied by high Fe, Ca and Ni. However also included in this group are samples CYD 635–639 and 643–644 from BH 10 which are described as calcareous biotite-schist, muscovite-quartz-schist and sericite-quartz-schist (A I, T X). These samples are enriched in barium however, with between 1.8 and 4.2% Ba (A II, T X) and they form part of the mineralised zone, being interbedded with quartz-celsian rock. The high titanium content of these rocks indicates that they are derived from metabasic rocks and this is also supported by their Fe, Ca and Ni contents, but they are significantly

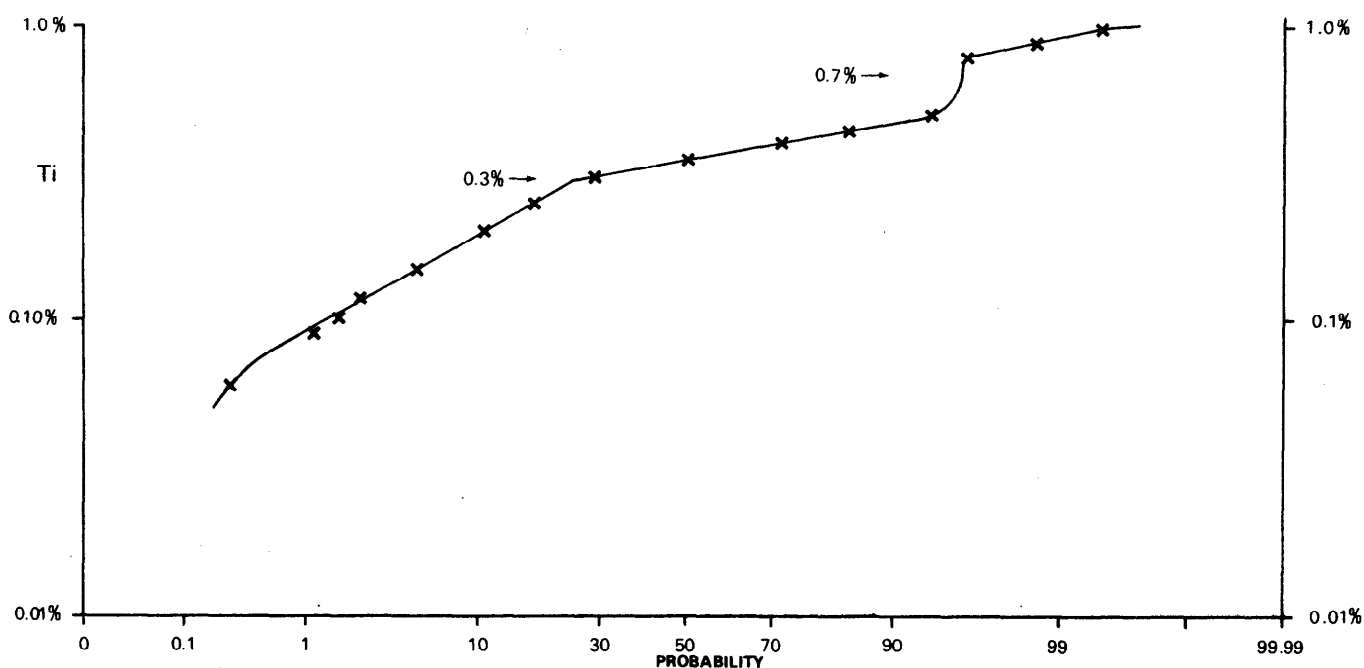


Fig 10 Cumulative frequency distribution of titanium in drill core samples

enriched in barium. From lithological and petrographic descriptions (A I, T X and A III, T X) it is likely that they formed as volcanic tuffs or thin lavas, which were, either metasomatically altered by slightly later hydrothermal or diagenetic solutions, or which scavenged barium from adjacent, still wet sediments.

Other rocks characterised by high titanium, accompanied by Fe, Ca and Ni, are CYD 766, 807 and 831 which are calcareous or garnetiferous biotite schists. Samples CYD 95 and 97 from BH 5 (A II T V) are enriched in titanium and also very high in barium but consist of folded intercalations of biotite-schist in baryte-rock which were aggregated during the sampling. If, as the chemistry suggests, these schists are metabasites then the close association with baryte-rock may be significant.

The recognition of volcanic rocks within the mineralised zone is clearly important in that it provides a possible source for the hydrothermal fluids. More likely, the ascent of the magma through the crust provided a heat source to drive the hydrothermal fluids upwards until they issued onto the sea floor. A similar hypothesis has been advanced for the mineralisation discovered in the Red Sea deeps (Weber-Diefenbach, 1977).

The above statistical treatments of the analytical data ignore the spatial distribution of the boreholes. One possible approach to the question of whether or not mineral zoning is present in the mineralised zone is a study of zinc and lead in a single lithology from the zone. Simple calculations based on core analyses appear to show that in the western sector graphitic schist contains approximately twice as much lead and zinc as the same lithology from the eastern sector.

	Zn ppm	Pb ppm	Cu ppm	Ba %	No. of samples
Western Sector BH's 9, 10, 11	1367	802	53	1.39	28
Eastern Sector BH's 7, 8	704	402	48	1.66	35

However, non-parametric statistical tests (Mann-Whitney U-test and Kruskal-Wallis test) show that there is a 95% probability that the zinc analyses from each sector, for example, are not drawn from the same population as regards central tendency and also that between each borehole in each sector there are significant differences at the 99% level. Much more work is clearly needed therefore to determine whether metal zoning is present and also to find sections of the strike length where base metals may be significantly concentrated.

## VLF MAPPING

### INTRODUCTION

Although the bedded baryte in the Ben Eagach Schist is locally well exposed, there are also broad tracts of drift-covered ground with little or no outcrop. A geophysical means to distinguish the mineralisation was required, to determine the lateral extent of the baryte bands and to investigate the drift-covered areas.

The most obvious method is gravity, which would respond to the  $2 \text{ g cm}^{-3}$  density contrast between baryte and schist. Detailed gravity surveys are slow and costly, however, and not well suited for us in rugged, peaty terrain. Simple calculations show that the effects of overburden thickness variations are of the same order as likely anomalies due to lenticular baryte (Table 6).

**Table 6** Comparison of gravity anomalies resulting from baryte bodies and overburden variations.

Source	Max. anomaly (mgals)
Vertical sheet, 85% baryte, 6 m wide 3 m below surface	0.19
Vertical sheet, 85% baryte, 10m wide 10 m below surface	0.13
Till thickness variations of 5 m	0.18
Till thickness variations of 10 m	0.35
Peat thickness variations of 5 m	0.33

Trial surveys to test the electrical and magnetic properties of the rocks were carried out over a limited area north of Creag an Fhithich. The mineralised zone here is a 50 m thick sequence of baryte-rock, quartz-celsian rock, and muscovite-schist accompanied by a 20 m band of calc schist, lying wholly within the graphitic schist characteristic of the Ben Eagach Formation. It contains sulphide segregations and is separated from the Ben Lawers calc schists to the south by about 100 m of graphitic schist.

The magnetic method was tried because it is rapid, although no susceptibility contrast was expected. In fact, a small magnetic anomaly does occur, near the northern margin of the mineralised band. Three electrical methods were tried despite misgivings caused by the presence of graphite in the Ben Eagach Formation. A gradient array induced polarisation (I.P.) survey gave an anomaly of 20–40 ms over the mineralised zone, probably due to the sulphides, but stronger effects (35–50 ms) were caused by the graphitic rocks to the north of the mineralisation. The gradient array resistivity results showed a contrast between the graphitic schist and the mineralised zone of about 1 to 3, with values for graphitic schist in the range 200–1000 ohm metres, and for the mineralisation of 1000–2500 ohm metres. The most successful method however was very low frequency electromagnetic (VLF–EM). Because of the resistivity contrast the mineralised zone showed up on the VLF–EM profiles as a weak reversed crossover or inflexion which could most clearly be seen by applying the filtering technique described by Fraser.

Following the encouraging results with VLF–EM in the pilot area, coverage was extended over almost the whole of the outcrop of the Ben Eagach Formation along a strike length of more than 8 km from Meall a'Choire (NN 877 572) to Coire an t'Suidhe (NN 797 545) (Fig. 13).

### OUTLINE OF THE VLF–EM METHOD

Powerful military and experimental radio communications transmitters produce signals in the VLF band (15–25 kHz). The magnetic component of these transmissions can be used in prospecting (Patterson and Ronka, 1971). It forms horizontal circular field lines centred on the antenna, propagating outwards. At large distances from the antenna, the magnetic field is effectively uniform over several square kilometers, and at  $90^\circ$  to the station direction.

Fig. 11 shows a thin dyke-like conductor in a more resistive half-space lying in a VLF field. Electric currents flow in the conductor due to induction. The secondary magnetic field produced by the currents flowing in the top of the conductor combines vectorially with the primary field. There is normally a phase difference between primary and secondary fields, causing the resultant vector to rotate in space, so as to describe an ellipse. The Geonics EM 16 instrument used for the present survey measures the tilt and ellipticity of this ellipse, which can be shown to be related to the vertical component of the secondary field. The

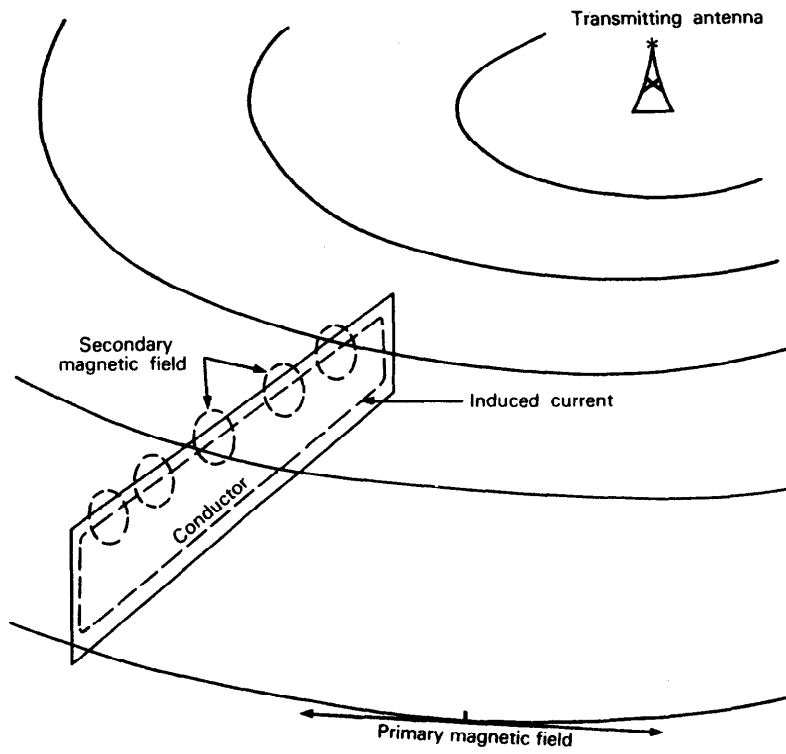


Fig 11 Sketch of magnetic fields around a conductor

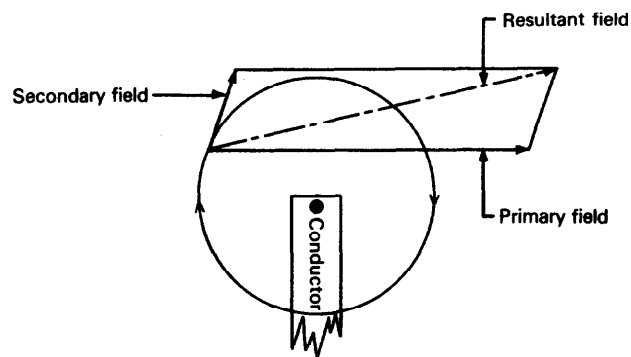
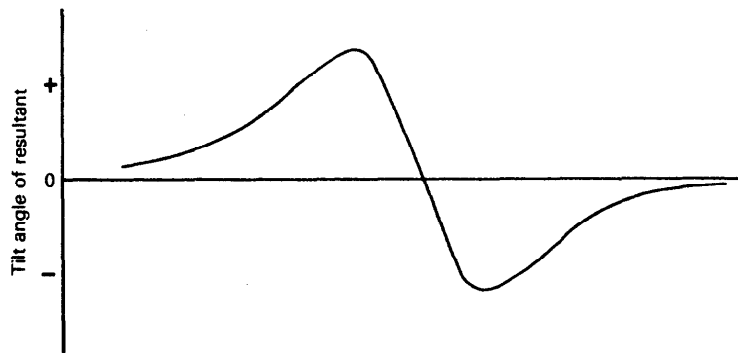


Fig 12 Sketch of magnetic vectors around the conductor in Fig11



tangent of the tilt angle is a good approximation to the in-phase part, and the ellipticity approximates to the out-of-phase part. In the EM 16 both parts are read off scales calibrated directly as percentages of the primary field. A mathematical treatment of the above, and a more detailed account of the EM 16 instrument, are given by Patterson and Ronka (1971).

The form of the anomaly produced by the conductor in Fig. 11 is shown on Fig. 12. Approaching the conductor, the in-phase component rises to a maximum, then falls steeply to a minimum, changing sign immediately over the conductor itself. A vertical boundary between rocks of different conductivities, which is the approximate general case at Aberfeldy, gives an anomaly which is simply half that over a narrow conductor; that is a maximum or minimum over the boundary with its steeper slope on the side of the more conductive rocks (Telford and others, 1977).

#### FILTERING VLF-EM DATA

The ideal conditions shown in Figs. 11–12 rarely occur in nature. The primary field is usually distorted by topography or broad geological effects, and it becomes necessary to separate local effects from regional ones. This can be done crudely by eye, but a better method is to calculate the slope of the in-phase component profile (Whittles, 1969). An improvement by Fraser (1969) effectively calculates the slope between adjacent averaged pairs of stations, providing some smoothing as well as the measure of slope. The Fraser filter is usually calculated to give maxima over zero-crossings due to conductors, but for the present survey was used in the form:

$$F_{2,3} = (M_4 + M_3) - (M_2 + M_1)$$

where  $M_1$  . . .  $M_4$  are the in-phase readings of stations 1 . . . 4, and  $F_{2,3}$  is plotted midway between stations 2 and 3. This gives positive F values over reverse-crossovers. Its simplicity makes the Fraser filter well suited to field use.

#### SURVEY METHODS

The area of the Ben Eagach Schist north of Aberfeldy is well suited to VLF-EM survey, being open moorland, with a few fences as the only artificial conductors present. Over most of the area slopes are relatively gentle, although locally steep topography, such as the south slope of Ben Eagach, gives both positioning problems and likely topographic distortion of the VLF primary field. For the extension of the original survey, a line spacing of 30 m was used. Further west, a spacing of 60 m was adopted for reconnaissance purposes, with intermediate lines in areas of interest or doubt, while over the steep topography and good exposure of Farragon Hill, a traverse spacing of 90 m was considered adequate. Readings were taken at 10 m intervals along the lines. The VLF station at Culter, Maine was used (NAA 17.8 kHz).

The baseline and, where necessary, additional parallel sub-base lines, were laid out by theodolite, except over Farragon Hill; where an approximate base line was laid using ranging poles and tape. Traverse lines were laid by tape and compass. Over Farragon Hill, the positions of the lines were fixed with reference to the 1:10000 O.S. map.

Data were reduced and plotted in the field, as far as possible. For consistency with the pilot survey the Fraser filter was calculated with the opposite sign to that used conventionally, in order to give a positive anomaly over the mineralised zone.

#### RESULTS AND INTERPRETATION

The data were plotted as profiles and as contour maps of the Fraser-filtered real component readings, at 1:2000 scale. These maps are available as supplementary illustrations (see page 1).

An empirical approach to interpretation was adopted. Comparison of geophysical and geological maps in areas of good exposure allowed interpretative criteria to be established. These criteria were then used to produce interpretations in areas of drift cover, from VLF-EM evidence alone.

As shown by the pilot study, reverse crossovers or inflexions, and therefore Fraser filter highs, indicate resistive rocks. Southern margins of resistive zones are shown by in-phase minima, and of conductive zones by in-phase maxima. The slope of the in-phase component profile is generally steeper on the side of the more conductive unit. This is in agreement with Telford and others (1977) who investigated the theoretical and practical VLF-EM response over vertical conductivity boundaries. Table 7 gives the relative resistivities of rocks in the Aberfeldy survey area.

**Table 7. Resistivities of rocks in Aberfeldy survey area**

Rock type	Resistivity <sup>1</sup> (ohm metres)
Overburden	150–300
Graphitic schist	200–1000
Mineralised zone <sup>2</sup>	1000–2500
Calc schist	1500

Notes <sup>1</sup>From pilot studies (Marsden, 1977); Schlumberger array probes for the present survey; and previous work in the L. Tay area (Smith and others, 1977) <sup>2</sup>Including massive baryte, quartz-celsian rock, muscovite-schist and calc schist.

The simplest case is shown in Fig. 14. As predicted, the greatest positive and negative in-phase component values occur over the margins of the Ben Eagach Schist and gradients are steepest on the more conductive side of the boundary. An unknown thickness of peat and till obscuring the northern margin broadens and flattens the anomaly, making precise identification of the boundary difficult. Its inferred positions from geological and VLF-EM data differ by about 15 m. Positive Fraser filter values in the centre of the Ben Eagach Schist outcrop have tentatively been ascribed to a zone of higher resistivity within the graphitic rocks. This interpretation is not really justified from this single profile, but the feature is stronger on adjacent lines, and interpretation more certain.

Detailed discussions of the VLF-EM results and interpretations have been included in the integrated reports on the target areas, pp 33 to 45. A summary of the geophysical interpretation is presented as a map in Fig. 15.

#### CONCLUSIONS

The VLF-EM method has shown its value as a rapid reconnaissance tool. In this case the problem was an unusual one in geophysical prospecting, namely a resistive target in a conducting host rock. The method was able to identify a number of resistive zones within the graphitic schist as targets for further investigation by geochemical surveys and drilling. The survey also aided geological mapping in areas of poor exposure by indicating the margins of the conductive schists as well as the location of several faults.

Four main problems were encountered. The method could not distinguish baryte from other resistive rocks, and its resolution was insufficient to allow interpretation in areas of complex local geology. Resistivity variations within the graphitic schist, probably due to variations in graphitic

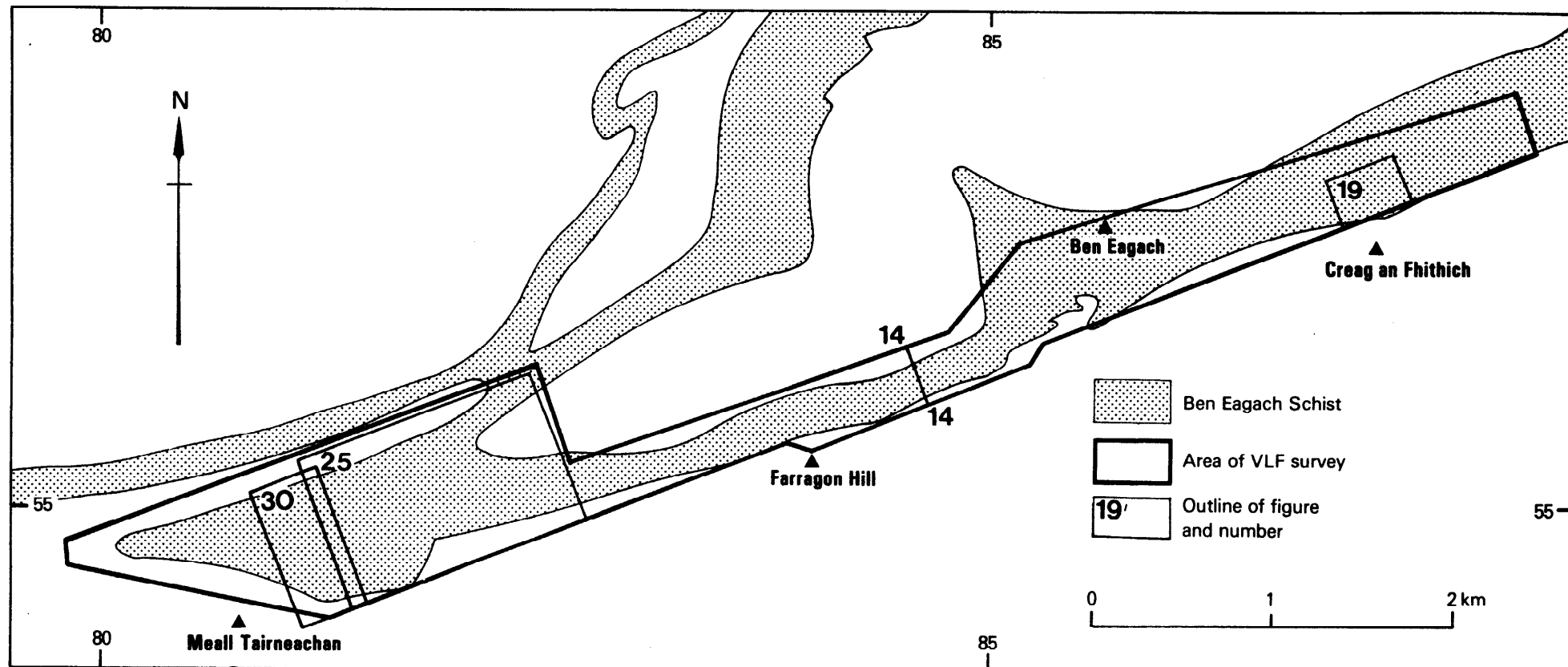


Fig 13 Sketch map showing area of VLF-EM survey near Aberfeldy and positions of profile Fig 14 and survey areas Figs 19, 25 and 30

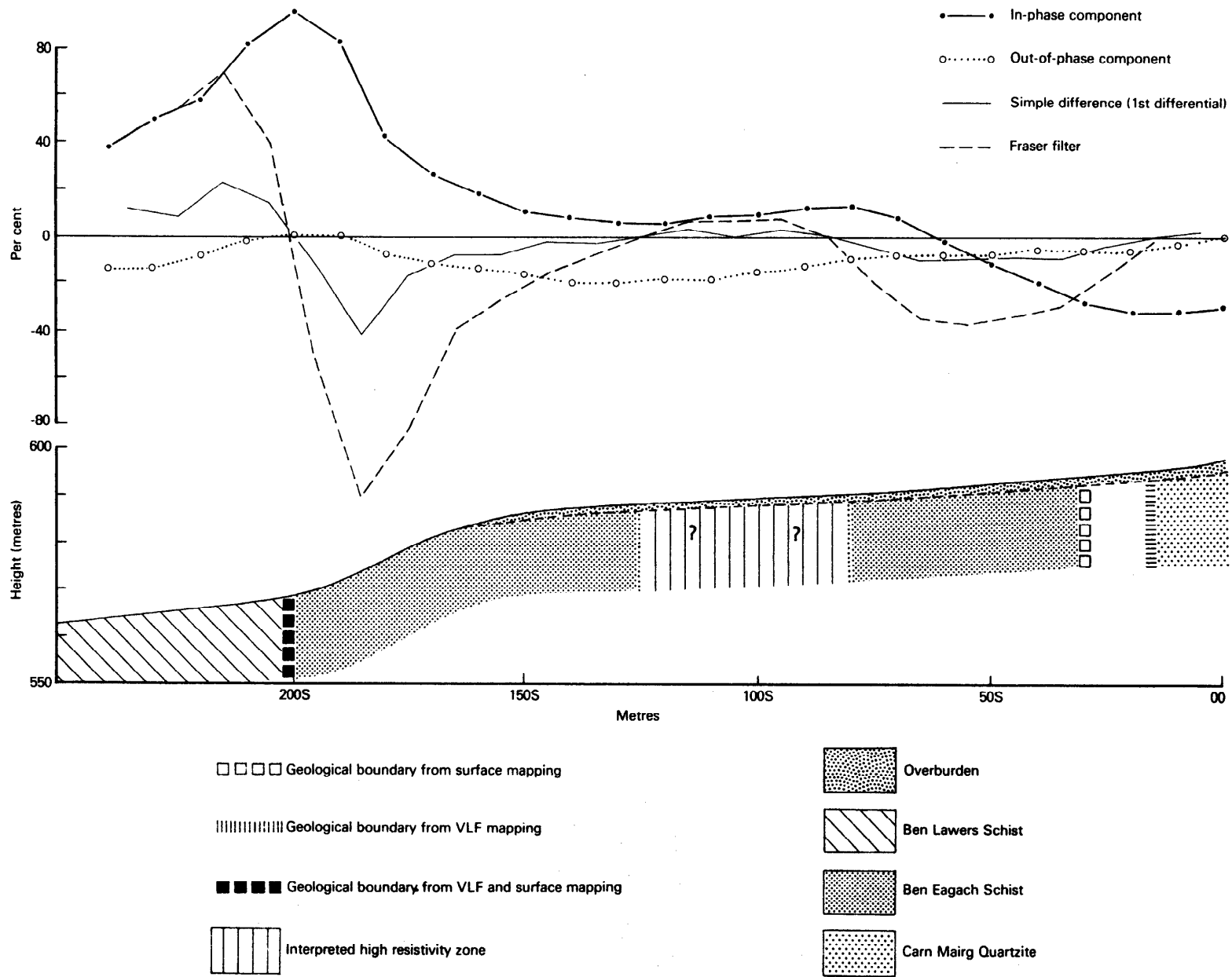


Fig 14 Interpretation of VLF-EM profile across the Ben Eagach Schist, east side of Farragon Hill (see Fig 13)

**Table 8** High resistivity zones worthy of investigation

Target	Borehole		
	IGS grid ref	Azimuth	Inclination
1. Western sector : northern most near-marginal anomaly. Quartz-celsian rock has been noted in stream exposure on this anomaly, which may represent the mineralised zone on the northern limb of the Creag na h-Iolaire anticline.	6060W 430N	340°	55°
2. Western sector : second most northerly marginal anomaly. Quartz-celsian rock noted in stream.	6060W 350N	340°	55°
3. Western sector : anomaly east of BH 3. Could be mineralised zone similar to that at BH 5/7 in eastern sector, or small fold nose of calc schist.	4050W 220S	340°	55°
4. Eastern sector : anomaly north of BH 5/7. An anomalous soil sample occurs over this anomaly, which is otherwise unexplained.	210W 130N	160°	55°

content, are often gradual and make interpretation of the data difficult. Finally, variations in overburden thickness may produce anomalies, although these effects were ignored in interpreting the present survey.

Beyond any programme to assess the known mineralised zones, some attempt should be made to investigate the other linear, high-resistivity zones within the Ben Eagach Schist. Since most occur where exposure is poor or non-existent, drilling or at least deep overburden geochemical sampling, will be necessary. Alternatively, a gravity survey could be tried, subject to the reservations expressed above. The most promising targets, and suggested boreholes, are listed in Table 8.

## MINERALOGY

### INTRODUCTION

Mineralogical investigations have been concerned with hand specimens selected from drill-core and surface outcrops. Forty-nine outcrop specimens were examined in 1976/7 by microscopic investigation of polished thin sections supported by X-ray diffractometry and electron microprobe analysis. In 1978 geological logging of BHs 1 to 5 was supported by examination of polished thin sections. Specimens from BHs 7 to 11 were examined later, together with further outcrop specimens, the methods employed again including XRD and microprobe analysis.

**Table 9** Minerals identified in the Ben Eagach Schist mineralised zone

Silicates	Oxides
QUARTZ	Magnetite
CELSIAN	Hematite
Hyalophane	Rutile
Cymrite	Ilmenite
Albite	Sulphates
K-feldspar	BARYTE
Hornblende	Sulphides
MUSCOVITE	PYRITE
Ba-MUSCOVITE	SPHALERITE
Biotite	GALENA
Fuchsite	PYRRHOTINE
Chlorite	Chalcopyrite
Illite	Covellite
Halloysite	Others
Clay (undifferentiated)	"GRAPHITE" (amorphous)
Almandine	Goethite
Tourmaline	Limonite
Sphene	Apatite
Clinozoisite	
Zircon	
Carbonates	
DOLOMITE	
CALCITE	
Cerussite	

Note: Major minerals in capitals.

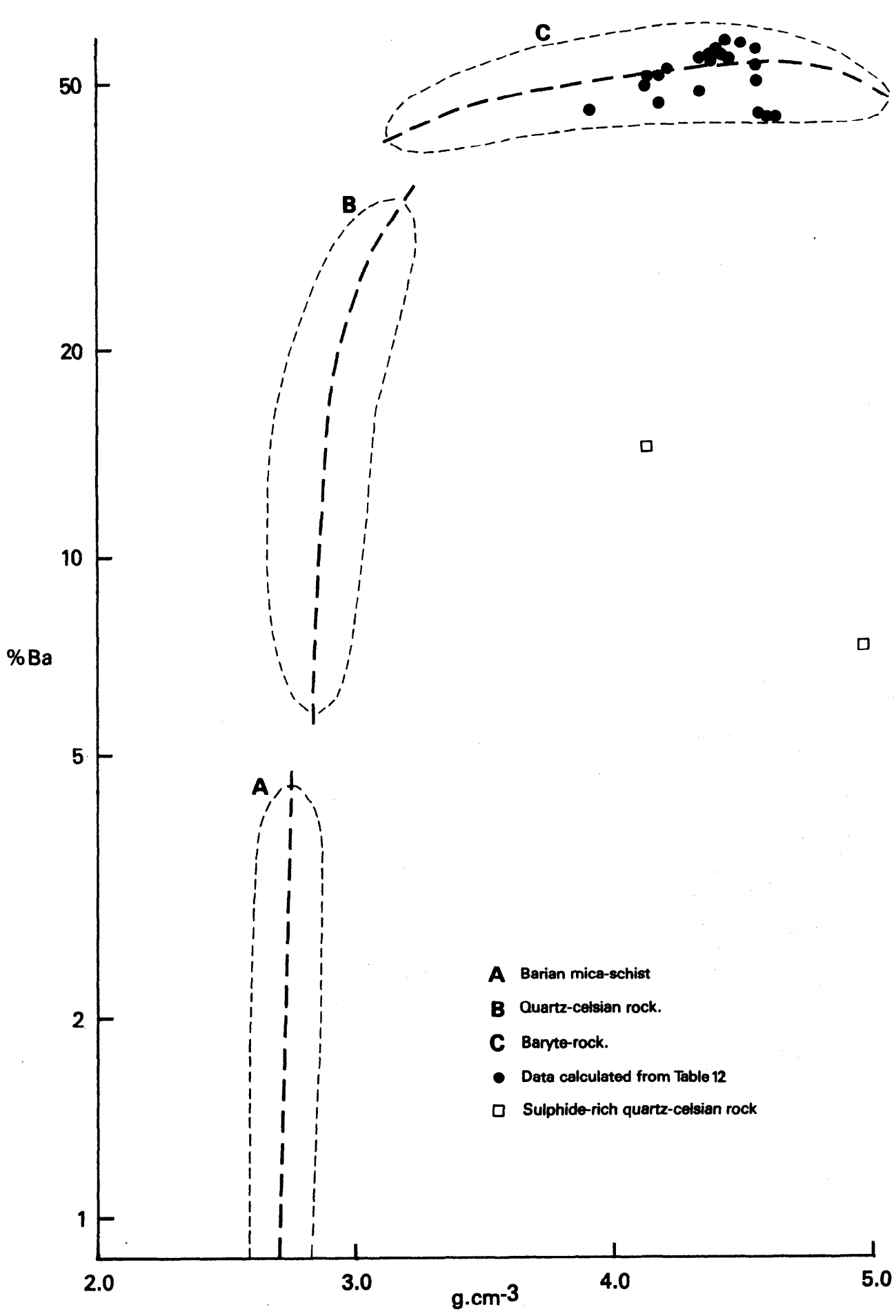


Fig.16 Plot of barium content against specific gravity for samples of borehole core from the mineralised zone near Aberfeldy.

**Table 10** Electron microprobe analyses of celsian and hyalophane (Analysts: J.A.T. Smellie, nos. 1 and 2; N.J. Fortey nos. 3 and 4; B. Beddoe-Stephens, no. 5 to 8).

Wt%	Celsian				Hyalophane			
	1	2	3	4	5	6	7	8
SiO <sub>2</sub>	37.3	34.7	31.8	31.1	32.6	33.2	33.3	53.9
TiO <sub>2</sub>	nd	0.08				nd	nd	0.11
Al <sub>2</sub> O <sub>3</sub>	24.5	26.0	27.7	28.4	27.3	27.1	26.8	21.0
Fe <sub>2</sub> O <sub>3</sub> *	0.03	0.03	0.28	0.30		nd	nd	0.03
MgO	0.01	nd	nd	nd		nd	nd	nd
CaO	nd	nd	nd	nd		nd	nd	0.02
BaO	35.8	36.5	39.8	39.9	39.4	38.3	38.2	13.6
Na <sub>2</sub> O	0.13	nd	0.08	nd	0.10	0.09	0.19	1.43
K <sub>2</sub> O	0.62	1.11	0.31	0.24	0.33	0.57	0.65	9.11
Total	98.39	98.42	99.97	99.94	99.73	99.26	99.14	99.18

Atomic Proportions (32 oxygens)

Si	9.01	8.51	7.90	7.74	8.07	8.19	8.23	10.9
Ti	0.00	0.02				0.00	0.00	0.02
Al	6.97	7.51	8.11	8.33	7.97	7.88	7.80	5.02
Fe	0.01	0.01	0.05	0.06		0.00	0.00	0.01
Mg	0.00	0.00	0.00	0.00		0.00	0.00	0.00
Ca	0.00	0.00	0.00	0.00		0.00	0.00	0.00
Ba	3.39	3.51	3.88	3.89	3.82	3.70	3.70	1.08
Na	0.06	0.00	0.04	0.00	0.05	0.04	0.09	0.56
K	0.19	0.35	0.10	0.08	0.10	0.18	0.21	2.36
X	3.65	3.87	4.07	4.03	3.97	3.92	4.00	4.01
Y	15.98	16.04	16.01	16.07	16.04	16.07	16.03	15.94
X+Y	19.63	19.91	20.08	20.10	20.01	19.19	20.03	19.91

\*Total Fe expressed as Fe<sub>2</sub>O<sub>3</sub>

Analysis	Specimen	PTS No.	Analysis	Specimen	PTS No.
1	CZR 3909 B	2890	5	BH 2 7.5 m	3896
2	CZR 3909 B	2890	6	BH 7 81.6 m	4314
3	CZR 3552 E	2473	7	BH 11 26.8 m	4691
4	CZR 3573 C	2477	8	BH 7 40.8 m	4309

Specific gravities of rocks (Fig. 16) were determined rapidly by use of a simple spring balance using specimens weighing c. 120 g. For BH 4 carbonates were examined by staining core specimens with Alizarin-Red dissolved in dilute HCl solution.

Table 9 lists the total mineral assemblage observed to date. This is probably incomplete. For instance, it is reasonable to suspect the presence of siderite and witherite though neither has been observed. Similarly, although no discrete manganous mineral has been observed during this investigation, Mn-enriched sphalerite and calcite have been noted and Sturt (1961) reported pyrolusite from the Ben Eagach area.

#### BARIUM FIELDSPARS

The abundance and textural variety of celsian in the mineralised zone is described in the following section. Microprobe data indicate that in most cases the mineral approaches pure celsian (Ba [Si<sub>2</sub>Al<sub>2</sub>O<sub>8</sub>]) in composition (Table 10). Potassium, though only a minor constituent, occurs in excess over sodium, and calcium is no more than a trace constituent. Substitution of K for Ba is a major source of variation in its composition, and is accompanied by

substitution of Si for Al.

In thin section, celsian crystals frequently show uniform extinction. Lamellar twinning is rare and normal cleavage inconspicuous. Coarse crystals, especially in celsian-rich bands, may exhibit a close-spaced, parallel, "ghost" cleavage derived from a laminar precursor of the present mineral. Textural evidence indicates that some celsian grew by replacement of muscovite. However, the presence of platy crystals of cymrite (BaAl<sub>2</sub>Si<sub>2</sub>O<sub>8</sub>.H<sub>2</sub>O) in certain rocks indicates that this mineral may have been the immediate precursor of celsian in many cases. Where celsian exhibits a massive, granular texture a platy precursor is unlikely, and its genesis may have involved direct replacement of pre-existing barium-fieldspar.

Compositional zoning is frequently absent or very restricted in celsian crystals. However, in a significant number of examples zoning of three structural types, each involving relatively potassic celsian, is present. In the most common, sets of fine oscillatory zones are present (e.g. BH 8, 143.6 m; A III, T VII). The second type involves development, as rims and overgrowths, of potassic celsian on normal celsian crystals, as in the case of outcrop specimen S64488 (NGR 8585 5662; A III, T XI) in which such zones occur both as incomplete rims intergrown with "pure"

**Table 11** Electron microprobe analyses of barium muscovite  
(Analyst: B. Beddoe-Stephens)

Wt%	1	2	3	4	5	6
SiO <sub>2</sub>	45.0	45.6	45.5	46.6	43.1	43.0
TiO <sub>2</sub>	0.99	0.97	1.74	1.69	1.16	1.13
Al <sub>2</sub> O <sub>3</sub>	30.8	30.9	29.5	29.3	32.0	32.0
Fe <sub>2</sub> O <sub>3</sub> *	1.05	1.33	0.71	0.61	0.33	0.38
MgO	1.94	2.08	3.80	3.58	2.27	2.43
CaO	nd	0.02	nd	nd	nd	0.01
BaO	3.94	4.03	6.40	5.96	8.17	8.25
Na <sub>2</sub> O	0.45	0.45	0.15	0.16	0.45	0.44
K <sub>2</sub> O	9.25	9.24	8.60	8.78	7.59	7.43
Total <sup>1</sup>	93.42	94.62	96.40	96.68	95.07	95.07

Atomic proportions (22 oxygens)

Si	6.27	6.28	6.24	6.34	6.05	6.04
Al <sup>iv</sup>	1.73	1.72	1.76	1.66	1.95	1.96
Z	8.00	8.00	8.00	8.00	8.00	8.00
Al <sup>vi</sup>	3.33	3.29	3.01	3.04	3.34	3.33
Ti	0.10	0.10	0.18	0.17	0.12	0.12
Fe	0.11	0.14	0.07	0.06	0.04	0.04
Mg	0.40	0.43	0.78	0.73	0.48	0.51
Y	3.94	3.96	4.04	4.00	3.98	4.00
Ca	0.00	0.00	0.00	0.00	0.00	0.00
Ba	0.22	0.22	0.34	0.32	0.45	0.45
Na	0.12	0.12	0.04	0.04	0.12	0.12
K	1.64	1.62	1.51	1.52	1.36	1.33
X	1.98	1.96	1.89	1.88	1.93	1.90

\*Total Fe expressed as Fe<sub>2</sub>O<sub>3</sub>. <sup>1</sup> - H<sub>2</sub>O may form 5% by weight.

Analysis	Specimen	PTS No.
1	BH 7 36.7 m	4308
2	BH 7 36.7 m	4308
3	BH 7 81.6 m	4314
4	BH 7 81.6 m	4314
5	BH 8 135.0 m	4178
6	BH 8 135.0 m	4178

celsian and as overgrowths which replaced muscovite adjacent to celsian crystals. In the third type, potassic celsian has replaced "pure" celsian to the extent that the latter is reduced to irregular relic patches in optical continuity (e.g. BH 3, 23.12 m; A III, T III).

Hyalophane (Cn <30%) is a minor constituent of the mineralised zone, occurring as discrete porphyroblasts in a few specimens of micaceous schist (e.g. BH 7, 40.8 m; A III, T VI).

#### CYMRITE

The hydrous barium silicate cymrite was identified during X-ray diffractometric study of a specimen from BH 11, 26.8 m (A III, T X). Although its precise distribution in the mineralised zone is not known, it is evidently a minor constituent probably confined to laminated quartz-celsian rocks. It is believed to have the composition BaAl<sub>2</sub>Si<sub>2</sub>O<sub>8</sub>·H<sub>2</sub>O (Essene, 1967), but in the present study has only been

identified by X-ray powder photography (cf. data given by Runnells, 1964).

#### MICAS

Muscovite is the major constituent of the graphitic schists and of pale schists usually associated with the more strongly mineralised rocks. It is a common, though minor constituent of quartz-celsian rock and baryte-rock. Within the mineralised zone the muscovite is frequently a barian variety containing up to 8.3% BaO (Table 11) and also somewhat enriched in TiO<sub>2</sub>. Similar material from Franklin, New Jersey (Heinrich and Levinson, 1955) has a 1M structure, but the most barium-rich muscovite observed from the Ben Eagach area has the normal muscovite 2M<sub>1</sub> crystal structure (D Atkin, *pers. comm.*). The density of the Ben Eagach mineral is ~3.01 g. cm<sup>-3</sup> (measured with a Berman balance).

Fuschite, the chromian muscovite, is a minor constitu-

**Table 12** Modal analyses of thin sections of baryte-rich rocks from Boreholes 1, 2, 4 and 5 [In all cases the number of points is between 1000 and 1100 (analyst B.R.H. Skilton)]

Borehole No.	1	1	1	1	1	1	1	1	2	2	2	2	2	2	2	2	4	4	5	5
Inclined depth, m.	13.2	14.6	15.3	16.8	17.2	18.6	25.2	25.9	1.7	4.3	8.2	10.5	10.5	10.7	11.3	13.3	16.4	17.0	6.6	23.2
PTS No.	4081	4082	4083	4084	4085	4086	4089	4090	3892	3893	3897	3900	3899	3898	3901	3902	3914	3915	4137	4142
Baryte	87.0	77.3	77.0	91.4	73.1	79.1	67.1	84.0	96.7	91.9	95.3	80.7	79.9	88.2	79.7	89.0	92.3	89.7	94.5	77.9
Opaque + sphalerite	12.2	22.5	22.9	3.2	5.2	7.8	0.8	<0.1	1.1	1.7	4.1	1.0	0.5	3.2	8.1	1.9	0.6	9.7	1.1	7.6
Pyrite <sup>1</sup>	11.0	14.4	20.8	0.5	4.7	6.8	0.3	<0.1	0.8	0.8	4.0	0.1	0.1	0.2	4.2	0.9	0.5	9.3	0.8	4.2
Sphalerite <sup>1</sup>	1.0	8.0	2.0	—	0.3	0.4	—	—	0.2	—	0.1	—	—	—	—	—	<0.1	0.2	0.2	0.2
Others <sup>1</sup>	0.2	0.1	0.1	2.6*	0.2	0.6	0.5*	—	0.1	0.9*	0.1	0.9*	0.4*	3.0*	3.9*	1.0*	0.1	0.2	0.1	0.2
Quartz	<0.1	<0.1	<0.1	4.7	4.0	3.4	29.4	10.2	1.3	3.8	0.1	18.2	19.4	8.5	9.3	8.0	7.0	0.6	3.2	10.7
Dolomite	<0.1	<0.1	<0.1	0.2	16.7	8.4	2.7	5.2	0.4	0.2	<0.1	0.1	<0.1	<0.1	2.2	<0.1	<0.1	<0.1	<0.1	2.5
Accessories	0.8	0.3	0.1	0.5	1.0	1.3	<0.1	0.6	0.5	2.5	0.5	<0.1	0.2	0.2	0.7	1.1	0.2	<0.1	1.1	1.2 <sup>x</sup>
Calculated s.g.(g.cm <sup>-3</sup> )	4.55	4.55	4.60	4.41	4.17	4.33	3.92	4.22	4.47	4.40	4.52	4.17	4.14	4.36	4.32	4.34	4.38	4.54	4.42	4.13
Estimated Ba content	49.32	43.82	43.18	53.46	45.22	47.12	44.15	51.34	55.80	53.87	54.38	49.92	49.78	52.18	47.59	52.90	54.36	50.96	55.15	48.65

<sup>1</sup> Subdivision of the opaques and sphalerite by visual estimation giving approximate contents.

\* Magnetite is the principal "other" opaque phase present.

<sup>x</sup> Celsian is a prominent minor constituent (BH 5, PTS. 4143).

Calculated specific gravities are based upon the following mineral densities (taken from Deare, Howie and Zussman, 1962) : baryte 4.5 g.cm<sup>-3</sup>; pyrite 5.0 g.cm<sup>-3</sup>; sphalerite 4.1 g.cm<sup>-3</sup>; galena 7.5 g.cm<sup>-3</sup>; magnetite 5.1 g.cm<sup>-3</sup>; quartz 2.65 g.cm<sup>-3</sup>; dolomite 2.88 g.cm<sup>-3</sup>; accessories (mostly micas) 2.77 g.cm<sup>-3</sup>; celsian 3.25 g.cm<sup>-3</sup>.

Porosity is not taken into account, but in all cases is very low.

Barium contents were estimated by the following formula:—

$$\text{Wt\%Ba} = (\text{Wt\%Ba in baryte}) \times \frac{\text{modal \% baryte} \times \text{density of baryte}}{(\text{calculated whole-rock s.g.} \times 100)}$$

The (Wt%Ba in baryte) term is given the value 57.32%, corresponding to a value of 64% BaO which is typical of baryte analyses given by Deer, Howie and Zussman (1962).



ent of non-graphitic muscovite-schist, quartz-celsian rock and baryte-rock. In thin section the crystals are normally pleochroic from pale green ( $\alpha$ ) to strong emerald-green ( $\beta$  and  $\gamma$ ). In some cases the mineral has a brown-green colour suggesting compositions transitional with biotite. In baryte-rock the occurrence of fuchsite is associated with that of magnetite (A III).

Biotite is a minor constituent of quartz-celsian rock and baryte-rock. It also occurs in the chloritic metabasites encountered in BH 7 (A III, T VI) and is common in rocks of the Ben Lawers Schist Formation (which also contain muscovite).

#### CHLORITE AND CLAY MINERALS

Chlorite is a minor but widespread constituent of the rocks examined. It occurs in several lithological environments and different varieties appear to be involved in each case. Most commonly, pale green chlorite occurs as a retrograde constituent of pale muscovite-schist, metabasite and rocks of the Ben Lawers Schist Formation. Strongly coloured green to brown "chlorite" forms interstitial pockets in baryte-rock (e.g. BH 2, 10.6m; A III, T VIII). Fibro-radial patches of pale chlorite occur in coarse carbonate areas in crudely banded dolomite-quartz rock (e.g. BH 8, 142.6m; A III, T VII). Chlorite replaces celsian in a few specimens (e.g. BH 3, 22.2m; A III, T III). As yet no detailed investigation of these minerals has been carried out.

Illite occurs as an alteration product of possible lithic fragments in the chloritic metabasite in BH 9 (e.g. 42.8m; A III, T VIII). Limonitic fractures and leached zones observed in borehole specimens sometimes contain the strongly fluorescent (bluish-white or yellow light emitted in response to short-wavelength UV light) clay mineral halloysite (XRD identification).

#### CARBONATES

Carbonate minerals are present in all specimens examined save for certain baryte-rocks and quartz-rich rocks. Specimens of the Ben Lawers Schist are abundantly calcareous as are the chloritic metabasites in BH 9. In the Ben Eagach Schist, including the mineralised zone, dolomite is frequently the dominant carbonate. No other carbonates have been located to date, save for cerussite present in weathered rocks near the site of BH 4.

Within the mineralised zone dolomite is common in most lithologies. Dolomite in graphitic schist from BH 8 (135.0m; A III, T VII) was examined qualitatively by microprobe and proved to be devoid of Ba and Sr while containing minor Fe. Dolomite is abundant in the banded celsian-bearing rocks, often forming discrete bands which

may be of considerable thickness as in BH 1 (A I, T I). In the baryte-rocks dolomite is a frequent minor constituent (see Table 12 and A I).

Calcite also occurs in many lithologies in the mineralised zone. In the baryte-rock intersection in BH 3, in which overlying celsian-bearing rocks are abundantly dolomitic, calcite is the sole carbonate present. In BH 4 (A I, T IV) occurs the "limestone" in which calcite contains approximately 9% MnO and 0.8% SrO (Table 13). This rock is rich in bands of sulphides and has given the highest Zn-Pb levels observed (A II, T IV).

Drill-core specimens from boreholes 3 and 4 were tested for witherite by staining with rhodizonic acid solution (Hutchinson, 1974) but with negative results.

#### BARYTE

Baryte occurs as coarse, polygonal, colourless crystals. Bladed baryte was observed only rarely in late cross-cutting veinlets (e.g. BH 1, 22.25m; A I, T I).

The normal polygonal crystals are invariably free from solid inclusions except for isolated grains 0.1 mm or more in diameter of quartz and opaque minerals. Minute fluid inclusions are, however, common, and often occur in discrete trails which run from grain to grain across the mosaic fabrics of the rocks in question.

Table 14 gives XRF results of partial analyses of baryte concentrates prepared from BH 2 material (see Appendix V). Allowing that the greater part of the  $\text{SiO}_2$ , MgO and CaO present occurs in quartz and dolomite impurities, it is clear that baryte in these specimens is a near-pure mineral with low Sr, Si and Ca contents.

#### IRON SULPHIDES

Sulphide minerals are important constituents of all the barian rocks, and occur in minor amounts in the barium-enriched graphitic and non-graphitic schists. Pyrite is the major sulphide mineral of the mineralised zone. Its principal mode of occurrence is as discrete, subrounded to euhedral grains disseminated and segregated into discrete bands. Thin massive bands of granular pyrite occur at a few points (e.g. BH 7, 55.8m; A III, T VI).

Pyrite is commonly accompanied by subordinate amounts of sphalerite and galena, and by traces of chalcopyrite. It coexists with pyrrhotine in graphitic schist and to a lesser extent in quartz-celsian rock. Pyrite grains often accompany magnetite in baryte-rock. In this situation other sulphides are usually absent and pyrite is subordinate to magnetite. Another mode of occurrence is that of grains and elongate patches of pyrite in calcareous cross-cutting hair veinlets seen in most of the boreholes.

Table 13 Semi-quantitative estimates of major elements in calcite from Borehole 4, 21.20 m by electron microprobe (Analyst: B. Beddoe-Stephens)

	Wt%			
CaO	43.0	44.9	45.7	42.7
MgO	1.61	1.34	1.50	1.25
MnO	9.40	9.39	9.93	9.34
FeO	2.00	2.06	1.52	1.95
SrO	0.74	0.64	0.79	0.82

Note: Owing to the high  $\text{CO}_2$ -content, ZAF corrections could not be made satisfactorily. The results given are raw measurements corrected only for background X-rays, dead-time and machine drift.

Table 14 Partial analyses of baryte concentrates by XRF (Analyst: D.J. Bland)

Sample	Sr	Fe <sub>2</sub> O <sub>3</sub>	CaO	SiO <sub>2</sub>	MgO
CYD 2	0.68	<0.1	0.83	5.9	0.4
CYD 3	0.50	<0.1	0.68	10.7	0.4
CYD 6	0.29	<0.1	0.42	4.9	0.4
CYD 7	0.51	<0.1	0.58	11.6	0.4
CYD 8	0.57	<0.1	0.51	7.8	0.2
CYD 9	0.46	<0.1	0.47	13.5	0.2
CYD 10	0.47	<0.1	0.50	10.6	0.1
A	tr	0.32	0.38	2.01	nd
B	2.79	nd	0.16	0.02	tr

A and B – baryte analyses from Deer, Howie and Zussman (1962, p. 189, analyses 1 and 4)

CYD 2 – BH 2, 1.85 – 3.56 m	CYD 8 – BH 2, 9.73 – 10.93 m
CYD 3 – BH 2, 3.56 – 5.75 m	CYD 9 – BH 2, 10.93 – 12.10 m
CYD 6 – BH 2, 7.68 – 8.47 m	CYD 10 – BH 2, 12.10 – 13.33 m
CYD 7 – BH 2, 8.47 – 9.73 m	

Table 15 Electron microprobe analyses of sphalerite (Analyst: B. Beddoe-Stephens)

	1	2	3	4	5	6
	Wt.%					
Zn	64.54	64.89	65.19	65.05	60.17	59.85
Fe	0.02	0.02	2.33	2.33	6.28	6.95
Mn	1.53	1.51	0.03	0.05	0.40	0.27
S	32.74	32.27	33.03	32.87	32.10	31.99
Sb <sup>1</sup>	0.02	0.02	nd	nd	nd	nd
Cu <sup>2</sup>	nd	nd	nd	nd	0.04	0.04
Total	98.85	98.81	100.58	100.30	99.99	99.10
	Atomic proportions					
Zn	0.969	0.978	0.964	0.965	0.901	0.896
Fe	0.000	0.000	0.040	0.040	0.110	0.122
Mn	0.027	0.027	0.001	0.001	0.001	0.005
Cu	0.000	0.000	0.000	0.000	0.001	0.001
S	1.003	0.995	0.995	0.994	0.980	0.976
%ZnS	97.3	97.3	95.9	95.9	88.5	87.6
%FeS	0.0	0.0	4.0	4.0	10.8	11.9
%MnS	2.7	2.7	0.1	0.1	0.7	0.5

<sup>1</sup>detection limit: 0.02% Sb; <sup>2</sup>detection limit: 0.03% Cu.  
Cd, Bi, Pb, As and Ag were looked for, but not detected.  
nd – not detected

Analysis	Specimen	PTS No.
1	BH 2, 8.2 m	3897
2	BH 2, 8.2 m	3897
3	BH 4, 17.8 m	3917
4	BH 4, 17.8 m	3917
5	BH 4, 21.2 m	3926
6	BH 7, 81.6 m	4314

**Table 16** Electron microprobe analyses of galena (Analyst: B. Beddoe-Stephens)

	1	2	3	4	Detection limit
	Wt%				
Zn	nd	nd	0.10	nd	0.08
Fe	nd	nd	0.06	0.04	0.06
Mn	nd	nd	nd	nd	0.08
Sb	0.15	nd	0.08	0.10	0.04
Cu	nd	nd	nd	nd	0.10
Pb	87.10	86.04	87.62	87.27	
Ag	0.15	0.07	nd	0.11	0.05
S	13.58	13.26	12.66	12.74	
Total	100.98	99.36	100.59	100.26	
	Atomic proportions				
Fe	<0.002	<0.002	0.003	<0.002	
Sb	0.003	<0.001	0.002	0.002	
Pb	0.993	1.001	1.029	1.027	
Ag	0.003	0.001	<0.001	0.002	
S	1.001	0.997	0.960	0.969	

The elements As and Bi were searched for but not detected.  
nd – not detected.

Analysis	Specimen	PTS No.
1	BH 4, 17.8 m	3917
2	BH 4, 17.8 m	3917
3	BH 4, 21.2 m	3926
4	BH 7, 81.6 m	4314

In some specimens, notably rocks with a breccia-texture, massive patches of pyrite display a colloform texture in which minute pyrite granules are arranged in fine, concentric sets of spherical bands. Examples include BH 3, 19.6 m and 22.2 m (A III, T III) and BH 10, 10.7 m, 16.5 m and 19.2 m (A III, T IX). This texture may be of metamorphic replacement origin akin to the "birds-eye" described by Ramdohr (1969, p. 595). It shows evidence of probably having replaced pyrrhotine, while being itself replaced by coarse, homogeneous pyrite. In another specimen from BH 10 (7.3m; A III, T IX) this texture occurs alongside developments of a skeletal, boxwork-like pyrite structure, an association similar to one described from the Rosh Pinah deposit (Page and Watson, 1976).

Irregular grains of pyrrhotine are common in graphitic schists including those intersected in boreholes 3, 7 and 9 (A I), and are also a frequent constituent of dolomitic quartz-celsian rock. In both lithologies pyrrhotine tends to be accompanied by chalcopyrite and, to a lesser degree, sphalerite and galena. It frequently coexists with pyrite (e.g. BH 3, 21.0 m; A III, T III; BH 5, 8.0 m; A III, T V). It is, however, rare in baryte-rock, though trace amounts were observed in BH 2 (16.8 m; A III, T II). Pyrrhotine forms massive granoblastic bands or lenses intersected at 76.3m in BH 9 (A I, T IX) and at 19.2m in BH 10 (A I, T X). No analytical data in this mineral are yet available.

#### SPHALERITE

Granoblastic grains of sphalerite occur disseminated or segregated into tenuous, and occasionally massive, laminae and bands. Sphalerite is particularly conspicuous in celsian-

bearing rocks, in barium-enriched micaceous schists and in the "limestone" encountered in BH 4 (A I, T IV). In the baryte-rock it is a common but minor constituent whose content rises very locally where pyrite is concentrated into discrete bands. Although widespread in the mineralised zone, sphalerite is abundant only on a very local scale.

The sphalerite varies widely in colour from a deep red ferroan variety to a pale, almost colourless variety. Microprobe data confirms that this reflects differences in Fe and Mn levels (Table 15). The pale, manganoan variety includes a fluorescent example (analyses 1 and 2) from baryte-rock in BH 2 (8.2 m; A III, T II) which gives an orange-yellow light in response to short-wavelength UV light. Analyses 3 and 4 refer to a second pale sphalerite (BH 4, 17.8 m; A III, T IV) which is low in both Fe and Mn, and correspondingly rich in Zn. This specimen, which does not fluoresce, occurs in a breccia containing baryte fragments. Analyses 5 and 6 refer to iron-rich examples from the banded "limestone" in BH 4 (21.2 m; A III, T IV) and from quartz-celsian rock in BH 7 (81.6 m; A III, T VI) respectively. In general it is apparent that there is an association of manganoan sphalerite with baryte-rock.

#### GALENA

Commonly associated with sphalerite, galena is a widespread minor constituent of the mineralised zone. Modal contents of sphalerite and galena given in Table 12 are visual estimations following determination of total sulphide-contents by point-counting, since galena levels were always too low for direct application of this technique. However, apart from the minor occurrence of cerussite, the only Zn and Pb

minerals observed were sphalerite and galena so that it appears that in general the assay data for these elements closely reflect the contents of these corresponding minerals, throughout the mineralised zone.

Microprobe analyses of galena are given in Table 16. Minor elements are low, with the exceptions of Ag and Sb which for the specimens from BH 4 (17.8 m; A III, T IV) and BH 7 (81.6 m; A III, T VI) give silver levels of 0.15% and 0.11% respectively, and antimony levels of 0.15% and 0.10% respectively.

#### **COPPER MINERALS**

Chalcopyrite is a widespread but very minor constituent of the mineralised zone. Covellite, of probable late supergene origin, was observed in one polished section (BH 5, 6.6 m; A III, T V).

#### **MAGNETITE**

Magnetite is a prominent constituent in some bands of baryte-rock, but is absent from others. It occurs as rounded grains disseminated and segregated into thin layers. A small number of magnetite grains have irregular, embayed forms, and some show partial replacement by pyrite or baryte. The mineral is often accompanied by fuchsite.

#### **RUTILE**

Minute rutile grains are closely associated with celsian and dolomite. They tend to occur as euhedral prisms and display geniculate twinning, indicating a metamorphic rather than a detrital origin.

#### **OTHER MINERALS**

Tourmaline, as minute, pale prisms, is a minor constituent of certain mica-schist (e.g. BH 8, 8.3 m; A III, T VIII). Sphene is a minor constituent of hornblende-bearing rocks of the Ben Lawers Schist encountered in BH 7 (e.g. 150.4 m, 152.7 m, 166.0 m; A III, T VI). Clinozoisite also occurs in these rocks as slender colourless prisms distinguished by the characteristic "Berlin blue" interference colour. Ilmenite was only observed in a specimen of chloritic metabasite from BH 9 (43.4 m; A III, T VIII), and has not been found to co-exist with magnetite.

### **PETROGRAPHY**

#### **BEN EAGACH SCHIST**

##### **Graphitic schist**

Widespread barium enrichment was encountered in graphitic schists from surface outcrop and drill-core (Appendix II) which had no obvious baryte or celsian. The relatively few specimens examined microscopically were found to be generally lacking in barium-rich minerals, and electron-microprobe investigations (Table 11) showed that most of the barium present resides in muscovite, which may form 50% or more of the rock. Accessory baryte was observed in one specimen (BH 8, 135.0 m; separated by laboratory panning of crushed rock). Certain other specimens contain minor amounts of barium feldspar. For instance, hyalophane is a prominent constituent of certain bands in a specimen from BH 7 (113.0 m; A III, T VI), and forms ovoid porphyroblasts in a second specimen of graphitic schist from this borehole (BH 7, 95.1 m; A III, T VI).

Apart from barium muscovite the major constituents of these rocks are quartz, carbonate (commonly dolomite, not yet found to contain significant barium) and sulphides. The graphitic component takes the form of microgranules of amorphous carbon occurring as solid inclusions in muscovite, on grain boundaries and concentrated into secondary cleavage planes. No crystalline graphite was observed in polished sections or located during X-ray diffraction investigations.

Pyrrhotine and pyrite, often coexisting, are the most common sulphides in these rocks (A I). Sphalerite is common locally, and tends to be accompanied by subordinate amounts of galena. Traces of chalcopyrite may accompany the pyrrhotine. Metal values are generally low in this rock type (A II) but are enhanced in certain dark carbonate bands (e.g. BH 3, 3.6 m; A III, T III).

The rock is highly schistose, with frequent development of cleavage crenulations and secondary cleavages. Primary banding on a fine scale is commonly expressed as alternations of micaceous and carbonate-rich (dolomite or marble) layers (e.g. BH 9, 31.5 m–37.31 m; A I, T IX). Thin sulphide-rich layers are locally common (e.g. BH 9, 56.0 m; A I, T IX). Larger-scale banding is less common, though conformable bands of black marble and dolomite are locally present (e.g. BH 3, 15.7 m–18.9 m; A I, T III; BH 7, 103.65 m–105.42 m; A I, T VII). Outside the zone of barium enrichment the graphitic schists contain sporadic minor pyrite and pyrrhotine but are not otherwise mineralised.

##### **Quartzite**

Over the Ben Eagach formation as a whole quartzite bands of detrital origin are common, being gritty and occasionally displaying graded bedding. In some areas such rocks may form up to 50% of the succession, but they are not well represented in the mineralised zone in which most of the quartzose rocks are believed to be of chemical origin. Examination of a small number of specimens of quartzite believed to be of detrital origin from the mineralised zone has shown them to be variable, some containing minor albite but no sulphide grains (e.g. BH 8, 68.3 m; A III, T VII) while others contain small amounts of pyrite or sphalerite (e.g. BH 9, 81.0 m; A III, T VIII).

##### **Muscovite-schist (including calc and dolomitic varieties)**

Schists in which graphitic material is effectively absent occur throughout the mineralised zone and may form considerable thicknesses adjacent to the mineralised zone. In BH 7, 3.14 m to 27.03 m (A I, T VII), dolomitic muscovite-schist in a hanging-wall situation stratigraphically underlying celsian and baryte mineralisation has low-level, cryptic barium enrichment with minor sulphides, and is distinctly banded owing to the presence of thin, cream-yellow, barren dolomite layers (A I, T VII and A II, T VII). Dolomitic muscovite-schists in BH 10A (A I, T XA) immediately overlie the mineralised Ben Eagach Formation. Thin bands of pale muscovite-schist occur within the mineralised zone and are interbanded with graphitic schist adjacent to strong mineralisation.

These schists are usually dolomitic, though in BH 9 (A I, T IX) calcareous examples bearing accessory pale tourmaline are present (e.g. 29.8m and 38.1m; A III, T VIII). Tourmaline was also observed as a minor constituent of muscovite-schist (referred to as calc-schist in Figs. 17, 18 and 20) in BH 11 (19.0 m and 127.3 m; A III, T X), the first example being a rock assigned to the Ben Lawers Schist, the latter a schist within the mineralised zone.

The muscovite-schists are frequently enriched in bar-

ium (Appendix II), largely due to the presence of barian muscovite (Table 11). As with graphitic schist, a few specimens proved to contain minor amounts of barium feldspar (BH 7, 40.5 m and 71.6 m; A III, T VI: BH 8, 115.8 m and 148.2 m; A III, T VII). One outcrop specimen (S 64488; NGR NN 8585 5662) not included in Appendix III, Table XI, contained common porphyroblasts of celsian with thin marginal zones of hyalophane.

The muscovite-schists often contain minor amounts of sulphides, commonly pyrite and/or pyrrhotine. In one unusually rich specimen from BH 10 (7.3 m; A III, T IX) pyrrhotine is seen to be part-replaced by "birds-eye" pyrite, itself part altered to marcasite. Sphalerite is not common in these rocks, and galena is apparently very rare (both much less common than in the graphitic rocks).

Biotite is rarely a major constituent of the mica-schists in the mineralised zone. In BH 1 (19.14 m to 19.32 m; A I, T I) a band or lens of pyritic quartz-biotite-schist occurs within the thick intersection of baryte-rock. Biotite also occurs as a minor constituent of muscovitic schists in the upper part of BH 7 (A I, T VII), in BH 10A (A I, T XA) and in BH 11 (A I, T XI).

#### Carbonate rocks

Carbonate-rocks are a widespread though relatively minor component of the mineralised zone. Rocks in which calcite is the dominant constituent occur notably in the form of thin dark marble bands seen to be interbanded with mica-schists in many of the boreholes and, more rarely, in surface exposures. In BH 4 (A I, T IV) an unusual limestone occurs in two intersections (18.00–18.07 m; 20.69–22.08 m) separated by a zone of calcareous breccia and brecciated dolomitic marble. In these rocks the calcite is a manganoan variety containing minor strontium (Table 13) and is accompanied by minor amounts of dolomite. The rock is rich in pyrite, sphalerite and galena and the brecciated zones contain celsian and baryte fragments. Metal levels here are c. 8% Zn and c. 4% Pb (A II, T IV). In the limestone the sulphides occur in discrete bands which impart a striped appearance to the rock, while in the brecciated rock they are congregated in the inter-fragment matrix. In BH 2 the baryte-rock is underlain by 0.8 m of a coarse, irregular-textured rock rich in Zn and Pb sulphides, quartz fragments and patches of coarse white calcite (A I, T II).

In addition to calcite bands, dark bands of dolomite also occur in the graphitic schists and may be enriched in sulphides (e.g. BH 3, 3.6 m; A III, T III). Thin bands of pale, barren dolomite occur in the muscovite-schist in the upper 27 m of BH 7 (A I, T VII) as already mentioned. A thick intersection of dolomite rock occurs in BH 3 from 19.56 m to c. 24.9 m (A I, T III). This rock varies in texture from a coarse, massive rock with minor celsian (21.0 m; A III, T III) to a banded, sulphide-rich, celsian-bearing rock (e.g. 24.6 m; A III, T III) and to breccia-textured rock in which sulphides are abundant in the rock's matrix (e.g. 19.6 m; A III, T III).

#### Quartz-celsian rock

Celsian-rich rocks occur throughout the mineralised zone in excess over baryte-rich rocks. They exhibit wide variations of modal composition, texture and grain size. Normally they are made of celsian, quartz, dolomite, sulphides and accessory rutile. Other common constituents include potassic celsian, barian muscovite, biotite, fuchsite and chlorite.

Coexistence of celsian and baryte is very restricted. Examples include bands of coarsely granular pyrite intersected in BH 1 (10.6 m; A III, T I) in which interstitial celsian

crystals appear to be set in a coarse, sub-poikilitic matrix of baryte and dolomite. In a second example from BH 1 (22.4 m; A III, T I) thin celsian-bearing and baryte-bearing bands alternate. In BH 5 at 23.2 m (A III, T V) bladed crystals of celsian occur in a massive, coarse-grained baryte-rock. However, a more common situation is one in which a celsian-bearing rock is cut by late, dilational hair veinlets carrying crystals of quartz, calcite and baryte. Examples of this were found in holes 2, 4, 5, 7 and 11 (A III).

In much of the mineralised zone occurs a fine-grained to medium-grained, granular, celsian-rich rock of cherty appearance. In BH 2 this rock was intersected from 6.7 m to 7.72 m (A I, T II). The texture here is equigranular, lacking any laminar fabric, though the rock is often crossed by parallel sulphide-rich bands. One such example from 6.8 m (A III, T II) consists of some 45% celsian, 35% quartz and 20% pyrite plus sphalerite (visual estimate). A second example from 7.5 m is sparingly dolomitic and not banded. Granular quartz-celsian rocks form the lower part of BH 4 and are a major constituent throughout BH 5 (A I, Tables IV and V). In these cases the sulphide contents are low and dolomite may be entirely absent (A III Tables IV and V). Celsian-bearing rocks in BH 11 (A I, T XI) have a similarly cherty appearance in hand specimen, but this is largely due to their high quartz contents. The contained celsian tends to be platy in habit (e.g. BH 11, 107.0 m and 114.9 m; A III, T X). In a further example, from BH 7 (32.6 m; A III, T VI), abundant celsian exhibits both granular and platy habits, to yield a rock of complex texture, and the celsian-bearing rocks from this borehole are generally of pale cherty appearance in hand specimen.

Celsian is quite commonly bladed in habit rather than granular. In one type the crystals are wafer-thin plates resembling mica crystals, which tend to occur thinly distributed through a granular quartz matrix. Good examples include the two specimens from BH 11 cited above. One of these was found to contain platy crystals of the hydrous barium silicate cymrite ( $\text{BaAl}_2\text{Si}_2\text{O}_8 \cdot \text{H}_2\text{O}$ ) in addition to platy celsian crystals. At the other extreme, very coarse crystals of celsian are the major constituent of certain bands. In these rocks the crystals tend to be of uniform optical properties and to lack twinning, yet they often display a relic lamination which runs through the rock parallel to the broad crystal faces in the strongly oriented fabric of bladed celsian (e.g. BH 5, 24.2 m; A III, T V: BH 10, 13.3 m; A III, T IX). The porphyroblastic character of these rocks is further emphasised by the presence in some examples of parallel inclusion trails of quartz and sulphide grains set in very coarse celsian (BH 9, 74.6 m; A III, T VIII). In extreme cases, such trails may preserve crenulation folds of the earlier fabric (e.g. S 63654; NGR NN 86645657). In another type, coarse celsian in a medium-grained quartz-rock takes on a peculiar branching-bladed form in which the individual celsian crystals again maintain optical homogeneity (e.g. surface specimen CZR 3573, NN 8073 5469: A III, T XI).

Coarse celsian crystals may also occur in bands closely associated with pyrite, pyrrhotine and sphalerite in certain strongly banded quartzose rocks (e.g. BH 3, 33.11 m; A III, T III). They also are a common major constituent of sulphidic brecciated rocks (described below), in which they may be part-chloritised (e.g. BH 3, 22.2 m; A III, T III).

Lastly, coarse blade-like porphyroblasts of celsian are a major constituent of certain very uncommon muscovitic schistose rocks, the one example observed in thin section being from BH 9 (28.6 m; A III, T IX). Here celsian "blades" up to 5 mm in length consist in detail of an irregular

mosaic of celsian patches set in more potassic celsian possibly formed by replacement. Similar bladed "porphyroblasts" in a muscovite-quartzite from surface outcrop (CYR 6, NN 8268 5506; A III, T XI) are pseudomorphs consisting of minute quartz grains set in baryte with minor goethite. Their precise paragenesis is obscure.

#### Brecciated rocks

Breccia is a minor component of the mineralised zone. Good examples have been examined from two of the boreholes (3 and 4; see A III), and similar rocks have been observed in other boreholes and at outcrop. In all cases the rock is made up of clast-like areas of a variety of quartz, dolomite, calcite, baryte and celsian-rich lithologies poor in sulphides set in a fine, sulphidic, quartzose or dolomitic matrix. The textures are thoroughly annealed, and are very probably of pre-metamorphic origin. The contrast between sulphide-rich matrix and sulphide-poor fragments may suggest a comparison with intra-formational breccias described from other stratiform base-metal deposits, such as the Footwall Breccias of the Rosh Pinah deposits (Page and Watson, 1976).

In BH 3 such rocks occur within the dolomite-rock intersected from 19.56 m to c. 24.5 m (A I, T III). One example, from 33.1 m (A III, T III), consists of fragments of quartz-rock set in a pyritic matrix containing small fragments of baryte and celsian. Another, from 22.2 m (A III, T III), is notable for the apple-green colour of coarse celsian fragments due to incipient chloritisation. In BH 4 breccias form three short intersections associated with the banded limestone (A I, T IV). One specimen from 17.8 m, (A III, T IV) has quartz and baryte fragments set in a dolomitic matrix rich in galena and sphalerite. In another (19.2 m; A III, T IV) the fragments include marble similar to that seen in adjacent intersections.

Other possible examples include the calcareous, crudely patchy rock from BH 2 (A I, T II) and breccia-texture developed in the dolomitic base to the baryte intersection in BH 1 (28.7 m to 29.0 m).

#### Baryte-rock

Massive baryte intersected in holes 1-5, 7 and 9 (A I) consists mostly of a coarse, granoblastic-mosaic rock in which anhedral, polygonal to irregular baryte grains frequently exceed 90% by volume. Modal analyses given in Table 12 show that the other common constituents are quartz, carbonate, magnetite and sulphides. These results do not include data for finely banded rocks, or for certain broad bands of opaque-rich baryte-rock. Banding is usually present to some degree, though the feature is often not well developed (e.g. BH 3 25.5 m to 32.5 m; A I, T III). The most common banding is expressed by layers of rock rich in sulphides and quartz, which alternate rhythmically with normal baryte-rock (e.g. BH 1, 8.3 m to 15.7 m; A I, T I). In such bands pale manganous sphalerite is a common minor constituent, galena less common and chalcopyrite an accessory. White baryte and quartz rock almost completely lacking opaque phases forms occasional layers (e.g. BH 1, 8.05 m to 8.30 m; A I, T I).

Table 12 illustrates an antipathetic relationship between the presence of magnetite and that of the sulphides. In BH 3 there is an abrupt change at 26.45 m from pyritic to magnetitic baryte-rock (A I, T III), but elsewhere the rock-types are often less clearly separated. Magnetite-bearing rocks commonly display a rhythmic banding with thin magnetite layers set in pale baryte-rock.

The carbonate present is commonly dolomite, though in BH 3 it is calcite (A I, T III). Other constituents include

micas and chlorites. Muscovite (probably barian) is a widespread minor constituent, fuchsite occurs locally in association with magnetite, and biotite is also locally present.

Common grain-sizes in these rocks are indicated by the following data:-

PTS 3898 (BH 2, 10.7 m)	Baryte 0.4-2.0 mm	Quartz 0.1-0.33 mm	Opaque 0.1-0.8mm
PTS 3902 (BH 2, 13.3 m)	Baryte 0.2-1.8 mm	Quartz 0.1-0.5 mm	Opaque 0.1-0.5mm
PTS 3898 (BH 2, 10.7 m)	Carbonate (trace)	Muscovite (trace)	
PTS 3902 (BH 2, 13.3 m)	Carbonate (minor)	Fuchsite (minor)	
		0.2-0.3 mm	0.4 x 0.05 mm
		0.1-0.5 mm	0.1 x 1.2 mm

Quartz tends to form small, irregular grains sited at interstices of the baryte fabric. Such grains may take the form of thin plates sited along boundaries between the baryte crystals. By contrast, the opaque minerals form rounded grains showing no preference for baryte grain boundaries. The micas occur as thin disseminated flakes frequently lacking a preferred orientation. Indeed, tectonic fabrics are uncommon in the baryte-rocks.

#### Massive sulphides

Massive bands and lenses of sulphide-rich rock more than about 5 cm thick are uncommon. In BH 2 a pyritic lens with minor galena is described at 13.8 m (A III, T II). In BH 4 broadly similar material has prominent sphalerite (17.5 m; A III, T IV). Similar pyritic bands occur in BH 7 (55.8 m and 64.8 m; A III, T VI). In holes 9 and 10 pyrite-rich bands are present (A I, T IX and T X). These rocks all have coarse, granular mosaic textures with various combinations of quartz, dolomite, baryte, celsian and other minerals occurring interstitially.

#### BEN LAWERS SCHIST

Rocks considered to have lithologies characteristic of the Ben Lawers Schist have been examined from the bottom part of BH 7 and the top of BH 11 (A I, T VII and T XI respectively). They are calcareous schists carrying major amounts of both biotite and muscovite together with common chlorite, and tend to be similar to some of the more chloritic muscovite-schists within the Ben Eagach Formation. However, they may display garbenschiefer texture in which coarse, randomly oriented, prismatic hornblende porphyroblasts are prominent. Equant porphyroblasts of pink garnet (almandine) are common. Clinzoisite is a common minor constituent of the Ben Lawers Schist seen in holes 7 and 11 (A III, T VI and TX respectively), and in the former it is accompanied by minor sphene. One specimen from BH 7 (150.5 m; A III, T VI) represents a coarse amphibolite with calcite, biotite, sphene and apatite.

#### METABASITES

Dark green calcareous and dolomitic chlorite-rocks, which are regarded as metabasites, are present in Creag an Chanaich (Fig. 29) and were intersected at depth by BH 9 (38.17-45.23 m and 48.49-53.45 m; A I, T IX). They are generally massive or poorly laminated with, in addition to chlorite and carbonate, biotite and accessory rutile and ilmenite. A similar rock from the more southerly of the two surface outcrops (Fig. 29) is dominated by orange calcite porphyroblasts and also carries magnetite. The sulphide content of these rocks is generally very low. Their high Fe

and Mn (A II, T IX) seems to confirm that they are metamorphosed basic igneous rocks and their massive character and absence of barium-enrichment points to an intrusive rather than extrusive origin.

## CHARACTERISTICS OF THE MINERALISED ZONE: GENERAL

Except in the Ben Eagach area, the outcrop of the Ben Lawers Schist is marked by a pronounced ridge with numerous rocky crags rising to over 700 m. The Ben Eagach Schist which crops out along the northern slope of the ridge is largely covered by glacial drift and peat. In most places the superficial deposits are less than 5 m thick but rock exposures are generally small and widely separated.

Between Meall a'Charra and Meall Tairneachan (Fig. 2) the Ben Eagach Schist consists principally of black graphitic muscovite-schist with impersistent bands of quartzite, non-graphitic mica-schist and limestone; but close to its boundary with the overlying Ben Lawers Schist it shows considerable lithological variation with, in addition to the suite of barian rocks, bands of calc-schist. The latter lithologically resembles the Ben Lawers Schist but is everywhere devoid of porphyroblastic hornblende and, since it is invariably enriched in barium, it is considered more likely to be a facies variant of the Ben Eagach Schist than an infold or thrust slice of Ben Lawers Schist. Unlike the quartz-celsian rock, which is considered to be a chemical sediment, the quartzite contains detrital albite and zircon and locally shows graded bedding.

Rocks of undoubted igneous origin are uncommon, but on Creag an Chanaich (Fig. 29) two conformable bodies of calc-chlorite-rock, ranging in thickness from 2 to 17 m, are almost certainly metabasite sills. They comprise a relatively massive and structureless dark green chloritic aggregate peppered with idiomorphic rhombs of brown calcite. Fine-grained margins, which were apparent where the larger of these two bodies was intersected by BH 9, are attributed to the effects of deformation. Although within the mineralised zone, the metabasites do not exhibit barium enrichment. A narrow band of dark rock, consisting mainly of randomly-oriented biotite porphyroblasts in a notably calcareous groundmass, is present close to the site of BH 3 (Fig. 24). Similar rocks intersected in BH 10 have high Fe and Ti contents suggesting a basic igneous origin. They are also enriched in barium.

The components of the mineralised zone have been described in the previous sections. Quoted thicknesses of of the mineralised zone include all barium-enriched rocks and not simply baryte-rock and quartz-celsian rock.

## CHARACTERISTICS OF THE MINERALISED ZONE: CREAG AN FHITHICH DISTRICT

### GEOLOGY

The Ben Eagach Schist in the Creag an Fhithich district dips steeply to the north and hence structurally overlies the Ben Lawers Schist. The southern margin of the mineralised zone roughly coincides with the Ben Eagach Schist-Ben Lawers Schist boundary but on a local scale is transgressive. For example, in BH 7 barium enrichment extends approximately 5 m into the Ben Lawers Schist (Fig. 20; A II, T VII) whereas in BH 6 the lowermost 5 m of Ben Eagach Schist has relatively little barium (Fig. 22). The northern limit of the zone is less well defined as boreholes 6, 7 and 8 inter-

sected mineralised rock immediately below superficial deposits. The mineralised zone in the Creag an Fhithich district has a minimum thickness of 100 m and is best exposed on the low hill immediately south of BH 7 (Fig. 17). The lower ground on the north side of this feature is underlain by a strip of calc schist, which dies out to the east but which thickens considerably towards BH 6. The northern boundary of the strip can be traced westwards along the strike to the Ben Eagach area where equivalent rocks are probably present. The calc schist contains anomalous quantities of barium and for this reason it is considered to be a band within the Ben Eagach Schist, rather than an infold of Ben Lawers Schist which it lithologically resembles. A sharp contact separates the calc schist from various barian rocks which form the summit of the low hill. Amongst these are three bands of bedded baryte, the most northerly of which is 11 m thick. The boreholes show that the bands are much thinner at depth (A I, T VII) and it is inferred that they are lenticular, although their strike-length has not been determined because of lack of exposure. Centimetre-scale layering within the baryte is well developed and shows no sign of folding or disruption. The baryte bands are separated by flaggy quartz-celsian rock which is generally rather fine grained and of cherty aspect. Contacts against baryte are seen at several localities and in boreholes 5 and 7, and in each case they are sharp with a complete absence of intermediate types (A I, T VII). Muscovite-schist is also present but poorly exposed.

Sphalerite and galena occur sporadically in quartz-celsian rock and muscovite-schist and in BH 7 the former rock type produced an assay of 0.45% Zn and 0.14% Pb over 2.0 m. A very small opening in quartz-celsian rock 57 m ENE of BH 5 may be an old trial adit excavated by early prospectors attracted by gossanous weathering or disseminated specks of galena.

The geophysical anomaly associated with mineralisation continues eastward from BH 5, but the zone itself diminishes in that direction and in an exposure 240 m ENE of BH 5 quartz-celsian rock interbanded with schistose quartzite provides evidence that barium-rich rocks interdigitate with, and pass laterally into, clastic metasediments. This is confirmed by BH 8 where the mineralised rocks are represented by quartzite and graphitic schist, the latter locally barium-enriched (A II, T VIII).

The area east of BH 8 is largely peat-covered but the ground north of Lochan Sgaradh Gobhair (Fig. 17) is well exposed and no baryte or quartz-celsian rock has been found. Samples collected in this area have been shown by XRF analysis to contain only slightly anomalous barium. The mapping was continued as far as Meall a'Charra, 2 km from BH 8, but all the rocks examined consist of clastic metasediments.

A band of quartz-celsian rock, at least 10 m thick, exposed in the stream 77 m north of the collar of BH 8 is situated stratigraphically below the mineralised zone but its strike extent is not known because of lack of exposure. Unusually thick bands of quartzite occur west of the stream and north of BH 7.

Geophysical evidence and one or two small exposures indicate that the mineralised zone extends westwards from BH 5 along the strike at least as far as the area near BH 6, where there is an exposure exhibiting, from north to south, quartz-celsian rock, quartz-pyrite-galena-rock and weathered muscovite-schist. The quartz-celsian rock is at least 7 m thick and dips towards the NNW at 75°. It is a medium to coarse-grained rock containing abundant crystals of celsian up to 10 mm across. The foliation, which is partly a litho-

logical layering and partly a crystal fabric, is well developed and allows the rock to be split into thin slabs. Some of the foliation planes and small cavities are coated with earthy brown material, presumably derived from the weathering of pyrite which is disseminated in small quantities through the rock. Galena and sphalerite are also present. The quartz-pyrite-galena-rock forms a band 1 m thick and has a sharp contact against the muscovite schist. It is coarsely crystalline, flaggy and somewhat weathered.

The absence of quartz-celsian rock and muscovite-schist in BH 6 is surprising since it passed directly beneath mineralised rocks exposed at the surface. The presence of much crushing and shattering shows that the borehole penetrated a fault and it is suggested that these rocks are displaced as shown in Fig. 22.

The band of graphitic schist adjacent to the Ben Lawers Schist contains, on the surface, a number of thin, probably impersistent, bands of quartz-celsian rock (Fig. 17). Boreholes 6, 7 and 8 show that the contact with the Ben Lawers calc-schist is sharp and that the latter contains abundant porphyroblasts of hornblende. Geophysical evidence indicates that the band of graphitic schist dies out in unexposed ground west of BH 6.

A mineralised band, 16 cm thick and dipping towards the NNW at 70°, is seen within graphitic schist in the stream (NN 8617 5656) west of BH 6. It consists of pale-coloured muscovite-quartz schist containing concordant streaks rich in sphalerite and galena and although it cannot be traced along strike and is not associated with quartz-celsian rock or massive baryte, it is nevertheless of interest because of the coincident geochemical (p34) and geophysical (p36) anomalies.

#### GEOCHEMISTRY

Shallow overburden sampling by hand auger was limited to four traverses 50, 250, 450 and 550 m east of BH 5 collar, running 160–340° (but not exactly coincident with the later geophysical traverses) and sampled at 20 m intervals. Deep overburden sampling using a power auger was confined to one geophysical line at 450E and a few samples on geophysical lines 410E and 510E, which were used to locate BH 8 (Fig. 18). Sample sites and analyses are given in Appendix IV.

The shallow sampling seldom reached the base of the overburden and the resultant samples contain >0.5% Ba in only three instances. These values are low in comparison with hand auger samples from further west in the mineralised zone. On the traverse 50 m east of BH 5, the absence of a strong barium anomaly close to the outcrop of the baryte rock is attributed to the greater thickness of the organic-rich A-horizon. However, at the southern end of this traverse a barium anomaly ( $\geq 0.3\%$  Ba) can be traced eastwards for 400 m. This anomaly is probably due to an increase in barium near the stratigraphic top of the Ben Eagach Schist and is also marked by an increase in resistivity. A similar rise in barium content occurs 20 m below the base of the Ben Lawers Schist in BH 8 (see A I, T VIII and A II, T VIII). Isolated barium peaks at 140 N on line 450E (NN 8734 5706) and 40N on line 550E (NN 8747 5699) (relative to an origin at BH 5) lie on the margins of high resistivity bands (Fig. 19a) and suggest the presence of quartz-celsian rock or possibly baryte rock.

Lead and zinc show a similar pattern to barium with an anomalous zone ( $\geq 150$  ppm Zn and  $\geq 100$  ppm Pb) coinciding approximately with the stratigraphic top of the Ben Eagach Schist in the west, but displaced southwards on line

450E. This southerly shift agrees with evidence, from elsewhere in the mineralised zone, for southerly glacial transport but contrasts with the results from the deep overburden sampling on the northern part of this traverse which are discussed below.

A feature with  $\geq 300$  ppm Zn and  $\geq 200$  ppm Pb is developed at the northern margin of the mapped mineralised zone but it is displaced slightly downslope, probably by hillcreep or hydromorphic transport, from the main resistivity high through BH 5. The most notable feature of the traverse 450E is the presence of high metal contents (up to 1040 ppm Pb and 900 ppm Zn at NN 8735 5702) in the northernmost samples. As this traverse is close to the stream course the anomaly may be due to alluvial transport; hydromorphic movement is unlikely because of the observed coherence between lead and zinc.

Deep overburden samples on line 450E show general barium enrichment in the  $-150 \mu\text{m}$  fraction, reaching a peak of 0.76% Ba at 50N coincident with the second resistive zone (Fig. 18). Zinc levels are more erratic but with a large peak at 10N. In the heavy mineral concentrates prepared from the basal till, a similar but more enhanced pattern is shown (Fig. 18) with up to 15% Ba at 60N, and baryte grains were identified optically in these concentrates (R C Jones *pers. comm.*). Borehole 8 was sited on the basis of the barium anomalies in the shallow and deep overburden, the presence of baryte grains, and the development of a coincident resistivity 'high'; but it failed to intersect baryte-rock. This is possibly due to the occurrence of thin beds of baryte-rock at surface-level which lens out rapidly with depth in the same way as was observed in boreholes 5 and 7 or are cut out by faulting. Alternatively, the presence of finely divided baryte in the basal till can be attributed to transport of baryte from the outcrops to the southwest by periglacial processes. Geochemical evidence for another mineralised band to the north is equivocal (Fig. 18) and the geochemical anomaly could be due to alluvial transport of mineralised material. However, this anomaly is coincident with a band of high resistivity and may indicate that a second mineralised band is present to the north of that investigated by BH 8.

Shallow overburden samples were also collected over an area between Ben Eagach and the site of BH 6 with an origin at NN 85605 56405 and baseline running at 070°. Five traverses at 200, 400, 600, 800 and 1000 m E were laid out at right angles to the baseline and sampled at 20 m intervals. Barium anomalies are mainly of low amplitude (<3000 ppm Ba) indicating that baryte-rock is not an important constituent of the underlying rocks. However, zinc and lead anomalies are stronger, particularly at NN 8655 5667 where 1050 ppm Pb was recorded. This lead anomaly is coincident with a high resistivity band, as illustrated by the contoured Fraser filter values (see Fig. 15) which can be traced eastwards to the galena-bearing outcrop just south of BH 6. Galena is also present at a small stream outcrop in the most southwesterly tributary of Middleton Burn (NN 8617 5656). The geophysical and geochemical anomalies die out quickly west of line 1000E. On the southern end of lines 200E to 1000E (from NN 8583 5628 to 8659 5655) an anomalous zone with greater than 1000 ppm Ba, 150 ppm Zn and 100 ppm Pb is interpreted as an enrichment at the junction of the Ben Lawers Schist and the Ben Eagach Schist and follows the Fraser filter contours associated with that boundary. Isolated lead and zinc anomalies further north on lines 600E and 400E are not considered to be very significant because of their generally low level (except for one value of 4050 ppm Pb at NN 8614



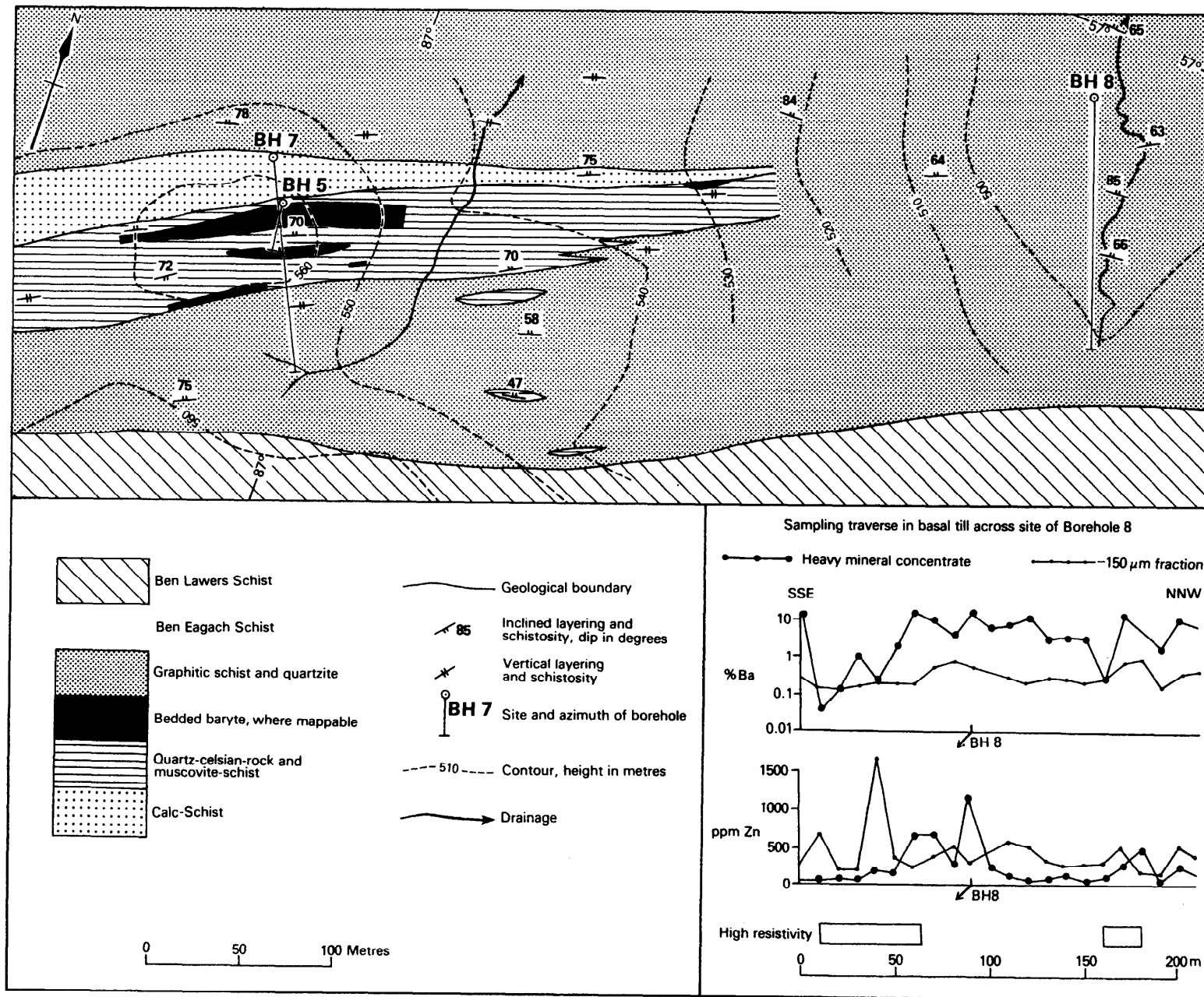


Fig 18 Geology, mineralisation and geochemical traverse in till, north of Creag an Fhithich

5662), and lack of continuity, although this may have been brought about by tectonic disruption. The depth of the overburden in this area is also uncertain.

Thus in the ground between Ben Eagach and BH 6, the geochemistry of the peat and shallow till exhibits few laterally persistent anomalies and fairly low barium levels. A slightly anomalous zone of Ba, Pb and Zn is found over the stratigraphic top of the Ben Eagach Schist. Isolated lead anomalies may be caused by a tectonically disrupted mineralised band similar to that seen at outcrop near BH 6.

#### VLF MAPPING

From the geophysical point of view this was the most straightforward area. The mineralised zone lies wholly within the conductive schists and causes a simple reversed crossover and Fraser-filter high (Fig. 19). Where the Fraser-filter anomaly does not agree in detail with the geological map, examination of the in-phase profiles and marking of the maxima and minima often gives better agreement. The anomaly extends both east and west from boreholes 5 and 7 (Fig. 19). To the east, it first becomes weaker, reaching its minimum amplitude at about 300 E, then becomes stronger and broader again. At about 600 E, the anomaly widens suddenly and splits in two, perhaps indicating a fault. West of boreholes 5 and 7, the anomaly extends more or less unchanging for 500 m until it runs into the anomaly associated with the base of the Ben Lawers Schist. The interpreted width of the mineralised zone varies from 40 to 140 m, averaging about 70 m. Drilling at boreholes 6 and 8, however, has shown that the resistive horizon causing this anomaly suffers lateral changes of composition. At BH 6 it is mica-schist, quartzite and graphitic schist containing up to 2.8% Ba, while at BH 8, a sulphide-rich quartz-celsian unit with up to 13.4% Ba accompanies graphitic schist, muscovite-schist and mica-ceous quartzite. Clearly the resistive zone represents a barium-enriched depositional episode, during which local conditions produced baryte (see pp. 33, 34 and A I, T VI and T VII).

About 50 m to the north of the known mineralisation a similar VLF-EM anomaly is developed. It is parallel to the strike, but not continuous. At one point, high barium values have been found in the soil over this feature (see Fig. 18) but otherwise its source is unknown.

The southern boundary of the Ben Eagach Schist can be seen clearly, giving an in-phase maximum and a steep gradient in the Fraser-filter.

At about 600 W occurs a hiatus in all three features described above. The boundary between the Ben Eagach Schist and the Ben Lawers Schist apparently swings northwards and round into the other two anomalies. A fault trending approximately NNE is indicated. To the west of this fault, the boundary continues on its previous bearing but the other anomalies are absent — only rather minor high resistivity zones are indicated, although one occurs over a small exposure of mineralisation at NN 8617 5655.

#### CHARACTERISTICS OF THE MINERALISED ZONE: BEN EAGACH TO FARRAGON HILL

#### GEOLOGY

A large outcrop of mineralised rock occurs in the core of the Ben Eagach antiform. This area, which has been mapped in detail (Fig. 23), lies immediately to the south-west of the summit of Ben Eagach and is drained towards the south,

the vertical relief being approximately 120 m. It is fairly well exposed with numerous rocky knolls separated by hollows filled with glacial drift overlain by peaty soil. A flat area in the NW is underlain by at least 2 m of peat dissected by gullies.

In the south-west a band of barium-enriched muscovite-schist and quartz-celsian rock approximately 40 m thick separates graphitic schist from calc schist. As this band is traced towards the north-east it enters an area of structural complexity and no longer lies along the contact between graphitic schist and calc schist. About 300 m ENE of BH 4, beyond the fence, exposures of graphitic schist and an absence of quartz-celsian rock debris show that the mineralised zone probably dies out and where last seen it is only 120 m across strike from the Carn Mairg Quartzite. In the south-east of the area covered by the detailed mapping, small scattered exposures suggest that graphitic schist lies in direct contact with calc-schist without intervening quartz-celsian rock and muscovite-schist.

The mineralised zone consists mainly of muscovite-schist, which has been shown by portable XRF analyser to contain up to 10% Ba, and quartz-celsian rock. The former contains ribs of quartzite, locally with well preserved detrital grains. The latter forms several discontinuous outcrops and includes fine-grained varieties resembling chert. It varies from massive, almost structureless, to flaggy and well banded and contains small quantities of disseminated pyrite and galena. Spots of fuchsite have also been identified. Weathering has locally produced a friable pale-coloured crust up to a few centimetres thick, and spots which are seen in thin section to be caused by the deposition of dark-coloured material along grain boundaries. Breccia occupying a few square metres at two localities (Fig. 23) consists of tightly packed centimetre-size fragments of quartz-celsian rock, the orientation of laminations varying from fragment to fragment. It is probably a syndepositional structure possibly related to contemporaneous faulting. Pods of creamy-coloured fine-grained limestone are found in quartz-celsian rock 280 m south of BH 4. The pods, which are closely spaced, have an irregular angular outline and vary from a few centimetres to 0.5 m across. Analysis of a specimen of the limestone using the portable XRF instrument indicates approximately 7% Ba. In the same area a 10 cm bed of quartzite within the quartz-celsian rock shows well preserved detrital grains. In quartz-celsian rock near BH 4 a number of veins, up to 30 cm thick, filling north-west trending fractures and consisting of coarsely crystalline galena, sphalerite and quartz can be traced for distances up to 10 m before tapering out.

Exposures of baryte and sulphide-bearing dolomitic limestone project through the scree slope at the base of a low cliff of quartz-celsian rock near BH 4 (Fig. 27). The baryte is at least 2.6 m thick (thinning to 2.0 m, 14 m below surface) with bedding dipping towards the south-east at 76°. It contains grains of pyrite in trails lying parallel to the bedding and also traces of sphalerite and galena. The baryte is followed to the SE by 4.5 m of flaggy dolomitic limestone, weathered to a deep brown colour, and containing streaks of pyrite, galena and sphalerite. Bands particularly rich in pyrite have weathered to a porous gossan which, in places, has cavities lined with small (1 mm) crystals of cerussite. In BH 4 this unit is 3 m thick and is mostly calcareous with some well developed sphalerite and galena (A I, T IV) containing up to 20.0% Zn and 6.6% Pb. The central part is brecciated with angular fragments of quartzite, celsian-quartz rock, dolomite and quartz-baryte rock set in a sulphide-rich quartzose and dolomitic matrix.

A band of muscovite-schist up to 14 m thick occurs

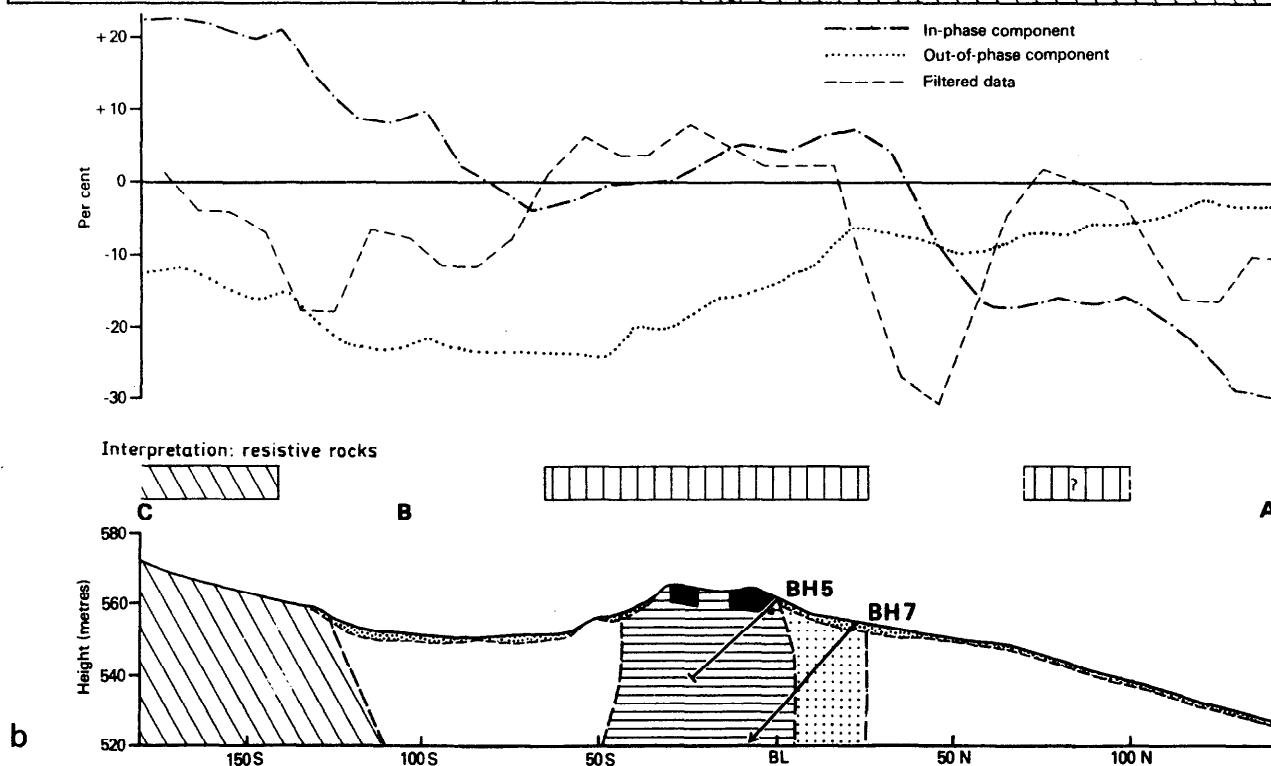
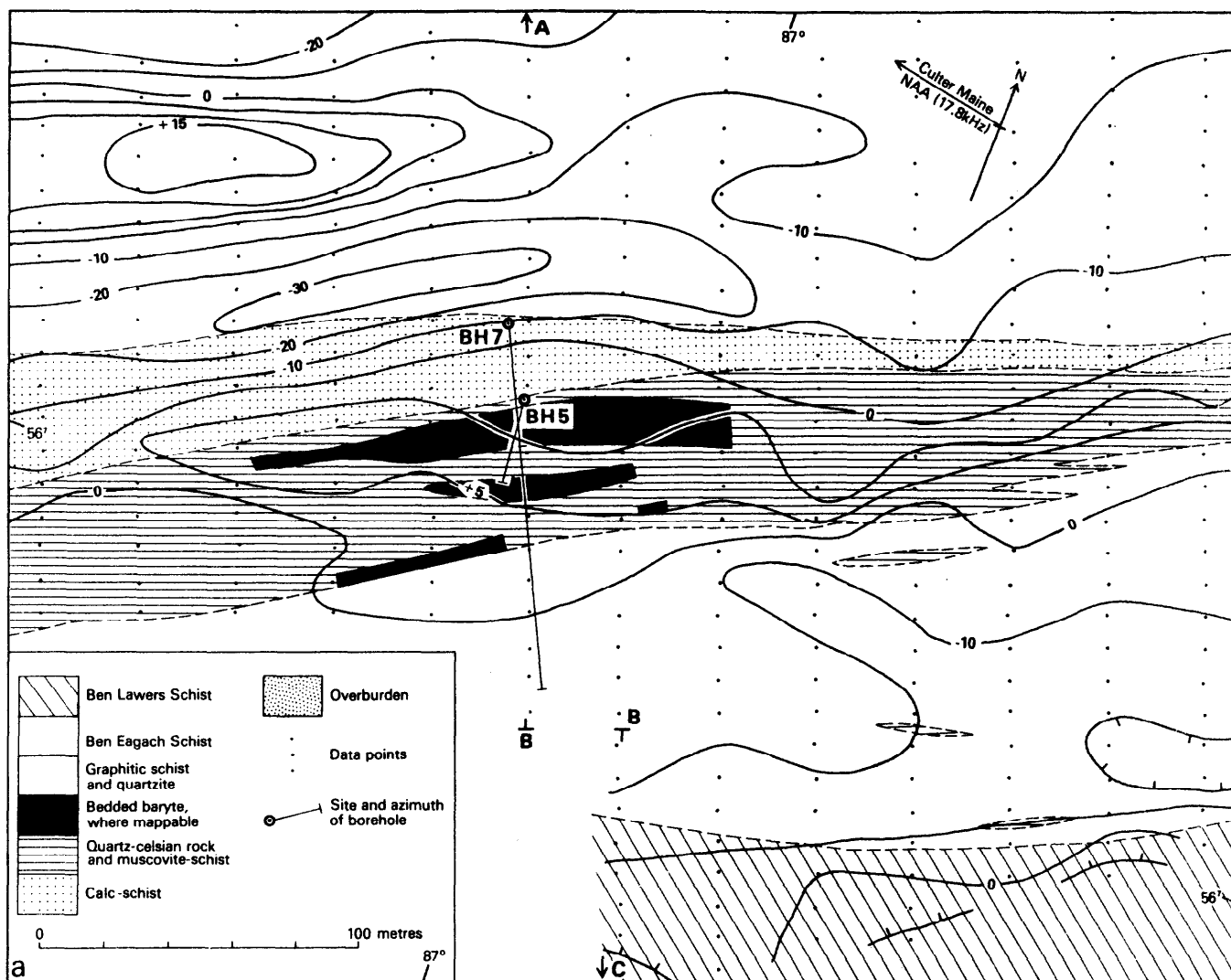
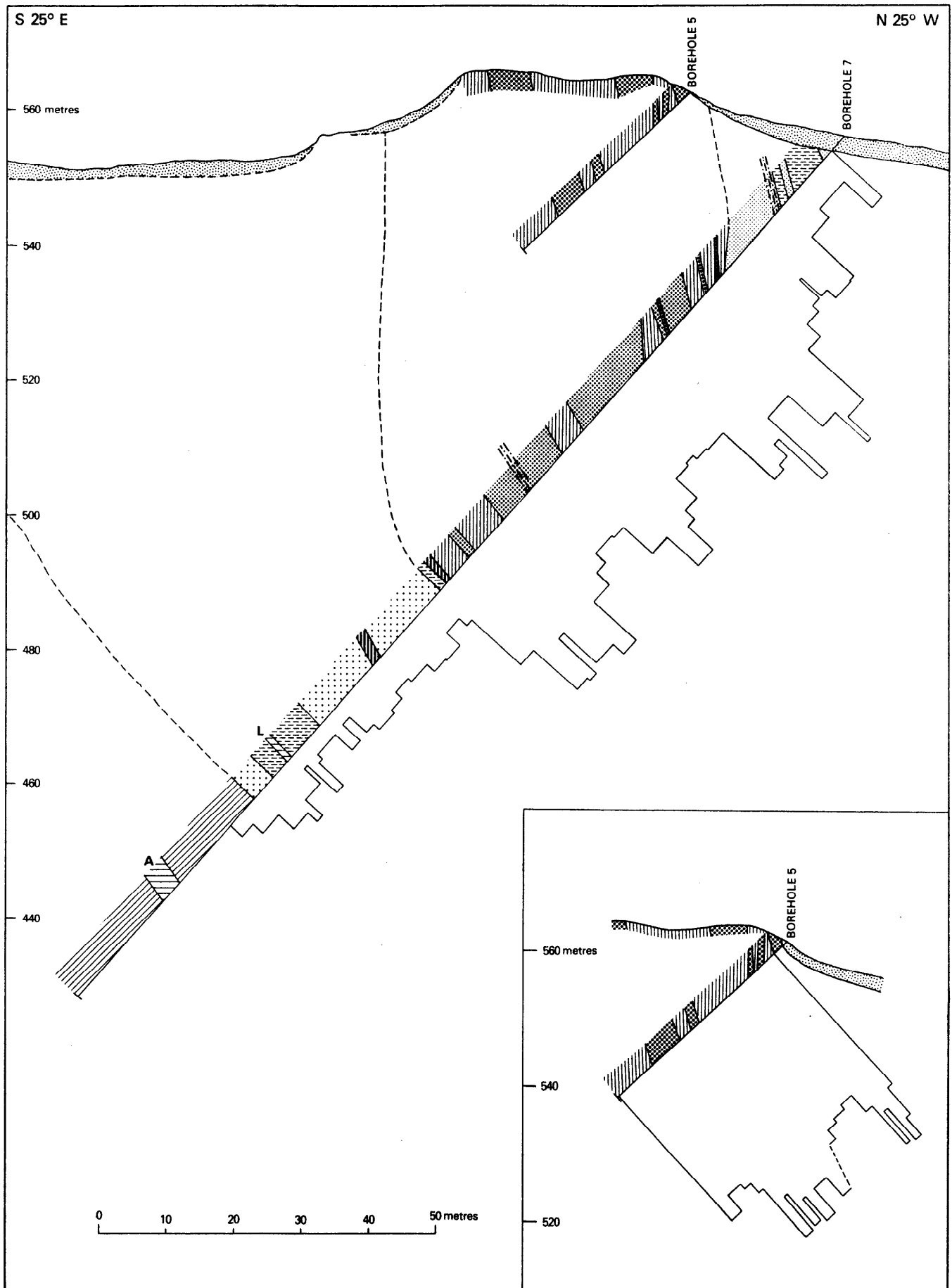
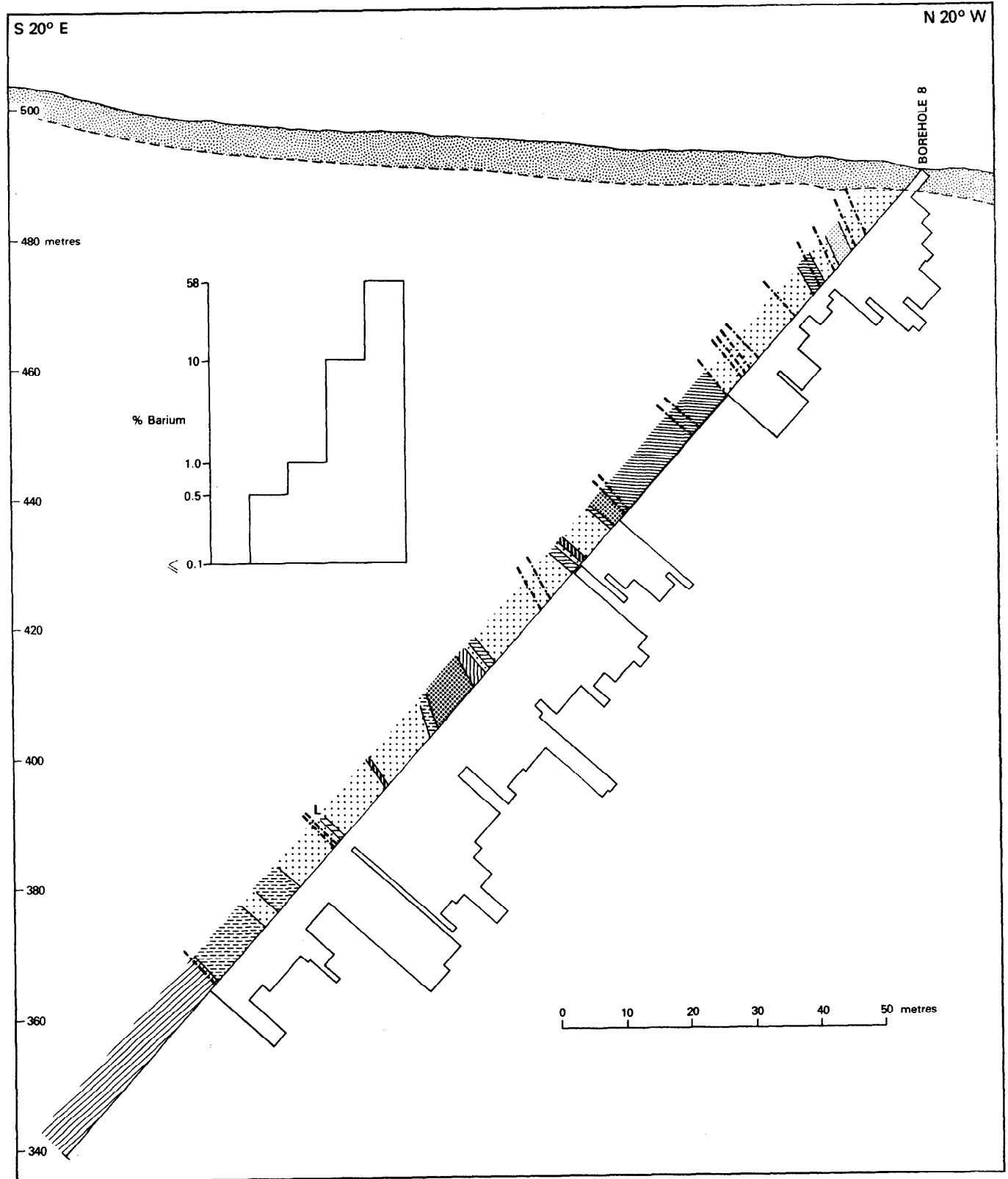


Fig 19 VLF-EM map of the area north of Creag an Fhithich (a) contour map of Fraser-filtered data, (b) profile along line ABC and its geophysical interpretation compared against the geological section in Fig 20

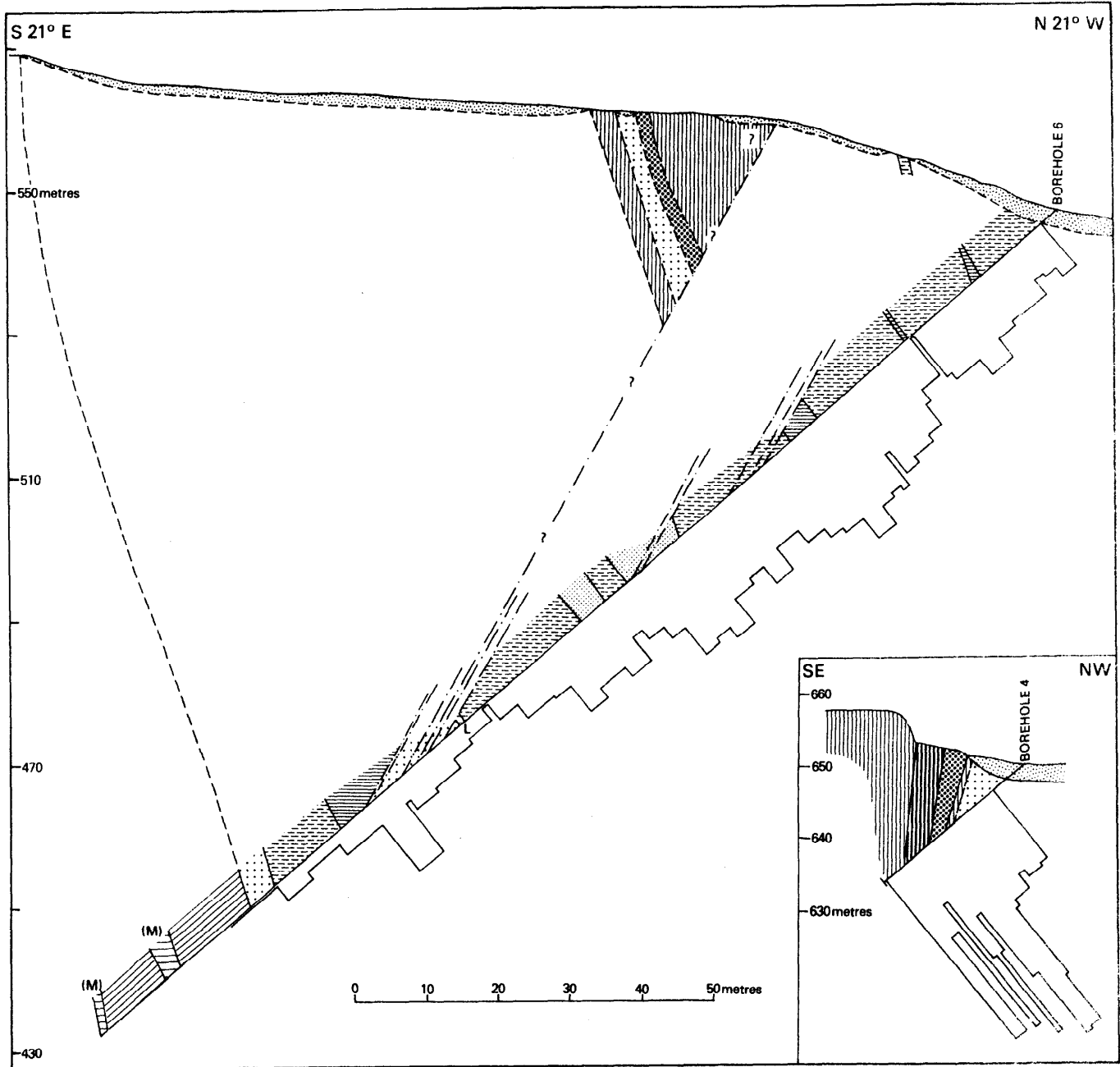


**Fig. 20. Section through boreholes 5 and 7, north of Creag an Fhithich, located on Fig. 17 and 18; legend as Fig. 21.**



- |  |   |  |
|--|---|--|
| Superficial deposits   | <b>BEN EAGACH SCHIST</b>  | Calc biotite-schist                      |
| Amphibolite (A), Metabasite (M), Lamprophyre (L)                     | Graphitic mica-schist   | Baryte-rock                              |
| <b>BEN LAWERS SCHIST</b>   | Quartzite and quartz-schist, including calcareous and dolomitic varieties | Quartz-calcian rock and muscovite-schist |
| Calc schist, including micaceous, chloritic and hornblende varieties | Carbonate-rock  | Muscovite-schist                         |
| Fault  | Mica-schist, including calcareous and dolomitic varieties                 |  |
|  | Chlorite-mica-schist including calcareous and dolomitic varieties         |  |

Figure 21. Section through borehole 8, north-east of Creag an Fhithich; located on figures 17-18



**Fig. 22** Section through borehole 6, north west of Creag an Fhithich, and borehole 4, south west of Ben Eagach; located on Figs. 17, 18 and 23; legend as Fig. 21.

within calc schist 360 m south of BH 4. It appears to die out towards the ENE and cannot be traced far in the opposite direction because of lack of exposure. It has been found to contain fuchsite and approximately 10% Ba. The calc schist to the north of this band is slightly enriched in Ba and is thus considered to be part of the mineralised zone; while that to the south appears to contain only background concentrations and is classified as Ben Lawers Schist.

The Ben Eagach area lies in the core of a major antiform (the F2 Ben Eagach Antiform of Sturt, 1961) which is tight in the north-west, dying out rapidly south-eastwards. The decrease in fold amplitude and the large increase in thickness of the Ben Eagach Schist has probably occurred as the result of movement of ductile graphitic schist from adjacent areas into the core of the structure. This movement may have been responsible for the detachment of part of the mineralised zone from its original stratigraphic position, although slightly Ba-enriched calc-schist, considered to be a part of the mineralised zone, is probably continuous along the boundary with the Ben Lawers Schist.

The only large structure which can be mapped within the area of detachment is a synform plunging at between 40° and 55° towards the W. An associated sub-vertical crenulation cleavage is well developed in graphitic schist, especially in the area SSW of BH 4 where it obscures the earlier schistosity (related to the F1 folds of Sturt, 1961). The axial trace of the synform crosses the outcrop of the mineralised zone twice and thus appears to be superimposed on an earlier structure which is difficult to define. Minor structures concordant with the Ben Eagach Antiform have not been recognised within the area of detailed mapping and the large synform and its associated cleavage probably record a deformation of local significance only.

Crenulations with axial planes dipping at 15° to 20° towards the NNW and sub-horizontal axes are present in almost every exposure of schistose rock. They refold the crenulation cleavage associated with the large synform and can be correlated with the F3 folds of Sturt (1961).

Sampling along a traverse across the outcrop of the graphitic schist on the east side of Ben Eagach showed that at most of the sample points the rock contains only background levels of Ba. However, in the north, (NN 8585 5662) close to the boundary with the Carn Mairg Quartzite, a thickness of at least 14 m of graphitic schist of normal appearance is strongly enriched in Ba (3.5% to >20%). Microscopic examination (p.31) shows that this zone contains abundant celsian as well as barian muscovite.

No mineralisation has been found in the Ben Eagach Schist where it crosses the coll south of Lochan a'Chait. However, there are few exposures in this area and the lower parts of the ground are largely peat-covered.

Two small exposures of mineralised rock are present on the eastern slopes of Farragon Hill at NN 8440 5563 and at NN 8425 5550. The more easterly consists of pyritous quartz-celsian rock and brecciated quartzite over 10 m thick. The celsian rock varies from a fine grained 'chert' to a coarse variety in which fuchsite porphyroblasts are prominent. Minor amounts of sphalerite are present and two shallow excavations, possibly made by early prospectors, were recorded in the more pyrite-rich bands. At the eastern extremity of the exposure the band is 4 m north of the Ben Lawers Schist-Ben Eagach Schist boundary but towards the west, possibly because of landslip, the gap increases to 15 m. The other exposure, 200 m to the south-west occurs at the boundary between the two formations and consists of a 1 m thick band of cherty, colour-banded quartz-celsian rock.

## GEOCHEMISTRY

The large outcrop of minerliased rocks which occurs in the core of the Ben Eagach Antiform (Fig. 23) was covered by five traverses running 160–340° at 0, 100, 200, 300 and 400 m W of an origin at NN 85605 56405 (the easterly continuation of the same grid has already been described in the Creag an Fhithich District). Soil samples were collected at 10 m intervals but in the rather irregular, craggy terrain it was difficult to collect representative samples of the C-horizon because either little or no soil was developed or the peat-filled hollows were too deep for the auger to reach the bottom of the organic layer.

High barium, lead and zinc anomalies are present with Ba reaching 17%, Pb 2.2% and Zn 1.3%. Barium values exceeding 1% were found in samples collected over quartz-celsian rock and baryte-rock (Fig. 23), to the south of BH 4 on line 300W and trending north-eastwards towards the summit of Ben Eagach which lies outside of the sampled area. Further west, barium values are much lower (generally <1000 ppm Ba) indicating that the mineralised rocks do not extend to line 400W but are cut off by a prominent NE-SW trending fault or by folding (Fig. 23). Lead shows a similar pattern with values  $\geq 0.5\%$  Pb immediately south of BH 4 and a generally southwards dispersion following a large peat-filled drainage hollow (line 300W). Further east, however, very high lead values were recorded with up to 2.2% Pb near the grid origin on line OW which was sited on the metal boundary fence leading to Ben Eagach. This fence could be a source of contamination because molten lead was used to 'solder' the iron posts into holes cut in the rock. However only slightly lower values of 0.47% Pb were found at 80S on line 100W, some distance away from the fence.

Zinc has a more irregular distribution than lead but the same general features are apparent, namely high values over the outcrop of the mineralised zone south of BH 4 and a belt of high values on the southern extremities of lines 0, 100 and 200W. This coherence of lead and zinc in the southern belt suggests that contamination is not the cause of the high lead values. However, the low silver values in these samples does tend to suggest the presence of industrial lead. The silver content of industrial lead will have been removed by cupellation whereas 'natural' lead should show some correlation with silver.

One interpretation of the very high lead and zinc values is that the sulphide-rich carbonate rock which outcrops near BH 4 is folded around the nose of an early structure and disrupted by ductile flow within the Ben Eagach Schist, leaving isolated fragments of sulphide-rich material within the schist. This area is obviously worthy of further investigation because of the high base metal values in the soil as well as in BH 4 cores, but its economic potential is limited by the short lateral extent of the mineralisation and the complex tectonic history.

Two sections of the Ben Eagach Schist outcrop on Farragon Hill were covered by shallow soil surveys. The first was on the north-east flank of Farragon Hill in the vicinity of two outcrops of quartz-celsian rock at NN 8446 5559 (CZR 3909, A III, T XI) and at NN 8455 5562 (CZR 3920). Chip sampling at the former locality assayed a maximum of 0.66% Zn, 0.018% Pb and 4 ppm Ag (CZR 3917) over 1 m. The origin of the soil grid was sited at NN 8447 5561 with the baseline at 070°, and four traverses at right angles (100W, 0, 100E and 200E) which were sampled at 10 m intervals.

The band of quartz-celsian rock could not be traced by soil sampling further than 10S on line 0 and 20S on line 100E, locations close to the outcrops. A peak value of 2.3%

Ba is associated with the outcrop. Barium values on the other lines are low but zinc enrichment near the outcrop continues to line 100W at 30S (NN 8439 5555) and 40S with up to 1160 ppm Zn. Another feature with high Pb and Zn, but lacking barium, was found at 100N on line 100W at NN 8434 5567, (460 ppm Pb, 840 ppm Zn) and 90N on line 0 at NN 8444 5569 (1800 ppm Pb, 390 ppm Zn) and this possibly continues through to 50N on line 200E (NN 8464 5573). This second feature may be correlated with the base of the mineralised zone whereas the quartz-celsian rock is near the top, only 15 m across strike from the base of the Ben Lawers Schist. Because of the low barium values in the fine fraction of the soil, baryte-rock is unlikely to be present and because high lead and zinc values are lacking, no further deep overburden sampling was carried out in this area. The presence of the mineralised zone is confirmed and some base metal sulphides are present.

A second, smaller grid was set up on the northern slopes of Farragon Hill with an origin at NN 8396 5541, a baseline running 071° and five traverses at 50W, 0, 50E, 100E and 150E which were sampled at 10 m intervals. The soil samples collected over the Ben Lawers Schist show low barium values with less than 1000 ppm Ba but values rise in the Ben Eagach Schist with up to 0.77% Ba at a distance of 20–30 m north of the junction of the two formations on line 50W. This band of high barium continues a similar distance from the formational junction for 100 m to the east but is not picked up on the two most easterly traverses. Lead and zinc contents are low and only two samples exceed the threshold levels.

Baryte-rock is probably absent from this part of the Ben Eagach Schist outcrop but a relatively thin band of barium-enriched schist or quartz-celsian rock is probably present some 20–30 m north of the Ben Lawers Schist–Ben Eagach Schist boundary. The mineralised zone is obviously reduced in thickness or grade when compared to the Creagan Loch area some 1.3 km to the west.

#### VLF MAPPING

The interpretation of the VLF-EM results in this area is included on Fig. 15. On the southern slopes of Ben Eagach itself (1400W to 2300W) the geology is complex, and the VLF-EM survey could not resolve sufficiently fine detail to allow a very credible interpretation. Further problems are introduced by the steep topographic slope, and a strong artificial anomaly caused by a fence. The boundary between the Ben Lawers Schist and the Ben Eagach Schist can be seen clearly, however, as can a strong anomaly due to a resistive zone near the northern margin of the Ben Eagach Schist. Between 1000W and 1200W this northern margin itself can be recognised. A nose of the northern resistive zone accompanies the mineralisation at BH 4. A few other tentative high resistivity zones have been marked on the interpretation map.

From Lochan a'Chait westwards across the north flank of Farragon Hill the interpretation is more confident, based on clear anomalies and quite good outcrop in an area which has a simple structure. A typical profile in this region has already been discussed (p.19). Although topographic slopes are steep, their effect on the VLF-EM field is probably small in comparison with the anomalies found. A discontinuous minor anomaly within the main Ben Eagach Schist outcrop has been tentatively interpreted as a less conductive band.

## CHARACTERISTICS OF THE MINERALISED ZONE: CREAGAN LOCH TO MEALL TAIRNEACHAN

### GEOLOGY

The geology of the country west of Farragon Hill is dominated by the two main structural features (Fig. 2), the Creag na h-Iolaire anticline and the Sron Mhor syncline, which Sturt (1961) considered to be primary folds. The former is an overturned structure which closes towards the south-east and plunges gently to the south-west. The Sron Mhor syncline, on the other hand, is a more symmetrical structure with a vertical axial plane. By virtue of these two early folds the Ben Eagach Schist outcrop has a strike-length of 10 km within an east-west distance of 3 km.

Between Creagan Loch and Meall Tairneachan the rocks lie on the southern limb of the Creag na h-Iolaire anticline and in general dip steeply southwards, though open folds with gentle westerly plunging axis (F3 of Sturt, 1961) cause local variations in orientation. This is particularly evident on the eastern flank of Creag an Chanaich (between boreholes 2 and 9) where baryte and quartz-celsian bands can be traced through at least three large fold closures.

Over the 1.8 km of strike-length between Creagan Loch (BH 3) and Creag an Chanaich (BH 9) the mineralised zone has far greater continuity both in lateral and vertical extension than to the east of Farragon Hill. The eastern-most mineralised exposure is on the northern slopes of Creagan Loch (BH 3). Immediately west of Creagan Loch exposure is sporadic but there is fragmentary geological and more definite geochemical evidence of continuity in the mineralised zone (Fig. 24, 26) towards Frenich Burn (BHs 1 and 11). To the west of Frenich Burn, bedrock is mantled by thick peat, but geophysical and geochemical surveys indicate that the zone is displaced to the south and connects with the mineralisation at the foot of Creag an Chanaich (BH 2). Westwards from BH 2 the mineralised zone is visible almost continuously for over 500 m and has an exposed vertical extension of at least 80 m (Fig. 29). The valley west of Creag an Chanaich is largely covered by peat but on the northern flank of Meall Tairneachan, some 300 m from the trig point (BH 10), there is a patch of quartz-celsian rock float in excess of 100 m<sup>2</sup>. Occasional boulders of baryte-rock occur to the west near the closure of the Creag na h-Iolaire anticline. Two small exposures of sulphide-bearing quartz-celsian rock are seen on the northern limb of the anticline, about 1.1 km ENE of the closure (Fig. 3), and there is strong geophysical evidence that the outcrop is considerably more extensive. However, despite the presence of several near-complete sections through the Ben Eagach Schist no further mineralisation has been recorded to the north and west.

In detail, the mineralised zone differs from that described in the area east of Farragon Hill, most noticeably in that between Creagan Loch and Creag an Chanaich, it comprises two distinct bands of barian rocks separated by quartzite which is, in part, enriched in barium.

At its eastern end (Creagan Loch; Figs. 24, 27) the upper or more southerly of the barian bands is 5 m below the lowermost Ben Lawers Schist and consists of about 2 m of pyritous quartz-celsian rock and 1.5 m of muscovite-schist. Between this and the lower barian band the succession is made up of 40 m of graphitic schist and quartzite which, though lacking barium, contains appreciable quantities of lead and zinc in the lowermost 10 m. The lower band is dominated by 3–7 m of baryte lying between narrow (<1 m) horizons of pyritous quartz-celsian rock. The northern margin consists of dolomite-rock with celsian,



pyrite and pyrrhotine ranging in thickness from 1 m at surface to 4 m at 16–20 m below. Within the dolomite-rock are several 'breccia' zones with abundant sphalerite and galena (A I, T III) producing assays of 2.1% Zn and 0.7% Pb over 4.7 m.

Below the lower band the barium content of the schist and quartzite diminishes rapidly downwards. The total thickness of the mineralised zone at Creagan Loch is therefore about 60 m.

At Frenich Burn (Figs. 24, 28), in contrast to Creagan Loch, the upper band, comprising quartz-celsian rock with interbedded limestone, is separated from the Ben Lawers Schist by only 1.3 m of dolomitic mica-schist. A zone of broken rock in BH 11 core and the absence of barium enrichment in the lower part of the Ben Lawers Schist, as in BH 9 (Fig. 32), suggest that the lowermost section of the Ben Lawers Schist and the uppermost part of the Ben Eagach Schist have been faulted out.

The lower barian band consists of 15–16 m of baryte at surface with an unknown thickness of dolomitic quartz-celsian rock on the south side. At about 90 m below surface the band has a total thickness of 27 m, comprising quartz-celsian rock interbedded with an almost equal thickness of graphitic schist and quartzite (A I, T XI). However, baryte bands ranging in thickness from 0.20 to 2.00 m and totalling 2.3 m are present in the lowermost 15 m of the mineralised zone.

The schist between the upper and lower bands is variably enriched in barium but, as at Creagan Loch, concentrations die out below the lower band. The total thickness of the mineralised zone at Frenich Burn is about 110 m.

The steep eastern face of Creagan Chanaich together with the core from BH 2 afford an almost complete 100 m vertical section through the mineralised zone (Fig. 29). The section is further enhanced by stacking of essentially flat-lying folds whose median limbs may be up to 40 m long.

The baryte is mostly confined to the upper zone and, as at Creagan Loch, is sandwiched between quartz-celsian rock. Over much of Creagan Chanaich the thickness of baryte is consistently between 3 and 4 m but in BH 2, at the foot of the eastern face, 5.4 m was recorded (A I, T II). This may result from slight tectonic thickening as the low inclination of the beds and the apparent repetition of the baryte band would seem to indicate that BH 2 pierced an F3 closure (Fig. 28). The lower barian band, which occurs 40 m to the north, is poorly exposed, its course being marked mostly by quartz-celsian rock and rare baryte debris. In BH 9 the probable down-dip extension of this band comprised 6 m of quartz-celsian rock with no visible baryte (A I, T IX). Bands of barium enrichment are particularly evident within the intervening graphitic schist (Fig. 32). Anomalous barium concentrations extend for about 4 m below the lower band and also 6 m into the overlying Ben Lawers Schist, giving the mineralised zone a total thickness of 75 m.

Pyrite and pyrrhotine are abundantly distributed throughout the Ben Eagach Schist on Creagan Chanaich and, within the mineralised zone, may be accompanied by sphalerite with minor galena and chalcocopyrite (A I, T IX). In BH 9 two sections totalling 6.3 m assayed 1.3% Zn and 0.4% Pb. Galena is particularly abundant at the westernmost exposure of the upper barian band. It occurs within quartz-celsian rock, but the absence of obvious stratification and the abundance of vein quartz strongly suggests that the enrichment results from remobilisation.

Despite the volume of quartz-celsian rock float on Meall Tairneachan only three bands, 0.14, 0.36 and 0.59 m thick

respectively, were intersected between 18 and 38 m below surface in BH 10 (Fig. 33; A I, T X). They form part of a zone of barium enrichment which extends from the base of the overburden for approximately 40 m down the hole. The mineralised zone intersected on Meall Tairneachan is thus considerably thinner than elsewhere in the district and lacks the upper band of barian rocks. This is almost certainly the result of faulting, since BH 10A intersected a 3 m wide zone of broken rock with poor core recovery at the junction of the Ben Lawers Schist and the Ben Eagach Schist (A I, T XA).

The distribution of base metal sulphides in BH 10 is anomalous in that it bears little relationship to the zone of barium enrichment. Traces of sphalerite, galena and chalcocopyrite are present in the uppermost 13 m of the borehole (A I, T X), but are not seen thereafter until 30 m below the base of the mineralised zone, with the greatest concentration 60–80 m below the main zone of barium enrichment.

### GEOCHEMISTRY

A shallow overburden survey was conducted in 1976 over the ridge known as Creagan Loch between the eastern tributary of Frenich Burn, which drains Lochan Lairig Laoigh, and the main headwater (Fig. 24). The origin was sited at NN 82682 55045, just south of the site of BH 3, and seven traverses from 0 to 600W laid out at 100 m intervals and at right angles to the baseline running 070°. Each traverse was sampled at sites 10 m apart. These traverses end some 130 m east of the site of BH 1. Deep overburden sampling was carried out two years later over the geophysical lines 4920, 5040, 5160, 5280, 5340, 5400, 5460, 5520, 5580, 5650, 5700, 5820, 5940 and 6000W (Appendix IV).

The shallow soil samples collected on the traverse line 0W running through the BH 3 site give the best reflection of the chemistry of the underlying rocks because soil cover is thin on the crags flanking the west side of the U-shaped valley. A very strong barium peak is found over the baryte-rock with up to 59% Ba in the fine fraction (analytical error of  $\pm 15\%$  Ba). This declines over 40 m on the southern side but drops much more sharply on the north to background levels of less than 1000 ppm. There is a slight rise in barium over the junction of the Ben Eagach Schist with the Ben Lawers Schist near the mapped quartz-celsian rock (Fig. 24). Lead and zinc show a similar distribution with a large peak (1.35% Pb, 0.75% Zn, 25 ppm Ag) just south of the sulphide-rich carbonate rock and a gentle decrease southwards.

This geochemical pattern which is seen near BH 3, may be compared to a saw-tooth with a sharp peak on the northern side and a gentle decline southward, followed by a second but smaller peak to the south. On other traverses this pattern is obscured or modified by glacial transport which produces a southerly shift or spread of anomalies. On a few north-facing slopes hill creep and hydromorphic transport produce a slight northward movement of the soil anomaly, and this is particularly noticeable for Zn.

When traced westwards of line 0 the barium values are lower, not exceeding 4% Ba, and this is attributed to dilution in the upper layers of the thicker overburden profile. Several anomalies of  $>0.5\%$  Ba follow the general strike of the mineralised zone and peak values of about 2–3% Ba indicate that quartz-celsian rock or baryte-rock is present (Fig. 26). The anomalous zone thins and is positioned nearer to the boundary of the Ben Eagach Schist and the Ben Lawers Schist on line 100W, widening to full thickness again on line 400W. Deep overburden sampling, however, shows that this impression is erroneous and barium values

$\geq 10\%$  (the emission spectrographic calibration limit) at 10S and 50S on geophysical line 4920W (equivalent to shallow soil line 300W) provide strong evidence that baryte-rock is present at the northern margin of the mineralised zone. Similar values were also found on lines 5040, 5160, and 5280W as far as the outcrop of baryte-rock in French Burn near BH 1 (Fig. 26). The deep overburden sampling therefore demonstrates that baryte-rock is most probably continuous from BH 1 eastwards for at least 420 m and may possibly continue to the site of BH 3, although the two shallow soil traverses 100W and 200W give little indication of its presence.

Lead in the shallow overburden samples shows a broad band of values  $>100$  ppm (the threshold) extending from the origin on line 0 to 80–100N on line 500W and 70–100N on line 600W (Fig. 26). The anomaly is unclosed to the north and west where the mineralised zone is not covered by the shallow overburden sampling grid (Fig. 26). Zinc shows a rather similar pattern with a high on line 0 over the exposed mineralisation, a gap on line 100W and a broad belt of anomalous values from 40N on line 200W to 90N on line 500W. The anomaly is open-ended northwards from 70–100N on line 600W (Fig. 26). An unusual feature is the presence of a small and coherent anomaly in Ba (up to 1%), Zn (300 ppm) and Pb (100 ppm) running from 80S on line 300W to 100S on line 600W. The anomaly is situated south of the southern boundary of the Ben Eagach Schist. It may be due to mineralised material glacially transported from the mineralised zone in the Ben Eagach Schist or it may represent a tectonic repetition of the mineralised zone.

The deep overburden traverses on lines 5160, 5040 and 4290W show the same geochemical pattern for barium as the shallow overburden traverse through BH 3, namely background values of about 1000 ppm Ba to the north of the zone, a sharp rise to  $\geq 10\%$  Ba at its northern edge due to baryte-rock, and an irregular decline to the south with some values of 1% Ba over the mineralised zone before a small rise (around 3% Ba) over the contact with the Ben Lawers Schist. Lead and zinc behave very similarly to barium with a sharp peak of up to 0.2% Pb and 0.3% Zn at the northern side of the mineralised zone, dropping off rather irregularly to the south to levels of about 40 ppm Pb and 100 ppm Zn over the Ben Lawers Schist. This geochemical pattern compares closely with the distribution of metals in BH 11 where there is a concentration of barium (up to 40% Ba) close to the base and an irregular decrease of barium (1–20% Ba) upwards with about 0.15% Pb and 0.3% Zn over some 34 m of core (Fig. 28 and CYD 777–779, A II, T XI). Lower values of barium (0.1–1%) lead (1–20 ppm) and zinc (15–140 ppm) are present until the Ben Lawers Schist junction where there is a rise to around 10% Ba, 0.12% Pb and 0.052% Zn (CYD 752). The observed correlation between the deep overburden geochemistry and the borehole data emphasises the value of the sampling method in gaining an accurate picture of the chemistry of the underlying rocks in this drift-covered district.

West of BH 1 deep overburden samples were collected only where the geophysical work showed a weak negative crossover or inflexion in the VLF in-phase component. This inflexion is not readily apparent on geophysical lines 5460W to 5640W and a fault was identified running NNE – SSW, approximately along the course of French Burn. The deep overburden traverse to the west of BH 1 (line 5400W) shows relatively low values of barium (maximum 1.0% Ba), lead and zinc, indicating that the baryte-rock does not continue with the same strike as seen at outcrop in the stream. Either the baryte-rock swings parallel to the fault or the

fault is situated some 10–20 m further east than indicated by the geophysical data (Fig. 25).

On traverses 5460W, 5520W, 5580W, 5640W and 5700W, barium levels are  $<1\%$  and generally in the range 1000–2000 ppm (see A IV). Baryte-rock and quartz-celsian rock are probably absent because of displacement by the fault. Zinc values, however, are anomalous on traverses 5700W and 5640W, reaching 7.6% (with 13.1% Fe but only 30 ppm Pb in sample CYS 55) at 130S on line 5640W, and 0.53% Zn at 130S on line 5700W (sample CYS 43). Zinc mineralisation is indicated, possibly as remobilised sulphide in the fault zone which is deduced from geophysical evidence to pass through 130S on line 5640W.

On the west side of the French Burn fault the baryte-rock was easily located by the deep overburden sampling on line 5820W with sites 210, 220, 230, and 240S all showing greater than 10% Ba in the fine fraction and up to 44% Ba in the heavy mineral concentrate. Traverse 5940W which runs just to the west of BH 2 shows lower barium levels (up to 0.87% Ba in sample CYS 13). This feature may be the result of failure to reach the base of the overburden as the anomalous sample was collected at a greater depth (2.60 m) than those from the rest of the traverse (see A IV). Zinc also reaches significant levels (0.36% Zn) in this sample. The next traverse to the west has one value of  $\geq 10\%$  Ba (sample CYS 6) showing that the baryte-rock continues to the foot of the steep crags of Creag an Chanaich which were not sampled.

Thus in the district of upper French Burn deep overburden sampling was very successful in demonstrating that the baryte-rock is continuous for some 420 m east of BH 1 and for over 200 m on the west side of the fault. Combined with the rapid VLF-EM geophysical method it is a very powerful technique for proving continuity of the baryte-rock. The occurrence of possible remobilised sulphide along the fault is also indicated.

The Ben Eagach Schist outcropping between the northern flank of Meall Tairneachan and the site of BH 9 was covered by a shallow overburden sampling survey with an origin near BH 10 at NN 80731 54704, with a base-line running 101° and seven perpendicular traverses at 0, 100, 200, 300, 400, 500 and 550E. Deep overburden sampling was limited to geophysical line 6480W and three samples on line 6540W.

Samples from the shallow soil traverses on the ridge east of BH 9 (500E and 550E) show a good geochemical response to the underlying rock types. Two parallel bands with anomalous barium levels are seen, a northern one with values  $>1\%$  Ba over the mapped quartz-celsian rock (baryte float also occurs on this band) and a southern one with values  $>10\%$  Ba over the baryte-rock and flanking quartz-celsian rock (Fig. 31). The southern anomaly continues at slightly lower levels to line 200E but the northern one is reduced to values of  $<1\%$  Ba on line 400E. Zinc and lead are anomalous over the whole mineralised zone in the east (Fig. 31) but the anomalies split further west into distinct northern and southern bands, which tend to be quite far apart on line 200E. This splitting may be illusory because of increased overburden thickness in the ground between the bands where the westernmost headwater of French Burn rises in a deep, peat-filled depression. Nearly all the samples from traverse 0 are anomalous with values peaking at 4.7% Ba near the area of loose quartz-celsian rock. Fairly extensive zinc anomalies are also found over 60 m of traverse length with zinc  $>150$  ppm, peaking at 720 ppm. Lead is less dispersed but again shows the pattern of two distinct bands, one near the Ben Lawers Schist contact and the other some 50 m to the north which reaches 880 ppm Pb.

Deep overburden sampling on geophysical lines 6480 and 6540W yielded marked barium anomalies with up to 5% Ba in the fine fraction at 200N on line 6480W (CYS 182) indicating that baryte-rock is most probably present. Similar levels in the three samples on line 6540W indicate that the baryte-rock extends to this point so that 900 m strike-length of baryte-rock can be predicted to occur west of the Frenich Burn fault. The mineralised zone continues for another 50 m west to BH 10 but from the borehole evidence baryte-rock is absent.

In conclusion the deep overburden sampling method provided evidence for the continuation of the baryte-rock for 900 m west of the Frenich Burn fault and nearly to BH 10. This evidence is crucial in the valley of the westernmost tributary of Frenich Burn where there is a relatively thick cover of peat and overburden. On the broad ridge near BH 9 which has good outcrop and only shallow soil cover geological mapping and shallow soil sampling are quicker and more efficient methods of investigation than deep overburden sampling.

### *VLF MAPPING*

Most of this area lies in the nose of the Creag na h-Iolaire Anticline, with the Ben Lawers Schist lying both north and south of the Ben Eagach Schist. The VLF-EM maps are relatively easy to interpret on the broad scale, but problems of resolution arise in attempts to define detail. Fig. 30 shows the eventual interpretation.

To the east of BH 3, conditions are straightforward, with the margins of the Ben Eagach Schist against the Carn Maig Quartzite in the north, and against the Ben Lawers Schist in the south reasonably well defined by a maximum and a minimum, respectively, in the in-phase component profiles. Within the Ben Eagach Schist lie several zones of higher resistivity. A particularly strong anomaly of this type lies between 3900W and about 4350W. It is about 40 m wide, and at its eastern end runs into the anomaly associated with the boundary of the Ben Lawers Schist and the Ben Eagach Schist.

Between boreholes 3 and 2 the graphitic schist outcrop is at its widest (approximately 1.3 km). The Fraser filter map of this area superimposed on the geological map is given as Fig. 25. At first glance there is good agreement between the geological and geophysical evidence, particularly with respect to the position of the northern boundary of the Ben Eagach Schist. To the south of this boundary linear, positive Fraser filter bands indicate resistive horizons within the graphitic rocks. There is little geological information on the causes of these features because of the mantle of drift in this area, but weakly mineralised quartzite debris is present and a high lead anomaly was obtained in the drainage survey.

The most striking feature of Fig. 25 is a NE-SW trending positive Fraser filter band with a negative to its south, which is likely to be due to a fault offsetting the Ben Eagach Schist-Ben Lawers Schist boundary by about 250 m. Reduced resistivities along the interpreted zone give rise to the crossover and the Fraser filter low; this is a normal "narrow conductor" type anomaly. The fault seems to divide in the north, one branch swinging west to join the slide forming the northern boundary of the Cairn Maig Quartzite and the other heading north to disrupt the northern margin of the Ben Eagach Schist.

The effect of closely interbanded conductive and non-conductive lithologies on VLF-EM readings is to produce only weak anomalies, giving a poor signal to noise ratio and rather poor agreement with the geological map in detail.

This is one of the principal drawbacks of the VLF-EM method, as endorsed by the poor results obtained near the southern boundary of the Ben Eagach Schist between Creagan Loch and Meall Tairneachan. Nevertheless, in areas of poor exposure, such as that between Creagan Loch and Creag an Chanaich, the VLF-EM survey, when combined with geochemical data, contributed significantly towards the geological interpretation.

The Carn Maig Quartzite in the nose of the Creag na h-Iolaire anticline plunges beneath the Ben Eagach Schist. The broad VLF-EM low due to the quartzite extends westwards as far as the interpreted fault, suggesting that the nose is longer and more tapered than indicated by outcrop evidence alone. It is not possible to recognise any feature which corresponds to the graphitic schist-quartzite boundary, however, suggesting that the plunge of the fold may be at a low angle.

Fig. 30 shows the VLF-EM profiles, Fraser filter contours and interpretation superimposed on the geological interpretation in the area west and north of BH 2. It shows how the geophysical interpretation was built up. The northern boundary of the graphitic schist is sharply defined by a real component minimum and a steep Fraser filter gradient. It does not agree precisely with the boundary inferred from geological evidence, but outcrop in this area is sparse. Two strong anomalies, each about 50 m wide and due to high resistivity bands within the graphitic schist, lie to the south of the boundary between the Ben Lawers Schist and the Ben Eagach Schist, coinciding with two exposures of weakly mineralised rocks in the stream. Both high resistivity zones can be traced for over 2 km from the fault truncating them in the east until they fade out in the west. Since outcrop is so poor here the causes of these anomalies are not adequately known. Several other, weaker resistive zones are indicated within the graphitic rocks further south.

The known mineralisation, along the southern edge of the Ben Eagach Schist around BH 9, occurs in an area of relatively complex geology — that is, thin bands of graphitic schist alternate with more resistive rocks, over about 100 m and the sequence has local folds of about 50 m wavelength. The resolution of the VLF-EM survey is not sufficient to expect perfect agreement with geology in ground of this type, but general agreement is reasonable. West of 6300W, the southern margin of the Ben Eagach Schist is clearly visible to 7200W and may extend further. The fading of these boundary features westwards may once again indicate a shallow angle of plunge for the Creag na h-Iolaire Anticline.

## **DISCUSSION AND CONCLUSIONS**

### *GENESIS OF MINERALISATION*

Dalradian sedimentation and diagenesis were followed by tectonism and metamorphism and, in considering the genesis of the Ben Eagach deposit, it is important to distinguish between primary features and later metamorphic effects. Textural and structural evidence show that the mineralised rocks have been subjected to strong recrystallisation and deformation, and the mineral assemblage and fabric of pelitic rocks adjacent to them indicate that this took place in several stages, the metamorphic maximum (amphibolite facies) being reached after development of an early penetrative schistosity. The deposit is thus clearly not of post-orogenic origin. The overall stratabound nature, the strongly interbanded character of the component lithologies and the frequency of sharp boundaries between them indicate that a pre-metamorphic origin is likely.

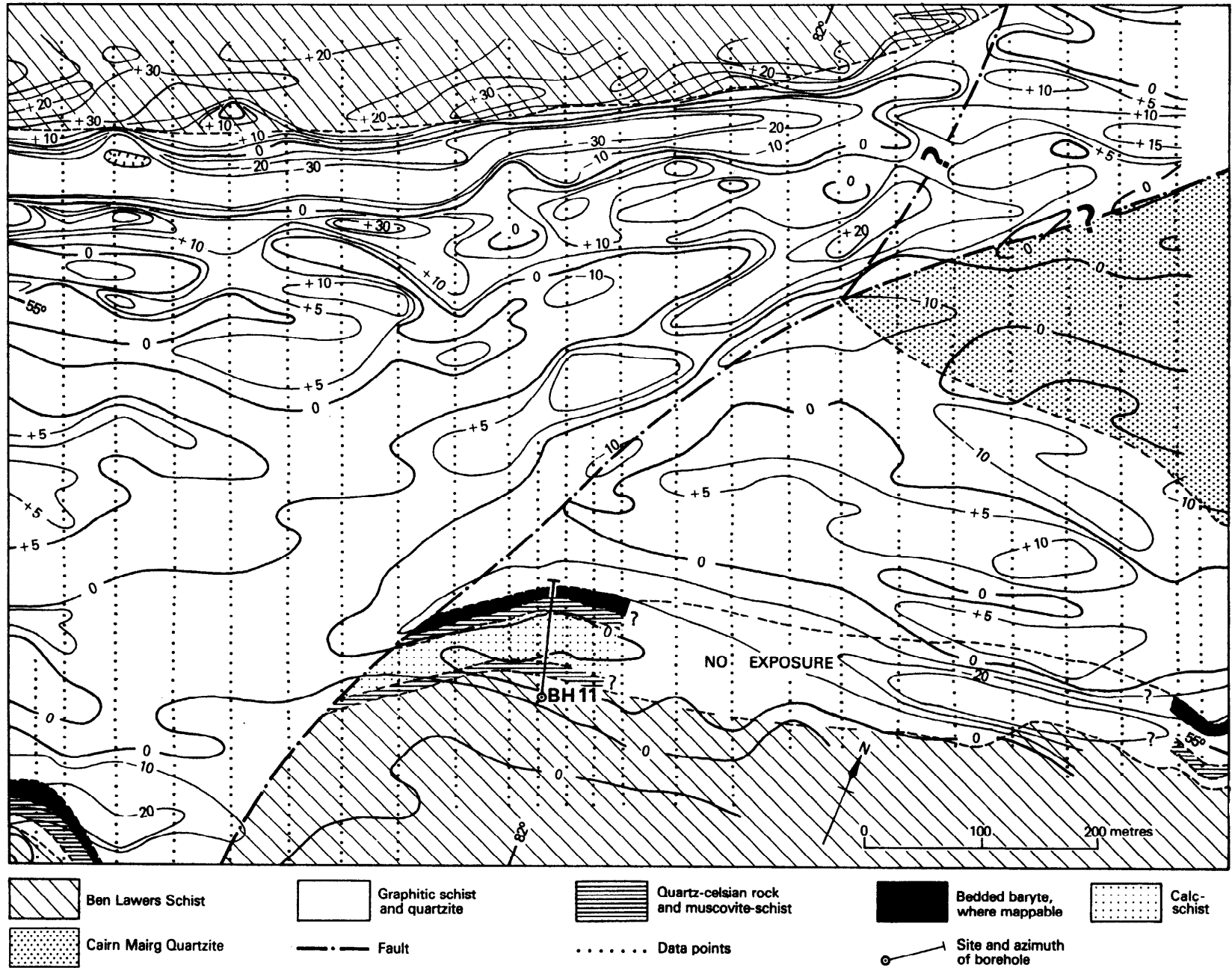


Fig 25 Fraser-filtered VLF real component data over the area of French Burn headwater; located on Fig 13

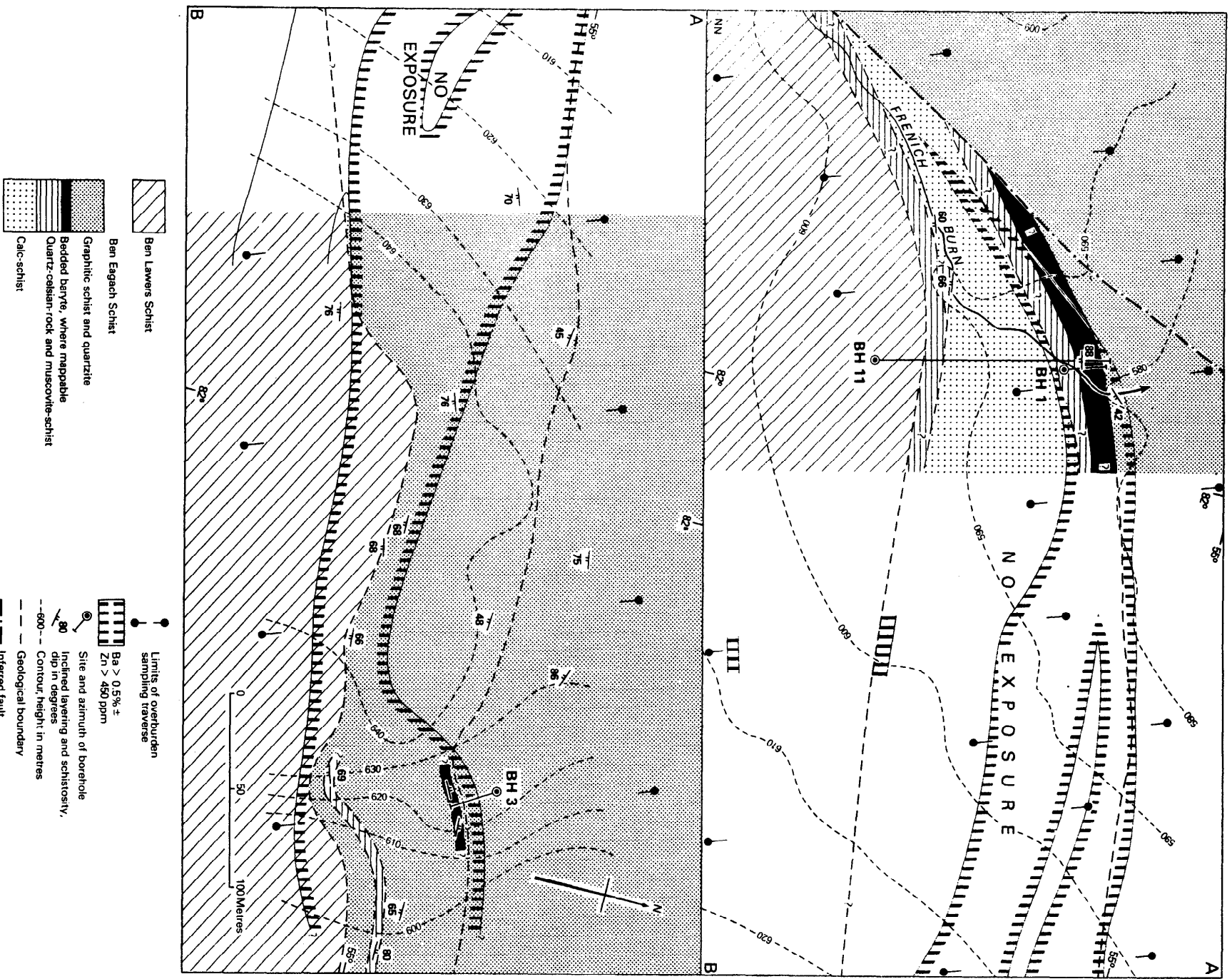
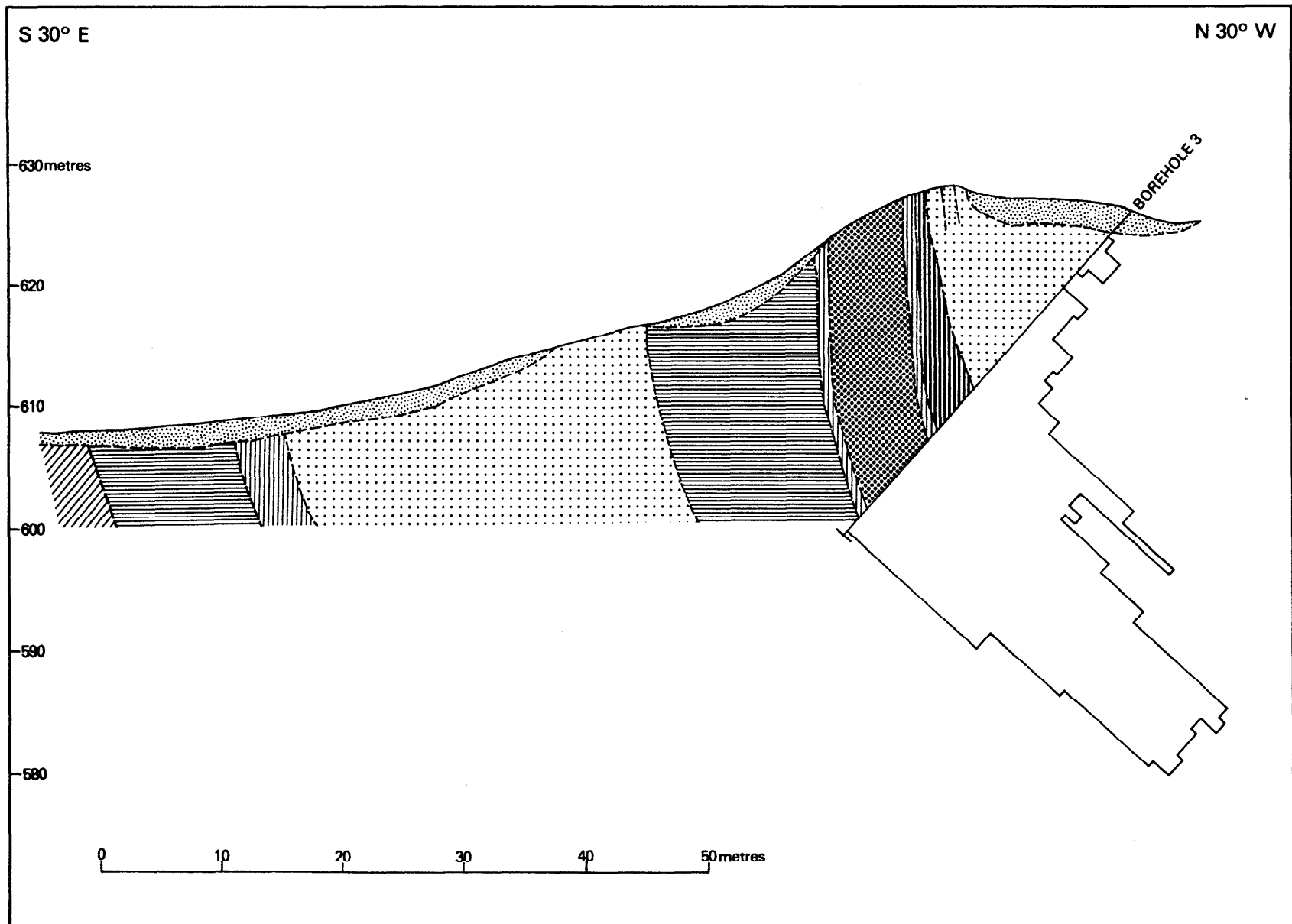


Fig 26 Geology, mineralisation and barium distribution in overburden, Upper French Burn (above) and the area north of Creagan Loch (below); A-B is a common boundary



**Fig. 27 Section through borehole 3, north of Creagan Loch; located on Figs. 24 and 26; legend as Fig. 21.**

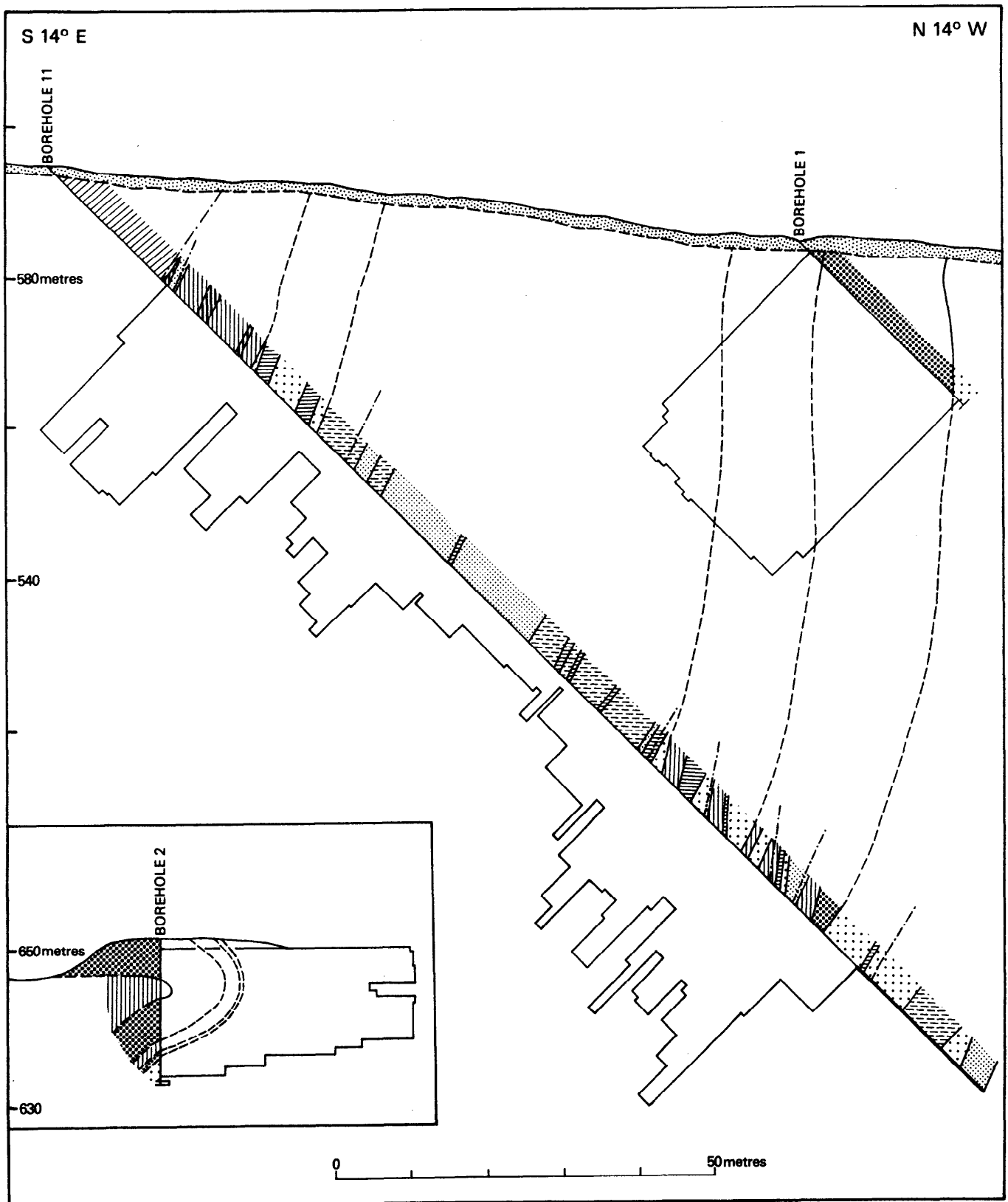


Fig 28 Section through boreholes 1 and 11, upper French burn, and borehole 2, Crag an Chanaich; located on Figs. 24 and 29; legend as Fig. 21

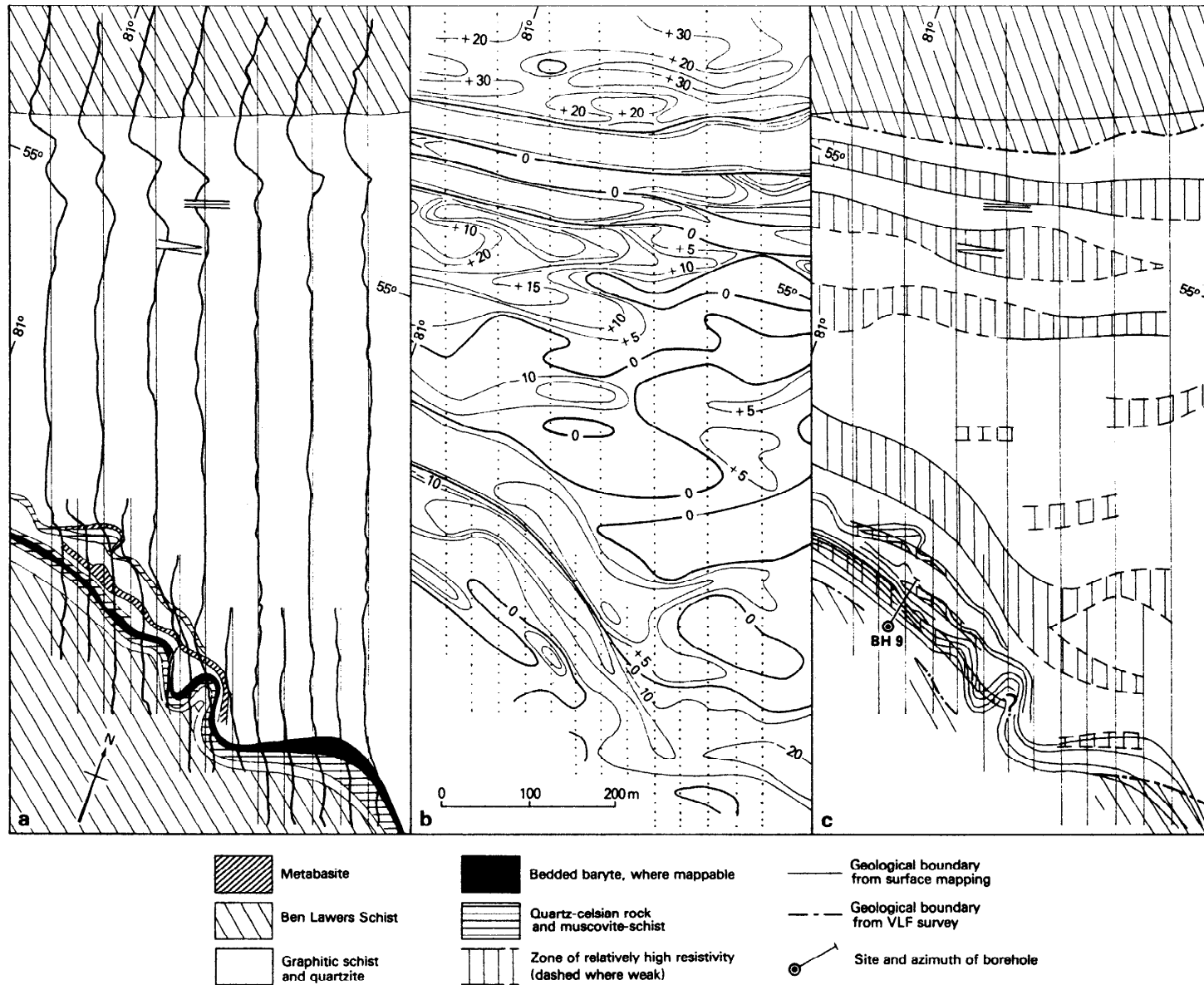


Fig 30 Real component profiles (a), Fraser-filtered real component data (b) and outline geology and geophysical interpretation (c) for part of the area located on Fig 13; the diagonally striped ornament on (c) represents the geophysically inferred suboutcrop on the Ben Lawers Schist



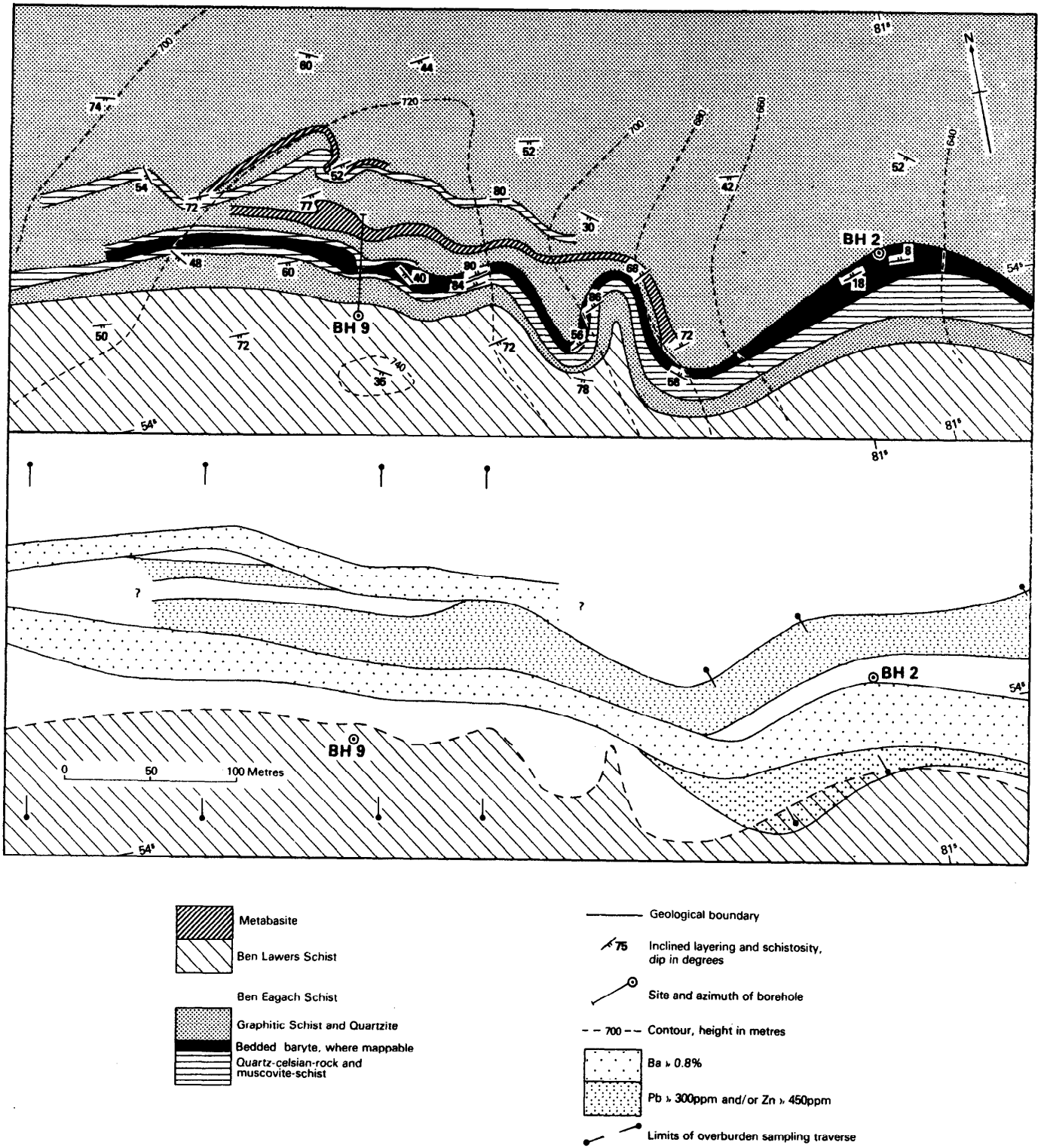


Fig 31 Geology, mineralisation and barium distribution in overburden, between Creag an Chanaich and Meall Tairneachan; zinc and lead anomalies are shown where not coincident with barium anomalies

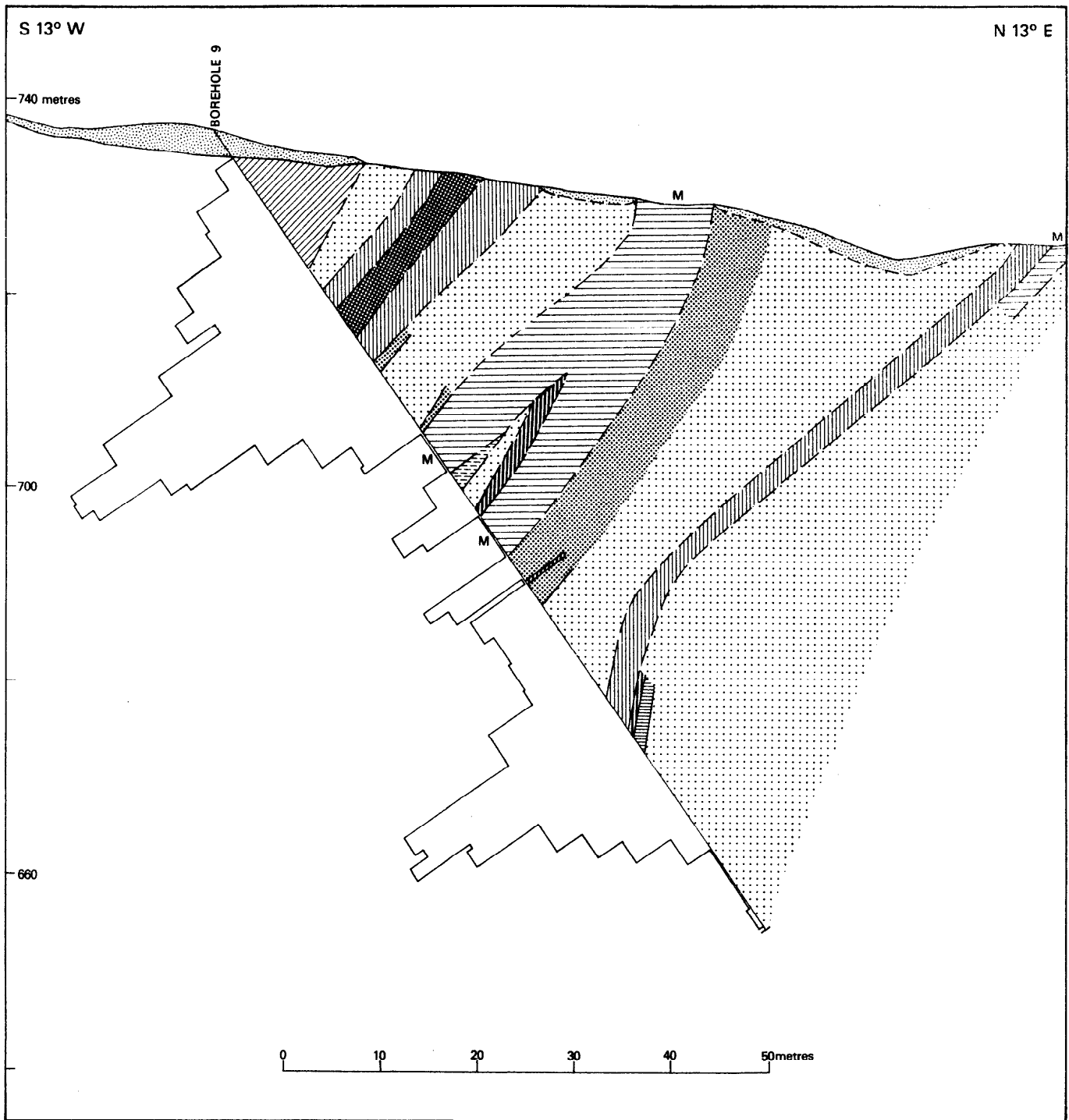
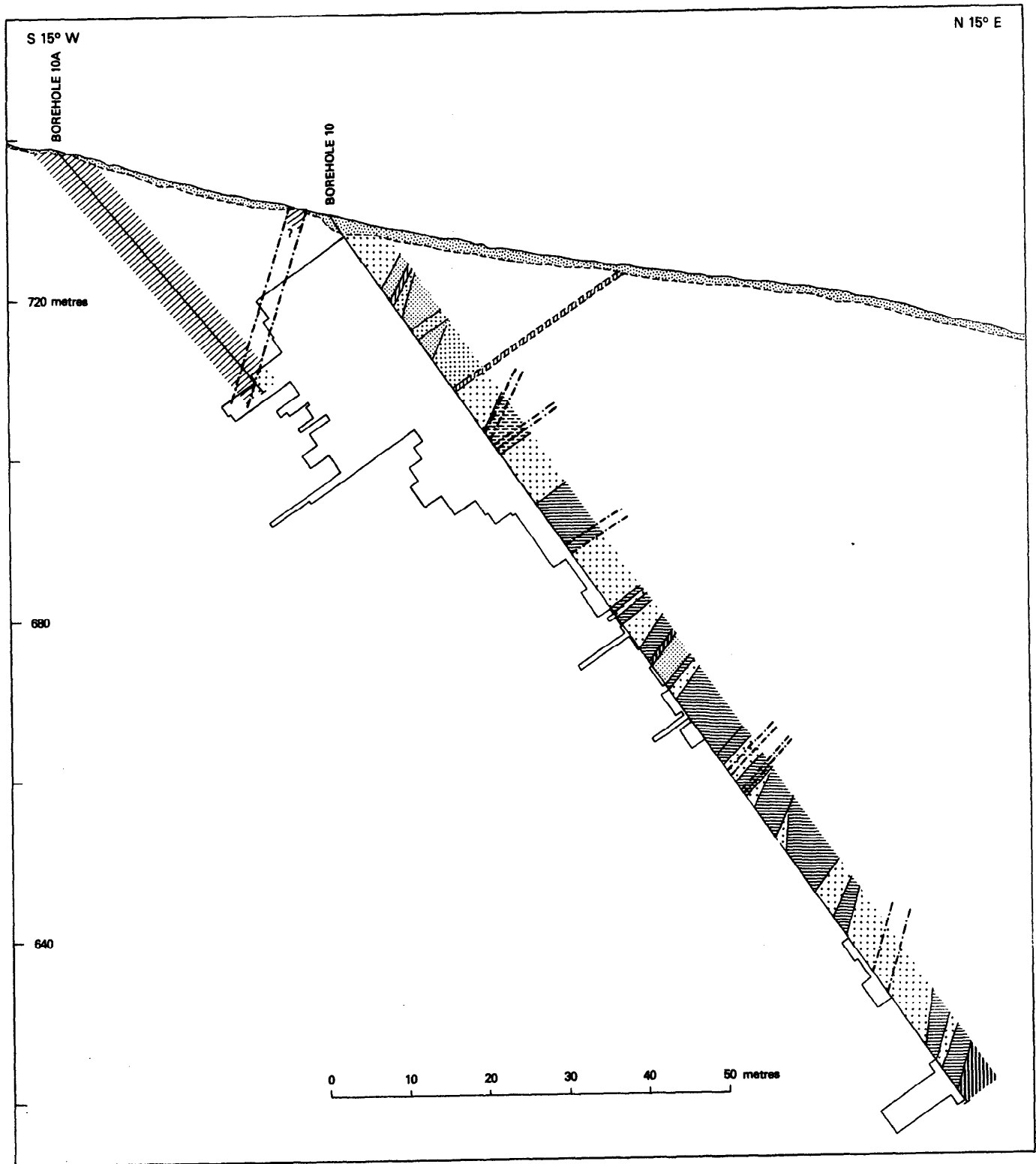


Fig. 32 Section through borehole 9, Creag an Chanaich; located on Fig. 29; legend as Fig. 21.



**Fig. 33 Section through boreholes 10 and 10A, north of Meall Tairneachan; located on Fig. 29; legend as Fig. 21.**

The deposit lacks many of the hallmarks of an epigenetic, replacement or vein-controlled origin. Its strictly stratiform nature and the presence of fine interbanding with undoubted metasedimentary rocks are difficult to reconcile with such an origin, such features being uncharacteristic of introduced hydrothermal lodes such as those of the Teign Valley (Beer and Ball, 1977). Systematic zonation of the mineralised sequence, such as might suggest the operation of diffusion fronts or a progressive sequence of episodic mineralisation, has not been observed save, perhaps, in the distribution of cryptic mineralisation which occurs, however, in rocks of metasedimentary origin. A small amount of local remobilisation is evident but may be attributed to metamorphic or later effects.

The unusual composition of the baryte-rock and carbonate-rock, together with their low content of clastic material, suggest formation by rapid chemical precipitation. The quartz-celsian rock commonly has a cherty, finely banded appearance and is interbanded with contrasting lithologies of metasedimentary origin. It also forms an envelope around the bodies of baryte-rock, but its chemical composition is distinct from both the baryte-rock and the barium-enriched schists (Coats, Smith and others, 1980). A compositional gap exists between the quartz-celsian rock, with up to 25% Ba, and the baryte-rock with greater than 35% Ba and this is confirmed mineralogically by the lack of samples containing both baryte and celsian. The formation of the quartz-celsian rock by a reaction between baryte and sedimentary material is therefore improbable. Celsian occurs in some of the barium-enriched schist, replacing mica, but the lack of samples with between 4 and 6% Ba, i.e. intermediate between the barium-enriched schist and the quartz-celsian rock, seems to preclude the operation of a continuous process of barium metasomatism of normal pelitic material. It can therefore be inferred that the quartz-celsian rock was derived from a precursor formed on the sea floor with substantially its present chemical composition, and that it had a predominantly chemical origin, although modern analogues for the deposition of such material are lacking. The adjacent graphitic schist and muscovite-schist have the appearance of normal pelitic metasediments but their chemical composition clearly indicates that metals such as barium, lead, zinc and manganese have been incorporated. It is concluded therefore that the deposit is of synsedimentary to diagenetic origin and was formed on or near the contemporaneous sea floor.

The association of conformable, lensoid beds of massive baryte with black shale and cherts has been recorded at many of the world's stratiform baryte - base-metal deposits including Meggen (Zimmerman, 1970; Amstutz and others, 1973), Barberton Mountain Land (Heinrichs and Reimer, 1977), Nye County, Nevada (Shawe and others, 1969) and North Pole, Western Australia (Hickman, 1973). However, with the possible exception of Rosh Pinah (Page and Watson, 1976), Aberfeldy differs from all other known baryte-base-metal deposits in its high barium silicate content, although such minerals could remain undetected where the metamorphic grade was insufficient to produce coarsely crystalline celsian.

The depositional environment that prevailed throughout much of the Dalradian trough at the time of deposition of the Ben Eagach Schist has been interpreted (Harris and others, 1978) as one of basins and swells, with organic-rich black mud accumulating in the former, whilst the highs were areas of non-deposition or of calcareous sedimentation. The graphitic, non-micaceous character of the host rock indicates slow sedimentation with anaerobic conditions in the substrata. In such an environment, sulphate-reducing

bacteria would generate  $\text{HS}^-$ , with the resultant production of an upward diffusing reduction front (Rickard, 1973), below which precipitation of sulphides could occur. The resulting mineral assemblage, dominantly now pyrrhotine and pyrite, would reflect metal-contents in pore-water. At present, similar depositional conditions are found in the Black Sea, the Red Sea, the Baltic and even in fairly open coastal waters (Rickard, 1973; Degens and Stoffers, 1979; Weber-Diefenbach, 1979).

The enrichment in Ba, Zn, Pb and other metals in the Ben Eagach deposit implies the participation of a metal-enriched brine of probable hydrothermal origin (Weber-Diefenbach, 1979). Direct evidence of hot spring activity has not been observed and the deposit does not appear to be proximal to major igneous bodies. However, there are some indirect pointers to the existence of thermal features in the area at the time of deposition. Rocks of metabasic character occur in one restricted part of the area (Figs. 29, 31, 32), and the overlying Ben Lawers Schist contains an appreciable volume of chloritic schist and minor amphibolites which can be interpreted as metamorphosed tuffs and lavas. When the Ben Eagach Schist is traced to the north-east it undergoes a facies change to quartzite and this is probably related to the emergence of the Ben Vrackie volcanic centre in Ben Lawers Schist times. Signs of basic igneous activity have also been noted in the older Killcrankie Schist. It may be postulated that thermal energy associated with the rising basic magma could have stimulated leaching of the underlying crust by meteoric or connate waters. Alternatively, the hydrothermal fluids could be of juvenile origin derived from an unrecognised or concealed igneous source rock. Whatever the origin of the fluids a source of brine with appreciable quantities of dissolved Ba, Fe, Zn, Pb, Mn, Si, and, perhaps Ca, Mg and Al must have been available for reaction and precipitation. The mineralised zone is located at or very close to the upper boundary of the Ben Eagach Schist and was therefore developed at a time of changing depositional environment. This change may have been accompanied by faulting which could have provided the passages necessary for the brine to circulate.

A possible model for the Ben Eagach deposit envisages the introduction of a metal-rich hydrothermal brine on to the sea floor under anaerobic, sulphate-reducing conditions. In a dense, cooling brine layer beneath the sulphate-sulphide reduction front, precipitation of  $\text{FeS}_2$ , ZnS and PbS would take place. The carbonate phases of the matrix could have been formed from the brine at very high salinities or have been precipitated from warm overlying marine waters. Under conditions of agitation or rapid input the brine could become mixed with overlying sulphate-bearing sea water, causing rapid precipitation of baryte with minor pyrite and sphalerite. Further dilution with sea water would cause the oxidation potential to rise sufficiently to precipitate magnetite and baryte. Factors including the rate of brine input, its density, sea water evaporation, degree of mixing and the rate of clastic sedimentation may have caused frequent changes, bringing about a succession of chemically contrasting layers.

The origin of the barium silicates is more problematic. Textural evidence indicates that during the formation of the metamorphic fabric, reaction between baryte and barium silicates did not occur and the fine interbanding was unaffected. Moreover, the baryte represents only a relatively minor part of the total barium within the mineralised zone. It is therefore suggested that the black organic-rich muds, which were the precursor of the graphitic schists, were enriched at the sedimentary or early diagenetic stage. Slow percolation of the hydrothermal fluids into the pore water

may have allowed adsorption of barium on to clay minerals and also enriched the rock in sphalerite and galena. This would explain the presence of this 'cryptic' mineralisation peripheral to, and of greater extent than, the more massive ore. The quartz-celsian rock may have been formed by complete diagenetic alteration of sedimentary material, precipitated on the sea floor as a barium-rich silica-alumina gel as suggested by its cherty aspect, or as a mixture of quartz and barium-zeolite such as harmotome which has been reported from deep sea cores in the Pacific (Boles, 1977). Barium-silicates formed at this early stage would have been reconstituted during metamorphism to yield celsian, hyalophane, barian muscovite and cymrite, whose present textures are thoroughly metamorphic.

#### ECONOMIC SIGNIFICANCE

The new baryte, sphalerite and galena mineralisation occurring near Aberfeldy forms part of a thick and persistent mineralised zone defined principally by a remarkable concentration of the barium silicates, barian muscovite and celsian. The zone is 60–110 m thick. It is known to occur, at least intermittently, over a 7 km strike length and through a vertical interval of 370 m, from the stratigraphic top of the Ben Eagach Schist in BH 8 at 370 m OD to the collar of BH 9 at 737 m OD. Repetition of the Ben Eagach Schist by folding over the westernmost 2 km of strike represents a significant addition to the potentially mineralised strike length.

#### Baryte.

On the available information, baryte-rock developed in the western part of the mineralised zone between Creagan Loch and Meall Tairneachan constitutes the material of most economic significance. The true thickness of the main baryte band in this area varies from 2.3 m to 15.5 m and it occurs over a vertical interval of 200 m in outcrops and borehole intersections at intervals along 1.8 km of strike length. The best evidence of lateral continuity is in the Creagan an Chanaich district, where a 3.6 m band of baryte at surface is the same thickness at 30 m depth (BH 9) and can be mapped along strike for about 400 m, despite the effects of open F3 folds some 30 m in amplitude. Folding of this kind probably accounts for the thicker intersection of nearly 10 m intersected in BH 2.

The sharp reduction in the thickness of baryte, from 15.5 m close to surface to 2.3 m at a depth of 90 m, in the Frenich Burn district (boreholes 1 and 11) is attributable to either folding, faulting or pronounced lenticularity of the baryte bands. A new NE–SW trending fault zone has been recognised in this district and evidence of faulting is present in the cores from BH 11.

The presence of strong barium anomalies in overburden along unexposed sections of the western part of the mineralised zone, notably for 300 m west of BH 9 on Meall Tairneachan and over 650 m between Frenich Burn and Creagan Loch, provides encouraging evidence of the continuity of the baryte bands, but the thickness is uncertain. Near Creagan Loch a 6.4 m band of baryte was recorded in BH 3.

Over the 5 km of strike length of the mineralised zone eastwards of Creagan Loch, the occurrence of baryte-rock is limited. On the south-western side of Ben Eagach a single band, 2.0–2.5 m thick, is recorded but because of structural complexity its strike-extension is probably small and certainly no more than 350 m. In the Creagan an Fhithich district, lenses or fault-disrupted bands of baryte have a projected lateral extent of 350 m. The thickness of baryte decreases

sharply, from 11.3 m at surface to 6.0 m at a depth of about 14 m (BH 5), and 1.4 m at about 28 m (BH 7). While there is some evidence of faulting in the section represented by boreholes 5 and 7 rapid lensing out of the baryte units is considered to be the main reason for the poor lateral continuity.

Thus, the main economic potential for baryte in the Aberfeldy mineralised zone clearly lies in the western sector. The influence of folding and faulting on the baryte bands will nevertheless require detailed study.

The chemical and mineralogical composition of the Aberfeldy baryte-rocks varies appreciably (see Tables 12 and 14), but because sulphide minerals are commonly present as impurities there is not a well-defined relationship between  $\text{BaSO}_4$  content and specific gravity. The  $\text{BaSO}_4$  content of typical samples of baryte-rock from boreholes 1–5 averages 86% (75–99%) and the specific gravity  $4.0 \text{ g cm}^{-3}$  (3.5–4.6  $\text{g cm}^{-3}$ ). Calcium and strontium levels are below 1%.

#### Base metals

The zinc and lead contents of certain units in the Aberfeldy mineralised zone are fairly high but reach levels comparable with those of economic deposits only at one locality. In BH 4 on Ben Eagach, the average metal content over an estimated true thickness of 4.3 m is 8.5% Zn and 3.6% Pb. The lateral persistence of the varied lithologies comprising this intersection is not likely to exceed that of the associated baryte-rock (350 m maximum) and the extension in depth could only be estimated by further boring.

Thinner intersections of moderately high grade, and several low grade intersections, were also located; for example 6.8% Zn and 0.49% Pb over 0.7 m (BH 2); 4.7 m of 2.1% Zn and 0.7% Pb (BH 3); 0.95% Zn and 0.25% Pb for 4.3 m and 1.7% Zn, 0.45% Pb over 2.0 m (BH 9). Sparse sphalerite-galena mineralisation was intersected in zones 10.5 m and 8 m thick in BH 11 and is persistently developed in units of quartz-celsian rock totalling 20 m in BH 7. The degree of lateral continuity of the sulphide mineralisation is best illustrated by the results of overburden sampling on Meall Tairneachan where well-developed zinc and lead anomalies occur over at least 0.5 km of strike length (see Fig. 31).

The rocks of the Aberfeldy mineralised zone exhibit general enrichment in silver as well as barium, zinc and lead (Table 5). Copper levels, however, are low. The mean metal ratio in rock samples from boreholes 1–5 is  $\text{Zn}_{73} \text{Pb}_{27}$ . The silver content of the galena itself is in the range 700–1500 ppm Ag (Table 16) and significant traces of antimony are also present.

#### Barium silicates

Although celsian and barian muscovite have no industrial application at the present time, their occurrence in such large quantities has not previously been recorded and some research on their properties for commercial usage might therefore be justified.

#### Mineral zoning

The lithological studies reported here suggest that variation in the metal content of individual lithologies could provide evidence of metal zonation along the strike length of the mineralised zone. From the limited number of analyses available, zinc and lead appear to be twice as abundant in graphitic schist samples from the western section than in those from the eastern sector but this simple conclusion is not born out by a more sophisticated statistical study. However, much more detailed sampling will be required to confirm this suggestion and to provide a basis for the study

of other lithologies. An assessment of the overall potential of the zone, and of the equivalent rocks in the Dalradian Succession, could well depend on the solution to this question of zoning.

#### ACKNOWLEDGEMENTS

The Institute would like to express gratitude to the several landowners in the Aberfeldy area for their co-operation and help over an extended period, and in particular to Major D.H. Butter, the Forestry Commission, Major N.G. Ramsay, Major T.W.M. Whitson, and Major W.D. Gibson.

This investigation arose from the initial stimulus of G.S. Johnstone who provided helpful advice and encouragement throughout. Other colleagues who contributed substantially to the work in this report are:

R. Falconer, B. Scarth and K. Jacobs for drilling and power auger sampling; G.D. Easterbrook, J.A.T. Smellie, A.M. Shilston, B.R.H. Skilton and B. Beddoe-Stephens for mineralogy; D.J. Bland, D. Hutchison, B.P. Vickers, D. Peachey, B.A.R. Tait and T.K. Smith for chemical analysis; D.A. Briggs, D.A.W. Bernard, D.J. Bland and J.A. Bain for beneficiation studies, and Ms. S. Pease for geophysical and levelling work.

Figs. 2, 4a, 5a, 11, 12, 13, 14, 18, 19, 25, 26, 30 and 31 are reproduced by permission of the Institution of Mining and Metallurgy.

#### REFERENCES

- Amstutz, G.C., Zimmermann, R.A. and Schott E.H. 1971. The Devonian mineral belt of Western Germany (the mines of Meggen, Ramsbeck and Rammelsberg). In *Sedimentology of parts of central Europe: guidebook to 8th international sedimentology congress, Heidelberg, 1971*. Muller G. ed. (Frankfurt-on-Main: Waldemar Kramer), 253–272.
- Beer, K.E. and Ball, T.K. 1977. Mineral investigations in the Teign Valley, Devon, Part 1 – Barytes. *Mineral Reconnaissance Programme Rep. Inst. Geol. Sci.*, No 12, 26p.
- Boles, J.R. 1977. Zeolites in deep-sea sediments. In *Mineralogy and Geology of natural zeolites*. Mumpton, F.A. ed., *Mineral. Soc. Amer. Short Course Notes*, Vol. 4, 137–163.
- Chayes, F. 1960. On correlation between variables of constant sum. *J. Geophys. Res.*, 65, 4185–93.
- Coats, J.S., Smith, C.G. and others, 1978. Stratabound barium-zinc mineralisation in Dalradian schist near Aberfeldy, Scotland: Preliminary report. *Mineral Reconnaissance Programme Rep. Inst. Geol. Sci.*, No. 26, 43p.
- Coats, J.S., Smith, C.G. and others 1980. Strata-bound barium-zinc mineralisation in Dalradian schist near Aberfeldy, Scotland: *Trans. Instn. Min. Metall. (Sect. B: Appl. Earth Sci.)*, 89, B110–22.
- Deer, W.A., Howie, R.A. and Zussman, J. 1962. Rock-forming minerals, Vol. 5. *Non-Silicates*. (Longmans), 371p.
- Degens, E.T. and Stoffers, P. 1979. Phase boundaries as an instrument for metal concentration in geological systems. In *Time and Strata-bound ore deposits*. Klenn, D.D. and Schneider, H.J. eds (Berlin: Springer-Verlag), 25–45.
- Essene, E.J. 1967. An occurrence of cymrite in the Franciscan formation, California. *Amer. Mineral.*, 52, 1885–1890.
- Fraser, D.C. 1969. Contouring of VLF-EM data. *Geophysics*, Vol. 34, 6, p. 958–967.
- Grout, A. and Gallagher, M.J. 1980. Barium determination in rock and overburden by portable XRF spectrometer. *Trans. Instn. Min. Metall. (Sect. B: Appl. Earth Sci.)*, 89, B 130–3.
- Harris, A.L., Baldwin, C.T., Bradbury, H.J., Johnson, H.D. and Smith, R.A. 1978. Ensialic basin sedimentation: the Dalradian Supergroup. In *Crustal evolution in Northwestern Britain and adjacent regions*. Bowes, D.R. and Leake, B.E. eds. (Seel House Press: Liverpool), 115–138.
- Harris, A.L. and Pitcher, W.S. 1975. The Dalradian Supergroup. In *A correlation of the Pre-cambrian rocks in the British Isles. Spec. Rep. Geol. Soc. London*, 6, 52–75.
- Heinrich, E.W. and Levinson, A.A. 1955. Studies in the mica group; X-ray data on roscoelite and barium-muscovite. *Amer. Journ. Sci.* 253 39–43.
- Heinrichs, T.K. and Reimer, T.O. 1977. A sedimentary barite deposit from the Archaean Fig Tree Group of the Barberton Mountain Land (South Africa). *Econ. Geol.*, 72, 1426–1441.
- Hickmann, A.H. 1973. The North Pole barite deposits, Pilbara Goldfields. *Geol. Surv. West. Aust. (Ann. Rep. 1972)*, 57–60.
- Hutchinson, C.S. 1974. Laboratory handbook of petrographic techniques. (Wiley Interscience, New York), 527p.
- Johnstone G.S. and Gallagher, M.J. 1980. Compilation of strata-bound mineralisation in the Scottish Caledonides. *Mineral Reconnaissance Programme Rep. Inst. Geol. Sci.*, No. 37, 6p.
- Kamp, P.C. van de, 1970. The Green Beds of the Scottish Dalradian Series: geochemistry, origin, and metamorphism of mafic sediments. *Journ. Geol.*, 78, 281–303.
- Lambert, I.B. and Sato, T. 1974. The Kuroko and associated ore deposits of Japan: a review of their features and metallogenesis. *Econ. Geol.*, 69, 1215–1236.
- Leake, R.C. and Aucott, J.W. 1973. Geochemical mapping and prospecting by use of rapid automatic X-ray fluorescence analysis of panned concentrates. *Br. Geochemical Exploration (London: IMM)*, 389–400.
- Lepeltier, C. 1969. A simplified statistical treatment of geochemical data by graphical representation. *Econ. Geol.*, 64, 538–550.
- Marsden, G.R. 1977. Geophysical surveys near Creag an Fhithich. *Inst. Geol. Sci. Applied Geophysics Unit [Unpublished report]*.
- Page, D.C. and Watson, M.D. 1976. The lead-zinc deposit of Rosh Pinah Mine, South-West Africa. *Econ. Geol.*, 71, 306–327.
- Parker, M.E. 1980. VLF electromagnetic mapping of strata-bound barium-zinc mineralization in Dalradian schist near Aberfeldy, Scotland. *Trans. Instn. Min. Metall. (Sect. B: Appl. Earth Sci.)*, B: 123-9.
- Paterson, N.R. and Ronka, V. 1971. Five years of surveying with the VLF-EM method. *Geoexploration*, 9, 7–26.
- Ramdohr, P. 1969. The ore-minerals and their intergrowths. (Pergamon Press: Oxford) 1174p.
- Rickard, D.T. 1973. Limiting conditions for synsedimentary sulphide ore formation. *Econ. Geol.*, 68, 605–617.
- Runnells, D.D. 1964. Cymrite in a copper deposit. Brooks Range, Alaska. *Amer. Mineral.*, 49, 158–165.
- Shawe, D.R., Poole, F.G. and Brobst, D.A. 1969. Newly discovered bedded barite deposits in East Northumberland Canyon, Nye County, Nevada. *Econ. Geol.*, 64, 245–254.
- Smith, C.G. and others. 1977. Investigation of stratiform mineralisation in parts of central Perthshire. *Mineral Reconnaissance Programme Rep. Inst. Geol. Sci.* No. 8, 83p.
- Sturt, B.A. 1961. The geological structure of the area south of Loch Tummel. *Q. Jl. Geol. Soc. London*, 117, 131–156.
- Tait, B.A.R. and Coats, J.S. 1976. A rapid method for the analysis of trace elements in rocks, stream sediments and soils by photographic emission spectrography

using a semi-automated method of plate evaluation.  
*Rep. Inst. Geol. Sci.*, No. 76/11, 30p.

**Telford, W.M., King, W.F. and Becker, A.** 1977. VLF mapping of geological structure. *Geol. Surv. Canada* Paper 76-25.

**Vine, J.D. and Tourtelot, E.B.** 1970. Geochemistry of black shale deposits – a summary report. *Econ. Geol.*, 65, 253–272.

**Weber-Diefenbach, K.** 1979. Geochemistry and diagenesis of recent heavy metal ore deposits at the Atlantis II Deep (Red Sea). In Time and Strata-bound ore deposits. Klenn, D.D. and Schneider, H.J. eds. (Berlin: Springer-Verlag), 419–436

**Wedepohl, K.H.** (Ed), 1969. Handbook of geochemistry.

**Whittles, A.B.L.** 1969. Prospecting with Radio Frequency EM-16 in mountainous regions. *Western Miner*, Feb. 1969. p. 51–6.

**Zimmerman, R.A.** 1970. Sedimentary features of the Meggen barite-pyrite-sphalerite deposit and a comparison with the Arkansas barite deposits. *Neues Jahrb. Miner. Abh.*, 113, 179–214.

## APPENDIX I

### BOREHOLE LOGS AND SUPPLEMENTARY NOTES

Detailed logs of the 11 boreholes drilled in this investigation are given here, preceded by notes on each borehole intended to supplement the logs. Tables I to XI represent boreholes 1 to 11 respectively.

In the logs, the column headed "Structure angle" contains the following angular measurements:

- F: angle of foliation plane relative to core axis.
- B: angle of compositional banding relative to core axis.
- C: angle of crenulation cleavage relative to the plane of foliation at the same location.

In the columns headed "Lithology" and "Mineralisation" reference is made to polished thin sections (PTS), detailed descriptions of which are given in the corresponding tables in Appendix III. Note that where baryte-rock is a principal lithology it is not referred to in the Mineralisation column. The final column in the logs shows "Assay Sample" numbers, permitting cross-reference to the corresponding tables in Appendix II.

#### *Borehole 1 (Table I)*

This borehole was drilled at 45° to the NNW immediately below the extensive baryte outcrop in French Burn. A true thickness of 15.5 m of baryte-rock was intersected, sandwiched between two bands of dolomitic quartz-celsian rock below which were 15 m of graphitic schist. Banding in the baryte-rock is generally inclined at 55° to the core axis implying a steep southerly dip (Fig. 28).

The calculated BaSO<sub>4</sub> content of the baryte-rock is 77–99%, quartz and dolomite forming the main impurities. Sulphides are locally concentrated in bands, for example at 12.80–14.13 m where the core assays 1.1% Zn (see A II, T I). The overall iron content of the baryte-rock is less than 1% Fe attributable to pyrite and magnetite. Celsian occurs unusually in certain sulphide-rich bands within the baryte-rock.

#### *Borehole 2 (Table II)*

This vertical hole was sited on a knoll of baryte-rock in which finely-developed banding dips northwards at 8–18°. In the borehole core the dip is apparently more variable (20–50°), probably due to folding. The following sequence was intersected:

Lithology	True thickness (m)
Baryte-rock	4.4
Quartz-celsian rock and quartzite	1.1
Baryte-rock	5.5
Quartz-celsian rock and muscovite-schist	1.5
Graphitic schist	3.5

The sequence of units immediately below the upper baryte band is similar to that seen on the eastern slopes of Creag an Chanaich and together with the unusually low dip of the banding suggests that the upper baryte band may represent a folded repetition of the lower band (Fig. 28). Flat-lying folds are visible on Creag an Chanaich (Fig. 29). The somewhat greater thickness of the baryte bands intersected in the borehole, compared with measurements on surface exposures, may have resulted from tectonic thickening in a fold closure.

In the lower band of quartz-celsian rock 6.8% Zn and 0.49% Pb were present over a true width of c. 0.7 m. High levels of Ag and Sb are associated with this lithology (see A II, T II). Sphalerite and galena also occur in the graphitic schists in the lowest part of the borehole.

#### *Borehole 3 (Table III)*

This hole was collared 17 m north of the mineralised exposure at Creagan Loch and inclined 45° SE to provide a continuous section through the mineralised rocks. The borehole intersection correlated closely with the surface exposures except for the absence of the calc-biotite rock found at the northern margin of the outcrop. Foliation measurements in the upper part of the borehole indicate a constant and steep northerly dip but lower in the intersection dips based on compositional banding are very variable, implying the effects of folding.

The schists encountered in the upper part of the borehole are locally enriched in sphalerite and to a lesser extent in galena. They are followed by a sulphidic dolomite-rock previously referred to as a calcareous quartz-celsian rock (Coats, Smith and others, 1978, p23). Assays over the interval 19.63–25.02 m, a true thickness of approximately 4.7 m, average 2.1% Zn and 0.7% Pb (A II, T III). The dolomite-rock contains coarse crystals of apple-green celsian and in places exhibits a fragmental texture similar to that observed in BH 4. Beneath it lies a thick band of baryte-rock about 6.4 m in true thickness, having a calculated BaSO<sub>4</sub> content of 75–85%. Sphalerite and galena are quite common in quartz rock and graphitic schist below the baryte-rock.

Thus sphalerite and galena are present at significant levels in several different lithologies in this section through the mineralised zone.

#### *Borehole 4 (Table IV)*

In this section schists containing about 1% Ba are followed by a band of massive baryte-rock, estimated to have a true thickness of 2.0 m and a BaSO<sub>4</sub> content of 90%. Sphalerite and galena are common in subsequent units of calcite- and dolomite-rock, fragmental rock and quartz-celsian rock. The average metal content of this varied assemblage over the interval 17.31–23.44 m, an estimated true thickness of 4.3 m, is 8.5% Zn and 3.6% Pb (A II, T IV).

#### *Borehole 5 (Table V)*

Three thin bands of baryte-rock totalling about 2.3 m in true width and a thicker band of about 3.6 m were intersected in this borehole. The baryte-rocks are fairly pure, having an equivalent BaSO<sub>4</sub> content of 83–99%. The remainder of the section is essentially made up of quartz-celsian rock, some of which is dolomitic. One example, at 19.01–21.42 m depth, was originally referred to as a quartz-rock with some baryte (Coats, Smith and others, 1978, p 33). Correlation between the borehole section and surface exposures requires some lensing out or sharp folding of quartz-celsian bands and the thinner baryte-rock.

#### *Borehole 6 (Table VI)*

This hole was drilled southwards beneath some small exposures of quartz-celsian rock and muscovite-schist on the crest of a low ridge 350 m WSW along strike from holes 5 and 7 (see Fig. 17). It was intended to explore the extension of the mineralisation in depth but, because of faulting, no mineralisation was intersected (see Fig. 22).

Core recovery in the fault zones was poor (66% at 54.15–60.22 m; 79% at 112.15–136.30 m) but overall a recovery of 96.5% was achieved. There was also a marked shallowing of the hole from 45° at surface to 35° at the base, probably due to the acute angle made by the fault planes to the borehole (Fig. 22). Above the main fault zone at around 120 m inclined depth the foliation angles measured on the cores suggest that the schists dip northwards at a moderate angle. Below this zone, where shallowing of the borehole is most likely to have taken place, measurements



indicate that the foliation in the schists is closer to the vertical.

The main part of the borehole section from the collar to the lamprophyre at 110 m is formed of chlorite-mica-schists and quartz-mica-schists which are variably dolomitic or calcareous and occasionally garnetiferous. Geochemically, the rocks are consistently enriched in barium, notably between 32 and 83 m, attaining a maximum of nearly 3% Ba around 49 m inclined depth (see A II, T VI). Pyrite and pyrrhotine are erratically developed in this zone of schists. Despite the absence of graphitic lithologies these rocks are regarded as part of the Ben Eagach Schist. Below the lamprophyre intrusion and within the main fault zone are graphitic schists and a quartzite at 127–132 m which is barium-enriched, followed by dolomitic, graphitic and chlorite-sericite-schists previously assigned to the Ben Lawers Schist (Coats, Smith and others, 1978). Although barium values in these rocks are low it is considered that on lithological criteria the rocks should be retained in the Ben Eagach Schist. The junction with the stratigraphically higher Ben Lawers Schist is taken at 149 m inclined depth with the appearance of calc schist, hornblendic in part and occasionally garnetiferous.

#### *Borehole 7 (Table VII)*

This borehole was drilled beneath BH 5 in order to determine the extension of the baryte bands in depth. The topmost 20 m of the borehole section (see Fig. 20) lies in calc-schist which is appreciably enriched in barium and zinc (see A II, T VII). The next 50 m consists of nine units of massive quartz-celsian rock, three sharply-bound thin bands of baryte-rock and muscovite-schist. The total true thickness of baryte is only about 1.4 m compared with nearly 6 m in BH 5. The quartz-celsian rock totals about 20 m and has weighted average contents of 0.45% Zn and 0.14% Pb. Sphalerite and galena also occur in the muscovite-schist.

Below the celsian-rock are some 40 m of the graphitic schist characteristic of the Ben Eagach Schist. They contain low but anomalous barium values and can be regarded as part of the mineralised zone which is therefore at least 110 m thick in this section. Barium values decrease sharply at the contact of the graphitic schists with hornblendic calc schists of the Ben Lawers Schist.

#### *Borehole 8 (Table VIII)*

The objective of this borehole was to investigate coincident geochemical and geophysical anomalies lying on the strike extension of the mineralised zone defined by BH 7 some 430 m to the WSW (Fig. 17). The hole was inclined southwards, approximately at right-angles to the strike of the schists exposed near the borehole collar in Allt Coirein a' Chinn (usually referred to as Middleton Burn).

Faulting is common in the topmost 90 m of the borehole (see Fig. 21) and core recovery, at 91% overall, was significantly reduced in the vicinity of the fault zones, namely:

Inclined depth, m	% recovery
12.50–18.25	61
38.78–49.00	78
49.40–53.18	49
54.46–62.09	80
69.32–72.68	80
80.90–91.03	92

The junction of the Ben Lawers Schist with the Ben Eagach Schist in the inverted sequence is at 165.60 m. In the Ben Eagach Schist baryte-rock is absent and the development of quartz-celsian rock is limited to a unit about 2.5 m

thick intersected at just below 100 m inclined depth. The barium content of the Ben Eagach Schist is nevertheless anomalous throughout much of the intersection and zinc and lead values commonly exceed 0.1% (A II, T V III).

#### *Borehole 9 (Table IX)*

This hole was sited in the basal units of the Ben Lawers Schist and inclined northwards to obtain a full section through the mineralised zone in the Ben Eagach Schist (see Fig. 29–31).

The northerly azimuth of the borehole runs approximately at right angles to the foliation observed in exposures of Ben Eagach Schist dipping at 40–60° southwards. Measurements of foliation on the upper 50 m of core suggest the dip may steepen, but readings over the lower part of the borehole are more in keeping with surface observations. The additional presence of crenulation cleavage and orientation variations in banded quartz-celsian rock would seem to confirm that the rocks have been affected by more than one episode of faulting. Direct evidence of faulting is very limited but broken and lost core recorded at 26 m inclined depth may mark a minor fault.

Although the top of the Ben Eagach Schist is taken as the first appearance of graphitic muscovite-schist at 17.7 m there is evidence of metal enrichment in the Ben Lawers Schist in the interval 6.2–17.7 m (see A II, T IX). In addition, garnet and hornblende are absent from the basal calcareous and dolomitic muscovite-schists of the Ben Lawers Schist intersected in BH 9.

The Ben Eagach Schist consists of graphitic and dolomitic muscovite-schists which are sometimes chloritic and occasionally biotitic. Dolomites or dolomite-rich schists are fairly common and thin limestones form a minor lithology. Units of quartz-celsian rock enclose the single baryte band which is equivalent in thickness (3.4 m true width) to that seen at surface. Anomalous barium values are widespread in the muscovite-schists within the mineralised zone. Porphyroblastic celsian and, unusually, porphyroblastic tourmaline and almandine garnet are locally present in the schists.

Two massive units 4–5 m thick with ill-defined contacts are correlated with the southernmost of the two metabasite sills mapped at surface (see Fig. 32).

Pyrite is particularly common in quartz-celsian rock and pyrrhotine in graphitic schist. Sphalerite and subsidiary galena are enriched in a wide range of lithologies – quartz-celsian rock, celsian-bearing schist, muscovite-schist, dolomite and limestone. Values of 0.95% Zn, 0.25% Pb were obtained over a true width of 4.3 m (26.60–31.52 m depth) and 1.7% Zn, 0.45% Pb over 2.0 m (54.89–56.95 m depth). The sulphides occur in bands parallel to the bedding plane foliation, as disseminations and also in hair-line veinlets signifying local remobilisation during deformation of the Ben Eagach Schist. In the rocks regarded as Ben Lawers Schist, levels of barium and base metals are fairly low but so too are metal levels in the weakly garnetiferous Ben Eagach Schist intersected in the bottom-most 10 m of the bore. Traces of chalcopyrite may occur but copper contents rarely exceed 100 ppm.

#### *Borehole 10 (Table X)*

This hole was drilled in an area of relatively poor exposure to investigate barium anomalies in soil and a large area of celsian-rich float. It was intended to collar the hole in Ben Lawers Schist but unsuitable ground conditions necessitated the rig being sited approximately 3 m north of the Ben Lawers–Ben Eagach Schist boundary. Because the hole was subsequently found to have commenced in barium-enriched schist a second hole (BH 10A) was sited 30 m to the south

and drilled on the same azimuth ( $015^{\circ}$ ) and inclination ( $50^{\circ}$ ). This azimuth is perpendicular to the strike of the foliation recorded in nearby exposures of Ben Lawers Schist.

Borehole 10 is cored entirely in Ben Eagach Schist and the average inclination of foliation relative to the core axis is  $62^{\circ}$ , which may be interpreted as a southerly dip of  $68^{\circ}$ . Considerable disruption of the core is evident ranging from minor crumpling to intense buckle folding. Crenulation cleavage is often well developed in the more pelitic lithologies. Fault zones, as evidenced by broken core and/or core loss were noted at 33.71–34.70 m; 50.77–52.64 m, 80.72–89.38 and 117.18–120.18 m. In the latter zone incipient brecciation and clay gouge are also present.

The core consists mainly of interbanded graphitic muscovite-schist and quartzite with minor limestone and chlorite-mica-schist which is in part calcareous and in other places quartzose. The quartzite is also patchily calcareous, commonly micaceous and invariably carries garnets. Between 14 m and 26.68 m there are three bands of calcbiotite-rock which because of their high iron and titanium contents are thought to be basic metavolcanic rocks.

Pyrrhotine and usually lesser pyrite occur ubiquitously in trails and patches while pyrite occurs commonly in veinlets which are thought to be products of remobilisation. Traces of sphalerite, galena and chalcopyrite appear in the uppermost 13 m and again below 67 m. Sphalerite is the commonest being particularly in evidence between 98 and 104 m and between 113.14 and 113.42 m.

#### *Borehole 10 A (Table XA)*

This borehole was drilled to determine the Ben Lawers-Ben Eagach contact which was not located in the poorly exposed ground explored by BH 10. Foliation angles in the cores average about  $70^{\circ}$ , suggesting that the schists dip southwards at approximately  $60^{\circ}$ . Muscovite-chlorite-schists attributable to the Ben Lawers Schist were intersected until just above the Ben Eagach Schist contact where only muscovite-schist is present. Here, the foliation angle in the core suggests that the schists are vertical and core recovery was also very poor, features possibly related to faulting close to the formation contact. A short intersection of graphitic schist in the bottom of the borehole is typical of the Ben Eagach Schist found in the upper part of BH 10.

It is notable that garnet and porphyroblastic hornblende are absent from this basal section through the Ben Lawers Schist and the lowermost 7 m, as in BH 9 have enhanced barium values which are attributed to barian muscovite.

#### *Borehole 11 (Table XI)*

This hole was 100 m SSE of BH 1 with the same azimuth and inclination and was intended to intersect the lower mineralised band at about 90 m below surface. It was also hoped that the siting would permit more detailed investigation of the calc schist above the lower mineralised band which was known to have anomalously high barium concentrations.

The uppermost 23 m or so were cored in Ben Lawers Schist and the remainder in Ben Eagach Schist. The average angle of intersection with the bedding is  $66^{\circ}$  giving a true southerly dip of about  $69^{\circ}$  which is in accord with surface measurements. Variations in the bedding inclination with respect to the core axis range from  $15$  to  $90^{\circ}$ . Crumpling and more intense buckle folding are evident with occasional crenulation and rare boudinage. Signs of movement (e.g. shearing, slickensiding, rock polish) are common and a major fault zone cuts the Ben Lawers Schist between 21.50

and 21.85 m within which the rocks are reduced to small slices with intervening clay bands. Further fragmentation of the rock was noted at 56.14–56.34 m, 123.50–123.60 m and 132.18–132.27 m with incipient brecciation in parts.

The Ben Lawers Schist consists almost exclusively of calcareous chlorite-sericite-schist with randomly orientated (garbenschiefer) hornblende and garnet porphyroblasts. The hornblende crystals become smaller and less abundant in the lowermost 3 m. A limestone band is present just above the contact.

A notable feature of this section is the dearth of graphitic schist in the upper 80–90 m of the Ben Eagach Schist, the section being dominated instead by calcareous and dolomitic mica-schists and chlorite-mica-schist which superficially resemble Ben Lawers Schist though lacking the garbenschiefer rocks. Graphitic muscovite-schist predominates below 90 m inclined depth in the hole. The Ben Eagach Schist also includes minor amounts of mica-schist, quartzite and limestone.

The mineralised zone has a total (true) thickness of about 110 m and comprises two bands of barian rocks separated by 65–70 m of barium-enriched schist. The uppermost band consists of approximately 15 m of interbanded quartz-celsian rock and subordinate limestone, whereas the lower is made of quartz-celsian rock and minor baryte interbanded with an almost equal volume of graphitic schist and quartzite, and has a total thickness of 30 m.

Pyrite and pyrrhotine occur throughout the core in varying amounts with notable concentrations in some of the quartz-celsian bands where pyrite may form up to 50 per cent of the core. Both iron sulphides form patches and trails; pyrite in addition is present in veinlets. Sphalerite and lesser galena are consistently present in the lower barian bands and in the immediately underlying graphitic schists. Values of 0.55% Zn, 0.21% Pb were obtained over an estimated true width of 10.5 m (140.90–152.83 m depth). Higher in the borehole (111.33–120.42 m) values of 0.50% Zn, 0.37% Pb are developed over a true width of about 8 m.

Inclined depth #	Inter-section #	Structure angle	Lithology	Mineralisation	Sample CYD No
0.00					
2.50	2.50		Superficial deposits		
			Dolomite-rock with celonian, pyrite, minor quartz, and local calcite. Base of unit marked by 10cm of broken, iron-stained core transitional to the following bed.	Pyrite occurs as low level dissemination and discrete thin layers 0.5 to 10cm apart. Minor sphalerite	45
4.50	2.00	F 55			46
			Baryte-rock; coarse, massive rock with thin pyritic bands, minor quartz and accessory fuchsite. Minor dolomite is likely	Pyrite, in layers and thin disseminations, accompanied by minor magnetite	
5.45	0.95	B 60			47
			Baryte-rock; conspicuously banded with thin <0.5cm layers of baryte-, quartz-, and pyrite-rich rocks. Below 5.95m becomes more uniform, white, sulphide-free baryte-rock crossed by thin pyritic bands, some with accessory chlorite. Limonitic fracturing prominent at c.6.50m	Discrete layers of pyrite and magnetite are common. Below 5.95m magnetite exceeds pyrite in volume	
6.60	1.15	B 60			
			Baryte-rock; massive with poorly developed layers spaced 1-3cm apart. Biotite occurs as an accessory in the layers	Pyrite and magnetite are thinly disseminated and in thin discrete layers	48
7.20	0.60	B/F 70			
			Baryte-rock; banding generally present and becomes prominent from 7.70 to 8.00m, and 8.30m onward. From 8.00 to 8.30m the rock is white baryte-rock lacking opaque grains. Quartz, chlorite and ?fuchsite present. Calcite occurs at 7.80m. In all baryte-rocks dolomite is a likely constituent (Appendix III, Table I)	Pyrite and magnetite are common in thin conformable layers and thinly disseminated	49
8.90	1.70	B 60			
			Baryte-rock [PTS 4080, 4081, 4082, 4083]; banded monotonously with minor quartz and likely dolomite. Chlorite is an accessory but micas rarely observed in hand specimens. An opaque-rich band at 10.60m [PTS 4080] contains celonian as major constituent. Celonian also occurs at 15.35m. Dark mica is an accessory from 14.90 to 15.90m. At 12.40m is a thin band of fragmental rock rich in sulphide-bearing veinlets	Pyrite is accompanied by varying subordinate amounts of red sphalerite and galena. Limonitic staining of fractures is frequently present. ?Magnetite is a rare minor constituent and traces of chalcocopyrite are present	50
15.80	6.90	B 60 - 45			51
			Baryte-rock [PTS 4084, 4085, 4086] more variegated than above. 15.90 - 16.15m is a chloritic baryte-rock. Below this the rock is broadly banded. A slightly cross-cutting quartzose layer occurs at 16.48m. Dolomitic bands occur at 16.57 and 18.90m. Fragments of baryte-rock set in a chloritic matrix occur in a fissure at 17.25m. Limonitic fractures are also found below 17.70m. Calcite hair veinlets with minor pyrite at 16.65 and 17.50m. Below 17.50m the rock is porous and possibly leached. The base of the bed is enriched in sulphides and the 20cm above contain ovoid, sulphide-rich patches up to 5cm across. Fuchsite occurs in all three thin sections and rutile in PTS 4084	Pyrite and lesser sphalerite are common, mostly present in parallel bands. Galena is a minor constituent, observed at 18.50m and in PTS 4085 and 4086. Pyrrhotine occurs in PTS 4084 (16.80m) and chalcocopyrite is present in all three thin sections	52
19.14	3.34	B 65			53
			Quartz-biotite-schist; lamination thrown into tight pygmaic folds	Pyrite grains observed	54
19.29	0.15				
			Baryte-rock [PTS 4087, 4088, 4089, 4090]; commences as baryte-bearing quartz-rock for c.20cm, then baryte-rock with minor quartz and dolomite. Chlorite, muscovite, biotite and fuchsite are also present. Limonitic fractures are common from 19.70 to 20.10m and at 28.05m. From 20.50 to 22.00m the rock is monotonously banded. Hair veinlets with calcite and grains of remobilised pyrite are found at some points. Calcite is disseminated at 21.60m and 24.10 - 24.60m. Below 22.00m the banding is slightly irregular with sulphide lenses, chlorite-veined pyritic quartz-rock [PTS 4088 from pyritic rock adjacent to the band of quartz-rock contains celonian in sulphide-rich layers interbanded with baryte-rock and quartz-rock], and zones of fragmental-textured rock 25.60-26.60m, 28.00-28.40m, and below 28.80m to the dolomite-rich end of the intersection. These textures include breccia-like structures and rocks with "cognate clasts" set in baryte-rock	Pyrite is the main opaque phase throughout, although magnetite is common from 19.32 to 21.50m and intermittently below this depth. Sphalerite occurs as a minor, intermittent constituent, often accompanied by galena and traces of chalcocopyrite. Opaque minerals occur thinly disseminated as well as in common, parallel mineral bands	55
28.75	9.46	B 70			56
					57
					58
					59
29.00	0.25	B 60			
			Dolomite-rock [PTS 4091]; pale fragmental rock merging into the foregoing. Quartz, celonian, rutile and chlorite are present	Pyrite is a minor constituent	59
30.50	1.50	F 60			60
			Carbonaceous muscovite-schist [PTS 4092]; texturally uniform rock variously dolomitic and calcareous. At 29.72 and 30.27 are 10cm bands of calcareous schist with sulphides. Quartz is a minor but ubiquitous constituent	Pyrite occurs disseminated and in drawn-out clusters of grains. Sphalerite is present in the calcareous band at 29.72m, in which galena and chalcocopyrite also occur	60
			END OF HOLE AT 30.50m		

Inclined depth m	Inter-section m	Structure angle	Lithology	Mineralisation	Sample CYD No
0.00					
1.42	1.42		Baryte-rock; coarse, weakly banded rock, iron-stained but some relicts of grey baryte with thin, pyritic bands	Pyrite, in bands and thinly disseminated forms <0.1 to 5% of the rock	
5.75	4.33	B 55	Baryte-rock [PTS 3892, 3893]; broken and iron-stained rock, crossed by a few thin, pyritic bands. Below 2.30m becomes less broken and stained. The rock contains minor quartz, fuchsite, muscovite and local, accessory dolomite. From 5.60 to 5.67m the core becomes broken and iron-stained again	Pyrite and magnetite occur weakly disseminated and in discrete bands. Ore content <1% overall though locally higher	1 2 3
6.31	0.56		Goesan; angular fragments set in a porous, goethitic matrix which constitutes >50% of the rock	All sulphides destroyed by leaching	
6.82	0.51		Quartz-rock [PTS 3894]; massive, fine-grained rock with minor muscovite. Limonitic fractures present. No barian mineral was identified but celsian is probably present as can be inferred from the chemical analysis	Pyrite occurs in weak dissemination and in cross-cutting hair veinlets	4
7.68	0.86	B 70	Celsian-quartz rock [PTS 3895, 3896]; fine to medium grained, massive rock with granoblastic texture. Banding is expressed by the presence of thin bands spaced ~1cm apart which are enriched in sulphides and quartz. Dolomite is commonly present, and rutile ubiquitous	Pyrite and subordinate sphalerite are disseminated and locally >10%. In places the sulphide-distribution is strongly banded	5
13.33	5.65		Baryte-rock [PTS 3897-3902]; massive, coarse grained rock containing minor amounts of quartz, dolomite, muscovite, chlorite, fuchsite and opaque minerals. Sulphide-rich bands are ubiquitous but subordinate. At c.11.70m and from 12.50 to 13.40m sulphide bands are strongly developed. The texture throughout is a coarse, granoblastic mosaic	Pyrite with minor sphalerite and galena (total sulphide < 3%) occur in bands and disseminations. Below 8.6% magnetite suddenly becomes important and remains so until end of unit. Chalcocopyrite, pyrrhotine and goethitic material identified in thin section	6 7 8 9 10
13.45	0.12		Sulphide-celsian band [PTS 3903]; sulphide dominated band containing major amounts of quartz and celsian, with minor rutile, chlorite, and goethitic material. Fine lithological banding is present	Pyrite, sphalerite and minor galena dominate the rock	
14.16	0.71		Mineralised quartz-rock [PTS 3904, 3905]; coarse irregularly segregated rock whose major constituents include quartz, calcite, celsian, pyrite and sphalerite. Baryte in PTS 3904 is in part replaced by calcite	Pyrite, sphalerite, galena, chalcocopyrite and pyrrhotine are present	11
14.81	0.65	F 40	Mineralised quartz-rock [PTS 3906, 3907]; grey, calcareous rock rich in irregular disseminations and bands of sulphides. Celsian, chlorite, rutile, and baryte are present	Pyrite is variable and often abundant, accompanied by minor chalcocopyrite	12
15.23	0.42	F 40	Muscovite-schist; pale, foliated rock with quartz and accessory fuchsite	Pyrite is common in certain bands and in cross-cutting hair veinlets	13
19.14	3.91		Graphitic muscovite-schist [PTS 3908]; monotonous dark grey schist with varying contents of calcite. Minor constituents include baryte and rutile. Bands of paler greenish (?chlorite) schist are found at 16.77 to 16.91m and 17.92 to 18.75m. Strong strain slip cleavage and crinkling in parts	Pyrite grains are common. Sphalerite and a trace of galena also occur [PTS 3908]	14 15 16
			END OF HOLE		17

Inclined depth m	Inter-section m	Structure angle	Lithology	Mineralisation	Sample CYD No
0.00					
0.00	3.00		Superficial deposits - no recovery		
			Graphitic quartz-muscovite-schist [PTS 3957]; dolomitic, highly fissile rock whose pronounced cleavage is crenulated throughout. Quartz lenses and veins are intersected at 4.12m, 4.85m, 6.16 to 6.29m, 6.56 to 6.96m, 7.40 to 8.00m, 8.28 to 8.45m and from 8.74m to 8.93m. At 7.04m the highly fissile schist gives way abruptly to laminated but non-fissile dolomite-rich rock which merges back into fissile schist by 7.72m. The rock is uniformly graphitic, but the carbon occurs as microscopic granules rather than discrete crystals.	Limonitic staining is prominent to 3.70m and in restricted zones below this point. Small amounts of pyrrhotine and sphalerite (but the latter mineral can be significant, see Appendix II), and accessory galena occur as streaked out grains. Some microgranular marcasite and framboidal pyrite is present. Sulphides conspicuous in and adjacent to quartz segregations.	18 19 20 21 22
9.30	6.30	F 65°	Dolomite-rock; band of laminated, non-fissile but still graphitic rock. Minor quartz occurs in conformable layers. Muscovite and possible biotite are present.	Pyrite is a minor, disseminated constituent along with lesser amounts of sphalerite.	23
9.46	0.16				
14.00	4.54		Graphitic muscovite-quartz-schist; fissile, soft, monotonous rock, probably with minor amounts of dolomite throughout.	Trace amounts of pyrite occur throughout and in cross-cutting veinlets at 13.39m, and 13.63m.	24 25
18.86	4.86		Graphitic schist with frequent dolomitic bands; soft, fissile schist forms c.60% of the intersection. Fourteen dark grey dolomitic bands ranging in thickness from 5 to 12cm, and a few thinner bands, are encountered.	Pyrite is a common though minor constituent, as discrete elongate blebs and masses, and in cross-cutting hair veinlets. Sphalerite and galena occur as minor constituents.	26 27 28
19.46	0.60		Muscovite-quartz-schist; less carbonaceous than the preceding beds, this unit has a uniform, fissile character. Dolomite is a minor constituent.	Pyrite and subordinate sphalerite occur in minor amounts, mainly disseminated through the rock.	29
			Mineralised dolomite-rock [PTS 3958-3962]; coarse, purple rock rich in celsian and sulphides. The distribution of celsian is irregular, with some rich bands. Minor constituents include quartz, rutile and chlorite. The rock frequently displays a fine banding. In certain bands between 19.46 and 20.83m it has a breccia-like texture in which fragments of coarse dolomite, quartz and celsian are set in a finer, quartzose, sulphide-rich matrix. Another 25cm thick band of similar breccia occurs at 22.47m. Below 24.00m no breccia-like textures are present but frequent sulphide-rich bands up to 1cm thick occur. These are dominated by pyrite, pyrrhotine now being absent. At 23.60m a 2cm calcite band crosses the core. Then comes a quartz segregation (24.34 to 24.40m), and the intersection finishes with 10cm of pyrite-enriched calcite-rock.	Pyrrhotine and lesser amounts of pyrite, sphalerite, galena, chalcocopyrite and marcasite (secondary) occur disseminated and enriched in the matrix of the fragmental rocks. Pyrite also occurs in cross-cutting hair veinlets. In thin section this mineral shows a framboidal texture. Overall sulphide levels are visually estimated to be from 3 to 10%, with levels in enriched bands much higher than these.	30 31 32 33 34
24.50	5.04				
			Pyritic calcareous quartz-rock; fine-grained at first, the intersection coarsens downward. Banding is chiefly expressed in changes in the sulphide content. An isolated cross-cutting veinlet is present.	Pyrite and lesser sphalerite are disseminated, being enriched in certain bands. The overall sulphide content is c.10%.	35
25.07	0.57				
			Baryte-rock [PTS 3963, 3964]; an abrupt rise in specific gravity marks the incoming of baryte as the major constituent, while calcite assumes a minor role. The rock is chiefly coarse grained baryte and lesser quartz with minor amounts of calcite, fuchsite, biotite, magnetite and sulphides. Banding, often poorly developed, is expressed by increase in the opaque content. The quartz content is generally considerable, the rock having s.g. values generally well below 4.0 g.cm <sup>3</sup> . From 29.40 to 29.75m the porosity, normally quite low in the baryte-rocks, is appreciable.	Pyrite, magnetite, and lesser amounts of sphalerite and galena are prominent in certain bands. Elsewhere the opaque minerals are thinly disseminated.	36 37 38 39 40 41
32.45	7.38	B 20-40			
			Calcareous baryte-rock (PTS 3965); finely banded rock in which calcite is accompanied by baryte, quartz, minor chlorite and sulphides.	Common pyrite, and minor sphalerite and galena occur disseminated throughout	42
32.90	0.45				
			Quartz-rock [PTS 3966]; grey, massive quartz-rock with common disseminated sulphides, minor calcite, baryte, possible celsian, rutile, muscovite and chlorite.	Common pyrite with lesser sphalerite and galena, trace chalcocopyrite and marcasite.	43
33.61	0.71	B c90			
			Graphitic muscovite-rich schist; the preceding quartz-rock merges into phyllitic schist in which light-coloured rock (little carbonaceous material) is interbanded with dark (graphitic rock).	Pyrite and lesser amounts of sphalerite, galena and pyrrhotine are sparse to common, as streaked-out grains.	44
35.45	1.84	F 40			
			END OF HOLE		

## APPENDIX I TABLE IV BOREHOLE 4

Inclined depth m	Inter-section m	Structure angle	Lithology	Mineralisation	Sample CYD No
0.00					
3.30	3.30		Superficial deposits		
4.68	1.38		Chlorite-muscovite-schist; graphite material is important only in isolated thin bands. Limonitic/goethitic staining is present intermittently		
		F 50°	Grey muscovite-rich schist [PTS 3909, 3910], soft fissile rock more graphitic than the foregoing. The intersection is generally uniform, though banding locally is present, expressed by bands of lighter, more quartzose rock. Biotite and Chlorite occur as minor constituents. At 12.06m the rock is chloritic and contains fragments of calcite-rock. At 12.51m there is a 3cm quartz vein with coarse pyrite and ? siderite. At 11.8m and 12.35m there are thin bands of granoblastic dolomite-rock	Pyrite is a minor constituent, present in irregularly distributed patches and in cross-cutting veinlets	62 63 64
		F 10°			65
13.00	8.32				
13.14	0.14	c 40°	Quartz-dolomite rock; fine-grained saccharoidal rock with quartz and muscovite	Pyrite grains elongate parallel to bedding and in cross-cutting hair veinlets	66
			Dolomitic schist [PTS 3911]; quartz, muscovite, and dolomite are the major constituents. The rock has a crumpled lamination marked by discrete muscovite-rich laminae	Pyrite, a minor constituent, occurs as conformable wisps and stringers	67
13.90	0.76	variable			
			Impure quartz-rock [PTS 3912, 3913]; dolomite is the other principle mineral, with some baryte. The texture is fine grained granoblastic	Disseminated sulphides are common; pyrite with lesser sphalerite and galena	68
14.50	0.60				
			Baryte-rock [PTS 3914, 3915]; coarse, massive rock of which pyrite is the other principal constituent. Quartz is an ubiquitous minor mineral. No other transparent phase was observed. The rock is banded, with alternations of pyrite-rich and pyrite-poor lithologies. Bands at 15.03m to 15.15m and 16.31m to 16.50m are of white rock from which pyrite is almost completely absent	Pyrite occurs in disseminations and in ore-rich bands. It is accompanied by sphalerite and lesser galena	69
17.35	2.85				
17.57	0.22		Sulphide band [PTS 3916]; porous, ochreous, granular aggregate with minor quartz and clay constituents	Pyrite and sphalerite are accompanied by minor galena	70
			Brecciated quartz-baryte rock [PTS 3917]; fragments of coarse quartz-rock and coarse baryte-rock are set in a sulphide-rich dolomitic matrix. A crude banding is shown by the presence of fragments of calcareous rock	Pyrite is accompanied by sphalerite, galena and accessory chalcocopyrite	
18.00	0.43				
			Banded mineralised carbonate-rock [PTS 3918, 3919]; close spaced sulphide-enriched laminae alternate with sulphide-poor rock rich in both calcite and dolomite. Quartz is a minor constituent. This structure has been thrown into open undulations. At the base of the intersection the rock has a major dolomite content [PTS 3919]	Pyrite and sphalerite are abundant; galena is also important	71
18.78	0.78	B 0 ± 45			
			Brecciated quartz-dolomite rock [PTS 3920]; celestian-bearing rock in which fragments of quartz-rock and dolomite are set in a sulphide-rich, celestian-bearing quartzose matrix. The texture is consequently irregular and does not display banding	Pyrite with lesser sphalerite and galena are common to abundant. Chalcocopyrite is an accessory phase	72 73
19.65	0.87				
			Dolomite-baryte rock [PTS 3921]; banded, granoblastic rock. Baryte forms ~ 50%, Quartz is a major constituent. A fine banding arises from wide variations in the baryte/dolomite ratio	Pyrite with lesser sphalerite and galena are abundant, disseminated throughout the rock	
19.76	0.11	B 40			
20.00	0.24		Baryte-rock; a thin band of calcareous baryte-rock	Sphalerite, galena and pyrite are disseminated	74
			Breccia [PTS 3922, 3923, 3924]; dolomitic brecciated quartz-baryte rock, iron-stained and porous due to leaching to 20.10m, then it is little oxidised to 20.27m, and is again limonitic to 20.47m	Pyrite, sphalerite and galena are abundant	
20.47	0.47				
20.69	0.22		Dolomite-rock [PTS 3925]; a band of massive, coarse dolomite with disseminated sulphide and minor quartz	Pyrite, sphalerite and galena are abundant. Chalcocopyrite is an accessory constituent	75
			Banded mineralised calcite-rock [PTS 3926-3929]; very similar to the calcareous 18.00 to 18.78m intersection. Coarse calcite-rock with appreciable amounts of dolomite, quartz and sulphides. Banding, resulting from sharp fluctuations in the sulphide-content, is developed to 21.78m, imparting a marked, striped appearance to the rock. At c.21.80m is a 5cm massive sulphide band. Below 21.82m to 22.09m the rock is a massive quartzitic calcite-rock [PTS 3929]	Pyrite and sphalerite are abundant, while galena is a minor but constant constituent	76
22.09	1.40	B 55			
			Banded celestian-quartz rock [PTS 4077]; celestian imparts a green shade to this rock in which banding is shown by varying feldspar and mica content. Baryte occurs in cross cutting hair veinlets	Minor amounts of disseminated pyrite, sphalerite and galena	77
22.86	0.77	B 10			
			Quartz-celestian rock [PTS 4078, 4079]; massive grey rock in which dolomite is patchily developed. Alignment of blade-like celestian crystals gives a laminar, schistose fabric to the rock. Baryte occurs in cross-cutting hair veinlets. Fine, sulphide-banding occurs only at c.23.50m. From 24.45m to 25.40m the rock carries very fine, dispersed spots of a grey mineral (not identified in thin-section; PTS 4079) which tend to be elongated parallel with the length of the core	Pyrite and lesser sphalerite occur disseminated through the rock, forming ~ 1% on average. Chemical analysis shows more in the upper part of the unit	78 79
25.40	2.54	B 0			

END OF HOLE

Inclined Depth m	Inter-section m	Structure angle	Lithology	Mineralisation	Sample GTD No
0.00					
2.30	2.30		Superficial deposits		
			Dolomitic quartz-celsian rock [PTS 4135]; often possessing a lamination due to the alignment of celsian blades. Pyritic bands occur at c 2.52m and c 3.40m. An isolated 2cm thick band of coarse baryte-rich rock occurs at c 3.34m	Pyrite and lesser sphalerite and galena occur as low-level (< 1%) disseminations and in occasional sulphide-rich bands	80 81
4.08	1.78	B 40°	Baryte-rock; massive, coarse-grained rock in which thin sulphide-rich bands alternate with sulphide-poor bands	Pyrite is common, both in low-level disseminations and in enriched bands	82
5.30	1.22	B 60°	Quartz-celsian rock [PTS 4136]; commences (c 5.30m, PTS 4136) with a 6cm band of strongly laminated quartz-celsian rock in which cross-cutting baryte veinlets are seen. Below this the rock is of a massive, weakly foliated type	Pyrite is a minor constituent throughout. In PTS 4136 sphalerite and a trace of chalcocopyrite are seen	83
6.01	0.71		Baryte-rock [PTS 4137]; massive, coarse-grained rock much broken at limonite-lined fractures. From 6.64m to 6.88m fracturing has reduced core recovery to disjointed fragments set in limonitic coatings. Quartz and sulphides are the principal minor constituents of the primary rock	Pyrite is common, and sphalerite and galena often are present. Magnetite and covellite were identified, but both only as trace constituents	84
6.93	0.92	B 45°	Quartz-celsian rock [PTS 4138, 4139, 4140, 4141]; this long intersection consists of massive though often foliated rocks in which a number of zones of fissile, schistose rock occur. The principal schistose zones are from 6.88m to 7.50m, 7.65m to 7.80m, 11.15m to 11.70m, 12.10m to 12.80m, 13.35m to 14.00m, 16.45m to 17.00m and 17.15m to 17.35m. The foliation of the more massive rock becomes relatively pronounced below 11.0m. Zones in which dark interstitial spots are common occur at c 10.70m, c 11.70m and c 13.10m. The precise identity of the dark material is not fully known, but it may be rich in carbonaceous "graphitic" material [PTS 4140]. At certain points the feldspar present is hyalophane (eg XRD at 8.58m) rather than celsian. Dolomite is an essential constituent	Disseminated pyrite is common, and in places is accompanied by sphalerite. Pyrrhotine, chalcocopyrite and galena were identified in the thin sections. Segregation of sulphides into conformable bands is common	85 86 87 88
17.45	10.52	F 50°			89
		F 45°			90
		F 60°			
18.20	0.75	B 40°	Baryte-rock; coarse rock, massive, though with weakly developed pyritic bands	Pyrite occurs in very minor amounts	
c 18.60	c 0.40		Celsian-quartz-rock [PTS 4142]; the core here is very porous, probably due to solution of a carbonate and/or sulphide mineral. It is well banded, the principal lithologies being pyritic quartz-celsian rock and celsian-rich rock	Pyrite is common in this well banded rock	
19.01	c 0.41		Baryte-rock; very similar to the 17.46m to 18.20m intersection.	Pyrite	92
21.42	2.41	F 50°	Quartz-celsian-rock; this intersection is much fractured and core loss was considerable. The material recovered is porous due to leaching, and the rock is generally limonitic.	All sulphides are absent due to leaching	93
23.30	1.88	B 40°	Baryte-rock [PTS 4143]; coarse, massive rock in which banding due principally to sulphide-enrichment is moderately developed. Porphyroblasts of celsian occur in PTS 4143, which also contains minor quartz, dolomite, apatite, rutile, and sulphides. It is likely that quartz and dolomite are more generally present in this intersection	Pyrite and lesser sphalerite and galena occur in bands and as a low-level dissemination	94
23.62	0.32	5.30°	Quartz-biotite-schist; probably dolomitic	Pyrite grains are common	
			Baryte-rock [PTS 4144]; coarse, massive-textured rock. At c 24.27m and c 24.60m bands of foliated dolomitic celsian-quartz rock [PTS 4146] occur in which baryte, biotite, rutile, muscovite, and pyrite are minor constituents. From 25.04m to 25.47m quartz-biotite-schist is intercalated into the intersection. The foliation and the quartz-biotite-schist intercalation are folded around a fold nose and there is repetition of the schist band.	Pyrite is common in this rock mostly as a dissemination. Some sphalerite is also present	95 96 97
27.07	3.45	Bc 45°	Quartz-celsian rock [PTS 4145, 4146]; foliated rock with well-laminated zones showing evidence of such leaching at c 27.5m and c 28.35m. Dark poikiloblastic spots are common between 29.12m and 29.32m (of PTS 4140). Muscovite is present in some parts, such of the foliation is due to parallel alignment of thin, blade-like crystals of Ba-feldspar. Minor constituents include rutile and baryte (which occurs in cross-cutting hair-veinlets), as well as sulphides. From 31.0m to c 33.3m the core is heavily leached and broken with some core loss	Pyrite, often with lesser sphalerite and galena occurs as a dissemination	98 99
33.27	6.20	F 45°	Quartz-muscovite-schist; the continuing sulphide-bearing and non-calcareous character of the rock indicates that this rock probably is still within the mineralised zone	Disseminated pyrite is a minor constituent, and sphalerite is also present	100 101
33.81	0.54				102

END OF HOLE

APPENDIX I TABLE VI BOREHOLE 6			G E O L O G I C A L R E C O R D		
Inclined depth m	Inter-Section m	Structure angle	Lithology	Mineralisation	Sample CYD No
0.00					
2.15			Superficial deposits		
			BEN EAGACH SCHIST		
7.22	5.07	{ C 52 F 60	Chlorite-muscovite-schist, weakly calcareous with minor quartz and a strong foliation, locally intensely folded, and penetrative strain-slip cleavage; thin interbanded dolomitic quartzite 5.90 - 6.16 m	Minor pyrite in small vein at 2.60 m	805 806
8.95	1.73	F 60	Dolomitic biotite-chlorite-schist, with minor quartz and sericite; strong foliation and distinctive 'speckled' texture due to numerous small flakes of biotite; rare calcareous bands; quartz segregations relatively common with associated dolomite clasts at 7.65 m and 8.21 m		807
13.60	4.65	{ F 75 C 40	Chlorite-biotite-schist, weakly calcareous quartz-schist with interbanded dolomitic quartzite units 13.10 - 13.30, 13.54 - 13.60 m; foliation intensely folded with incipient strain-slip cleavage developed locally; garnet porphyroblasts noted at 11.40 m; quartz-dolomite segregations 9.75 - 9.81 m	Minor pyrite and pyrrhotine	808
15.18	1.58	F 70	Muscovite-quartz-schist silvery schist with variable foliation due to intense folding; dolomitic circa 13.75 m	Minor pyrite	809
26.42	11.24	F 90 F 50 F 80	Quartz-chlorite-schist finely laminated in parts, with minor biotite a strong foliation; locally folded, and thin quartzite bands; quartz segregations relatively common with associated dolomite clasts at 20.04 m	Sporadic pyrite and rare subordinate pyrrhotine	810 811 812
27.10	0.68	F 85	Quartz-mica-schist, (varying to micaceous quartzite) dolomitic with good foliation; small scale (?) early fold structure at 26.69 m		813
27.77	0.67		Dolomitic quartzite, white with rare biotite flakes; prominent quartz veining in uppermost 15 cm		814
31.23	3.46	F 90	Dolomitic muscovite-chlorite-schist, laminated silvery schist with minor quartz and biotite and a prominent foliation, locally intensely folded; quartz segregations common below approximately 30 m with associated dolomitic clasts		815
32.15	0.92		Chlorite-biotite-schist; variably sericitic calcareous grey schist with minor quartz and a prominent highly contorted foliation	Trace of pyrite	816
38.03	5.88	F 85 F 90	Dolomitic biotite-chlorite-schist; dark grey homogeneous quartz-schist with prominent regular foliation sericitic in parts and local thin dolomitic bands; garnet porphyroblasts noted below 34.85 m	Traces of pyrite and pyrrhotine in thin trails; limonite coating joint surfaces in lowermost 30 cm	817 818
42.20	4.17		Chlorite-sericite-schist; inhomogeneous quartz-schist with minor biotite and a poorly defined foliation which when developed is highly contorted; variably dolomitic throughout with quartz segregations common, and prominent dolomitic quartzite band 40.36 - 41.00 m	Minor pyrite; possibly finely disseminated barium mineralisation	819 820 821
43.84	1.64	F 90	Micaceous quartzite, (varying to quartz-mica-schist) weakly dolomitic with generally well developed foliation, apart from uppermost 15 cm, and prominent quartz veins/segregations	Traces of pyrrhotine in small trails	822
49.00	5.16	F 85 F 90	Quartz-muscovite-schist, transitional with previous unit; good foliation locally variable due to minor folding; dolomite bands and segregations common below 45.40 m with prominent dolomitic quartzite noted 46.10 - 46.55 m; core highly broken 44.45 - 45.30 m - (?) fault	Pyrrhotine and subordinate pyrite relatively common in thin trails parallel to the foliation. Possibly finely disseminated barium mineralisation.	823 824
57.02	8.02	F 90 F 90	Biotite-chlorite-schist, with strong, locally folded foliation and interbanded dolomitic quartzite units; small garnet porphyroblasts noted below 52.20 m; core highly broken, with significant core loss between 54.15 - 57.02 m - (?) fault	Coarse pyrite and finer pyrrhotine present throughout	825 826
60.22	3.20		Chlorite-quartz-schist, highly broken unit with conspicuous quartz veining and 'clay-gouge'; garnet porphyroblasts noted at 59.20 m and below - fault	Pyrite in coarse patches	827
64.30	4.08	F 90 F 70	Biotite-chlorite-schist, locally dolomitic with minor quartz and a strong foliation; quartz segregations common 61.00 - 61.50 m;	Occasional pyrite noted	828
67.10	2.80		Chlorite-muscovite-biotite-schist, dark schist with poorly defined foliation and distinct garnet porphyroblasts; locally dolomitic with interbanded dolomitic quartzite unit 66.49 - 66.60 m	Occasional pyrite in veins and patches; traces of pyrrhotine	829
69.40	2.30		Chlorite-sericite-schist, weakly dolomitic dark schist with minor quartz and biotite; local quartzite unit and abundant quartz veins	Pyrite and pyrrhotine in trails and small patches	830
73.09	3.69	F 90 F 85	Garnetiferous biotite-chlorite-schist, dark schist with prominent garnet porphyroblasts - locally highly dolomitic with abundant dolomite lenses, bands and thin interbanded dolomitic quartzites throughout	Common pyrite throughout with local minor pyrrhotine	831
76.26	3.17	F 85	Muscovite-biotite-schist, dark schist with prominent quartz segregations and chloritic pseudomorphs after garnet; minor dolomite locally associated with the quartz segregations	Relatively common pyrrhotine and minor pyrite; trace of (?) chalcocopyrite	832
78.37	2.11	I 90	Sericite-biotite-schist, finely striped with quartz and chlorite and thin interbanded dolomitic quartzite units; core highly broken 76.73 - 77.40 m - (?) fault	Pyrite in coarse patches	833
83.28	4.91	F 85	Chlorite-biotite-schist, with minor sericite, a poorly defined foliation and interbanded dolomitic quartzite units	Common pyrite with traces of pyrrhotine	834 835
85.85	2.57	F 90	Sericite-biotite-schist, weakly dolomitic, finely striped with quartz and a strong foliation locally folded		836
87.75	1.90	F 90	Sericite-quartz-schist, with thin interbanded dolomite-quartz units		837
101.10	13.95	F 90	Dolomitic chlorite-sericite-schist, dark locally biotitic schist with characteristic intensely folded foliation and interbanded dolomitic quartzite units; prominent quartz segregations locally	Minor pyrite dominantly in thin trails and small patches	838 839 840 841
103.46	2.36		Carbonaceous chlorite-sericite-schist; highly calcareous dark schist with interbanded fine-grained dark limestone units; foliation locally intensely folded	Minor pyrite	842
109.24	5.78		Chlorite-sericite-schist; highly calcareous quartz schist with intensely folded foliation and local interbanded sericite-quartz-schist units; biotitic in parts	Pyrite in sporadic patches and minor veins	843 844



## GEOLOGICAL RECORD

Inclined depth m	Inter-Section m	Structure angle	Lithology	Mineralisation	Sample CID No
110.00	0.76		Lamprophyre		845
			Graphitic sericite-schist with minor quartz and chlorite; inhomogeneous dark schist with interbedded chlorite-schist and dark dolomitic limestone units; locally garnetiferous, with quartz veins/segregations common throughout; (?) minor faulting 114.40 - 114.50 m and 117.70 - 117.80 m	Common pyrite dominantly in thin trails and veinlets, with sporadic coarser patches	846 847 848 849
117.90	7.90	F 85	50% core loss 118.25 - 121.25 m - <u>fault</u>		
			Micaceous quartzite; calcareous, slightly dolomitic, grey quartzite with variable biotite content and local graphitic partings		850
127.60	9.70		127.00 - 127.60 m core reduced to very small pieces, (?) brecciation, with probable core loss - (?) <u>fault</u>		
			Quartzite, pale grey with chlorite-sericite partings; abundant calcite veins and rarer dolomite veins; broken core below 128.60 m with noticeable core loss circa 130.00 m - (?) <u>fault</u>	Minor pyrite	851
132.16	4.56		Dolomitic sericite-chlorite-schist; striped schist with minor quartz and biotite and a characteristically crumpled foliation; rare bands of dolomitic quartzite		
		F 70 F 80			
133.88	1.72		Biotite-sericite-schist; slightly carbonaceous dolomitic schist with poorly defined foliation		
134.60	0.72		Sericite-chlorite-schist with minor biotite and dolomite, well striped, with rare interbedded dolomitic quartzite; locally abundant quartz segregations, net veined by calcite; rare carbonaceous zones; tight minor folds developed throughout		852
		F 70 F 80	core reduced to small chips 134.80-136.30 m with approx. 1.05 m lost - <u>fault</u>		
138.46	3.86		Graphitic muscovite-dolomite-schist, with quartz and garnet; well developed strain-slip cleavage	Minor pyrite	
139.05	0.59	F 90 C 60			
			Dolomitic limestone, slightly graphitic with bands of chlorite-sericite-schist and limestone (139.24 - 139.30 m); concordant lenses of quartz-dolomite; incipient strain - slip cleavage	Traces of pyrite	
139.60	0.55	F 80			
144.31	4.71	F 70	Sericite-biotite-schist with chlorite and dolomite; striped due to interbedded quartz-dolomite laminae, with local folding		853
145.50	1.19	F 75	Graphitic muscovite-dolomite-schist, with prominent interbedded dolomitic limestones and garnet porphyroblasts	Sporadic pyrrhotine trails	
145.75	0.25	F 75	Chlorite-sericite-schist, with minor biotite and dolomite, and bands of dolomitic quartzite and local quartz segregations		
147.72	1.97	F 70 C 40	Graphitic dolomite-muscovite-schist, varying to a dolomitic limestone, with a variably developed foliation, garnet porphyroblasts, and local quartz segregations rarely with associated dolomite clasts	Minor pyrrhotine trails with rarer pyrite	
148.94	1.22		Dolomite-sericite-biotite-schist, with minor chlorite and interbedded quartz-muscovite-schist and hornblende-sericite-schist units, typically calcareous; small lenses of quartz and dolomite and larger quartz segregations relatively common; garnet and rarer hornblende porphyroblasts irregularly distributed throughout	Traces of pyrrhotine	854
			<b>NEW LAWERS SCHIST</b>		
157.34	8.40	F 70 F 80 F 70	Calcareous hornblende-sericite-schist, with typical garbenschiefer texture and rare garnet porphyroblasts; local, large quartz segregations present and interbedded grey "limestone" bands		855
160.87	3.53		Chlorite-sericite-schist, with minor biotite and rare thin dolomitic bands; sporadic garnet and hornblende porphyroblasts locally	Rare pyrite and pyrrhotine	
161.61	0.74		Chlorite-biotite-schist with rare sericite, and variably developed calcite-quartz lenses		
164.55	2.94	F 75	Metabasite, dark calcareous chlorite-amphibole-schist with variably developed foliation, locally biotitic; quartz-dolomite and quartz-calcite lenses relatively common and in places result in distinct striped texture	Traces of pyrite locally as sporadic anhedral crystals	
165.15	0.60	F 75	Hornblende-quartz-schist, slightly dolomitic with garbenschiefer texture and concordant dolomite-quartz units	Traces of pyrite	
166.51	1.36	F 50	Metabasite, dark calcareous hornblende-chlorite-schist locally highly dolomitic, passing down into striped quartz-chlorite-hornblende-schist	Traces of pyrite	
168.44	1.93	F 55	Calcareous chlorite-biotite-schist, finely laminated, with rare thin calcareous bands and quartz-calcite segregations; locally hornblende	Rare pyrite cubes	
169.60	1.16	F 60	Calcareous hornblende-chlorite-schist with minor sericite; typical garbenschiefer texture and thin calcareous quartzite	Rare pyrite	
170.25	0.65	F 30	Calcareous quartzite with crude foliation defined by chlorite and biotite	Trace of pyrite	
172.31	2.06	F 20	Calcareous chlorite-sericite-schist with minor hornblende, quartz-calcite segregations and interbedded calcareous chlorite-quartzite units; varying to chlorite-schist	Sporadic pyrite cubes	
173.20	0.89	F 15	Calcareous chlorite-biotite-schist, locally sericitic with occasional hornblende porphyroblasts and rare quartz segregations	Trace of pyrite	
173.90	0.70	F 20	Calcareous quartzite with aligned chlorite-biotite pseudomorphs after (?) amphibole		
175.03	1.13	F 50	Calcareous chlorite-sericite-schist, with minor biotite and rare hornblende porphyroblasts; interbedded calcareous quartzite units and occasional quartz segregations noted	Occasional pyrite porphyroblasts	
176.20	1.17	F 60	Metabasite, finely laminated calcareous chlorite-biotite-hornblende-schist with rare quartzose laminae and locally important quartz-calcite, and chloritic, patches		
176.20			End of borehole		

G E O L O G I C A L R E C O R D						
Inclined Depth	Inter-section	Structure angle	Lithology	Mineralisation	Sample	CYD No
0.00						
3.14	3.14		Superficial deposits BEN EAGACH SCHIST			
5.00	1.86	F 065	Muscovite-schist, calcareous, limonitic and weathered; foliation contorted	Contorted quartz veinlet contains probable baryte at 3.92m	501	
6.20	1.20	F 070	Muscovite-chlorite-schist, highly calcareous in places with appreciable biotite, minor hornblende and thin bands of yellow dolomite; minor quartz in eyes and veinlets	Trace of pyrite		
6.45	0.25		Schist, limonitic and porous due to weathering along foliation planes with numerous contorted lenses of white (?) illite	Isolated tarnished grains of sulphide		
7.59	1.14	F 060	Biotite-chlorite-schist with minor muscovite, quite limonitic in places; dolomitic laminae and quartz lenses common; brown calcite crystals in contorted quartz bands		502	
10.40	2.81	F 060	Dolomite-schist, striped, with muscovite, quartz and lesser biotite and chlorite; yellow-white dolomite c 50% of rock; local limonitic zones up to 10cm thick and occasional quartz segregations; foliation highly contorted in lower part [PTS 4305]	Trace of tarnished pyrite	503	
10.50	0.10	F 45	Muscovite-dolomite-schist with minor chlorite			
10.64	0.14		Biotite-schist			
10.97	0.33		Muscovite-schist with alternating calcareous and dolomitic, quartzose bands; the strong foliation is refolded			
11.63	0.66		Biotite-muscovite-chlorite-schist, striped as a result of alternating quartzose and dolomitic layers	Minor pyrite and (?) pyrrhotine on hair fractures		
12.01	0.38		Dolomitic muscovite-schist with minor biotite, striped and pale in colour; foliation refolded	Trace of (?) pyrrhotine; limonitic fractures		
12.35	0.34	C 025	Muscovite-schist, leached and limonitic in central part; conspicuous fold closures			
12.49	0.14		Muscovite-schist, pale, probably dolomitic, unbanded		504	
12.74	0.25		Biotite-schist with sericite, chlorite, quartz and dolomite			
13.22	0.48		Biotite-muscovite-schist, dolomitic, with minor chlorite; minor grey quartz contrasts with yellow dolomite and white (?) baryte; limonitic and leached	(?) baryte in a few thin layers and segregations		
14.31	1.09	F 45	Biotite-schist with chlorite, sericite, quartz and dolomite; rare calcareous laminae and quartz segregations	Trace of pyrite	505	
15.20	0.89		Quartz-muscovite-schist with minor biotite; core broken and lost indicating (?) fault		506	
18.45	3.25		Muscovite-biotite-schist, dolomitic and striped below 15.97m; F parallel to core axis around 15.4m indicating a fold		507	
18.55	0.10		Quartz lens or vein incorporating limonitic, micaceous slivers			
18.77	0.22		Muscovite-schist, dolomitic, pale with dark spots of (?) hornblende; fold closure exhibited			
19.79	1.02	B45 - 80	Muscovite-dolomite-schist, pale with contorted banding	Traces of pyrrhotine, pyrite in sub-conformable streaks	508	
19.83	0.04		Quartz segregation with angular patches of (?) celsian and dolomite, wedging out	Irregular patches and grains of pyrite and dark sphalerite		
19.86	0.03		Dolomite and (?) celsian, saccharoidal with mica streaks	Pyrrhotine streaks		
20.06	0.20		Massive sulphide in a quartz matrix, wedging out, leached	Pyrite (c.40%), (?) sphalerite	509	
21.78	1.72	F 55	Muscovite-schist with numerous eyes and contorted bands of quartz and some biotitic bands; interspersed are creamy-white friable bands of dolomite - (?) baryte	Minor pyrrhotine with subordinate (?) chalcocopyrite 21.18 - 21.34m; probable baryte	510	
24.37	2.59		Muscovite-schist with minor biotite and quartz, and dolomitic streaks; highly micaceous; contorted towards base with grey quartz layers and a band of pale calcite (23.85m)	Accessory pyrrhotine in conformable wisps mostly with quartz layers	511	
25.25	0.88		Muscovite-schist as above but core broken, iron-stained and leached; white colouration related to (?) baryte-bearing assemblage forming discrete conformable streaks	Pyrite and a (?) pyrrhotine-sphalerite(?) baryte-quartz assemblage		
27.03	1.78		Muscovite-schist with minor quartz and carbonate, thin white layers of quartz and (?) celsian at 27.0m, and black laminae possibly altering from pyrite; leached and limonitic especially at 25.91 - 26.43m	Pyrite as smears and in bands containing traces of bornite and chalcocopyrite at 25.73m; (?) celsian	512	
27.98	0.95	F 40	Quartz-celsian rock, banded due to abrupt variations in quartz and celsian content; medium-grained and mosaic-textured with accessory pale "phlogopitic" biotite; pyritic throughout [PTS 4306]; dolomite, biotite and rutile also present	Pyrite in conformable laminae and disseminated; sphalerite common with minor galena in laminae at 27.74 - 27.98m		
28.56	0.58	F 45	Baryte-rock with pyrite disseminated and in layers with limonite, galena and sphalerite; "cherty" band 28.31 - 28.33m	Baryte; pyrite common, minor galena and sphalerite		
29.09	0.53		Quartz-celsian rock with minor disseminated sulphides and sulphide-rich laminae up to 1cm thick; some dolomitic layers	Pyrite throughout plus minor brown sphalerite		
29.74	0.65		Quartz-celsian rock, dolomitic and thinly banded; banding contorted	Pyrite and minor sphalerite disseminated and in layers		
30.54	0.80		Quartz-celsian rock with more irregular banding, highly contorted at 30.3m where sulphides are common and large porphyroblasts of black (?) dolomite are present	Pyrite disseminated and in layers with minor sphalerite and lesser galena	513	
31.24	0.70		Baryte-quartz rock, sheared and infilled with quartz at top; pyrite concentrated at edges of quartz lenses indicating its mobility during metamorphism	Baryte; pyrite common in conformable layers and also as a minor disseminated constituent	514A	
32.32	1.08	F 60	Quartz-celsian rock, grey and "cherty" with contorted banding including sulphide-rich layers 31.24 - 31.34m, followed by poorly banded rock containing angular, flattened (?) celsian-rich fragments	Pyrite disseminated in irregular segregations with minor sphalerite and galena		
33.43	1.11		Celsian-quartz rock, generally similar to above, seen in section [PTS 4307] to consist of mosaic-textured quartz with abundant platy celsian crystals; medium-grained and finely banded; some folding evident in pyrite trails; rutile, dolomite and biotite also present	Pyrite in irregular segregations and also disseminated		

			G E O L O G I C A L R E C O R D		
Inclined Depth m	Inter- section m	Structure angle	Lithology	Mineralization	Sample CYD No
34.09	0.66	F40-55	Quartz-celsian rock, generally similar to above, grey and banded with irregular creamy-coloured patches	Pyrite disseminated and in irregular patches	514B
38.52	4.43	F 60	Muscovite-schist with quartz, dolomite and (?) celsian; "cherty" and well banded 34.09 - 34.59 followed by core with grey quartz segregations and yellow layers carrying celsian and dolomite; flattened lenses of soft, white mineral at 35.91 m; muscovite-quartz-schist below 36.0m [PTS 4308]	Pyrite grains common, also in cross-cutting veinlets (eg. at 35.79m); traces pyrrhotine and sphalerite	515
38.78	0.26	F 50	Quartz-celsian rock, grey, banded and "cherty"; minor calcite in pinkish-coloured (?) celsian band at 38.77m	Pyrite abundant, minor galena and sphalerite	
39.55	0.77		<u>Baryte-rock</u>	<u>Baryte</u>	
39.80	0.25		Quartz-celsian rock, grey, banded and "cherty"		516
40.93	1.13	F 45	Muscovite-schist in which quartzose layers contain grains of <u>hyalophane</u> [PTS 4309]	Pyrite in streaks and veinlets with accessory sphalerite	517
44.73	3.80		Quartz-celsian rock, grey, banded and "cherty" with streaked-out cream-coloured fragments and irregular laminae; more muscovitic in central part of unit and in lower part certain bands are broken and leached with soft, white clay	Pyrite disseminated and in occasional laminae; subsidiary sphalerite and galena	518 519
50.34	5.61	F 40	Muscovite-schist, much broken and apparently leached; lenses of soft, white mineral at 45.88m and of soft, yellow, dolomitic material at 46.29 - 46.46m and especially 50.38 - 51.74m; solution of dolomite in part may account for leached appearance	Pyrite in cross-cutting hair veinlets and with pyrrhotine in patches at edges of dolomitic lenses; also disseminated pyrite	520 521
51.74	1.40		Muscovite-schist as above, crossed by quartz vein at 50.88m and angular fragments of yellow dolomitic material in continuum with adjacent yellow band	Tarnished pyrite in quartz vein	522
54.62	2.88	F 35	Muscovite-schist as above with occasional quartz lenses and dolomitic laminae	Pyrite disseminated and in veinlets, minor	523
57.09	2.47	F 60	Muscovite-schist, initially more weathered than above, then possibly celsian-bearing; numerous quartzose layers and flattened lenses; pyritic segregation at 55.8m consists of sieve-like sulphide enclosing quartz, muscovite and a late-formed clay mineral and goethite assemblage [PTS 4310]	Pyrite common in weak disseminations, bands and cross-cutting veinlets; minor sphalerite and trace of galena	524
58.64	1.55		Muscovite-quartz-schist, initially heavily leached and broken with much soft, yellow clay, then more massive; at 57.70 - 57.90m the rock is a quartzite, fragmented and cemented by material now largely altered to clay (possible <u>fault</u> )	Disseminated sulphide common in more massive schist, sparse elsewhere	525
60.13	1.49	F 75	Quartz-celsian rock in which banding is expressed by the presence of thin, pale bands; flattened fragments of yellow dolomite also occur and at 59.10m a cross-cutting, yellow dolomite vein containing coarse, angular quartz is developed; some clay-rich altered zones around 5cm thick	Fine-grained, disseminated pyrite and isolated coarse pyrite porphyroblasts, some with quartz strain shadows	
61.91	1.78		Quartz-celsian rock, muscovitic foliation or schistosity is closely spaced	Pyrite-sphalerite bands, sometimes cross-cutting	526
63.22	1.31		Quartz-celsian rock, muscovitic; weakly dolomitic with occasional cross-cutting chlorite-pyrite and dolomite-pyrite veinlets; unit commences with an 8cm thick leached clayey zone and is initially less muscovitic than the unit above	Pyrite and lesser sphalerite disseminated and in conformable streaks; pyrite also in veinlets	
65.23	2.01	F 80	Muscovite-schist, dolomitic with quartz and celsian; dolomitic quartzite bands fairly common in upper 0.5m; pyritic segregation ( $\geq 50\%$ sulphide) at 64.34 - 64.38m [PTS 4311] incorporates angular white fragments of possible hyalophane and baryte	Pyrite disseminated and in bands; traces of chalcopyrite and galena and common sphalerite in massive sulphide bands	527
67.28	2.05	F 80	Dolomitic muscovite-schist, quartzose and probably celsian-bearing; the numerous yellow dolomitic layers are locally fragmented and recemented in quartz and pyrite	Pyrite in cross-cutting veinlets, lesser amounts in dolomitic layers and disseminations	528
69.60	2.32		Muscovite-schist, dolomitic, quartzose and probably celsian-bearing; dark laminae of biotite or chlorite occur throughout with associated sulphide and coarse quartz lenses are sometimes present	Minor pyrite	
69.80	0.20		Core broken and lost indicating possible <u>fault</u>		
70.33	0.53	F 55	Muscovite-schist with chloritic fractures and quartz lenses containing irregular chlorite segregations		
70.82	0.49		Crushed muscovite-schist indicating <u>fault</u>		529
72.85	2.03	F 75	Muscovite-schist, quartzose and dolomitic and relatively dark to 72.32m due to biotite; thin quartz layers are numerous [PTS 4312]	Pyrite weakly disseminated and at margins of quartz lenses; trace chalcopyrite	530
76.39	3.54	F 85	Quartz-rich muscovite-celsian-schist, weakly dolomitic, sometimes calcareous and with occasional quartz lenses; well banded due to contrasting grey quartz bands and pinkish dolomitic bands; small calcite fragments occur at 75.48m and the lamination is deflected around a quartz lens at 75.56m; at about 75.40 m core frequently broken on pyrite bands which herald incoming of the quartz-celsian rock	Sparse pyrite in streaks and as cross-cutting veinlets; galena associated with calcite at 75.48m; conspicuous pyrite bands below 75.40 m	531
79.10	2.71	F 85	Quartz-celsian rock, laminated due to parallelism of platy celsian crystals [PTS 4313] and fractured and veined by pinkish-coloured quartz; occasional dolomitic layers and grains of rutile are present; the celsian is relatively coarse in certain bands within typical fine-grained "cherty" quartz-celsian rock	Sulphide bands common (locally forming c. 20% of rock), consisting of pyrite, lesser sphalerite and accessory galena	532
82.83	3.73		Quartz-celsian rock, grey and "cherty" in aspect with bands of quartz and quartz-sphalerite and cut by dolomite-baryte veinlets [PTS 4314]; banded baryte occurs in a cavity at 82.15 m and a slump structure at 81.14 - 81.25m; a sphalerite-rich band is deflected around a quartz lens at 81.79m and a similar band at 81.59m encloses fragments of "chert"	Sulphide common in bands and as weak disseminations, consisting of pyrite, reddish-coloured sphalerite and minor galena; baryte veinlets	533
84.03	1.20		Pyritic muscovite-schist, dolomitic and laminated [PTS 4315] with a thin grey "chert" band, probably celsian-bearing, at 83.51m; a quartz lens occurs at 83.70m and the rock is cut by thin quartz-dolomite veinlets	Pyrite abundant in conformable bands and seams, also in cross-cutting veinlets	534
85.47	1.44		Quartz-celsian rock, grey with quartz lenses and relatively coarse-grained in places; the rock has an irregular patchy structure due to calcite patches [PTS 4316] and the disruption has affected a coarse quartz lens; this disruption may be tectonic and irregular chloritic segregations are associated with the quartz lenses; calcite-baryte veinlets at 84.68m	Pyrite and accessory sphalerite occur in bands and to a lesser extent form disseminations	535
88.16	2.69		Quartz-celsian rock, banded, dark grey with some quartz lenses; minor rutile; the rock is cut by calcite veinlets carrying minor baryte along faultlets, especially at 86.80-87.14 [PTS 4317] and 88.05m; this fragmented and recemented texture may be syndepositional in origin	Pyrite abundant plus minor sphalerite (locally forming c. 8% in bands up to 6cm thick); remobilised pyrite in calcite veinlets	536

			GEOLOGICAL RECORD		
Inclined Depth	Inter-section	Structure angle	Lithology	Mineralisation	Sample CTD No
88.83	0.67		Broken core of dark limestone with muscovite and chlorite; rock strongly fractured and containing quartz segregations	Pyrite and traces of sphalerite	
90.65	1.82	F 90	Biotite-muscovite-chlorite-schist with quartz bands and cross-cutting calcite veinlets; core broken and graphitic near base	Traces of disseminated pyrite	537
91.70	1.05		Graphitic muscovite-schist, contorted and broken; the rock is calcareous and contains a quartz lens near the base	Conformable pyrite smears occur locally	538
94.62	2.92	F 85	Graphitic muscovite-schist; foliation locally kinked and refolded; a little dolomite and calcite in introduced veinlets and irregular patches; a sieve-like pyritic segregation at 91.75 - 91.81m encloses quartz, calcite and celadon [PTS 4318]	Pyrite abundant in conformable layers and in cross-cutting veinlets	539
97.08	2.46	F 070	Graphitic muscovite-schist, black, commonly dolomitic and sometimes calcareous; much calcite veining; ovoid porphyroblasts of <u>hyalophane</u> are also present [PTS 4319]	Pyrite common in conformable layers and in cross-cutting fractures predating calcite veins	540
100.15	3.07		Graphitic muscovite-schist with quartz lenses abundant from 98.58 - 98.70m; calcite veinlets out pyrite patches which are common in the quartz lenses	Pyrite common in quartz lenses	541
100.81	0.66		Graphitic muscovite-schist		
101.49	0.68		Fractured graphitic muscovite-schist, indicating fault; much calcite veining, angular white crystals occurring marginally to pink calcite	Pyrite common adjacent to calcite veins but not apparently remobilised	
103.65	2.16	F 070	Graphitic muscovite-schist, black, somewhat shattered and calcite cemented, dolomitic; more quartzose from 102.36 - 102.56m	Pyritic quartz lense prominent at 102.78 - 102.92m	542
105.42	1.77	B/F 80	Limestone, dark grey with a medium-grained granoblastic texture [PTS 4320]; the finely developed regular foliation of the rock runs parallel to original lithological banding	Pyrite in chloritic cross-fractures	
106.33	0.91	F 80	Muscovite-schist, grey and calcareous containing graphitic layers and quartzose bands; a quartz lense at 106.15 m is cut by a dolomite-pyrite veinlet	Minor pyrite in conformable layers and in cross-fractures	543
108.72	2.39	B/F 80	Graphitic muscovite-schist, black with alternating dolomitic and calcareous bands and some calcite veinlets	Minor pyrite in smears and on fractures; (?) pyrrhotine	544
112.13	3.41	F 85	Graphitic muscovite-schist, banded with very low carbonate content; minor calcite in late veinlets	Moderate pyrite in smears and on fractures	545
113.84	1.71	F 80	Graphitic muscovite-schist, dolomitic in part with a calcareous band at 112.60 - 112.80m and quartz-pyrite lenses in contorted schist at 112.20m; a dolomite band rich in porphyroblasts of <u>hyalophane</u> occurs at 113.00 - 113.06m [PTS 4321]	Minor pyrite in smears and in cross-cutting hair-veinlets; also enclosed in quartz lenses	546
114.15	0.31		Limestone, grey, poorly banded	Disseminated pyrite	
114.54	0.39	F 85	Muscovite-schist, grey, weakly graphitic and dolomitic	Minor pyrite	
114.98	0.44		Limestone, grey	Minor pyrite in laminae	
115.15	0.17		Muscovite-schist		547
117.15	2.00		Graphitic muscovite-schist with quartz lenses	Pyrite grains and patches	548
121.06	3.91	F 80	Biotite-muscovite-chlorite-schist, dolomitic and quartzose with dolomite-quartz bands especially at 120.34-120.91m	Pyrite traces with calcite and chlorite in hair veinlets	549
121.27	0.21	B/F 45	Dolomitic quartzite, banded		
121.95	0.68	F 90	Dolomitic muscovite-biotite-chlorite-schist with a few quartzose layers	Trace of pyrite	550
122.05	0.10		Calcareous quartzite, banded		
123.30	1.25	F 85	Dolomitic muscovite-biotite-schist with many quartz bands, quartzose and chloritic		551
124.18	0.88		Lamprophyre sheet with phenocrysts of hornblende and pink and white feldspars set in an olive-green groundmass; hair veinlets of calcite		552
127.57	3.39		Muscovite-chlorite-schist, dolomitic and quartzose with some biotite; quartz-biotite lense at 124.45 - 125.15 m; pale muscovitic bands notably at 126.25 - 126.43m; some pinkish calcite veinlets	Minor pyrite in chlorite laminae	553
128.63	1.06		Graphitic muscovite-schist, massive and black, interbanded with paler rock containing quartz and dolomite; foliation deflected adjacent to quartz lens	Pyrite common in veinlets	554
131.71	3.08		Graphitic muscovite-schist, dark grey, moderately graphitic with some dolomite and calcite veining; quartz lenses from 130.07 to 130.37m; the schist appears to be rich in minute zircon grains and a lens of irregularly intergrown quartz and dolomite patches occurs at 130.29 - 130.37m [PTS 4322]	Pyrite locally common in conformable smears, also remobilised in cross-cutting hair veinlets	555
133.93	2.22		<b>BEN LAWERS SCHIST</b> Garnet-muscovite-schist with quartz eyes and lenses, some biotite and calcite; the garnet is almandine	Trace of pyrite	
135.17	1.24		Calcareous muscovite-schist with quartz eyes and lenses and hornblende porphyroblasts below 134.50m; a disrupted quartz lens is broken into fragments at 134.05 - 135.13m		556
135.55	0.38		Muscovite-schist, weakly graphitic with some large hornblende porphyroblasts	Pyrite minor in calcite hair veinlets	
137.88	2.33	F 90	Calcareous hornblende-muscovite-schist with abundant porphyroblasts of hornblende, locally biotitic and massive; calcite veins common, some with patches of dark green clay or chlorite		557
140.80	2.92		Calcareous muscovite-biotite-schist, massive		558
143.62	2.82	F 80	Calcareous muscovite-hornblende-biotite-schist consisting of alternating laminated biotitic bands and massive bands with little or no biotite; hornblende porphyroblasts abundant		559
146.45	2.83		Calcareous muscovite-hornblende-biotite-schist with quartz veins and lenses and some darker coloured graphitic bands; quartz segregations and white calcite veinlets present		560
148.31	1.86		Calcareous hornblende-biotite-schist with quartz eyes and lenses and bands of dolomitic muscovite-schist, cut by calcite veinlets		561

## APPENDIX I TABLE VII (CONTINUED)

				G E O L O G I C A L      R E C O R D		
Inclined Depth m	Inter- section angle m	Structure angle	Lithology	Mineralisation	Sample CYD No	
148.90	0.59		Amphibolite, consisting of coarse-grained hornblende porphyroblasts and muscovite in a compact green rock apparently interbedded with calcareous biotite-schist cut by calcite veinlets			
151.82	2.92		Amphibolite, coarse-grained and laminated, consisting of hornblende, quartz, biotite and calcite, possibly part of unit above; accessory sphene and apatite [PTS 4323]	Traces of pyrite and chalcopyrite	562	
159.60	7.78	F 70	Calcareous hornblende-muscovite-chlorite-schist with accessory biotite and fine, acicular crystals of probable clinzoisite [PTS 4324]; amphibole with characteristic garbenschiefer texture; quartz eyes and veins with minor white calcite also present; accessory sphene and rutile; cross-cutting quartz veins at 155.50m	Visible sulphides absent; trace of chalcopyrite in polished section	563 564 565	
162.20	2.60	F 080	Calcareous biotite-muscovite-schist with quartz eyes and lenses; hornblende porphyroblasts common at 160.50m; calcite occurs in cross-veinlets as well as in the rock fabric		566	
170.75	8.55	F 70	Biotite-hornblende-muscovite-schist, calcareous throughout; pale green colour possibly due to abundant chlorite; grey quartz in eyes and lenses; acicular crystals of probable clinzoisite at 166.0 m [PTS 4325]		567 568	
170.75			End of borehole		569	

## GEOLOGICAL RECORD

Inclined depth m	Inter-section m	Structure angle	Lithology	Mineralisation	Sample CYD No
0.00					
4.46	4.46		Superficial deposits, including boulders of siliceous schists and graphitic schist	Sphalerite abundant in siliceous schist	614
			BEN BAGACH SCHIST		
6.56	2.10	{ F 70 C 30	Graphitic muscovite-schist, mid grey, strongly foliated; quartz lense at 5.86 - 6.02m with rectangular crystals up to 15 mm across of soft greenish-white (?) chlorite; lensing quartz band 10 - 40mm thick at 10.20m	Minor pyrite as thin bands on foliation; more plentiful as patches up to 20mm across indenting quartz lens	615
8.92	2.36	F 70	Graphitic muscovite-schist, mid grey and strongly foliated; fine grained, compact and dolomitic at 7.56 - 7.70m and in thinner bands elsewhere; non calcareous [PTS 4510]	Thin pyrite bands and rare veinlets	616
10.44	1.52	F 65	Muscovite-quartz-schist, light grey, varying from intensely folded to simply laminated; the more compact laminated schist is dolomitic [PTS 4511]		617
12.14	1.70	F 60	Biotitic muscovite-quartz schist, sparingly dolomitic; greenish grey, ranging from intensely folded to simply laminated; weakly graphitic around 12.00m; biotite rare to absent below 12.40m; cherty quartz lens 15 mm thick at 10.96m; quartz lenses mostly small		618
15.74	3.60	F 65	Muscovite-schist, weakly graphitic and quartzose; thin (1-3mm, lensing) dolomitic band at 12.29m; broken badly cored quartz band at 12.50 - 12.55m. Very low core recovery below 13.32m - with probable additional presence of quartz-muscovite-schist and graphitic muscovite-schist. - fault [PTS 4512].	(?) Pyrrhotine disseminated and along foliation with traces in cross-cutting veinlets	
16.54	0.80	F 80	Muscovite-biotite-chlorite-schist	(?) iron sulphide disseminated and along foliation	619
17.58	1.04	F 70	Biotitic muscovite-quartz-schist, sparingly dolomitic; grey and strongly foliated	Pyrite disseminated along foliation with ? limonite	620
19.40	1.82	F 60	Muscovite-quartz-schist, characterised by muscovite in coarse grained books and in abundance along foliation; pinkish grey and well foliated with quartz lenses; below 18.25m more fine grained and weakly dolomite with small quartz knots in which sulphide is common. [PTS 4513]	Scattered fine grained pyrite; also very common on foliation	621
20.60	1.20	F 60	Muscovitic quartz-schist; probably weakly graphitic; grey, compact and finer grained than above; becomes more graphitic below 20.05m; band of dolomitic limestone 19.90 - 20.05m	Much (locally 10%) fine to medium grained pyrite	622
21.67	1.07	F 60	Muscovitic quartz-schist, grey laminated, graphitic at 21.26m, very fine grained and calcareous at 21.43 - 21.48m; quartzose at 21.62 - 21.67m; fault marked by calcite veining 20.60 - 20.70m, and quartz lens at 20.70 - 20.81m	Pyrite patches up to 10 mm in veined schist; small sphalerite and pyrite in vein; much pyrite in conformable bands up to 2 mm thick	623
23.17	1.50	{ F 70 C 20	Muscovitic quartz-schist, grey, compact with only minor folding; biotitic quartz schist between 21.80 and 22.10m and some darker, probably graphitic bands	Pyrite in conformable bands, especially at 22.10m, and as minor veins	624
24.55	1.38	F 70	Quartz-schist, weakly muscovitic, light grey, compact and weakly foliated with quartz lenses; minor fault at 24.07m and 24.35 - 24.48m	Pyrite weakly disseminated along foliation and as patches in calcite veinlets	625
25.80	1.25		Quartz-schist, biotitic, muscovitic and sparingly dolomitic with some darker (?) graphitic bands; folded	Minor pyrite in conformable bands	626
28.83	3.03	F 70	Graphitic muscovite-schist, dark grey, compact and finely laminated; very quartzose and essentially a micaceous quartzite between 27.10 and 27.43m; minor chlorite and, below 28.00m, dolomitic	Minor conformable pyrite except at 28.80m where it forms 0%	627
31.07	2.24		Graphitic muscovite-schist with micaceous quartzite at 29.37 - 27.51m and below 30 - 25m bearing garnet and chlorite pseudomorphs after garnet; fault at 29.33 - 30.25m	Pyrite common in fault zone and in veinlets in adjacent rock; (?) chalcocopyrite in thin veinlets at 28.85m	628
33.63	2.56		Graphitic muscovite-schist, dark grey well foliated and folded; calcareous with thin bands of fine grained dark limestone above 32.55m; bands of muscovite-quartz-schist prominent between 32.55 and 33.63m; cut by quartz vein at 32.88 - 33.46m	Trails and patches of pyrite with rare pyrrhotine; sulphide content increases in lowest 20cm	698
38.25	4.62		Muscovite-quartz-schist, silvery green with minor chlorite and interbedded graphitic muscovite-schist and mica-schist; strong foliation with minor crinkling at 34.20m; dolomitic patches at 35.78m and quartz with chloritic selvages and minor pyrrhotine at 33.63 - 33.85m	Pyrrhotine throughout in patches and trails - coarse development at 37.70m; pyrite less common, present in veins; (?) sphalerite at 34.64 - 34.73m and (?) chalcocopyrite at 37.38m	699
38.90	0.65		Quartz vein with lenses of graphitic muscovite-chlorite-schist; core broken below 38.78m - (?) fault; rare calcite veinlet at 38.45m	Coarse pyrite in patches and trails; silena at 38.25 - 38.85m in quartz-chlorite (?) breccia with possible schist fragments; trace (?) sphalerite at 38.31m	700
46.27	7.37		Graphitic muscovite-schist, dolomitic in parts with inter-banded dark fine-grained limestone and, more rarely, muscovite-schist and quartz-muscovite-schist; local crumpling and probable faults at 40.56m and 41.40-42.33m as evidenced by broken core and quartz veins [PTS 4674]	Pyrrhotine and pyrite trails and patches common in graphitic schist; pyrite also in veinlets; (?) sphalerite in limestone band at 40.11 - 40.18m	701
52.80	6.53		Micaceous quartzite, with garnets pseudomorphed in part by chlorite; coarse dolomite patch below 51.50m; poorly defined foliation and occasional quartz veins; core highly broken - (?) fault	Sporadic pyrite and pyrrhotine	702

## GEOLOGICAL RECORD

Inclined depth	Inter-section	Structure angle	Lithology	Mineralisation	Sample CYD No
53.32	0.52	F 90	Graphitic muscovite-schist, with fine grained homogeneous limestone bands and, below 53.07m micaceous quartzite	Minor pyrite	
53.82	0.50		Quartz vein, locally micaceous with dolomitic patches	Sporadic coarse pyrite	703
		F 90	Micaceous quartzite, sparingly dolomitic with local mottled texture [PTS 4675]; interbedded graphitic schist and limestone; grit band at 55.23 - 65.66m; garnets together with (?) biotite appear below 55.00m; local minor quartz and calcite veinlets; graphite-schist bands often highly contorted; strong foliation below 66.26m. Core highly broken at 54.46m and below 69.32m., the latter accompanied by calcite veining - (?) faults distinctly more schistose in lowermost 20 cm passing down into	Pyrite sporadically throughout, as patches and trails sub-parallel to foliation and in remobilised veins	704
70.18	16.36	F 80			705
72.64	2.46	F 90	Muscovite-schist, silvery green, with strong locally contorted foliation and quartz-calcite segregations	Pyrite and pyrrhotine as small patches and trails throughout decreasing below c 72.00m	706
73.53	0.89	F 90	Micaceous quartzite, greenish with good foliation and variably dolomitic.	Minor pyrite and pyrrhotine	707
79.15	5.62	F 80-90	Graphitic muscovite-quartz-schist, variably dolomitic with thin interbands of fine grained dark limestone; strong foliation with local crumpling and incipient strain-slip cleavage	Abundant pyrrhotine as trails and coarse patches; pyrite less common	708 709
80.00	0.85	F 90	Limestone, fine grained, dark, homogeneous	Minor pyrrhotine and pyrite	710
80.90	0.90	F 80-90	Graphitic muscovite-schist, with dark limestone; lowermost 20 cm highly broken	Veiniform, patchy and stratiform pyrite	711
82.63	1.73	F 90	Sparingly micaceous quartzite, 'fragmented texture' in uppermost 55-60 cm due to strong quartz (with chlorite clasts) veining; probably not a true breccia; distinctly more homogeneous below 81.47m with irregularly developed foliation	Abundant pyrite in coarse patches, stringers and veins; rare pyrrhotine; (?) sphalerite in quartz vein at 82.50m	712
84.85	2.22	F 80-85	Graphitic muscovite-schist, lead grey with prominent foliation showing minor crumpling and folding; thin homogeneous limestone bands common; cut by calcite and calcite-quartz veinlets, particularly below 83.81m	Pyrite common in trails, stringers and veinlets; minor sphalerite at 83.35, 83.61 and 84.50m	713
86.80	1.95		Muscovite-quartz-schist, green (notably between 86.55 and 86.78m.) with intensely crumpled foliation; some interbedded limestone and graphitic schist with occasional gradational junctions; quartz vein between 86.78 and 86.80m	Variable amounts of pyrite, pyrrhotine and some associated sphalerite	714
93.80	7.00	F 70	Graphitic muscovite-schist, variably calcareous with local limestone bands up to 25 cm thick; quartz veins and rare quartz-dolomite segregations; strong foliation with local crumpling and poorly developed strain-slip cleavage; core strongly fractured at 87.68 - 90.07m. - (?) minor fault	Pyrite and pyrrhotine occur variably throughout; trace sphalerite at 90.83 and 91.23m; (?) chalcocite with pyrrhotine in quartz lens at 90.78m	715 716
95.18	1.38	F 90	Muscovite-quartz-schist with biotite; silvery green with strong foliation enhanced by local quartz and dolomite lenses; interbedded graphitic schist below 94.65m, where core becomes darker and more massive; also dolomitic; grades down into	Pyrite and pyrrhotine variably throughout. Trace galena and sphalerite in quartz veins 95.12-95.18m	717
100.70	5.52	{ F 80 C 60	Graphitic muscovite-schist, lead grey, strongly and regularly foliated with intense crumpling below 97.05m; poorly defined strain-slip cleavage; interbedded limestone, calcite and quartz veining	Pyrite and pyrrhotine irregularly distributed in rock and vein	718
102.02	1.32		Quartz-mica-schist and micaceous quartzite with thinly interbedded graphitic schist; good foliation with minor crumpling; quartz veins common below 101.13m	Pyrite relatively common, with minor pyrrhotine	719
102.80	0.78		Graphitic muscovite-schist, well developed foliation with dolomite-quartz partings and quartz veins	Pyritic trails and rarer patches	720
104.31	1.51		Quartz-calcian rock, massive, unfoliated with mottled texture resulting from ubiquitous chloritic-micaceous knots and fracture infillings; <u>fracture</u> at 103.10m; minor quartz veining	Pyrite and pyrrhotine common throughout; massive sphalerite in vein at 103.83m and with pyrite and pyrrhotine at 104.10m; (?) chalcocite on broken surface at 103.75m	721
105.21	0.90		Quartz-calcian rock, greenish with crinkled foliation; coarsely crystalline calcian at 104.61m and below; cut by quartz vein and dolomitic patches	Pyrite disseminated throughout and in coarse patches	722
105.74	0.53		Quartz-calcian rock, initially identical with above having mottled and fractured texture and abundant chlorite; chlorite-infilled shears absent below 105.58m	Abundant pyrite throughout with subordinate pyrrhotine trace galena in vein with pyrite at 105.42m and 105.57m	723
114.29	8.55	F 70 F 85 F 90 F 65 F 65 F 65 F 45	Muscovite-schist, dolomitic and with chloritic partings; generally striped due to alternating dolomitic and micaceous laminae; principal variations in appearance result from variations in proportions of chlorite and dolomite; rare biotite; thin dark dolomitic limestone at 107.26 and 107.46m; and micaceous quartzite between 110.60 and 110.71m; well developed foliation throughout showing variable disruption ranging from minor crumpling to tight folding; veins and lenses of quartz, calcite and calcite; occasional chloritic hair veinlets [PTS 4514]	Pyrrhotine common above 107.00m. as coarse patches and stratiform trails; below this pyrite dominant; overall sulphide content markedly smaller; sulphide practically absent below 112.50m	724
115.94	1.65	F 60	Chlorite-muscovite-schist, dolomitic with very minor graphite; densely chloritic at 115.69 - 115.78m and at 115.81m small dolomitic patches with cavities; strong foliation folded with strain-slip cleavage [PTS 4515]	Pyrite and minor chalcocite dispersed throughout with addition of sphalerite below 115.71m	
116.30	0.36		Dolomite-schist, massive, gray; laminated but not fissile and graphitic; calcareous in parts and cut by white (?) calcite hair veinlets	Pyrrhotine in dispersed conformable streaks; rare pyrite	726

GEOLOGICAL RECORD						
Inclined depth m	Inter-section m	Structure angle	Lithology	Mineralisation	Sample CYD No	
118.13	1.83		Graphitic muscovite-schist, striped with minor quartz; little carbonate except in certain massive black limestone bands; lamination frequently crumpled; cross cutting veinlets of calcite, chlorite and pyrite and rare quartz lenses.	Pyrrhotine and pyrite disseminated throughout; pyrite also in veinlets. Sphalerite accompanies pyrrhotine and forms discrete patch adjacent to quartz lens.	727	
118.42	0.29		Dolomitic and calcareous limestone, grey, banded with conspicuous tight fold closure; cut by dolomitic veinlets; irregular chloritic hair veinlets at base of bed.	Pyrite in dolomitic veinlets; sphalerite in chloritic veinlets.		
		F 80	Graphitic muscovite-schist, with quartz and dolomite; frequently striped due to alternating dark grey graphite-muscovite and paler quartz-dolomite laminae; between 119.61 and 119.91m prominent pyrite-chlorite partings sub parallel to core axis; lamination well developed, frequently contorted with some u-shaped folds; rare quartz lenses; many irregular dolomite veins at 118.42 - 118.79m with open vuggy cavities; some obviously leached.	Pyrite in dolomitic veinlets; sphalerite in chloritic veinlets. Pyrite and pyrrhotine occur irregularly in rock with some associated sphalerite; pyrite also in veinlets.	728	
		F 70			729	
125.61	7.19		Dolomite, massive grey with quartz and minor muscovite; muscovite layers and bands of laminated graphitic muscovite schist; cross cutting pyrite-chlorite hair veinlets.	Disseminated pyrrhotine with trace (?) chalcocypsite; pyrite in hair veinlets.	730	
126.22	0.61	F 80	Graphitic muscovite-schist, with dolomite and quartz; consists of interlamated graphitic-muscovite and pale dolomite; foliation disrupted by secondary cleavage; rare quartz segregation and dolomitic veinlets [PTS 4516].	Pyrrhotine in variable amounts with minor pyrite and sphalerite; latter two also in quartz lens at 128.28m.	731	
129.60	3.38	F 80	Graphitic muscovite-schist, sulphide-rich, and dolomitic; sulphide in conformable massive bands with calcite, also dispersed grains and conformable streaks, at 129.90 m coarse segregation of quartz, dolomite, pyrrhotine, (?) celonian and rutile.	Pyrite, lesser sphalerite and minor pyrrhotine in massive bands and dispersed elsewhere.	732	
130.11	0.51	F 70-80			733	
		F 85	Graphitic muscovite-schist, calcareous and rich in pyrite; poor in quartz-carbonate laminae - in effect a dark and relatively massive rock; below 131.25m, becomes lighter and more striped with bands of massive dolomitic muscovite-quartzite; returns to dark schist between 133.68 - 134.63m; dolomitic limestone at 136.25 - 136.35m; foliation variably defined and frequently contorted; approximately 50% core loss between 134.67 and 136.05m; calcite and dolomite veinlets. [PTS 4478 & 4479].	Pyrite and pyrrhotine irregularly throughout with minor sphalerite.	734	
		F 75			735	
136.73	6.62	F 70			735	
		F 80			736	
137.49	0.76		Lamprophyre, green with dark amphibole phenocrysts and carbonate patches; both contacts concordant with foliation; calcite vein at 137.44m and slickensiding in upper 10 cm.		736	
		F 90	Graphitic muscovite-quartz-schist, dolomitic or, more rarely, calcareous in parts with (?) celonian; upper 60 cm relatively deficient in graphite; limestone band with calcite veining at 138.92 - 139.17m; foliation well developed being enhanced by the ubiquitous pyritic trails or, at 138.19m by quartzose band; quartz veins common some carrying dolomite and minor calcite clasts; calcite veins less common [PTS 4676, 4677]. Core highly broken at 138.53m and veined with calcite, and at 139.17 - 139.22m clay schist and fine debris - ? fault	Pyrite exceedingly common as stratiform trails and stringers with local coarse patches, trace pyrrhotine; quartz veins carry occasional pyrite, minor sphalerite and rare galena.	737	
		F 90			738	
146.18	8.69	F 90			738	
		F 85	Biotite-chlorite-quartz-schist, with minor muscovite; greenish with prominent striping due to interbanded quartz and chlorite-biotite; locally dolomitic; quartzose band at 147.95 - 148.10m underlain by chlorite-rich zone; notable increase in biotite content below 150.75m; inclination of foliation highly variable due to micro-folding; a few quartz veins and rare calcite veinlets. [PTS 4678]	Pyrrhotine and pyrite occur patchily and in veins.	739	
151.59	5.41	F 85-90	Graphitic muscovite-quartz-schist, lead grey with interbanded paler dolomite; good foliation with crumpling and micro-folding; quartz rich units (possibly a vein) with chlorite-biotite wisps present at 152.85 - 153.17m and 153.33 - 153.44m, fine grained limestone at 153.44 - 153.59m; quartz and calcite veins fairly rare.		740	
153.85	2.26	F 90			741	
154.63	0.78	F 70	Muscovite-chlorite-schist, green, with thin graphitic partings and local folding; quartz veining very common.	Pyrrhotine common in coarse patches and trails. Minor pyrite.	741	
		F 70	Graphitic muscovite-quartz-schist, lead grey with prominent dark graphitic partings producing a coarse foliation; partings frequently lensed and 'clast like'; dolomitic in parts.	Pyrrhotine common throughout with rare associated pyrite.	742	
155.03	0.40				743	
		F 90	Chlorite-mica-schist, with biotite and muscovite, dark green with local graphitic partings and below 155.65m garnet; variably dolomitic - generally as thin bands but may be up to 3 cm thick; minor folding occurs sporadically throughout, as do quartz veins; coarse carbonate (dolomite and minor calcite) segregation at 157.72 - 157.85m.	Sulphide content very low - principally pyrrhotine with rare pyrite.	744 745	
165.60	10.57				745	
			<b>NEW LAYERS SCHIST</b>			
		F 80-85	Calcareous hornblende-schist, with coarse bladed hornblendes, chlorite, muscovite and fine calcite; very poorly defined foliation with only minor folding evident; dolomite segregations with or without quartz common, particularly between 166.00 and 167.03 m; patches and veins of orange-red calcite; rare quartz veins. Core broken 167.03 - 167.44m with approximately 40cm breccia - fault	Coarse patchy pyrite at 165.85 - 165.9m; sulphide extremely rare below this.	746	
171.46	5.86	F 55				
		F 90	Calcareous quartzite, fine grained, grey-green with colour band; probably due to variable chlorite content; calcite vein on bands and red (?) calcite speckle- throughout.			
172.16	0.70					
		F 90	Calcareous hornblende-schist, very similar to above with bladed amphibole, chlorite, muscovite, calcite and irregularly developed foliation showing rare minor folds; quartz, quartz-calcite and dolomite segregations; orange-red calcite in vein with quartz at 173.12m calc-schist without amphibole but with well developed foliation present at 174.14 - 174.40m; interbanded dolomitic quartzite at 189.37 - 189.56m and calcareous quartzite at 198.60 - 198.86m and 199.70 - 199.86m.	Overall sulphide content very low; mostly traces of pyrite but occasionally present as massive patch with calcite.		
200.83	28.67	F 75-80				
200.83			End of borehole			



Inclined depth m	Inter-section m	Structure angle	Lithology	Mineralisation	Sample CYD No
0.00					
3.50	3.50		Superficial deposits		
			BEN LAWERS SCHIST		
6.19	2.69	{ F 40 C 155	Muscovite-biotite-dolomite-chlorite-schist composed of alternating micaceous and quartzose bands; some limonitic fractures; accessory rutile and albite [PTS 4326]		570
6.81	0.62	{ F 65 C 45	Weathered mica-schist, leached and limonitic but otherwise similar to above		
8.32	1.51	{ F 65 C 50	Calcareous biotite-muscovite-schist with quartz; calcite in fractures, limonitic and leached in parts		571
9.17	0.85	{ F 40 C 150	Banded dolomite-muscovite-schist with yellow dolomitic laminae less than 5mm thick except at 8.64 - 8.67 m where a medium-grained granoblastic dolomite has a laminated fabric due to drawn out quartz patches, and accessory muscovite, biotite, rutile and chlorite [PTS 4327]		
9.65	0.48	F 65	Quartz-calcite-muscovite-schist, limonitic, poorly banded		
10.60	0.95		Dolomitic muscovite-biotite-schist, limonitic and leached		
11.28	0.68	{ F 30 C 150	Dolomitic biotite-muscovite-schist with quartz, somewhat limonitic and leached with calcite veinlets on fractures	Accessory pyrite in calcite veinlets	572
16.50	5.22	{ F 30 C 145 F 60 C 40	Muscovite-schist with bands of dolomitic schist composed of dolomite, muscovite and quartz [PTS 4328]; sulphides occur on limonitic fracture surfaces and are drawn out with the contorted schistosity, accessory rutile	Flattened pyrrhotine grains within schistosity; pyrite in cross veinlets and trace of chalcopyrite	573 574
17.69	1.19	F 65	Dolomite-quartz rock, irregularly banded, iron stained in part; pyrite-muscovite-schist at base [PTS 4329] contains c 10% pyrite and minor calcite and rutile	Pyrite especially at base in grains and irregular patches flattened and within the foliation	575
			BEN HAGACH SCHIST		
20.03	2.34	{ F 70 C 150 F c 80	Graphitic muscovite-schist, dark grey and weakly dolomitic with alternating quartzose and graphitic laminae; core highly broken and below 19.43 m exhibits leached cavities containing a little quartz and from which calcite may have been leached	Pyrite common as disseminated flattened grains; high Ba content presumably located in muscovite	576
21.01	0.98	F 75	Banded "cherty" rock probably composed of quartz and celsian; alternating light and dark grey layers with some thin white quartz-(?) baryte laminae; baryte probably present with quartz in soft white veinlets	Baryte probably a minor constituent	
22.50	1.49	F 70	Quartz-celsian rock; pale grey, fine-grained and "cherty" in upper 20 cm with closely-spaced pyrite trails accentuating probable bedding; below this grain size increases with celsian crystals reaching 5 mm and there are bands of darker grey quartz; limonite common throughout giving rise to a distinctive banding and gossanous zones	Pyrite fairly common in disseminations and in conformable laminae and trails	577
25.98	3.48	F 60	Baryte-rock, massive, light grey, coarse-grained with limonitic fracture surfaces; a petrographical specimen [PTS 4679] at 25.12 - 25.17 m contains significant amounts of quartz and clay mineral plus minor rutile, chlorite, pyrite and goethite; the clay mineral replaces primary mica	Baryte abundant; pyrite disseminated, in laminae and on fractures; banded pyrite more common near base and often oxidised	578 579
26.60	0.62		Broken core (loss recorded) composed of limonitic fragments of a quartzite-like rock		580
28.35	1.75	F 75	Quartz-celsian rock, light grey, "cherty", carbonate-free; limonite-stained throughout with numerous leached cavities; lower part of unit is highly enriched in sphalerite	Pyrite common, accessory sphalerite in laminae, disseminated and in small irregular patches	581
29.14	0.79	F 75	Muscovite-quartz-celsian-schist, slightly banded and somewhat "cherty" in aspect; bladed porphyroblasts of celsian are strongly zoned and intergrown with hyalophane [PTS 4330]	Pyrite and sphalerite common as disseminations and in bands; also galena and chalcopyrite	582
29.54	0.40	{ F 60 C 145	Muscovite-schist, a little graphitic, carbonate-free	Pyrite and sphalerite common	
30.35	0.81		Muscovite-schist, quartzose and sphalerite-rich but carbonate-free; the pyrite is altered to microcrystalline, concentrically-banded patches [PTS 4331]	Sphalerite (c 6% in sectional specimen) in thin irregular segregations with equal pyrite, chalcopyrite and galena noted	
31.52	1.17	{ F 45 C 140	Graphitic muscovite-schist, quartzose, dark grey, carbonate-free limonitic in places indicating leaching of sulphides; graphitic bands, soft and broken at 31.28 - 31.33m	Sphalerite and equal pyrite locally common in streaks and disseminations	583
31.70	0.18		Dolomite band, massive and grey containing thin layers of dolomite and sphalerite which are somewhat limonitic (paleontological sample taken)	Sphalerite in thin layers	
35.18	3.48	{ F 45 C 165	Graphitic muscovite-schist, quartzose and weakly dolomitic with traces of calcite; limonitic in vicinity of sulphides; dolomite band 1 cm thick at 32.54 m	Pyrite, sphalerite, pyrrhotine and trace of chalcopyrite	584
35.38	0.20		Dolomite band, massive and grey, grading into schist below; the dolomite is medium-grained and contains subsidiary amounts of muscovite and quartz; rutile is an accessory and quartz-dolomite veinlets carry accessory sulphides [PTS 4680] (paleontological sample taken)	Sphalerite, galena and pyrite in veinlets	
37.31	1.93	{ F 55 C 140 F 80 C 45	Weakly graphitic muscovite-schist, interbanded with thin limestone beds, massive and fine-grained, and bands of grey muscovite-quartz-dolomite schist; the schists are quartzose and dolomitic, containing accessory biotite, zircon and sulphides [PTS 4681]	Pyrite, pyrrhotine, sphalerite and chalcopyrite present in minor amounts, disseminated and hair veinlets	585
38.17	0.86		Calcareous muscovite-schist, quartzose with small porphyroblasts of green tourmaline [PTS 4332]	Pyrrhotine mainly in hair veinlets	586
42.79	4.62		Metabasite; calcareous chlorite-schist with relatively minor muscovite and biotite and accessory rutile [PTS 4333]	Traces of pyrrhotine	587
43.20	0.41	F 70	Muscovite-chlorite-schist, dolomitic with accessory rutile [PTS 4334]	Minor pyrrhotine and pyrite	
45.23	2.03	F 75	Dolomite-chlorite-schist with relatively minor muscovite and biotite, and minute ilmenite crystals; poorly laminated [PTS 4335]	Traces of pyrrhotine, chalcopyrite and sphalerite	588
47.61	2.38	{ F 60 C 150	Graphitic and dolomitic muscovite-schist with minor calcite; top 40 cm non-graphitic		589

## GEOLOGICAL RECORD

Inclined Depth m	Inter-section m	Structure angle	Lithology	Mineralisation	Sample CYD No
48.49	0.88	F 70	Sphaleritic dolomite, granoblastic, schistosity defined by druse out quartz patches [PTS 4336]; subsidiary amounts of quartz and muscovite are present	Sphalerite common in conformable laminae; pyrite in cross veinlets	590
53.45	4.96		Metabasite; calcareous, massive, unbanded rock, possibly an epidiorite; limonitic fractures; contacts ill-defined	Trace of pyrrhotine	591
54.00	0.55		Dolomite-quartz-schist with muscovite, yellowish coloured	Trace of pyrrhotine	
54.89	0.89	F 75	Muscovite-schist with quartz veinlets, limonitic fractures and quartz-calcite segregations	Pyrrhotine, pyrite, galena and sphalerite around segregations	592
55.21	0.32	{ F 80 C 130	Muscovite-schist, dolomitic, massive		
56.58	1.37	{ F 90 C 135 F 70	Muscovite-schist, dolomitic, interbanded with sphaleritic dolomite; schist is carbonaceous in part; the dolomite [PTS 4337 at 56.0 m] is similar to that at 47.61 - 48.49 m	Sphalerite common in laminae in dolomite rock with pyrite; pyrrhotine smears in schist	593
56.95	0.37		Dolomitic and sphaleritic limestone, massive and grey with quartz-sphalerite bands and calcite-sulphide bands; calcite hair veinlets also present	Sphalerite common, lesser pyrite	594
58.50	1.55	{ F 85 C 145	Muscovite-schist, dolomitic, dark grey and somewhat graphitic; minor calcite veinlets	Pyrrhotine common, lesser pyrite	
59.78	1.28	{ F 80 C 60	Graphitic muscovite-schist, dolomitic with quartz lenses and veinlets	Pyrrhotine and pyrite	595
63.00	3.22		Graphitic muscovite-schist, dark grey with dolomite and chlorite; cut by calcite and quartz veinlets	Pyrite; sphaleritic bands at 62.90 m	596
66.09	3.09		Graphitic muscovite-schist, highly graphitic at 63.15 - 63.50 m; some highly calcareous bands some 15 cm in thickness and a dark grey, fine-grained limestone at 65.60 - 65.90 m	Pyrite locally common; pyrrhotine	597
66.68	0.59		Quartzose schist, weakly graphitic, coarse-grained and mid-grey in colour with subsidiary amounts of muscovite and dolomite; pyrite and pyrrhotine are segregation in section [PTS 4338]	Sphalerite, pyrite and pyrrhotine	
67.60	0.32		Graphitic muscovite-schist	Pyrite in calcite veinlets	598
71.62	4.02	{ F 90 C 70 F 45 C 120	Graphitic and dolomitic muscovite-schist, dark grey with minor quartz-calcite veinlets and some thin, massive limestone bands (palaeontological sample taken at 69.68 - 69.74 m); muscovite exceeds quartz in section [PTS 4339]	Pyrrhotine exceeds pyrite in coarse grained bands; trace of chalcocopyrite	599
72.18	0.56		Quartz-celsian rock, coarse-grained, poorly banded	Pyrite minor sphalerite	
73.60	1.42	F 60	Celsian-dolomite interbanded with quartz-celsian rock; the former is composed of a coarse-grained orientated mosaic of celsian porphyroblasts with sieve-textures in which quartz and sulphide grains are embedded, set in a coarse dolomite matrix [PTS 4340]; the quartz-celsian rock is well banded and dolomitic [PTS 4341]	Sphalerite and trace of chalcocopyrite occur in the dolomite rock; pyrite, pyrrhotine and galena have a strongly banded distribution in the quartz-celsian rock	600
74.58	0.98		Quartz-celsian rock, coarse-grained and dolomitic with a quartz veinlet; banding defined by celsian laminae and by sulphide-rich laminae	Sulphides common in laminae-pyrite, pyrrhotine and sphalerite	601
75.73	1.15	F 45 F 90	Celsian-quartz rock with minor dolomite and rutile [PTS 4342], finely banded by sulphide laminae	Pyrrhotine, pyrite and sphalerite in laminae	
76.07	0.34		Limestone bed with irregular grey, "cherty" bands, probably celsian-bearing	Sphalerite and pyrite	602
76.32	0.25		Pyrrhotine lens, massive with irregular contacts, the upper contact having a fragmented appearance; sulphide intergrown with quartz, celsian, dolomite and clay [PTS 4343]	Pyrrhotine exceeds 50% skeletal and intergrown with celsian-quartz rock at margins, minor chalcocopyrite	603
76.58	0.26		Limestone bed incorporating "cherty" bands with coarse celsian crystals in places	Pyrrhotine, sphalerite and galena in blebs	
76.68	0.10		Quartz-celsian rock, dark grey and banded	Sphalerite, pyrite and galena in bands up to 6 cm thick	604
78.37	1.69	F 45	Quartzite, banded with bands rich in dolomite porphyroblasts or in sulphides [PTS 4344]	Pyrrhotine and lesser sphalerite and pyrite in bands; galena in quartzite bands	605
81.80	3.43	{ F 80 C 53	Muscovite-schist, moderately graphitic; weakly foliated, biotitic and dolomitic at 78.37 - 78.87 m; quartzite band at 81.0 m [PTS 4345]	Pyrrhotine, pyrite and sphalerite in conformable laminae	606 607 608
90.53	8.73	{ F 70 C 30	Muscovite-schist, moderately graphitic with rare quartz lenses and some thin bands of dark limestone; rare calcite veinlets		
100.48	9.95	F 75 F 75 F 80	Graphitic muscovite-schist, dark grey, sparingly dolomitic with thin bands of dark grey, massive limestone at 91.18 - 92.27 m, 91.43 - 91.51 m and at 91.74 m and 92.19 m; sparse porphyroblasts of almandine garnet in lower part of unit	Pyrrhotine and pyrite sparse in laminae, cross veinlets and isolated grains	609 610 611 612
100.48			End of borehole		

## GEOLOGICAL RECORD

Inclined depth m	Inter-Section m	Structure angle	Lithology	Mineralisation	Sample CYD No
0.00					
3.05	3.05		Superficial deposits		
			BEN BAGACH SCHIST		
5.75	2.70	F 45	Muscovite-schist, silvery with darker ?graphitic partings; initial 50 cm of core broken into "slivers" along foliation	Rusty (?) limonite partings	629
		{ F 70 C 30	Graphitic-muscovite-schist, lead-grey with good foliation showing mostly minor crumpling; strain-slip cleavage sufficiently strongly developed in places as to obliterate foliation; concordant lenses of fine-grained (?) calcareous material occur locally viz 6.20, 6.45, 10.33 and 10.60 - 62m; between 10 and 10.05m 5cm thick siliceous band with very thin calcite veinlets; where present (viz 8.31 and 8.58 m) calcareous/calcite wisps and veinlets emphasise foliation; prominent calcite veins, generally subparallel to foliation occur at 10.66 - 74 m and 10.87 m [PTS 4517, 4518]	Pyrite and pyrrhotine in patches and trails throughout, and in calcite veins; traces of chalcopyrite and sphalerite	630 631 632
11.35	5.60	F c90	Muscovite-quartz-schist, more calcareous and less leaden than above, passing (c 12.60 m) down into calc schist with speckled texture resulting from small biotite and chlorite wisps; strong foliation with local crumpling; coarse patches of dolomite and quartzite eg at 12.04 - 12.10 m; irregular quartz lenses at 12.31 - 12.35 and 12.52 - 12.60 m with interbedded "talcoose-muscovite" partings defining foliation	Pyrite and pyrrhotine in trails and patches; galena and pyrrhotine adjacent to quartz lens	633
12.88	1.53	F 40	Graphitic muscovite-schist with strong foliation and incipient strain-slip cleavage; 1 cm thick muscovite lens at 19.04 - 19.05 m and quartz veining between 19.14 and 19.18 m	Pyrite with subordinate pyrrhotine	634
13.20	0.32	F 60	Celsian-quartz-schist with muscovite-schist at top and base, and coarse green celsian associated with quartz segregation at 13.35 m; foliation irregularly developed and absent between 13.50 and 13.60; some pinkish ? calcite patches and between 13.47 and 13.50 m quartz vein [PTS 4682]	Pyrite and sporadic pyrrhotine	
13.79	0.59	F 50	Calcareous biotite-schist, mottled texture defined by very irregular biotite and chlorite laminae in carbonate matrix; paler bands more prominent in lowermost 20 cm [PTS 4683]	Rare pyrite	635
15.74	1.95	F 45-50	Muscovite-quartz-schist with minor chlorite; calcite "augens" at 16.23, 16.41 and 16.52 m; green ?chlorite-rich area at 16.30 - 16.38 m followed by 20 cm quartz vein with chlorite and ? celsian; traces of fuchsite at 16.02 m. Lowest 14 cm comprise fairly coarse-grained greenish celsian rock [PTS 4519]	Pyrite and pyrrhotine disseminated throughout and concentrated in lowest 15 cm	636
16.70	0.96	F 50	Sericite-quartz-schist with biotite, and dolomite patches; trace of fuchsite at 17.35 m; minor crumpling at 17.27 m [PTS 4520]	Minor pyrite, some remobilised	637 638
17.46	0.76	F 90	Calcareous biotite-schist as above; poorly defined foliation	Remobilised pyrite in veins	639
18.98	1.52	F 90	Muscovite-chlorite-schist with quartz and occasional calcite patches; chlorite concentration with sulphide 19.17 - 19.22 m; band of more quartzose schist 19.35 - 19.46 m [PTS 4521]	Abundant pyrrhotine particularly below 19.44 m with minor pyrite	640
19.66	0.68	F 90	Graphitic muscovite-schist, lead grey with highly crumpled foliation	Abundant coarse patchy pyrrhotine with rare associated pyrite	641
20.45	0.79	F 80-90	Muscovite-quartz-schist, greenish grey with irregularly developed foliation and local minor folds; quartz vein with chlorite and sulphide patch between 21.63 and 21.86 m [PTS 4522]	Abundant pyrrhotine and minor pyrite	642
22.13	1.68	F 60	Calcareous-biotite-schist, similar to above but with the addition of muscovite; indeed between 22.71 and 22.97 m muscovite practically the only mica; chloritic zones locally developed; foliation distinctly crumpled below c 26.67 m below which passes gradually into green coarsely crystalline celsian-rock	Pyrite and pyrrhotine increase below 26.67 m	643 644
26.68	4.0		Celsian-rock, coarsely crystalline, green, with irregular foliation	Abundant pyrrhotine and pyrite	645
27.04	0.0		Muscovite-quartz-schist, silvery green with well developed foliation and minor crumpling	Minor pyrite and pyrrhotine	646
27.36	0.2	F 80	Graphitic muscovite-schist, foliation and strain-slip cleavage variably developed, latter in parts picked out by sulphides; limestone bands occur 29.12 - 29.18 m, 32.53 - 32.76 m and 33.04 - 33.25 m; also rare calcite veins [PTS 4523]	Pyrite common pyrrhotine more rare	647 648 649
33.25	5.89	{ F 80-90 C 0 F 90 C 165	Muscovite-chlorite-schist, silvery, calcareous and slightly carbonaceous with thin bands of dark limestone eg 33.41 - 33.46 m; foliation essentially constant and regular with no evidence of folding; a few quartz lenses present eg at 35.26 m Fault zones - 33.71 - 34.70 m and 35.60 - 36.10 m as evidenced by rubbly core, core loss and iron staining	Minor pyrite and pyrrhotine; content increased downwards	650
36.52	3.27	F 90	Graphitic-muscovite-schist, much as above with good foliation and irregularly developed strain-slip cleavage; intensely crumpled below 40.50 m into series of relatively light buckle folds [PTS 4524]	Pyrite with subordinate pyrrhotine present throughout	651 652 653
43.45	6.93	F 80-90	Quartz-biotite-schist, greenish, with chlorite and poorly developed foliation	Pyrite very common with some pyrrhotine	654
43.62	0.17	F 90	Graphitic muscovite-schist, as above with good foliation and quartz lenses	Sporadic patchy pyrite and pyrrhotine	
44.10	0.48		Micaceous quartzite, well laminated, with interbanded graphitic units up to 10 cm thick		655
47.43	3.33	{ F 90 C 150	Graphitic muscovite-schist with quartz lenses; chlorite throughout and sparingly dolomitic	Minor pyrrhotine and subordinate pyrite	
47.97	0.54	F 60	Micaceous quartzite, grey-green with prominent garnet porphyroblasts and variably developed foliation. Uppermost 30 cm and lowermost 79 cm comprise quartz-mica-schist; strong foliation and local crumpling c 51.60 m; below c 50.77 m core distinctly more broken and iron stained - fault	Rare pyrrhotine and very minor pyrite	656
52.04	4.07	F 70	Graphitic muscovite-schist striped in parts with garnetiferous micaceous quartzite, and more rarely, dark dolomitic limestone bands	Finely divided pyrrhotine and pyrite; latter also in veinlets; limonite on joints	657 658
60.46	8.42	{ F 65-70 F 60 C 20-30			

## GEOLOGICAL RECORD

Inclined depth m	Inter-Section m	Structure angle	Lithology	Mineralisation	Sample CYD No
61.21	0.75	F 70	Quartzite, garnetiferous and micaceous with laminae, bands and lenses of graphitic muscovite-schist; foliation disrupted in parts and rare calcite segregations	Finely divided pyrrhotine	659
61.86	0.65		Graphitic muscovite-schist, little different from above, with quartzose stripes and garnets	Disseminated pyrrhotine richer than above	660
63.09	1.23		Quartzite, garnetiferous and micaceous with graphitic muscovite-schist bands, laminae and lenses showing in parts, strong folding	Disseminated pyrrhotine	661
63.95	0.86		Graphitic muscovite-schist with bands of quartzose garnet-mica-schist and some contorted thin quartz segregations	Pyrite throughout	662
64.48	0.53		Quartzite, sparsely micaceous and garnetiferous	Pyrrhotine streaks	663
66.72	2.24	F 70-80	Graphitic muscovite-schist with interbanded garnet-mica-quartzite and garnet-mica-schist; pale green ? chlorite also very common; foliation contorted in parts	Pyrrhotine disseminated throughout with crystals	664
68.83	2.11	F 70	Quartzite, highly micaceous and schistose with garnet and chlorite; unit includes graphitic laminae, garnetiferous-mica-schist bands and, near base, rare dolomitic segregations	Pyrrhotine throughout in varying amounts with associated chalcopyrite and ? sphalerite at 67.66 and 68.35 m	665
69.31	0.48		Limestone; upper 20 cm fine-grained, dark with irregular pale stripes; below this slightly paler and probably more impure with faint striping and garnet porphyroblasts	Sporadic pyrite; thin trails of sphalerite with chalcopyrite in upper 20 cm	666
72.10	2.79	F 80-50	Garnet-mica-schist with rare micaceous quartzite	?Pyrrhotine and pyrite trails of ? sphalerite	667
72.96	0.86	F 70	Quartzite, garnetiferous and micaceous with rare thin bands of graphitic muscovite-schist; poorly foliated	Disseminated pyrrhotine and rare ? sphalerite; pyrite in hair veinlet	668
74.43	1.47		Garnet-mica-schist, graphitic with thin bands of garnetiferous micaceous quartzite	Pyrrhotine disseminated throughout; trace of sphalerite; pyrite in lower 10 cm	669
76.26	1.83		Quartzite, garnetiferous, micaceous and slightly calcareous, darker than above with graphitic partings and bands; uppermost 10 cm broken into small pieces with limonite on joints	Pyrrhotine disseminated throughout with rare pyrite in hair veinlets; stratiform sphalerite trails, common particularly between 75.20 and 75.29 m; trace chalcopyrite	670
76.69	0.43		Quartzite, pale grey, sparsely micaceous, patchily calcareous and garnetiferous with small calc quartz segregations	Disseminated pyrrhotine, pyrite rarer; sphalerite common, galena rare	671
77.30	0.61		Graphitic muscovite-schist, extremely homogeneous	Disseminated pyrrhotine with rare pyrite and limonite	672
77.79	0.49	F 60	Quartzite, pale grey, much as above but with micaceous and graphitic wisps, garnets and small calcite lenses; patchily calcareous	Finely disseminated pyrrhotine with rare pyrite and sphalerite	673
80.63	2.84	F 65 C 10-30	Interbanded grey micaceous garnetiferous quartzite with graphitic laminae, and graphitic muscovite-schist; patchily calcareous; band of dark fine-grained limestone between 79.86 and 80.18 m; occasional calcite-quartz segregations with quartz vein 79.44 - 79.50 m	Pyrrhotine disseminated throughout; traces of sphalerite in uppermost metre	674
83.15	2.52	F 60-75	Dolomitic quartzite, spotted, pale grey with muscovite; includes quartz-calcite segregations which on occasions have chlorite selvages	Iron and zinc sulphides rare	675
83.98	0.83		Graphitic muscovite-schist, with dolomitic stripes and spots	Fine ? pyrrhotine throughout; occasional pyrite veinlets with limonite	676
85.36	1.38		Quartzite, calcareous and muscovitic with graphitic partings and bands which in general are thicker in lowest 35 cm	Disseminated pyrrhotine	677
87.30	1.94	F 70-80 C 30	Graphitic muscovite-schist, calcareous in parts with quartzitic stripes and bands; between 85.83 and 86.55 m core reduced to small fragments with traces of limonite and solution cavities - ? fault	At 85.90 m small cavity containing amorphous grey mineral with pyrite; disseminated pyrrhotine with pyrite and traces of sphalerite	678
89.58	2.28		Quartzite, calcareous and garnetiferous with bands and lenses of graphitic muscovite-schist and rare quartz-calcite segregations; core broken 88.72 - 89.38 m with approximately 20 cm lost - fault	Disseminated pyrrhotine with pyrite generally in veinlets; thin films of galena 87.93 - 88.05 m	679
91.38	1.80		Graphitic quartz-mica-schist, slightly calcareous with occasional quartzite bands	Disseminated pyrrhotine very common throughout with traces of sphalerite; rare pyrite and chalcopyrite at 90.43 m	680
95.94	4.56	F 60	Quartzite, garnetiferous and micaceous (muscovite and biotite) with graphitic partings and bands; foliation contorted; patchily dolomitic with rare quartz-carbonate segregations; thin dark limestone band 91.48 - 91.53 m	Disseminated pyrrhotine and, below 92.70 m, sphalerite; traces of chalcopyrite; pyrite in hair veinlets	681
98.06	2.12	F 60 C 25-30	Graphitic muscovite-schist with paler (?quartzose) stripes and, rarely, bands; dolomite noted in quartzitic bands 96.79 - 96.29 m; quartz-calcite segregations common occupying over half core between 97.10 and 97.46 m with occasional schist fragments and rare muscovite	Pyrrhotine disseminated throughout with sporadic associated sphalerite; rare pyrite in hair veinlets; quartz calcite segregations have pyrrhotine but with minor amounts of galena, pyrite and traces of chalcopyrite around 97.30 m whilst sphalerite occurs at base	682
104.32	6.26	F 40 F 60 F 70	Quartzite, with muscovite, biotite and sporadic garnets and bands and partings of graphitic muscovite-schist; dolomite disseminated throughout quartzite but absent from graphitic schist; dark limestone band with black porphyroblast 99.10 - 99.11 m; between 103.01 and 103.22 m core comprises quartz segregation and is very broken	Sphalerite with subordinate pyrrhotine common in uppermost 45 cm; decreases below this but prominent again 100.92 - 100.99 m and 101.96 - 102.01 m; traces of chalcopyrite; pyrite restricted to quartz-calcite segregations * increases again below 102.95m	683

## GEOLOGICAL RECORD

Inclined depth m	Inter-Section m	Structure angle	Lithology	Mineralisation	Sample CYD No
108.26	3.94	F 60	Graphitic muscovite-schist with, below 105.15 m, interbanded micaceous quartzite; all dolomitic; foliation noticeably folded with prominent strain-slip cleavage; between 104.81 and 104.99 m core reduced to small pieces; quartz segregations also occur in this section; dark limestone band with black porphyroblasts present 107.84 - 107.88 m	Sporadic disseminated pyrrhotine; traces of sphalerite below 105.70 m with slight concentration 106.13 - 106.23m trace of pyrite	684
108.54	0.28		Limestone, fine-grained, dark with black porphyroblasts and thin graphitic partings; foliation affected by rather open folds; quartz veinlets and segregations	Finely divided pyrrhotine and pyrite; traces of sphalerite and chalcocopyrite	685
111.34	2.80	F 50 C 25 F 70	Quartzite, micaceous and dolomitic with bands and partings of graphitic muscovite-schist; foliation intensely disrupted in places	Pyrrhotine disseminated throughout with associated subordinate sphalerite; traces of pyrite and chalcocopyrite	686
				Disseminated pyrrhotine throughout with associated sphalerite; occasional pyrite with rare chalcocopyrite and galena; between 113.14 and 113.42 m enriched in sphalerite and pyrrhotine (possibly related to increased number of quartz carbonate segregations) - out by chalcocopyrite veinlets; such veinlets common below 114.20 m	687
		F 70	Graphitic-muscovite-schist with rare dolomitic bands and a few bands of micaceous quartzite; bands of dark limestone 112.52 - 112.54 m with black biotite porphyroblasts 114.45 - 114.52 m, 117.78 - 117.80 m and 121.43 - 121.51 m; mineralised quartz-dolomite segregations appear below 113.14 m, occupying entire core between 113.96 and 114.25 m; folding apparent below 114.60 m; core reduced to relatively small pieces 117.18 - 120.18 m with incipient brecciation and clay zone 117.18 - 117.37 m - <u>fault</u>		688
121.56	10.22	F 30 F 50			689
125.75	4.19	F 30	Graphitic quartz-muscovite-schist with interbanded dolomitic micaceous quartzite and quartz segregations; signs of strong crumpling	Disseminated pyrrhotine with subordinate to rare sphalerite; pyrite present occasionally in schist and in veinlets with ? chalcocopyrite	691
126.49	0.74	F 20-40 F 30	Quartzite, pale grey, sparsely micaceous with quartz segregations and rare graphitic muscovite-schist bands; green calcite film on joints	Pyrrhotine content reduced relative to above with rare associated sphalerite; pyrite veinlets common	692
128.36	1.87	F 0-90	Graphitic quartz-muscovite-schist with occasional quartzite bands; crumpled	Disseminated pyrrhotine, in parts subordinate to pyrite which occurs both in rock and in veinlets; rare sporadic sphalerite ? chalcocopyrite 127.30 - 127.40 m	693
130.04	1.68	F 50	Micaceous quartzite patchily dolomitic and garnetiferous below 129.00m pink quartz -feldspathic veins in upper 20 m with trace of dolomite; in lowest 40m passes into striped graphitic quartz-muscovite-schist	Disseminated pyrrhotine with subordinate sphalerite; pyrite mostly in veinlets but in lowest 40 m some stratiform with sphalerite; quartz-feldspar veins carry pyrrhotine and rare chalcocopyrite	694
131.38	1.34		Graphitic muscovite-schist, crumpled with small calcareous patches	Pyrite throughout; rare sphalerite	695
134.85	3.47		Graphitic quartz-muscovite-schist, finely striped in parts with bands of quartzite and graphitic muscovite-schist; disseminated dolomite almost throughout with dark limestone bands 131.56 - 132.03 m and 134.10 - 134.24 m; crumpled, with strain-slip cleavage common	Disseminated pyrrhotine (absent from limestone); occasional associated pyrite and rare chalcocopyrite; sphalerite rare to abundant	696
136.25	1.40	F 0-90	Limestone, with pale and dark bands; graphitic bands and partings in pale rock; small quartz calcite segregations; folding evident	Pale bands have pyrrhotine (dominant sulphide), sphalerite, pyrite and rare chalcocopyrite	697
136.25			End of borehole		

			GEOLOGICAL RECORD	
Inclined depth m	Inter-section m	Structure angle	Lithology	Mineralisation
0.00				
1.15	1.15		Superficial deposits	
			<b>BEN LAVERS SCHIST</b>	
		F 70	Muscovite-schist, grey, rather massive to 2.15m followed by muscovite-chlorite-schist, greyish green with yellow-white dolomitic laminae up to 6cm thick [palaeontological sample 1.82 - 1.95 m]; several leached limonitic zones possibly related to fractures; quartz lenses and some minor biotite in lower part	
13.63	12.48	F 55 F 60		
13.89	0.26	F 75	Calcite-quartz-muscovite-schist with minor chlorite and pale yellow dolomitic laminae; limonitic	
14.05	0.16		Muscovite-quartz-schist with yellow dolomitic laminae; minor chlorite and biotite	
14.18	0.13	F 80	Dolomitic quartz-muscovite-schist	
14.28	0.10		Dolomitic quartz-muscovite-schist with minor chlorite and biotite	
15.13	0.85	F 75	Dolomitic quartz-muscovite-schist with a limonitic calcareous band at 14.78 m and some relatively dark bands containing minor chlorite and biotite	
18.33	3.20	F 65 F 65	Highly calcareous quartz-muscovite-chlorite-dolomite-schist; the calcite is limonite - stained and also forms a white veinlet at 18.24 m	
20.77	2.44	F 70	Dolomite-muscovite-chlorite-schist with quartz, minor biotite; calcite veinlet at 18.9 m	
21.05	0.28	F 75	Dolomitic muscovite-schist with quartz and cross-cutting calcite hair veinlets	
25.20	4.15	F 70	Muscovite-chlorite-schist, dolomitic with minor quartz and biotite and some quartz-calcite lenses; massive dolomite band at 23.85 - 23.90 m	
25.92	0.72	F 75	Muscovite-chlorite-schist with minor quartz; calcite and lesser dolomite common in laminae	
27.00	1.08	F 80	Muscovite-schist with chlorite and minor biotite, quartz and dolomite; bedding cleavage somewhat deformed by second cleavage	
28.43	1.43	F 65	Muscovite-schist as above with numerous orange calcareous laminae; broken and leached with chloritic fractures	
29.96	1.53		Muscovite-chlorite-schist with dolomite and calcite laminae; cut by calcite hair veinlet with a red limonitic alteration envelope at 29.43 m; calcareous parts leached and broken	
30.94	0.98	F 65	Muscovite-chlorite-schist with minor quartz and biotite; dolomitic but without discrete carbonate laminae; quartz lenses and veinlets	Pyrite speck in quartz lens at 30.28 m
31.49	0.55	F 60	Muscovite-schist with minor chlorite, calcareous; quartz lens at 31.43 m; leached and fractured	Hematitic band adjacent to quartz lens
34.70	3.21	F 65	Muscovite-schist, sparingly dolomitic and with only minor quartz in layers; dark carbonaceous laminae reaching a maximum of 4 cm at 32.39 - 32.43 m; often iron-stained especially at base	Finely divided pyrite is associated with the thick carbonaceous band
34.87	0.17		Limestone, brown, massive with calcite veinlets	Minor hematite grains
35.37	0.50		Chlorite-muscovite-schist exhibiting a fold closure	
35.69	0.32	F 40	Muscovite-schist, greyish brown, friable	
38.50	2.81		Muscovite-schist, broken and limonitic with 0.16 m thick quartz segregation at top and fragments of muscovite-quartzite (both calcareous and non-calcareous) below in a zone of very poor core recovery (27.5%) <b>Amh</b>	
			<b>BEN BAGACH SCHIST</b>	
39.65	1.15		Highly graphitic muscovite-schist exhibiting crumpled schistosity	Minor pyrite in sub-conformable bands and in veinlets
39.65			End of borehole	

MB. No chemical analyses were performed on the rocks from this borehole; measurements of specific gravity average 2.7 in the Ben Lavers Schist and 2.8 in the Ben Bagach Schist.

Inclined depth m	Inter-Section m	Structure angle	Lithology	Mineralisation	Sample CYD No
0.00					
2.14	2.14		Superficial deposits		
			BEN LAWERS SCHIST		
		F 15-90°	Calcareous chlorite-sericite-schist with randomly orientated (garbenschiefer) hornblende and sporadic garnet porphyroblasts; calcite, mostly in finely divided form but also forms brown 'spots'; foliation not always apparent but where seen has variable inclination with folding evident; core in small pieces 5.34 - 5.45m; quartz-chlorite segregations throughout with occasional garnet. Pale limestone bands with [ PTS 4684, 4685, 4686, 4687] micaceous partings and occasional garnets 7.53 - 7.64, 12.65 - 12.82 and 16.80 - 16.95m; quartz vein with chlorite at 3.00 m	Pyrrhotine sporadically throughout with pyrite and rare (?) chalcocopyrite; pyrite also in quartz vein; limonite on joints and spec hematite in quartz segregation	
18.21	16.07	F 70	Calcareous chlorite-sericite-schist, striped and more schistose than above; also hornblende smaller and less common; garnets particularly well developed in uppermost 80 cm; quartz segregation with, on occasion orange calcite; pale limey bands and between 18.90 and 19.15 m more leaden schist. [PTS 4688]	Trace of pyrite	
21.56	3.35	F 80	FAULT ZONE		
			Mostly thin slices of chlorite-sericite-schist with clay bands at base	Thin film of pyrite on foliation	
21.85	0.29		Limestone, brown and grey, dominantly massive but banding evident in parts; cut by network of calcite veinlets; upper 20 cm broken		
22.81	0.96		BEN RAGACH SCHIST		
		F 70	Dolomitic mica-schist, slightly carbonaceous below 23.20 m; minor folding near base; lowest 30 cm broken into relatively small pieces suggesting fault; quartz-calcite segregations at base [PTS 4689]	Pyrite stratiform and in veinlets; often weathered to limonite	747
24.13	1.32	F 70	Celsian-quartz rock, white to pale greenish grey, slightly micaceous with traces of calcite [PTS 4690]; cut by thin discontinuous shears; quartz segregations appear below 25.38 m and between 26.63 and 26.93 m occupy the entire core; carry celsian and orange calcite [PTS 4691]; dark limestone bands 28.14 - 28.17 m	Pyrite almost exclusively in veinlets. Above 27.30 m pyrrhotine occurs sparsely; below this forms parallel plates which define crude foliation; traces of (?) covellite on joints between 26.30 and 26.50 m	748
28.33	4.20	F 70	Limestone, pale and dark bands, with micaceous and carbonaceous partings; upper 5 cm comprises dolomitic mica-schist; slightly thicker pale band at 29.42 - 29.57 m beneath which banded limestone becomes more foliated and chloritic	Pyrite, mostly in veinlets; trace of pyrrhotine	749
30.08	1.75	F 70	Celsian-quartz rock, pale grey to green, with discontinuous dark wisps consisting predominantly of pyrrhotine but also some biotite; rare muscovite partings; graphitic limestone 30.83 to 30.90 m and carbonaceous mica-schist with good strain-slip-cleavage at 33.60 - 33.96 m; quartz segregations carrying some celsian appear below 32.40 m; shearing apparent 32.90 - 33.40 m [PTS 4692]		
35.53	5.45	C 50	Dolomitic limestone, fine grained dark grey with pale stripes; quite schistose with carbonaceous partings in lowest 20 cm; rare lenses of chlorite around 35.70 m; a few quartz-calcite veins [PTS 4693]	Occasional pyrrhotine traces of pyrite	751
36.46	0.93	F 65	Celsian-quartz rock, pale grey, sparsely micaceous with rare graphitic partings; calcite lenses and veinlets common in lowermost metre; slightly coarser grained pale green rock 36.92 - 37.06 and 38.11 - 38.14 m possibly reflecting higher celsian content; dark green (?) chlorite infilling shears	Pyrite, sporadic small spots and on shear planes	752
38.45	1.99	F 75	Graphite-muscovite-schist, well foliated with calcareous bands	Patchy pyrite	753
39.38	0.93	F 60	Quartzite, pale to mid grey, much finer grained than quartz-celsian rocks above, almost cherty and with micaceous partings; thin dolomitic partings near base	Pyrite common in shears, more rarely as stratiform trails	754
41.30	1.92	F 70	Graphitic muscovite-schist with calcareous and, more rarely quartzitic bands; between 42.84 and 42.90 m pale green muscovitic band with lens of dark schist; incipient strain-slip-cleavage; quartz segregations occur sporadically between 44.07 and 44.16 m and carry calcite together with angular schist fragments; uppermost 5 - 15 m cut by quartz veins with chlorite	Pyrrhotine present throughout; pyrite in irregular patches associated with quartz segregations in uppermost metre	755
46.44	5.14	F 70	Quartzite, highly micaceous with pale grey and buff colour banding; rare muscovite-schist and graphitic bands though, in general more micaceous and foliated between 48.27 and 48.50 m; a few quartz calcite segregations	Pyrrhotine as isolated patches and trails	756
49.17	2.73	F 65	Graphitic quartz-muscovite-schist, slightly calcareous with pale and dark limestone bands between 49.32 and 50.60 m; much folding	Pyrrhotine common above 49.80 m and rare below; pyrite, both stratiform and in veinlets in and around limestone bands	757
50.64	1.47		Calcareous chlorite-mica-schist, with chlorite, biotite, sericite and quartz in varying proportions; traces of graphite and rare garnets which may be partly or wholly replaced by chlorite; orange calcite appears at 54.90 m; quartz segregations present occasionally crumpled	Fine pyrite on foliation planes, often associated with quartz segregations	758
54.80	4.16		Calcareous chlorite-mica-schist, with biotite and sericite; considerably more pelitic than above; highly crumpled; quartz segregations with occasional chlorite selvages occupy bulk of core between 56.56 and 56.93 m; core reduced to relatively small fragments between 56.14 and 56.34 m - fault; slickensiding noted 55.87 - 55.78 m; some calcite especially around quartz vein between 55.70 and 55.85 m	Rare pyritous veinlets	759

GEOLOGICAL RECORD						
Inclined depth m	Inter-Section m	Structure angle	Lithology	Mineralization	Sample CYD No	
58.40	0.70		Calcareous muscovite-quartz-schist, with minor biotite, paler than above due to suppression of biotite and chlorite	Disseminated (?) pyrrhotine; some pyrite on foliation planes	760	
60.00	1.60	F 70	Calcareous mica-quartz-schist, with muscovite and biotite and concordant quartz segregations	Finely divided (?) pyrrhotine	761	
62.85	2.85		Quartz-mica-chlorite-schist, dolomitic with biotite and sericite; chlorite probably after garnet, absent below 62.25 m; some quartz-calcite segregations; between 61.15 and 61.60 m prominent joint sub parallel to core axis; slickensiding with chlorite "rock polish"	Traces of pyrite associated with quartz segregations	762	
65.10	2.25	F 65	Calcareous quartz-mica-schist, muscovite, biotite and rare quartz-calcite segregations; crumpled with incipient strain-slip cleavage	Pyrrhotine, mostly as fine dissemination, more rarely in quartz segregations	763	
68.37	3.27		Muscovite-quartz-schist, dolomitic with some biotite partings; strain-slip cleavage often well developed and in part difficult to distinguish from bedding schistosity; quartz-calcite segregations and quartz veins	Pyrrhotine disseminated throughout; quartz veins carry some pyrite but mainly pyrrhotine	764	
69.70	1.33	F 70	Quartz-muscovite-schist with rare biotite partings and quartz-calcite segregations; some tight buckle folds	Pyrrhotine disseminated throughout occasionally forming stratiform trails and concentrations near quartz segregations	765	
70.25	0.55		Calcareous biotite-quartz-schist, striped in parts with occasional quartz segregations	Trace of pyrrhotine	766	
75.45	5.20	F 70	Calcareous mica-quartz-schist, striped with biotite, sericite and (?) chlorite, and bands of calcareous quartzite; quartz-calcite-chlorite segregation, rather sheared in parts, occupies most of core 73.40 - 73.55 m; about 30 cm below schist much more pelitic; noticeably folded and partly schistinated near base;	Pyrite in quartz-calcite segregations. Pyrite in quartz veins and on fractures	767	
75.91	0.46		Calcareous quartzite, with irregular (?) chlorite filled shears; lowermost 20 cm comprise quartz - calcite segregation and sericite-schist	Pyrite and pyrrhotine co-existing in quartz segregation	768	
90.38	14.47	F 70	Quartz-mica-schist, laminated and dolomitic, with sericite and biotite and bands of dolomitic quartzite and biotite-sericite-schist; small amounts of chlorite and (?) graphite also present; some folding evident but foliation in general not strongly disrupted; (?) cross-bedding at 77.40 m younging downwards; quartz lenses occur intermittently throughout, mostly parallel to foliation; strain-slip-cleavage occasionally evident; shears and tension gashes; considerable folding [PTS 4694, 4695]	Pyrite and pyrrhotine occur patchily throughout, pyrite also in shears and tension gashes	769 770	
95.15	4.77	F 70-80	Chlorite-mica-quartz-schist, dolomitic with biotite and sericite - considerably more pelitic than above - and poorly developed striping; quartz-calcite lenses widely distributed, as above; foliation considerably disrupted [PTS 4696]	Trace pyrite in quartz segregations. Rare pyrrhotine	771	
95.98	0.83		Quartzite, pale greenish grey with irregular bands and partings of chlorite-biotite-sericite-schist; rare quartz segregations	Traces of pyrite on foliation planes	772	
97.44	1.46		Chlorite-mica-schist, with biotite and sericite and irregular quartz-dolomite stripes; above 96.50 m core in small pieces with (?) talc; quartz segregations	Trace of pyrite adjacent to quartz segregations	773	
98.06	0.62	F 70	Quartzite, pale grey with irregular partings of chlorite, biotite and sericite; also irregular thin quartz lenses, slightly cherty in parts	Trace of pyrite	774	
103.09	5.03	F 80	Chlorite-mica-quartz-schist, dolomitic with sericite and biotite and occasional dolomitic quartzite bands; conspicuous folding and quartz segregations.	Pyrite relatively common in hair veinlets and occasionally on foliation; also rare pyrrhotine	775	
103.68	0.59		Quartzite, pale grey, dolomitic with chlorite and biotite partings	Pyrite in hair veinlets		
110.60	6.92		Chlorite-mica-quartz-schist, striped and dolomitic much as above but with bands of dolomitic quartzite and chlorite-sericite-biotite-schist; quartz-dolomite segregations common throughout; foliation affected by small scale folding throughout; lowest 30 - 35 cm consist of muscovite-quartzite	Pyrite in hair veinlets and rarely in rock; pyrrhotine occurs sporadically, often elongated along foliation; trace of (?) chalcopyrite with pyrrhotine in quartz segregation at 105.85m	776	
111.33	0.73	F 75	Mica-quartz-dolomite-schist, finely striped, darker than above rock with less folding	Irregularly distributed pyrrhotine	777	
113.07	1.74	F 75	Quartzite, very fine grained dark grey with muscovite and graphite and with paler dolomitic bands and quartz segregations; incipient brecciation with small calcite-filled shears between 112.57 and 112.72 m - ? fault	Abundant pyrite, both stratiform, with subordinate sphalerite and rare chalcopyrite, and in minor veinlets	778	
115.03	1.96	F 60	Graphite-muscovite-schist, calcareous in parts with rare thin bands of dark limestone; bands of quartz-celsian rock appear below 114.47 m and eventually dominate lowermost 30 cm; small fractures infilled with calcite [PTS 4698]	Pyrite throughout schist with mostly subordinate, sphalerite; sulphide content of quartz-celsian rock lower, mainly (?) pyrrhotine with minor sphalerite and pyrite	779	
117.13	2.10	F 60	Quartz-celsian rock, pale grey to green, fine grained with dark micaceous laminae; calcite, mostly as isolated spots but occasionally concentrated into discontinuous laminae; rock becomes noticeably more dolomitic below 116.60 m; trace of fuchsite at 115.37 and 117.00 m [PTS 4697]	Sulphide extremely common throughout forming up to 50% of core at 116.70 - 117.00 m. Comprise pyrite; pyrrhotine - 50; 50 and subordinate sphalerite; latter absent from enriched zone; pyrrhotine and sphalerite exclusively stratiform but pyrite also in veinlets	780	



Inclined depth	Inter Section	Structure angle	Lithology	Mineralisation	Sample CYD No
			Dolomite-celsian rock with bands of quartz-celsian rock and rare quartz segregations [PTS 4699]	Fine dissemination and concordant trails of sphalerite with subordinate pyrrhotine and pyrite; quartz-celsian rock has almost exclusively pyrrhotine with only trace of sphalerite; galena noted at 117.57, 117.45 m and elsewhere below	781
118.06	0.93	F 35	Quartzite, dark grey, very fine grained - almost a chert, with occasional dolospots and at 118.13-118.20 m dolomite-rich band; also bands of dolomite-graphite-mica-schist at 118.80 - 119.00 and 119.96 - 120.25 m; quartz - (?) chlorite segregation or vein at 118.21 - 118.63 m	Sulphide throughout; dominantly pyrite and sphalerite with pyrrhotine replacing pyrite in parts; sphalerite notably enriched at 118.50 - 118.63 m in and around quartz segregations; galena at 118.40 m, also in quartz segregation	782
120.42	2.36	F 70	Graphitic quartz-muscovite-schist, with bands of muscovite-schist and quartz-dolomite segregations between 121.72 and 122.08 m; also bands of dark dolomitic limestone at 120.90 - 121.00 m, 122.18 - 122.25 m and 122.72 - 122.74 m; some crumpling evident	Pyrrhotine and pyrite common throughout in approx 50 : 50 ratio; mostly in co-parallel trails; minor associated sphalerite and trace of chalcopyrite	783
122.82	2.40	F 75 F 65	Micaceous quartzite, pale grey, slightly graphitic and faintly laminated	Pyrite common, mostly in stratiform trails but also in veinlets, with associated sphalerite; pyrrhotine rare	784
123.21	0.39	F 40	Quartz-celsian rock, very fine grained dark grey 'chert' with small pools and streaks of pale quartz and rarer green (?) chlorite; also rare quartzite bands; occasional thin graphitic partings - concentrated with mica in lowest 20 cm to give distinct schistose fabric; incipient brecciation at 123.50 - 123.60 m with calcite infilling shears - <u>fault</u> [PTS 4700]	Pyrite in stratiform trails and veinlets dominant sulphide; pyrrhotine also noted; finely divided sphalerite	785
126.37	3.16	F 50	Micaceous quartzite, pale grey, slightly graphitic with dolomite and graphitic schist band between 126.72 and 126.84 m; calcite veinlets very common 126.44 - 126.51 m	Pyrite throughout, in stratiform trails with sphalerite and in veinlets	786
126.92	0.55	F 65	Graphitic quartz-muscovite-schist, slightly dolomitic with dolomite-rich bands and lenses; quite finely laminated in places; trace of chlorite around 127.30 m; minor gentle folding with incipient strain-slip cleavage; quartz segregation with angular schist pieces occupies core between 128.05 and 128.12 m [PTS 4701]	Pyritous streaks and blebs throughout; traces of sphalerite	787
129.11	2.19	{ F 70 C 20	Interbanded muscovite-schist, graphitic muscovite-schist and dolomitic limestone; foliation generally wavy with strain-slip cleavage in parts; quartz segregation at base	Pyritous trails and veinlets with traces of sphalerite	788
129.90	0.79	F 40	Quartz-celsian rock, pale greyish green, spottily dolomitic with interbanded barite-rock; distinctly dolomitic between 14 and 20 m above base; unit includes quartzose and, rarely, dolomitic stripes with occasional micaceous partings; barite rock forms two main bands at 130.21 - 130.44 m and 130.52 - 130.78 m and several thin (less than 0.5 cm) stripes; consists of pale grey slightly dolomitic rock with pepper and salt texture	Ubiquitous pyrite trails; sphalerite in variable amounts in quartz-celsian rock; notably concentrated with pyrite and galena in dolomitic zone 14 - 20 cm above base; galena present in both lithologies below 130.70 m	789
131.12	1.22	F 40	Graphitic muscovite-schist and graphitic quartz-muscovite-schist with interbanded quartzite and muscovite-schist; incipient brecciation between 132.18 and 132.27 m - <u>fault</u>	Pyrite with subordinate sphalerite disseminated throughout	790
132.60	1.48		Quartz-celsian rock, fine grained, dark grey and 'cherty' with calcareous and quartzose bands and stripes, particularly well developed in uppermost 12 cm; cut by calcite infilled shears, notably in lowermost 20 cm where rock appears brecciated	Pyrite patchily in upper half, finely disseminated and stratiform below; minor sphalerite	791
133.75	1.15	F 50	Quartz-celsian rock, very pale grey to off white; quite distinctive rock, resembling quartz-segregation, particularly in upper 55 cm where rocks devoid of dark quartz, stripes and co-parallel pyritic trails; minor calcite and chlorite; dolomite-rich band 135.05 - 135.11 m; shearing throughout, particularly intense in uppermost 55 cm and at 135.05 - 135.50 m where brecciation evident - <u>fault</u> [PTS 4702]	Pyrite as discrete crystals throughout; also in stratiform aggregates and in veinlets; accompanied in upper metre by minor sphalerite (?) magnetite and traces of galena	792
136.36	2.61		Quartzite, mid grey, dolomitic, muscovitic and slightly carbonaceous with paler (probably non-carbonaceous) bands; cut by innumerable calcite veinlets	Pyrite throughout with associated sphalerite in upper 20 cm	793
137.17	0.81	F 50	Graphite-muscovite-schist, dolomitic with bands of dark dolomitic limestone and, more rarely, of muscovite-schist; rare quartz-calcite segregations; core reduced to quite small fragments	Pyrite dominantly in veinlets	794
138.18	1.01	F 60	Sericite-dolomite-quartz-schist with (?) chlorite and biotite; occasional bands of dolomitic quartz-celsian rock; late brittle folding with associated shearing	Pyrite irregularly distributed in trails and veinlets	795
140.00	1.82	F 40	Quartz-celsian rock, pale green, soft with dark (?) biotite wisps; dolomitic above 140.60 m; noticeably sheared in upper 20 cm with incipient brecciation - <u>fault</u>	Pyrite trails and veinlets throughout; some disseminated sphalerite	796
140.90	0.90	F 80	Quartz-celsian rock, pale brownish grey 'chert' with some paler bands and biotite wisps in upper 10 cm; pale dolomitic stripes appear below 141.80 m and at 142.10 m passes down into pale grey dolomitic 'chert'; lowermost 28 cm comprises massive calcite with quartzose stripes	Pyrite exceedingly common, mainly disseminated but also in trails; pyrite, galena and (?) sphalerite disseminated through massive calcite	797
142.87	1.97	F 60			

## GEOLOGICAL RECORD

Inclined depth	Inter Section	Structure angle	Lithology	Mineralisation	Sample CYD No
		F 65	<u>Pyrite</u> -rock, massive with pepper and salt texture; main variant is pyrite content; rare stripes of biotite and, above 143.60 m, dolomite; calcite appears below about 143.70 m and is noticeably concentrated in massive pyrite bands; lowest 13 cm comprise pale grey fine quartz-calcian rock with thin muscovite schist	Pyrite throughout, ranging from fine dissemination to sub-massive bands, latter with interstitial sphalerite; abundant limonite and traces of galena; fine grained baryte at 143.60 m (?) remobilised	798
144.92	2.05				
		F 80	Graphite-muscovite-schist, very dark and relatively homogeneous with very thin dolomitic partings and lenses; rare calcite veinlets	Pyrite and sphalerite disseminated throughout, latter decreasing towards base	799
145.67	0.75				
		{ F 80 C 30 F 70 C 30	Graphite-muscovite-quartz-schist, slightly dolomitic with bands of mostly dark dolomitic limestone 1 - 10 cm in thickness and, between 147.90 and 148.15 m dolomitic sericite-schist; rare quartz-calcite segregations; strongly foliated apart from limestone bands	Iron sulphide throughout; pyrite dominant above 148.50 m, pyrrhotine below; sphalerite above 148.50 m and below 151.34 m	800
151.88	6.21				
		F 70	Interbanded dark graphitic dolomitic limestone and pale grey micaceous quartzite with rare bands of graphitic schist; quartz-dolomite lenses in both main lithologies; rare calcite veinlets; some tight folding	Pyrite, both stratiform and veiniform, throughout with (mostly) subordinate sphalerite	801
152.83	0.95				
		F 80	Graphitic quartz-muscovite-schist, finely laminated and dolomitic in parts; traces of chlorite; closely spaced schistosity with occasional open folds	Except for uppermost 40 cm pyritic trails and veinlets common; traces of limonite and (?) sphalerite	
154.20	1.37				
			Quartz-vein, sheared with trace of (?) chlorite	Cut by patches and veinlets of pyrite	
154.50	0.30				
			Quartz-muscovite-schist, dolomitic, with traces of graphite and chlorite and a few garnet porphyroblasts; separated from preceding unit by 5 - 7 cm thick micaceous gouge (?) fault	Pyrite, dominantly in veinlets	
155.11	0.61				
		F 70	Graphitic muscovite-quartz-schist, crudely laminated and slightly dolomitic, with (?) biotite and, above 155.55 m, garnet and chlorite; foliation/laminae frequently disrupted and lensed; band of dark fine grained limestone 155.55 - 155.80 m with garnet porphyroblasts up to 5 mm; rare quartz-calcite segregations	Iron sulphide throughout with limonite; exclusively pyrite above 155.30 m, below this stratiform pyrrhotine with pyrite veinlets	802
159.95	4.84				
		F 70 - 80	Chlorite-mica-quartz-schist, pale grey, slightly dolomitic with muscovite biotite and garnet; latter more common below 162.00 m though below 163.00 m may be replaced by chlorite; band of graphitic schist above 161.18 m and below 161.60 m, almost dying out again below 165.70 m; rare thin limestone bands	Disseminated pyrrhotine above 160 m; then decreases as pyrite content increases; pyrrhotine again dominant below 161.50; graphitic schist bands relatively deficient in sulphides	
166.95	7.00				
		F 90	Graphitic mica-quartz-schist, with muscovite, biotite, minor chlorite and garnet; quartz and biotite form stripes and lenses which impart vague lamination; rare bands of graphite-free schist and occasional quartz segregations; (?) cross bedding at 168.05 m younging downwards	Disseminated pyrrhotine throughout - enriched in psammitic parts; pyrite in streaks, patches and veinlets, both sulphides present in quartz segregations	803
170.57	3.62				
		F 70	Mica-quartz-schist, with sericite, biotite, garnet and rare chlorite; graphitic schist partings increase markedly in number below 173.69 m; garnets extremely abundant between 173.05 and 173.10 m	Pyrite above 172.00 m in streaks and veinlets; below this disseminated pyrrhotine predominates	804
174.90	4.33				
174.90			End of Borehole		

## APPENDIX II

### GEOCHEMICAL ANALYSES OF BOREHOLE CORES

Tables I to XI represent boreholes 1 to 11 respectively. The sample numbers are cross-referenced to the borehole logs given in the corresponding tables of Appendix I. Note that the core-lengths assayed do not always correspond exactly with the lithological units in Appendix I. The brief lithological descriptions given in this Appendix are of necessity very generalised.

The specific gravity measurements listed here are based on simple weighings using a spring balance and are therefore not better than  $\pm 0.2 \text{ g/cm}^3$  in accuracy.

Analyses were performed on representative samples collected by splitting the core in half, crushing all the material in a jaw crusher to less than 1–2 mm particle size, cone and quartering, and grinding approximately 200 g in an agate terra mill to less than 50  $\mu\text{m}$  grain size. Samples from boreholes 1 to 5 were analysed for Cu, Pb, Zn and Ag by atomic absorption spectrophotometry (AAS) using a hot  $\text{HNO}_3$  attack (analyst M.E. Stuart), for Mg, Al, Si, S, K, Ca, Fe, Mn, Sr and Ba by X-ray fluorescence spectrometry (XRF) on a Siemens XRF spectrometer (analyst D.J. Bland); and for Ti, Ni, Rb, Y, Zr, Nb, Sb and U by XRF on a Philips 1450/20 spectrometer (analyst T.K. Smith).

In boreholes 6–11 (samples CYD 501–855), the elements Ca, Ti, Mn, Fe, Ni, Cu, Zn, Ag, Sb, Ba and Pb were determined by XRF on the Philips instrument. The XRF results for zinc were found to be unreliable above 1% Zn and 48 samples were reanalysed by AAS. Agreement was found to be acceptable below 0.5% Zn but the XRF results were consistently low above this level and in the presence of high barium values, probably because of insufficient correction for mass absorption effects. There is also a consistent bias between the Philips XRF barium values and those from the earlier boreholes and this was checked by determining barium in 5 samples with between 30 and 54% Ba using a gravimetric method which was taken as the standard or 'correct' method (analyst D. Hutchison). The Philips XRF barium values were consistently low and converted by multiplying by a factor of  $1.1427 \pm 0.0161$  to agree with the gravimetric method. The standard error of the estimate is  $\pm 1.499\%$  Ba which is an estimate of the accuracy of the XRF method at these barium levels. Less consistent results were obtained at lower barium levels (10–15% Ba) and a mineralogical matrix effect of celsian as compared to baryte is likely. The earlier Siemens XRF barium results do not show a consistent bias compared to the gravimetric method but appear to be less precise probably because of differential compaction of the powdered sample. Some of the high barium values (ca 58% Ba) are probably statistically random overestimates of the 'true' content. Accuracy of the Siemens XRF method is estimated to be  $\pm 3.5\%$  Ba at the 50% Ba level (based on reanalysis of 3 samples).

APPENDIX II TABLE I BOREHOLE 1

SAMPLE NO.	DEPTH		INTER-SECTION (M)	GENERALISED LITHOLOGY	SP.GR.	MGO %	AL2O3 %	SiO2 %	S %	K2O %	CaO %	TI %	MNO %	FE2O3 %
	FROM (M)	TO (M)												
45	2.50	3.73	1.23	DOLOMITIC QUARTZ-CELSIAN-ROCK		2.4	6.55	51.00	3.71	0.812	3.85	0.260	0.200	3.6
46	3.73	4.65	0.92	DOLOMITIC QUARTZ-CELSIAN-ROCK		2.2	5.92	43.10	6.40	0.881	3.61	0.242	0.000	4.4
47	4.65	6.05	1.40	BARYTE-ROCK	3.9	0.4	0.00	13.30	11.50	0.009	1.05	0.100	0.000	0.6
48	6.05	7.25	1.20	BARYTE-ROCK	3.9	0.8	0.00	6.95	11.70	0.015	1.63	0.107	0.000	0.7
49	7.25	8.48	1.23	BARYTE-ROCK	4.1	1.1	0.00	4.35	11.80	0.000	2.29	0.102	0.000	0.6
50	8.48	10.96	2.48	BARYTE-ROCK	3.9	3.3	0.00	0.49	12.10	0.001	5.99	0.092	0.000	1.1
51	10.96	12.80	1.84	BARYTE-ROCK	4.0	1.2	0.00	0.77	13.40	0.000	1.94	0.105	0.000	0.6
52	12.80	14.13	1.33	BARYTE-ROCK	4.4	0.4	0.00	0.12	15.60	0.007	0.50	0.108	0.000	1.1
53	14.13	16.67	2.54	BARYTE-ROCK	4.3	0.2	0.00	2.33	15.30	0.001	0.58	0.108	0.000	1.1
54	16.67	19.11	2.44	BARYTE-ROCK	4.1	0.2	0.00	4.04	13.90	0.002	0.68	0.107	0.000	0.8
55	19.29	20.60	1.31	BARYTE-ROCK	3.7	0.6	0.00	8.88	11.50	0.001	0.92	0.105	0.000	0.5
56	20.60	22.54	1.94	BARYTE-ROCK	3.9	0.3	0.00	7.14	11.80	0.004	0.82	0.106	0.000	0.5
57	22.54	25.68	3.14	BARYTE-ROCK	4.0	0.1	0.00	6.93	11.70	0.003	0.86	0.105	0.000	0.5
58	25.68	26.85	1.17	BARYTE-ROCK	3.9	0.5	0.00	8.32	11.60	0.003	1.12	0.108	0.000	0.4
59	26.85	29.03	2.18	BARYTE-ROCK WITH DOLOMITE-ROCK AT BASE	3.9	0.3	0.00	8.02	12.70	0.006	0.87	0.107	0.000	0.9
60	29.03	30.15	1.12	GRAPHITIC MUSCOVITE-SCHIST		2.3	7.96	33.70	5.38	2.740	4.08	0.253	0.100	2.4

SAMPLE NO.	DEPTH		INTER-SECTION (M)	GENERALISED LITHOLOGY	SP.GR.	NI PPM	CU PPM	ZN PPM	RB PPM	SR %	Y PPM	ZR PPM	NB PPM	AG PPM	SB PPM	BA %	PB PPM	U PPM
	FROM (M)	TO (M)																
45	2.50	3.73	1.23	DOLOMITIC QUARTZ-CELSIAN-ROCK		23	15	370	14	0.110	16	163	8	1	0	18.00	500	0
46	3.73	4.65	0.92	DOLOMITIC QUARTZ-CELSIAN-ROCK		27	15	1500	15	0.157	14	178	9	1	0	21.00	150	0
47	4.65	6.05	1.40	BARYTE-ROCK	3.9	9	20	90	0	0.471	0	137	2	0	0	50.00	130	0
48	6.05	7.25	1.20	BARYTE-ROCK	3.9	9	35	150	0	0.541	0	149	1	1	6	52.00	200	0
49	7.25	8.48	1.23	BARYTE-ROCK	4.1	11	20	880	0	0.537	0	145	0	10	0	51.00	450	0
50	8.48	10.96	2.48	BARYTE-ROCK	3.9	9	45	4500	0	0.357	0	122	2	13	4	45.00	1000	0
51	10.96	12.80	1.84	BARYTE-ROCK	4.0	13	45	4300	0	0.329	0	122	0	6	5	54.00	1350	0
52	12.80	14.13	1.33	BARYTE-ROCK	4.4	11	95	11000	0	0.395	0	127	1	6	0	58.00	2400	0
53	14.13	16.67	2.54	BARYTE-ROCK	4.3	12	75	7000	0	0.434	0	134	0	8	3	56.00	4200	0
54	16.67	19.11	2.44	BARYTE-ROCK	4.1	12	100	3900	0	0.478	0	136	5	4	2	55.00	2100	0
55	19.29	20.60	1.31	BARYTE-ROCK	3.7	12	15	490	0	0.536	0	140	1	0	2	54.00	230	0
56	20.60	22.54	1.94	BARYTE-ROCK	3.9	11	50	740	0	0.552	0	152	1	2	1	54.00	1700	0
57	22.54	25.68	3.14	BARYTE-ROCK	4.0	12	25	150	0	0.669	0	172	3	1	0	54.00	450	0
58	25.68	26.85	1.17	BARYTE-ROCK	3.9	12	30	470	0	0.560	0	149	0	0	9	52.00	480	0
59	26.85	29.03	2.18	BARYTE-ROCK WITH DOLOMITE-ROCK AT BASE	3.9	13	105	3800	0	0.509	0	136	1	3	5	52.00	1550	0
60	29.03	30.15	1.12	GRAPHITIC MUSCOVITE-SCHIST		20	55	3500	98	0.137	9	158	8	4	0	21.00	1100	0

APPENDIX II TABLE II BOREHOLE 2  
 =====

SAMPLE NO.	DEPTH FROM TO		INTER-SECTION (M)	GENERALISED LITHOLOGY	SP.GR.	MOO %	AL2O3 %	SI02 %	S %	K2O %	CAO %	TI %	MNO %	FE2O3 %
	(M)	(M)												
1	1.05	1.85	0.80	BARYTE-ROCK	4.0	1.4	0.00	3.89	11.90	0.098	3.01	0.106	0.000	0.8
2	1.85	3.56	1.71	BARYTE-ROCK	4.1	0.6	0.00	3.54	12.10	0.001	1.36	0.106	0.000	0.4
3	3.56	5.75	2.19	BARYTE-ROCK	4.0	0.5	0.00	3.39	12.20	0.096	0.74	0.116	0.000	0.5
4	5.75	6.82	1.07	GOSSAN WITH QUARTZ-ROCK AT BASE		0.4	1.18	58.80	2.57	0.206	0.42	0.097	0.000	9.7
5	6.82	7.68	0.86	QUARTZ-CELSIAN-ROCK		2.0	8.15	44.70	4.36	2.200	2.83	0.303	0.000	4.3
6	7.68	8.47	0.79	BARYTE-ROCK	4.2	0.1	0.00	2.67	13.10	0.167	0.43	0.121	0.000	0.5
7	8.47	9.73	1.26	BARYTE-ROCK	4.1	0.3	0.00	6.59	11.80	0.019	0.59	0.107	0.000	0.5
8	9.73	10.93	1.20	BARYTE-ROCK	4.3	0.2	0.00	4.42	12.00	0.000	0.52	0.108	0.000	0.4
9	10.93	12.10	2.40	BARYTE-ROCK	4.0	0.2	0.00	6.81	11.60	0.002	0.47	0.107	0.000	0.6
10	12.10	13.33	1.23	BARYTE-ROCK	4.1	0.3	0.00	7.44	11.60	0.008	0.57	0.107	0.000	0.6
11	13.33	14.26	0.93	SULPHIDE-RICH QUARTZ-ROCK WITH CELSIAN	0.8	1.35	43.50	12.50	0.064	6.12	0.060	0.700	5.9	
12	14.26	14.70	0.44	SULPHIDE-RICH CALCAREOUS QUARTZ-ROCK	1.8	3.43	43.90	13.10	0.200	7.68	0.112	2.800	17.7	
13	14.70	15.23	0.53	QUARTZ-MUSCOVITE-SCHIST	3.2	10.40	50.40	2.40	3.550	5.69	0.492	0.100	6.0	
14	15.23	16.77	1.54	GRAPHITIC MUSCOVITE-SCHIST	2.3	15.40	56.50	1.56	5.620	5.61	0.338	0.300	5.1	
15	16.77	17.92	1.15	GRAPHITIC MUSCOVITE-SCHIST	3.1	16.70	54.60	1.32	5.860	4.85	0.452	0.300	6.2	
16	17.92	18.75	0.83	CALCAREOUS CHLORITE-MICA-SCHIST	5.5	11.30	45.60	0.42	2.550	10.70	0.893	0.300	12.4	
17	18.75	19.14	0.39	GRAPHITIC MUSCOVITE-SCHIST	3.2	16.30	54.80	0.67	5.850	6.26	0.358	0.500	5.9	

SAMPLE NO.	DEPTH FROM TO		INTER-SECTION (M)	GENERALISED LITHOLOGY	SP.GR.	NI PPM	CU PPM	ZN PPM	RB PPM	SR %	Y PPM	ZR PPM	NB PPM	AG PPM	SB PPM	BA %	PB PPM	U PPM
	(M)	(M)																
1	1.05	1.85	0.80	BARYTE-ROCK	4.0	11	40	2300	0	0.546	0	164	4	14	5	46.00	1300	0
2	1.85	3.56	1.71	BARYTE-ROCK	4.1	11	25	820	0	0.742	0	195	1	5	0	49.00	980	0
3	3.56	5.75	2.19	BARYTE-ROCK	4.0	12	15	250	0	0.058	0	165	1	3	2	52.00	220	0
4	5.75	6.82	1.07	GOSSAN WITH QUARTZ-ROCK AT BASE		4	40	190	5	0.060	2	71	2	3	0	17.00	330	0
5	6.82	7.68	0.86	QUARTZ-CELSIAN-ROCK		37	80	300	43	0.052	21	155	10	4	1	19.00	200	6
6	7.68	8.47	0.79	BARYTE-ROCK	4.2	13	20	510	5	0.336	0	132	2	2	0	52.00	430	0
7	8.47	9.73	1.26	BARYTE-ROCK	4.1	11	10	120	0	0.605	0	169	4	3	2	51.00	100	0
8	9.73	10.93	1.20	BARYTE-ROCK	4.3	12	15	90	0	0.628	0	165	2	2	0	52.00	150	0
9	10.93	12.10	2.40	BARYTE-ROCK	4.0	10	35	110	0	0.551	0	159	2	2	2	53.00	180	0
10	12.10	13.33	1.23	BARYTE-ROCK	4.1	10	20	130	0	0.521	0	158	2	2	1	53.00	180	0
11	13.33	14.26	0.93	SULPHIDE-RICH QUARTZ-ROCK WITH CELSIAN	15	75	68000	5	0.195	0	89	1	49	20	14.00	4900	0	
12	14.26	14.70	0.44	SULPHIDE-RICH CALCAREOUS QUARTZ-ROCK	17	390	1450	2	0.075	7	81	3	2	0	7.20	100	2	
13	14.70	15.23	0.53	QUARTZ-MUSCOVITE-SCHIST	31	95	1650	110	0.081	16	129	7	2	0	7.20	300	1	
14	15.23	16.77	1.54	GRAPHITIC MUSCOVITE-SCHIST	29	75	5100	181	0.031	18	136	8	2	1	1.30	1200	5	
15	16.77	17.92	1.15	GRAPHITIC MUSCOVITE-SCHIST	28	80	6000	194	0.014	21	154	12	2	3	0.47	1600	1	
16	17.92	18.75	0.83	CALCAREOUS CHLORITE-MICA-SCHIST	39	90	1200	99	0.026	18	113	7	2	0	0.07	230	2	
17	18.75	19.14	0.39	GRAPHITIC MUSCOVITE-SCHIST	28	55	3800	186	0.010	18	152	10	2	7	0.12	900	3	

APPENDIX II TABLE III BOREHOLE 3

SAMPLE NO.	DEPTH		INTER-SECTION	GENERALISED LITHOLOGY	SP.GR.	MGO %	AL2O3 %	SiO2 %	S %	K2O %	CaO %	TI %	MNO %	FE2O3 %
	FROM CYD (M)	TO CYD (M)												
18	3.00	4.04	1.04	GRAPHITIC QUARTZ-MUSCOVITE-SCHIST	5.3	11.70	45.80	0.75	4.740	11.00	0.261	1.700	7.2	
19	4.04	6.10	2.06	GRAPHITIC QUARTZ-MUSCOVITE-SCHIST	3.6	18.80	52.10	0.63	7.020	5.10	0.404	0.760	7.2	
20	6.10	6.86	0.76	GRAPHITIC QUARTZ-MUSCOVITE-SCHIST	2.8	14.10	66.40	0.82	4.750	3.32	0.278	0.200	5.6	
21	6.86	7.36	0.50	GRAPHITIC QUARTZ-MUSCOVITE-SCHIST AND DOLOMITE	7.2	9.60	39.80	0.42	4.130	16.00	0.225	2.300	7.2	
22	7.36	8.59	1.23	GRAPHITIC QUARTZ-MUSCOVITE-SCHIST	3.5	12.10	59.60	1.29	4.380	5.61	0.272	0.600	10.0	
23	8.59	9.60	1.01	DOLOMITE-RICH QUARTZ-MUSCOVITE-SCHIST	4.3	18.40	48.60	0.64	7.170	6.73	0.413	0.700	7.0	
24	9.60	12.23	2.63	GRAPHITIC QUARTZ-MUSCOVITE-SCHIST	3.3	17.90	55.70	0.69	6.730	4.13	0.397	0.200	6.4	
25	12.23	14.13	1.90	GRAPHITIC QUARTZ-MUSCOVITE-SCHIST	2.8	19.10	55.40	0.50	6.980	2.99	0.411	0.300	6.9	
26	14.13	15.25	1.12	GRAPHITIC MICA-SCHIST WITH DOLOMITE BANDS	3.6	16.40	55.40	0.60	6.060	5.35	0.367	0.100	6.0	
27	15.25	16.88	1.63	GRAPHITIC MICA-SCHIST WITH DOLOMITE BANDS	4.5	14.40	52.60	0.85	5.510	7.44	0.326	0.600	6.1	
28	16.88	18.38	1.50	GRAPHITIC MICA-SCHIST WITH DOLOMITE BANDS	5.3	13.40	47.20	0.80	5.500	10.10	0.311	0.900	6.5	
29	18.38	19.63	1.25	MUSCOVITE-QUARTZ-SCHIST	4.1	11.50	54.70	1.76	4.130	6.76	0.272	0.700	6.3	
30	19.63	20.08	0.45	SULPHIDE-RICH DOLOMITE-ROCK	7.3	2.88	35.90	6.84	0.227	13.00	0.623	2.500	11.3	
31	20.08	21.47	1.39	SULPHIDE-RICH DOLOMITE-ROCK	14.0	0.87	5.01	2.24	0.027	32.20	0.032	0.700	7.0	
32	21.47	22.28	0.81	SULPHIDE-RICH DOLOMITE-ROCK	13.8	0.95	1.57	2.77	0.046	32.10	0.018	0.700	7.7	
33	22.28	22.75	0.47	SULPHIDE-RICH DOLOMITE-ROCK	11.4	0.85	1.73	8.43	0.005	23.90	0.016	0.500	10.6	
34	22.75	24.12	1.37	SULPHIDE-RICH DOLOMITE-ROCK	11.7	1.46	2.62	6.07	0.088	26.40	0.038	0.400	7.7	
35	24.12	25.02	0.90	SULPHIDE-RICH CARBONATE-QUARTZ-ROCK	9.1	1.31	12.80	13.40	0.091	18.80	0.052	0.300	8.6	
36	25.02	26.36	1.34	BARYTE-ROCK	4.3	0.9	0.00	2.27	18.50	0.014	3.04	0.095	0.000	2.6
37	26.36	27.25	0.89	BARYTE-ROCK	4.2	0.7	0.00	5.74	11.50	0.005	1.26	0.104	0.000	0.5
38	27.25	28.46	1.21	BARYTE-ROCK	3.9	1.2	0.00	5.40	11.20	0.011	2.47	0.105	0.000	0.7
39	28.46	29.40	0.94	BARYTE-ROCK	3.8	1.1	0.00	7.02	11.10	0.006	2.00	0.103	0.000	0.3
40	29.40	30.87	1.47	BARYTE-ROCK	3.7	0.9	0.00	12.20	10.70	0.010	1.90	0.099	0.000	0.4
41	30.87	32.46	1.59	QUARTZITIC BARYTE-ROCK	3.6	0.6	0.00	15.10	10.50	0.003	2.41	0.097	0.000	0.5
42	32.46	32.94	0.48	CALCITE-QUARTZ-BARYTE-ROCK	0.7	0.26	19.40	9.51	0.015	9.12	0.077	0.200	1.0	
43	32.94	33.61	0.67	PYRITIC QUARTZ-ROCK	1.7	7.48	49.70	11.90	2.710	1.97	0.213	0.100	8.2	
44	33.61	35.20	1.59	GRAPHITIC MUSCOVITE-QUARTZ-SCHIST	4.1	12.30	58.60	1.69	4.510	5.57	0.290	0.500	5.1	

SAMPLE NO.	DEPTH		INTER-SECTION	GENERALISED LITHOLOGY	SP.GR.	NI PPM	CU PPM	ZN PPM	RB PPM	SR %	Y PPM	ZR PPM	NB PPM	AG PPM	SB PPM	BA %	FB PPM	U PPM
	FROM CYD (M)	TO CYD (M)																
18	3.00	4.04	1.04	GRAPHITIC QUARTZ-MUSCOVITE-SCHIST	26	40	15500	152	0.014	14	165	8	6	8	0.11	3900	0	
19	4.04	6.10	2.06	GRAPHITIC QUARTZ-MUSCOVITE-SCHIST	25	45	800	230	0.008	23	189	14	1	7	0.15	200	3	
20	6.10	6.86	0.76	GRAPHITIC QUARTZ-MUSCOVITE-SCHIST	25	45	1600	154	0.004	17	106	9	0	6	0.11	90	2	
21	6.86	7.36	0.50	GRAPHITIC QUARTZ-MUSCOVITE-SCHIST AND DOLOMITE	8	25	3800	126	0.017	13	148	8	1	0	0.07	200	0	
22	7.36	8.59	1.23	GRAPHITIC QUARTZ-MUSCOVITE-SCHIST	50	80	800	139	0.016	19	169	9	1	5	0.10	80	3	
23	8.59	9.60	1.01	DOLOMITE-RICH QUARTZ-MUSCOVITE-SCHIST	22	45	1800	227	0.010	21	189	14	1	0	0.16	220	4	
24	9.60	12.23	2.63	GRAPHITIC QUARTZ-MUSCOVITE-SCHIST	24	40	280	219	0.007	21	191	12	1	3	0.15	600	4	
25	12.23	14.13	1.90	GRAPHITIC QUARTZ-MUSCOVITE-SCHIST	27	45	1430	226	0.006	23	177	12	1	0	0.22	80	2	
26	14.13	15.25	1.12	GRAPHITIC MICA-SCHIST WITH DOLOMITE BANDS	19	40	3300	200	0.009	19	196	10	1	1	0.21	180	3	
27	15.25	16.88	1.63	GRAPHITIC MICA-SCHIST WITH DOLOMITE BANDS	18	40	6600	186	0.014	14	165	11	3	3	0.24	2700	3	
28	16.88	18.38	1.50	GRAPHITIC MICA-SCHIST WITH DOLOMITE BANDS	17	45	900	180	0.016	17	155	8	2	0	0.36	1150	2	
29	18.38	19.63	1.25	MUSCOVITE-QUARTZ-SCHIST	22	105	7400	132	0.019	14	132	9	2	5	2.10	1700	1	
30	19.63	20.08	0.45	SULPHIDE-RICH DOLOMITE-ROCK	15	520	11000	6	0.099	17	110	8	5	0	6.00	2600	2	
31	20.08	21.47	1.39	SULPHIDE-RICH DOLOMITE-ROCK	0	205	260	0	0.158	9	43	2	3	0	0.95	250	0	
32	21.47	22.28	0.81	SULPHIDE-RICH DOLOMITE-ROCK	1	200	10000	0	0.143	7	42	0	3	2	1.20	500	0	
33	22.28	22.75	0.47	SULPHIDE-RICH DOLOMITE-ROCK	15	490	56000	23	0.219	0	64	1	26	25	1.00	24000	1	
34	22.75	24.12	1.37	SULPHIDE-RICH DOLOMITE-ROCK	8	175	37000	12	0.129	1	57	2	12	16	2.70	13000	0	
35	24.12	25.02	0.90	SULPHIDE-RICH CARBONATE-QUARTZ-ROCK	11	100	26000	11	0.107	0	70	2	12	13	6.50	9300	0	
36	25.02	26.36	1.34	BARYTE-ROCK	4.3	14	70	13000	0	0.257	0	115	0	8	8	44.00	3300	0
37	26.36	27.25	0.89	BARYTE-ROCK	4.2	12	30	230	0	0.558	0	149	0	1	4	50.00	200	0
38	27.25	28.46	1.21	BARYTE-ROCK	3.9	12	20	420	0	0.510	0	145	1	1	2	47.00	280	0
39	28.46	29.40	0.94	BARYTE-ROCK	3.8	12	5	260	0	0.534	0	153	1	1	0	47.00	200	0
40	29.40	30.87	1.47	BARYTE-ROCK	3.7	10	15	320	0	0.541	0	156	0	0	0	47.00	180	0
41	30.87	32.46	1.59	QUARTZITIC BARYTE-ROCK	3.6	11	20	300	0	0.453	0	142	1	1	0	45.00	330	0
42	32.46	32.94	0.48	CALCITE-QUARTZ-BARYTE-ROCK	8	15	7200	0	0.142	0	94	4	6	3	33.00	3900	0	
43	32.94	33.61	0.67	PYRITIC QUARTZ-ROCK	33	860	64000	95	0.053	2	136	4	16	30	5.90	16000	1	
44	33.61	35.20	1.59	GRAPHITIC MUSCOVITE-QUARTZ-SCHIST	22	70	8500	149	0.015	13	180	9	3	2	1.40	2000	3	

APPENDIX II TABLE IV BOREHOLE 4  
 =====

SAMPLE NO.	DEPTH FROM CYD (M)	INTER-SECTION (M)	GENERALISED LITHOLOGY	SP.GR.	MG0	AL203	SI02	S	K20	CA0	TI	MNO	FE203	
					%	%	%	%	%	%	%	%		
62	5.77	7.04	1.27	QUARTZ-MUSCOVITE-SCHIST	8.3	16.60	57.00	0.64	5.510	3.60	0.326	0.300	6.3	
63	7.04	9.40	2.36	QUARTZ-MUSCOVITE-SCHIST	3.5	17.60	57.30	0.58	5.460	1.84	0.418	0.100	6.8	
64	9.40	10.34	0.94	QUARTZ-MUSCOVITE-SCHIST SLIGHTLY GRAPHITIC	3.5	16.90	57.50	0.54	4.950	2.63	0.410	0.100	6.5	
65	10.34	11.82	1.48	QUARTZ-MUSCOVITE-SCHIST CHLORITIC IN PARTS	3.2	19.50	53.70	0.78	6.280	1.56	0.444	0.100	7.2	
66	11.82	13.10	1.28	QUARTZ-MUSCOVITE-SCHIST DOLOMITIC AT BASE	4.3	17.70	49.50	1.13	5.900	4.82	0.384	0.300	8.0	
67	13.10	13.84	0.74	QUARTZ-MUSCOVITE-DOLOMITE-SCHIST	7.8	8.83	38.90	1.18	3.670	14.70	0.209	0.900	5.2	
68	13.84	14.43	0.59	DOLOMITIC QUARTZ-ROCK	4.9	6.19	39.90	2.98	1.630	8.03	0.205	1.100	3.2	
69	14.43	16.26	1.83	BARYTE-ROCK	4.3	0.2	0.00	1.99	18.40	0.015	0.52	0.106	0.000	2.1
70	16.26	17.31	1.05	BARYTE-ROCK	4.0	0.3	0.00	2.88	14.10	0.005	0.56	0.107	0.000	0.8
71	17.31	18.11	0.80	SULPHIDE-RICH CARBONATE-ROCK	4.3	1.32	10.10	25.70	0.082	9.46	0.039	0.400	11.8	
72	18.11	18.81	0.70	SULPHIDE-RICH CARBONATE-ROCK	2.8	0.49	30.10	7.39	0.000	22.30	0.007	1.000	5.0	
73	18.81	19.51	0.70	BRECCIATED SULPHIDE-QUARTZ-DOLOMITE-ROCK	4.1	0.93	16.10	34.10	0.102	7.71	0.025	0.300	12.8	
74	19.51	20.03	0.52	DOLOMITIC BARYTE-ROCK	4.4	1.6	0.06	4.72	18.80	0.013	5.82	0.076	0.000	3.5
75	20.03	20.75	0.72	DOLOMITIC QUARTZ-BARYTE- AND DOLOMITE-ROCK	4.6	0.63	5.71	28.40	0.020	10.50	0.017	0.400	10.0	
76	20.75	21.34	0.62	BANDED QUARTZ-CALCITE-ROCK	1.1	0.65	34.10	5.52	0.000	22.60	0.005	1.100	4.3	
77	21.34	22.22	0.88	BANDED QUARTZ-CELSIAN-ROCK	1.2	6.09	49.90	2.89	0.344	1.83	0.287	0.200	4.3	
78	22.22	23.44	1.22	SULPHIDE-RICH QUARTZ-CALCITE-ROCK	1.7	0.55	25.70	16.70	0.000	17.50	0.007	1.100	8.4	
79	23.44	25.39	1.95	QUARTZ-CELSIAN-ROCK	4.3	5.73	39.30	2.81	0.434	7.37	0.261	0.200	2.8	

SAMPLE NO.	DEPTH FROM CYD (M)	INTER-SECTION (M)	GENERALISED LITHOLOGY	SP.GR.	NI	CU	ZN	RB	SR	Y	ZR	NB	AG	SB	BA	PB	U	
					PPM	PPM	PPM	PPM	%	PPM	PPM	PPM	PPM	PPM	%	PPM	PPM	
62	5.77	7.04	1.27	QUARTZ-MUSCOVITE-SCHIST	31	40	150	175	0.010	20	200	9	1	0	0.94	40	3	
63	7.04	9.40	2.36	QUARTZ-MUSCOVITE-SCHIST	33	30	110	179	0.011	21	243	12	1	0	1.00	20	4	
64	9.40	10.34	0.94	QUARTZ-MUSCOVITE-SCHIST SLIGHTLY GRAPHITIC	24	40	150	152	0.007	20	286	12	1	2	0.82	20	4	
65	10.34	11.82	1.48	QUARTZ-MUSCOVITE-SCHIST CHLORITIC IN PARTS	35	55	230	192	0.009	23	239	14	0	1	1.30	20	4	
66	11.82	13.10	1.28	QUARTZ-MUSCOVITE-SCHIST DOLOMITIC AT BASE	32	45	450	172	0.014	21	158	10	1	1	1.30	20	3	
67	13.10	13.84	0.74	QUARTZ-MUSCOVITE-DOLOMITE-SCHIST	22	45	1700	102	0.040	16	127	6	1	2	1.50	230	2	
68	13.84	14.43	0.59	DOLOMITIC QUARTZ-ROCK	27	10	25000	54	0.131	12	166	8	12	8	13.00	8400	0	
69	14.43	16.26	1.83	BARYTE-ROCK	4.3	13	75	7000	0	0.219	0	106	3	12	10	53.00	2100	0
70	16.26	17.31	1.05	BARYTE-ROCK	4.0	11	210	6400	0	0.263	0	111	1	15	15	56.00	3700	0
71	17.31	18.11	0.80	SULPHIDE-RICH CARBONATE-ROCK	27	165	105000	33	0.128	0	80	0	49	76	7.60	36000	0	
72	18.11	18.81	0.70	SULPHIDE-RICH CARBONATE-ROCK	8	90	42000	34	0.489	0	92	0	42	59	0.90	36000	0	
73	18.81	19.51	0.70	BRECCIATED SULPHIDE-QUARTZ-DOLOMITE-ROCK	31	30	160000	51	0.091	0	70	1	70	82	2.90	48000	0	
74	19.51	20.03	0.52	DOLOMITIC BARYTE-ROCK	4.4	15	140	60000	16	0.140	0	98	2	30	44	35.00	20000	0
75	20.03	20.75	0.72	DOLOMITIC QUARTZ-BARYTE- AND DOLOMITE-ROCK	34	40	200000	66	0.128	0	82	1	85	113	2.80	64000	0	
76	20.75	21.34	0.62	BANDED QUARTZ-CALCITE-ROCK	9	165	54000	31	0.518	0	92	0	41	54	0.43	36000	0	
77	21.34	22.22	0.88	BANDED QUARTZ-CELSIAN-ROCK	27	10	12500	8	0.033	9	149	9	3	5	22.00	1400	0	
78	22.22	23.44	1.22	SULPHIDE-RICH QUARTZ-CALCITE-ROCK	18	35	71000	43	0.351	0	77	1	56	71	0.95	42000	0	
79	23.44	25.39	1.95	QUARTZ-CELSIAN-ROCK	21	15	750	7	0.126	13	152	9	1	0	20.00	200	0	

APPENDIX II TABLE V BOREHOLE 5  
 =====

SAMPLE NO. CYD	DEPTH			GENERALISED LITHOLOGY	SP.GR.	MGO %	AL2O3 %	SiO2 %	S %	K2O %	CAO %	TI %	MNO %	FE2O3 %
	FROM (M)	TO (M)	SECTION (M)											
80	2.30	3.25	0.95	DOLOMITIC QUARTZ-CELSIAN-ROCK		0.4	8.08	68.30	0.61	3.350	0.55	0.244	0.000	2.0
81	3.25	4.15	0.90	DOLOMITIC QUARTZ-CELSIAN-ROCK		1.3	4.58	34.50	7.48	1.300	2.35	0.205	0.100	3.0
82	4.15	5.26	1.11	BARYTE-ROCK	4.3	0.2	0.00	3.03	13.50	0.227	0.46	0.132	0.000	0.6
83	5.26	6.02	0.76	QUARTZ-CELSIAN-ROCK		0.2	4.27	67.10	1.93	1.640	0.44	0.181	0.000	1.9
84	6.02	6.87	0.85	BARYTE-ROCK	4.1	0.2	0.21	6.53	11.60	0.279	0.40	0.137	0.000	2.6
85	6.87	7.94	1.07	QUARTZ-CELSIAN-ROCK		1.1	11.10	55.10	0.94	5.220	0.94	0.362	0.000	3.4
86	7.94	10.06	2.12	QUARTZ-CELSIAN-ROCK		6.1	7.32	42.10	1.23	4.010	10.50	0.236	0.600	3.3
87	10.06	11.06	1.00	QUARTZ-CELSIAN-ROCK		3.6	11.30	51.40	1.35	5.410	4.36	0.324	0.100	3.3
88	11.06	12.26	1.20	QUARTZ-CELSIAN-ROCK		3.1	13.40	49.90	1.22	6.080	3.48	0.391	0.100	3.1
89	12.26	13.45	1.19	QUARTZ-CELSIAN-ROCK		1.4	11.90	56.10	1.43	5.310	1.36	0.358	0.000	4.1
90	13.45	15.20	1.75	QUARTZ-CELSIAN-ROCK		1.0	11.60	49.80	1.08	5.660	0.42	0.423	0.000	4.2
92	17.37	19.00	1.65	BARYTE-ROCK	4.5	0.2	0.48	18.30	9.79	0.180	0.54	0.171	0.000	1.7
93	19.00	21.42	2.42	QUARTZ-CELSIAN-ROCK		0.2	1.13	48.80	3.67	0.173	0.41	0.145	0.000	10.2
94	21.42	23.27	1.85	BARYTE-ROCK	4.3	0.1	0.00	3.42	13.66	0.035	0.41	0.115	0.000	0.5
95	23.27	23.70	0.43	BIOTITE-QUARTZ-CELSIAN-SCHIST		5.8	3.98	26.10	5.09	1.280	6.67	0.736	0.300	4.2
96	23.70	24.92	1.22	BARYTE-ROCK		0.6	0.06	5.24	12.70	0.107	1.39	0.214	0.000	0.9
97	24.92	25.62	0.70	BARYTE-ROCK AND BIOTITE-QUARTZ-SCHIST BANDS		6.3	6.81	38.30	1.58	2.260	5.74	1.013	0.200	6.7
98	25.62	27.07	1.45	BARYTE-ROCK		0.2	0.00	3.37	14.10	0.069	0.47	0.128	0.000	0.8
99	27.07	27.95	0.88	QUARTZ-CELSIAN-ROCK WITH MUSCOVITE IN PARTS		3.3	11.00	51.30	1.45	4.680	4.24	0.320	0.200	3.1
100	27.95	29.12	1.17	QUARTZ-CELSIAN-ROCK WITH MUSCOVITE IN PARTS		1.8	17.70	50.10	2.05	5.210	1.01	0.379	0.000	4.8
101	29.12	31.10	1.98	QUARTZ-CELSIAN-ROCK WITH MUSCOVITE IN PARTS		3.2	13.70	52.00	1.96	5.320	3.86	0.350	0.100	4.3
102	31.10	33.81	2.71	QUARTZ-CELSIAN-ROCK WITH MUSCOVITE IN PARTS		2.7	10.60	53.40	2.25	4.370	3.13	0.294	0.100	3.5

SAMPLE NO. CYD	DEPTH			GENERALISED LITHOLOGY	SP.GR.	NI PPM	CU PPM	ZN PPM	RB PPM	SR %	Y PPM	ZR PPM	NB PPM	AG PPM	SB PPM	BA %	FB PPM	U PPM
	FROM (M)	TO (M)	SECTION (M)															
80	2.30	3.25	0.95	DOLOMITIC QUARTZ-CELSIAN-ROCK		7	10	500	74	0.033	9	208	7	2	0	12.00	450	1
81	3.25	4.15	0.90	DOLOMITIC QUARTZ-CELSIAN-ROCK		20	35	2800	32	0.203	16	172	8	5	1	31.00	2150	0
82	4.15	5.26	1.11	BARYTE-ROCK	4.3	14	15	950	3	0.348	2	136	1	2	0	57.00	1300	0
83	5.26	6.02	0.76	QUARTZ-CELSIAN-ROCK		5	20	1000	38	0.070	6	227	5	2	0	18.00	800	0
84	6.02	6.87	0.85	BARYTE-ROCK	4.1	12	60	1200	3	0.342	1	139	1	5	0	53.00	1400	0
85	6.87	7.94	1.07	QUARTZ-CELSIAN-ROCK		19	40	890	135	0.053	13	204	9	1	0	13.00	200	3
86	7.94	10.06	2.12	QUARTZ-CELSIAN-ROCK		22	40	1350	101	0.109	15	156	7	1	0	7.20	50	0
87	10.06	11.06	1.00	QUARTZ-CELSIAN-ROCK		29	60	600	156	0.067	17	172	10	1	0	8.40	60	2
88	11.06	12.26	1.20	QUARTZ-CELSIAN-ROCK		32	30	420	185	0.056	19	184	11	2	0	8.20	710	1
89	12.26	13.45	1.19	QUARTZ-CELSIAN-ROCK		13	80	840	159	0.054	16	206	11	1	0	9.50	60	2
90	13.45	15.20	1.75	QUARTZ-CELSIAN-ROCK		7	30	150	165	0.067	12	206	12	4	0	13.00	2000	2
92	17.37	19.00	1.65	BARYTE-ROCK	4.5	15	30	580	0	0.315	1	150	2	5	3	49.00	1100	0
93	19.00	21.42	2.42	QUARTZ-CELSIAN-ROCK		5	90	280	6	0.067	0	96	5	12	5	24.00	3100	0
94	21.42	23.27	1.85	BARYTE-ROCK	4.3	13	20	1600	0	0.652	0	156	3	5	4	58.00	1450	0
95	23.27	23.70	0.43	BIOTITE-QUARTZ-CELSIAN-SCHIST		107	180	1800	58	0.335	22	203	10	4	0	24.00	230	0
96	23.70	24.92	1.22	BARYTE-ROCK		22	15	1100	0	0.491	2	149	3	2	8	52.00	470	0
97	24.92	25.62	0.70	BARYTE-ROCK AND BIOTITE-QUARTZ-SCHIST BANDS		145	285	1750	103	0.202	22	209	12	4	0	16.00	50	0
98	25.62	27.07	1.45	BARYTE-ROCK		15	20	2350	0	0.564	0	148	2	3	0	56.00	880	0
99	27.07	27.95	0.88	QUARTZ-CELSIAN-ROCK WITH MUSCOVITE IN PARTS		25	55	4300	123	0.093	16	198	10	2	0	9.50	440	2
100	27.95	29.12	1.17	QUARTZ-CELSIAN-ROCK WITH MUSCOVITE IN PARTS		43	125	1900	170	0.036	13	167	10	1	0	6.80	640	3
101	29.12	31.10	1.98	QUARTZ-CELSIAN-ROCK WITH MUSCOVITE IN PARTS		34	70	3650	167	0.043	16	163	11	1	0	5.70	600	2
102	31.10	33.81	2.71	QUARTZ-CELSIAN-ROCK WITH MUSCOVITE IN PARTS		30	110	1900	128	0.071	14	158	9	1	0	10.00	530	0



APPENDIX II      TABLE VI      BOREHOLE 6  
 \*\*\*\*\*  
 \*\*\*\*\*  
 \*\*\*\*\*

SAMPLE CYD NO.	FROM		TO M	INTER- SECTION M	GENERALISED LITHOLOGY	SP.GR.	CA	TI	MN	FE	NI	CU	ZN	AG	SB	BA	PB
	M	M					%	%	%	%	PPH	PPH	PPH	PPH	PPH	%	PPH
805	2.15	5.42	3.27		CHLORITE-MUSCOVITE-SCHIST	2.8	2.90	0.398	0.088	4.99	42	23	171	1	0	0.40	37
806	5.42	7.22	1.80		"	2.9	3.55	0.484	0.081	5.99	48	25	152	0	0	0.31	25
807	7.22	8.95	1.73		DOLOMITIC BIOTITE-CHLORITE-SCHIST	2.9	5.44	0.844	0.112	7.08	115	77	122	0	0	0.27	18
808	8.95	13.60	4.65		CHLORITE-BIOTITE-SCHIST	3.0	3.58	0.455	0.074	5.53	49	39	169	3	0	0.42	10
809	13.60	15.18	1.58		MUSCOVITE-QUARTZ-SCHIST	3.0	6.47	0.306	0.082	4.45	45	53	111	1	0	0.41	9
810	15.18	18.25	3.07		QUARTZ-CHLORITE-SCHIST	2.8	5.34	0.329	0.088	4.57	33	22	172	0	0	0.46	6
811	18.25	22.08	3.83		"	2.8	3.57	0.429	0.101	5.00	37	50	218	1	0	0.82	6
812	22.08	26.42	4.34		"	2.8	5.58	0.317	0.098	5.02	32	6	109	2	0	0.49	7
813	26.42	27.10	0.68		QUARTZ-MICA-SCHIST	2.8	6.05	0.342	0.090	4.11	29	23	94	2	0	0.42	7
814	27.10	27.77	0.67		DOLOMITIC QUARTZITE	-	3.52	0.099	0.045	2.38	10	1128	34	1	0	0.01	11
815	27.77	31.23	3.46		DOLOMITIC MUSCOVITE-CHLORITE-SCHIST	2.8	6.95	0.297	0.089	4.50	30	16	67	0	0	0.34	6
816	31.23	32.15	0.92		CHLORITE-BIOTITE-SCHIST	2.9	5.76	0.320	0.085	4.84	34	16	97	0	0	0.49	4
817	32.15	34.53	2.38		DOLOMITIC BIOTITE-CHLORITE-SCHIST	2.9	3.94	0.414	0.114	4.63	29	29	134	2	0	0.92	7
818	34.53	38.03	3.50		"	2.8	2.42	0.493	0.105	5.53	44	28	210	1	0	1.10	17
819	38.03	40.35	2.32		CHLORITE-MUSCOVITE-SCHIST	2.9	4.35	0.302	0.187	4.20	28	31	475	2	0	1.38	17
820	40.35	41.00	0.65		"	2.9	8.78	0.163	0.324	4.21	16	6	1042	0	0	0.66	20
821	41.00	42.20	1.20		"	2.9	1.12	0.509	0.061	5.40	52	40	625	1	0	1.78	18
822	42.20	43.84	1.64		MICACEOUS QUARTZITE	2.7	4.36	0.259	0.167	3.87	25	54	200	1	0	1.54	23
823	43.84	46.14	2.30		QUARTZ-MUSCOVITE-SCHIST	2.7	3.87	0.314	0.162	4.18	34	52	101	2	0	1.62	19
824	46.14	49.00	2.86		"	2.8	3.48	0.312	0.139	3.35	25	53	79	2	0	2.85	17
825	49.00	52.20	3.20		BIOTITE-CHLORITE-SCHIST	2.8	2.56	0.405	0.111	4.93	45	133	158	0	0	1.49	22
826	52.20	54.15	1.95		"	2.8	2.38	0.460	0.099	5.19	44	38	171	2	0	1.26	17
827	54.15	60.22	6.07		CHLORITE-QUARTZ-SCHIST	2.8	2.35	0.415	0.090	4.84	45	44	126	3	0	0.99	17
828	60.22	64.30	4.08		BIOTITE-CHLORITE-SCHIST	2.9	5.10	0.321	0.096	4.66	31	7	87	1	0	0.65	12
829	64.30	67.10	2.80		CHLORITE-MUSCOVITE-BIOTITE-SCHIST	2.9	3.01	0.480	0.113	5.65	46	17	116	0	1	1.23	12
830	67.10	69.40	2.30		CHLORITE-SERICITE-SCHIST	2.9	3.88	0.277	0.147	5.17	38	66	107	2	0	0.77	17
831	69.40	73.09	3.69		GARNETIFEROUS BIOTITE-CHLORITE-SCHIST	2.9	4.24	0.897	0.121	7.26	128	58	186	1	0	0.84	22
832	73.09	76.26	3.17		MUSCOVITE-BIOTITE-SCHIST	2.8	4.28	0.401	0.107	4.47	36	54	103	2	0	1.78	23
833	76.26	78.37	2.11		SERICITE-BIOTITE-SCHIST	2.9	3.81	0.279	0.128	3.81	27	24	79	1	5	1.39	16
834	78.37	81.00	2.63		CHLORITE-BIOTITE-SCHIST	2.8	3.57	0.498	0.139	5.91	68	67	177	0	2	1.51	18
835	81.00	83.28	2.28		"	2.8	4.15	0.351	0.116	5.00	31	22	97	0	1	0.64	17
836	83.28	85.85	2.57		SERICITE-BIOTITE-SCHIST	2.8	5.50	0.294	0.073	4.06	25	14	53	2	6	0.44	9
837	85.85	87.75	1.90		SERICITE-QUARTZ-SCHIST	2.8	6.45	0.318	0.092	4.52	30	41	45	1	1	0.32	6
838	87.75	91.00	3.25		DOLOMITIC CHLORITE-SERICITE-SCHIST	2.8	4.82	0.363	0.100	5.05	36	20	133	2	2	0.68	15
839	91.00	95.56	4.56		"	2.8	3.14	0.378	0.079	5.07	35	40	93	0	1	0.50	12
840	95.56	98.50	2.94		"	2.8	3.35	0.362	0.067	4.76	26	29	68	0	5	0.67	9
841	98.50	101.10	2.60		"	2.7	3.75	0.352	0.076	5.12	30	18	72	2	0	0.29	16
842	101.10	103.46	2.36		CARBONACEOUS CHLORITE-SERICITE-SCHIST	2.8	6.79	0.313	0.115	4.83	37	55	29	0	0	0.26	12
843	103.46	106.00	2.54		CHLORITE-SERICITE-SCHIST	2.8	4.44	0.345	0.094	4.99	33	29	57	0	0	0.27	11
844	106.00	109.24	3.24		"	2.8	3.35	0.380	0.100	5.03	39	50	80	0	0	0.18	19
845	109.24	110.00	0.76		LAMPROPHYRE	2.8	2.06	0.867	0.050	8.64	69	29	59	2	5	0.08	7
846	110.00	114.40	4.40		GRAPHITIC SERICITE-SCHIST	2.8	5.03	0.251	0.154	4.11	21	45	96	1	4	0.15	23
847	114.40	117.90	3.50		"	2.8	4.33	0.338	0.136	5.50	48	62	138	1	0	0.18	27
848	117.90	122.54	4.64		"	2.8	2.19	0.404	0.075	5.51	45	54	119	0	0	0.23	24
849	122.54	126.34	3.80		"	2.8	4.13	0.374	0.090	4.98	43	41	61	1	3	0.25	16
850	126.34	127.00	0.66		MICACEOUS QUARTZITE	2.8	6.41	0.364	0.133	4.79	32	20	45	0	8	0.18	11
851	127.00	132.16	5.16		QUARTZITE	2.8	5.27	0.278	0.101	3.74	28	46	48	1	2	0.85	8
852	132.16	138.46	6.30		DOLOMITIC SERICITE-CHLORITE-SCHIST	2.7	4.69	0.319	0.101	4.71	29	28	76	1	2	0.19	8
853	138.46	144.31	5.85		SERICITE-BIOTITE-SCHIST AND LIMESTONE	2.8	4.35	0.340	0.082	5.08	35	39	77	0	2	0.14	12
854	144.31	148.94	4.63		DOLOMITIC MICA-SCHIST	2.8	4.16	0.391	0.091	5.21	46	45	92	0	7	0.17	5
855	148.94	157.34	8.40		CALCAREOUS HORNBLende-SERICITE-SCHIST	-	4.64	0.350	0.080	5.23	43	26	114	3	1	0.10	16

APPENDIX II      TABLE VII      BOREHOLE 7  
 =====      =====      =====

SAMPLE CYD NO.	FROM M	TO M	INTER-SECTION M	GENERALISED LITHOLOGY	SP.GR.	CA	TI	MN	FE	NI	CU	ZN	AG	SB	BA	PB
						%	%	%	%	PPM	PPM	PPM	PPM	PPM	%	PPM
501	3.14	5.00	1.86	CALCAREOUS MUSCOVITE-SCHIST	-	0.53	0.466	0.088	7.12	68	47	2360	0	4	0.45	128
502	5.00	7.59	2.59	BIOTITE-MUSCOVITE-CHLORITE-SCHIST	2.8	2.42	0.475	0.084	6.75	60	25	721	0	3	0.23	21
503	7.59	10.40	2.81	MUSCOVITE-BIOTITE-CHLORITE-DOLOMITE-SCHIST	2.5	3.89	0.347	0.071	5.48	30	31	269	0	0	0.23	11
504	10.40	12.49	2.09	.	2.6	7.28	0.295	0.091	4.47	29	38	275	0	1	0.32	14
505	12.49	14.31	1.82	.	2.6	3.14	0.374	0.136	5.13	43	8	1504	0	0	0.99	17
506	14.31	15.20	0.89	MUSCOVITE-SCHIST	-	4.35	0.333	0.125	4.09	32	19	305	0	0	1.50	10
507	15.20	18.45	3.25	MUSCOVITE-BIOTITE-DOLOMITE-SCHIST	2.6	2.95	0.377	0.115	4.83	51	32	963	0	2	1.58	83
508	18.45	19.79	1.34	MUSCOVITE-DOLOMITE-SCHIST	2.5	4.36	0.284	0.171	3.54	22	39	149	0	0	1.16	11
509	19.79	20.06	0.27	MASSIVE PYRITE	-	3.05	0.141	0.384	14.57	51	495	2752	0	0	0.53	6
510	20.06	21.78	1.72	MUSCOVITE-SCHIST	2.6	4.36	0.292	0.138	3.86	31	41	1051	0	0	1.14	69
511	21.78	24.37	2.59	.	2.7	1.45	0.372	0.066	3.56	31	58	578	0	0	1.41	26
512	24.37	27.03	2.66	.	2.6	0.23	0.412	0.034	3.54	39	86	1458	0	2	2.33	340
513	27.03	30.54	3.51	QUARTZ-CELSIAN-ROCK AND BARYTE-ROCK	3.3	2.80	0.194	0.227	2.86	19	48	5350	0	0	17.45	730
514A	30.54	31.24	0.70	BARYTE-ROCK	3.7	1.38	0.127	0.098	0.92	15	0	1550	0	2	41.78	872
514B	31.24	34.09	2.85	QUARTZ-CELSIAN-ROCK	2.9	1.01	0.292	0.074	2.58	25	2	993	0	0	12.45	993
515	34.09	38.52	4.43	MUSCOVITE-DOLOMITE-CELSIAN-SCHIST	2.9	0.85	0.362	0.069	3.67	22	66	541	0	0	3.52	42
516	38.52	39.80	1.28	QUARTZ-CELSIAN-ROCK AND BARYTE-ROCK	2.7	0.52	0.165	0.071	1.91	22	1	2900	0	0	32.79	2787
517	39.80	40.93	1.13	MUSCOVITE-SCHIST WITH HYALOPHANE	2.7	0.60	0.342	0.060	3.84	40	35	1717	0	1	7.02	894
518	40.93	42.61	1.68	QUARTZ-CELSIAN-ROCK	2.9	3.15	0.327	0.226	2.20	26	11	520	0	0	10.49	57
519	42.61	44.73	2.12	.	2.9	0.33	0.239	0.122	5.56	53	15	13800	0	10	12.13	7343
520	44.73	48.12	3.39	MUSCOVITE-SCHIST	2.7	1.61	0.403	0.099	3.92	46	55	2461	0	0	1.84	432
521	48.12	50.34	2.22	.	2.6	1.15	0.378	0.082	3.83	34	54	2562	0	0	1.75	266
522	50.34	51.74	1.40	.	2.8	4.31	0.290	0.126	3.21	22	51	370	0	3	1.46	16
523	51.74	54.62	2.88	.	2.7	2.10	0.363	0.149	4.33	28	49	2358	0	0	1.62	86
524	54.62	57.09	2.47	.	2.8	1.00	0.355	0.131	6.21	48	166	4476	0	0	3.54	569
525	57.09	58.64	1.55	.	2.9	0.11	0.314	0.010	3.22	32	534	1960	0	4	5.06	1719
526	58.64	61.91	3.27	QUARTZ-CELSIAN-ROCK	2.7	0.20	0.384	0.033	2.06	37	12	2376	0	0	12.40	349
527	61.91	65.23	3.32	QUARTZ-CELSIAN ROCK AND MUSCOVITE-SCHIST	2.6	2.38	0.305	0.244	3.98	31	49	3463	0	0	3.99	268
528	65.23	67.28	2.05	DOLOMITE-MUSCOVITE-SCHIST	2.7	4.51	0.304	0.221	4.66	32	45	2102	0	3	1.35	47
529	67.28	70.82	3.54	MUSCOVITE-BIOTITE-DOLOMITE-SCHIST	2.8	3.88	0.351	0.126	4.71	51	32	113	0	0	1.25	6
530	70.82	72.85	2.05	.	2.8	3.11	0.405	0.116	4.60	40	57	97	0	6	1.80	8
531	72.85	76.39	3.54	MUSCOVITE-CELSIAN-DOLOMITE-SCHIST	3.0	1.90	0.338	0.118	3.23	28	73	1097	0	0	2.84	275
532	76.39	79.10	2.71	QUARTZ-CELSIAN-ROCK	3.1	1.32	0.219	0.114	2.76	21	6	3900	0	0	13.81	707
533	79.10	82.83	3.73	.	2.9	1.43	0.161	0.112	2.59	17	20	10300	0	0	9.19	2442
534	82.83	84.03	1.20	MUSCOVITE-CELSIAN-DOLOMITE-SCHIST	2.9	2.27	0.323	0.147	2.81	23	51	2408	0	4	2.74	824
535	84.03	85.47	1.44	QUARTZ-CELSIAN-ROCK	2.9	3.28	0.211	0.145	4.26	33	27	1481	0	0	11.39	309
536	85.47	88.16	2.69	.	2.9	2.16	0.177	0.114	5.00	30	7	589	0	0	10.06	264
537	88.16	90.65	2.49	LIMESTONE AND BIOTITE-MUSCOVITE-SCHIST	2.8	3.29	0.412	0.085	5.25	33	17	253	0	0	1.95	103
538	90.65	91.70	1.05	GRAPHITIC MUSCOVITE-SCHIST	2.8	1.72	0.382	0.038	4.65	26	30	152	0	6	0.35	40
539	91.70	94.62	2.92	.	2.7	4.35	0.277	0.149	4.98	25	41	425	0	5	0.26	36
540	94.62	97.08	2.46	GRAPHITIC MUSCOVITE-DOLOMITE-SCHIST	2.8	1.08	0.437	0.033	4.38	29	53	271	0	1	0.43	34
541	97.08	100.15	3.07	GRAPHITIC MUSCOVITE-SCHIST	2.7	2.68	0.353	0.079	4.08	25	52	284	0	5	0.39	30
542	100.15	103.65	3.50	.	2.7	6.60	0.271	0.131	3.82	30	38	224	0	4	0.30	30
543	103.65	106.33	2.68	LIMESTONE AND MUSCOVITE-SCHIST	2.7	11.76	0.237	0.099	3.57	33	16	43	0	0	0.27	21
544	106.33	108.72	2.39	GRAPHITIC MUSCOVITE-DOLOMITE-SCHIST	2.8	1.21	0.411	0.038	4.45	35	54	125	0	0	0.33	26
545	108.72	112.13	3.41	GRAPHITIC MUSCOVITE-SCHIST	2.8	1.55	0.398	0.047	4.11	31	42	171	0	0	0.38	24
546	112.13	113.84	1.71	GRAPHITIC MUSCOVITE-DOLOMITE-SCHIST	2.9	3.83	0.306	0.113	4.36	24	29	96	0	2	0.31	21
547	113.84	115.15	1.31	LIMESTONE AND MUSCOVITE-SCHIST	2.9	11.63	0.148	0.291	5.01	11	12	80	0	3	0.16	16
548	115.15	117.15	2.00	GRAPHITIC MUSCOVITE-SCHIST	2.8	4.13	0.292	0.104	4.48	28	34	241	0	0	0.31	20
549	117.15	121.06	3.91	DOLOMITE-MUSCOVITE-BIOTITE-CHLORITE-SCHIST	2.8	4.56	0.345	0.083	5.10	33	11	82	0	7	0.17	8
550	121.06	121.95	0.89	.	2.8	3.79	0.422	0.070	5.22	43	33	70	0	0	0.19	10
551	121.95	123.30	1.35	.	2.8	5.38	0.310	0.106	4.38	32	4	63	0	0	0.49	3
552	123.30	124.18	0.88	LAMPROPHYRE	2.7	3.95	0.395	0.077	5.05	36	14	75	0	3	0.30	8
553	124.18	127.57	3.39	DOLOMITE-MUSCOVITE-BIOTITE-CHLORITE-SCHIST	2.8	3.54	0.703	0.076	6.63	84	32	75	0	0	0.18	5
554	127.57	128.63	1.06	GRAPHITIC MUSCOVITE-SCHIST	2.8	0.97	0.502	0.030	4.45	39	73	117	0	0	0.56	24
555	128.63	131.71	3.08	.	2.8	3.17	0.397	0.082	5.09	48	36	117	0	5	0.40	10
556	131.71	135.17	3.46	CALCAREOUS MUSCOVITE-HORNBLende-SCHIST	2.7	4.24	0.418	0.074	5.87	55	7	143	0	0	0.23	28
557	135.17	137.88	2.71	.	2.8	7.75	0.394	0.075	4.05	32	12	78	0	3	0.16	15
558	137.88	140.80	2.92	CALCAREOUS MUSCOVITE-BIOTITE-SCHIST	2.7	8.46	0.417	0.074	4.28	31	9	72	0	3	0.07	11
559	140.80	143.62	2.82	CALCAREOUS MUSCOVITE-HORNBLende-SCHIST	2.7	8.80	0.320	0.070	4.27	34	14	86	0	0	0.07	8
560	143.62	146.45	2.83	.	2.8	6.21	0.317	0.062	4.67	47	24	105	0	2	0.09	17
561	146.45	148.31	1.86	.	2.6	4.00	0.363	0.095	5.43	38	24	123	0	2	0.08	37
562	148.31	151.82	3.51	AMPHIBOLITE	2.9	4.86	0.852	0.116	8.21	94	69	188	0	0	0.05	56
563	151.82	153.51	1.69	CALCAREOUS HORNBLende-MUSCOVITE-SCHIST	2.8	4.45	0.350	0.099	5.50	42	0	134	0	0	0.10	63
564	153.51	156.46	2.95	.	2.7	5.23	0.344	0.095	5.21	37	14	114	0	3	0.09	48
565	156.46	159.60	3.14	.	2.7	4.78	0.343	0.114	5.90	46	16	135	0	0	0.07	38
566	159.60	162.20	2.60	CALCAREOUS BIOTITE-MUSCOVITE-SCHIST	2.8	4.19	0.391	0.100	5.48	46	7	126	0	0	0.10	39
567	162.20	165.07	2.87	.	2.8	3.21	0.381	0.082	6.17	43	8	126	0	2	0.06	33
568	165.07	167.91	2.84	.	2.7	2.79	0.387	0.078	6.08	43	39	127	0	6	0.06	35
569	167.91	170.75	2.84	.	-	2.81	0.500	0.076	6.58	58	23	129	0	0	0.07	29

APPENDIX II      TABLE VIII      BOREHOLE 8  
 \*\*\*\*\*      \*\*\*\*\*      \*\*\*\*\*

SAMPLE CYD NO.	FROM M	TO INTER- SECTION		GENERALISED LITHOLOGY	SP.GR.	CA %	TI %	MN %	FE %	NI PPM	CU PPM	ZN PPM	AG PPM	SB PPM	BA %	PB PPM
		M	M													
614	0.00	4.46	4.46	SPHALERITE-BEARING BOULDER IN TILL	-	2.15	0.230	0.127	2.80	15	34	5485	2	5	0.13	1644
615	4.46	6.56	2.10	GRAPHITIC MUSCOVITE-SCHIST	2.8	2.68	0.343	0.078	3.78	21	25	73	2	0	0.27	19
616	6.56	8.92	2.36	"	2.8	2.83	0.372	0.082	3.82	24	32	76	1	5	0.41	22
617	8.92	10.44	1.52	MUSCOVITE-QUARTZ-SCHIST	2.5	4.73	0.367	0.099	4.30	31	24	41	1	1	0.62	6
618	10.44	12.14	1.70	BIOTITIC MUSCOVITE-QUARTZ-SCHIST	2.7	4.71	0.340	0.102	4.57	31	10	57	2	0	0.61	5
619	12.14	16.54	4.40	BIOTITIC MUSCOVITE-SCHIST	2.7	2.67	0.364	0.097	3.72	36	43	48	1	1	1.34	7
620	16.54	17.58	1.04	BIOTITIC MUSCOVITE-QUARTZ-SCHIST	2.7	2.90	0.401	0.073	4.17	31	23	67	2	1	0.81	8
621	17.58	19.40	1.82	MUSCOVITE-QUARTZ-SCHIST	2.9	2.79	0.392	0.094	3.79	32	48	91	1	3	1.90	11
622	19.40	20.60	1.20	"	2.8	3.13	0.304	0.254	4.40	28	73	4054	4	2	1.56	2393
623	20.60	21.67	1.07	"	2.7	2.60	0.242	0.174	3.63	19	56	6800	3	5	0.37	2689
624	21.67	23.17	1.50	"	2.6	0.60	0.428	0.044	4.82	33	36	130	1	7	0.70	38
625	23.17	24.55	1.38	"	2.5	0.95	0.249	0.056	3.63	16	21	77	0	4	0.14	15
626	24.55	25.80	1.25	"	2.8	1.26	0.388	0.062	4.69	19	14	81	2	6	0.17	22
627	25.80	28.83	3.03	GRAPHITIC MUSCOVITE-SCHIST	2.7	0.97	0.433	0.064	5.52	29	25	101	1	2	0.21	17
628	28.83	31.07	2.24	"	2.8	1.84	0.309	0.100	5.24	28	30	82	1	0	0.14	18
698	31.07	33.63	2.56	"	3.1	4.16	0.338	0.196	5.36	28	20	103	2	4	0.19	25
699	33.63	38.25	4.62	MUSCOVITE-QUARTZ-SCHIST	2.7	1.27	0.328	0.062	4.10	22	53	106	0	0	0.47	38
700	38.25	38.90	0.65	QUARTZ VEIN	-	0.89	0.093	0.050	1.54	11	21	28	1	0	0.21	184
701	38.90	46.27	7.37	GRAPHITIC MUSCOVITE-SCHIST	2.9	2.38	0.319	0.151	3.90	27	49	1393	1	0	0.65	585
702	46.27	52.80	6.53	MICACEOUS QUARTZITE	2.6	2.02	0.167	0.098	3.15	8	13	40	1	1	0.07	15
703	52.80	58.45	5.65	MICACEOUS QUARTZITE AND GRAPHITIC SCHIST	2.7	2.03	0.290	0.095	4.43	22	22	67	0	2	0.09	11
704	58.45	65.08	6.63	"	2.5	1.32	0.193	0.063	2.70	9	20	26	1	6	0.07	4
705	65.08	70.18	5.10	"	2.7	1.75	0.225	0.082	2.76	11	18	78	2	0	0.07	32
706	70.18	72.64	2.46	MUSCOVITE-SCHIST	2.9	3.64	0.364	0.127	4.23	33	72	35	0	4	1.79	9
707	72.64	73.53	0.89	MICACEOUS QUARTZITE	2.7	6.93	0.288	0.110	3.86	28	15	101	1	0	0.73	26
708	73.53	77.04	3.51	GRAPHITIC MUSCOVITE-QUARTZ-SCHIST	2.7	1.19	0.405	0.041	5.24	41	72	711	0	0	1.03	601
709	77.04	79.15	2.11	"	2.8	2.02	0.367	0.060	4.46	28	39	82	0	1	0.39	25
710	79.15	80.00	0.85	LIMESTONE	2.7	10.25	0.173	0.246	4.52	9	12	51	0	2	0.21	24
711	80.00	80.90	0.90	GRAPHITIC MUSCOVITE-SCHIST	-	2.67	0.356	0.076	3.92	23	30	134	0	6	0.50	38
712	80.90	82.63	1.73	SPARSELY MICACEOUS QUARTZITE	2.7	0.77	0.178	0.024	3.04	21	45	432	2	0	0.09	19
713	82.63	84.85	2.22	GRAPHITIC MUSCOVITE-SCHIST	2.8	0.99	0.372	0.035	5.29	43	74	943	2	0	1.59	801
714	84.85	86.80	1.95	MUSCOVITE-QUARTZ-SCHIST	3.0	3.79	0.375	0.125	4.14	34	59	710	0	0	2.44	44
715	86.80	91.30	4.50	GRAPHITIC MUSCOVITE-SCHIST	2.7	1.77	0.400	0.065	4.26	37	53	866	1	3	1.83	652
716	91.30	93.80	2.50	"	2.8	1.45	0.393	0.045	4.77	36	73	1312	1	0	1.21	223
717	93.80	95.18	1.38	BIOTITIC MUSCOVITE-QUARTZ-SCHIST	2.9	4.27	0.348	0.151	3.73	27	70	566	3	0	2.34	405
718	95.18	100.70	5.52	GRAPHITIC MUSCOVITE-SCHIST	2.8	0.91	0.391	0.057	3.66	28	50	1990	3	3	0.94	1227
719	100.70	102.02	1.32	QUARTZ-MICA-SCHIST AND QUARTZITE	2.7	1.27	0.332	0.067	3.78	23	30	52	0	0	0.50	27
720	102.02	102.80	0.78	GRAPHITIC MUSCOVITE-SCHIST	-	2.78	0.335	0.123	3.99	28	38	61	0	4	0.68	25
721	102.80	104.31	1.49	QUARTZ-CELSIAN-ROCK	3.0	0.57	0.225	0.046	4.74	61	215	5800	8	2	13.43	455
722	104.31	105.21	0.90	"	2.8	1.35	0.315	0.188	2.20	29	22	357	3	1	12.34	176
723	105.21	105.74	0.53	"	-	0.69	0.232	0.069	3.84	32	83	3200	7	0	12.08	1700
724	105.74	110.60	4.86	MUSCOVITE-SCHIST	2.8	4.99	0.321	0.115	4.26	29	32	266	0	0	1.41	32
725	110.60	114.29	3.69	"	2.8	6.81	0.294	0.109	4.21	28	26	37	2	5	1.32	26
726	114.29	116.30	2.01	CHLORITE-MUSCOVITE-SCHIST	2.9	4.90	0.309	0.121	3.77	26	32	182	0	0	1.82	154
727	116.30	118.24	1.94	GRAPHITIC MUSCOVITE-SCHIST AND LIMESTONE	2.8	1.16	0.397	0.042	3.98	20	37	354	0	0	0.38	61
728	118.24	121.14	2.90	"	2.8	1.99	0.336	0.062	4.79	32	65	1240	2	0	1.81	639
729	121.14	124.13	2.99	"	2.8	3.79	0.299	0.104	4.47	28	71	1314	4	0	1.82	986
730	124.13	126.22	2.09	"	2.8	4.33	0.329	0.110	4.55	34	81	868	2	0	2.36	370
731	126.22	128.70	2.48	GRAPHITIC MUSCOVITE-SCHIST	2.9	3.28	0.390	0.082	4.04	37	62	874	3	0	3.68	886
732	128.70	131.25	2.55	"	3.3	1.44	0.305	0.057	4.67	48	37	1302	8	0	12.81	2659
733	131.25	133.14	1.89	"	2.8	3.72	0.366	0.090	4.15	38	62	798	4	0	3.70	151
734	133.14	136.05	2.91	"	2.8	2.33	0.285	0.065	3.82	34	47	3125	5	0	3.34	2077
735	136.05	136.73	0.68	"	2.8	3.18	0.319	0.099	3.30	31	34	1425	6	0	6.05	1461
736	136.73	137.49	0.76	LAMPROPHYRE	-	2.02	0.851	0.055	7.30	63	22	88	0	3	0.15	35
737	137.49	141.75	4.26	GRAPHITIC QUARTZ-MUSCOVITE-SCHIST	2.8	2.16	0.305	0.069	3.34	46	36	2743	6	0	9.15	2154
738	141.75	146.18	4.43	"	3.0	1.76	0.301	0.078	3.01	36	48	1702	8	0	11.68	894
739	146.18	151.59	5.41	BIOTITE-CHLORITE-QUARTZ-SCHIST	2.8	4.21	0.462	0.086	5.60	52	28	96	0	0	0.26	21
740	151.59	153.85	2.26	GRAPHITIC MUSCOVITE-QUARTZ-SCHIST	2.9	6.27	0.327	0.116	3.95	28	28	54	1	7	0.70	33
741	153.85	154.63	0.78	MUSCOVITE-CHLORITE-SCHIST	-	2.04	0.332	0.067	4.77	41	80	128	2	1	1.29	46
742	154.63	155.03	0.40	GRAPHITIC MUSCOVITE-QUARTZ-SCHIST	2.7	1.27	0.329	0.050	5.53	51	112	167	1	0	0.38	45
743	155.03	159.82	4.79	CHLORITE-MICA-SCHIST	2.7	1.45	0.425	0.074	6.10	54	14	221	0	1	0.35	37
744	159.82	162.44	2.62	"	2.7	0.92	0.449	0.054	6.13	53	24	204	1	3	0.36	25
745	162.44	165.60	3.16	"	2.8	1.94	0.391	0.081	5.36	54	17	183	1	5	0.27	142
746	165.60	168.42	2.82	CALCAREOUS HORNBLende-SCHIST	2.8	3.19	0.350	0.085	5.08	37	0	103	3	2	1.12	21

APPENDIX II      TABLE IX      BOREHOLE 9  
 =====

SAMPLE CYD NO.	FROM M	TO M	INTER- SECTION M	GENERALISED LITHOLOGY	SP.GR.	CA	TI	MN	FE	NI	CU	ZN	AG	SB	BA	PB
						%	%	%	%	PPM	PPM	PPM	PPM	PPM	%	PPM
570	3.50	6.19	2.69	CALCAREOUS MUSCOVITE-BIOTITE-SCHIST	2.7	4.10	0.362	0.067	5.13	33	9	99	0	2	0.15	6
571	6.19	8.32	2.13	"	2.7	6.07	0.338	0.089	4.91	38	5	71	0	0	0.32	4
572	8.32	11.28	2.96	"	2.6	5.76	0.312	0.092	4.57	31	17	60	0	1	0.34	5
573	11.28	14.12	2.84	MUSCOVITE-DOLOMITE-SCHIST	2.8	5.16	0.374	0.105	3.95	29	59	19	0	1	0.97	3
574	14.12	16.50	2.38	"	2.8	5.28	0.444	0.107	4.53	46	63	22	0	3	1.47	0
575	16.50	17.69	1.19	DOLOMITE-QUARTZ-ROCK	-	9.66	0.268	0.239	3.20	20	45	227	0	6	0.80	7
576	17.69	20.03	2.34	GRAPHITIC MUSCOVITE-SCHIST	2.8	0.87	0.339	0.068	3.34	20	76	381	0	4	3.43	451
577	20.03	22.50	2.47	QUARTZ-CELSIAN-ROCK	3.2	0.06	0.294	0.009	2.85	21	58	809	0	0	17.23	598
578	22.50	23.59	1.09	BARYTE-ROCK	4.2	0.01	0.130	0.010	0.10	13	1	84	0	1	51.43	122
579	23.59	25.03	1.44	"	4.6	0.01	0.125	0.009	0.14	11	1	151	0	1	52.64	95
580	25.03	26.60	1.57	"	4.3	0.01	0.168	0.009	0.85	15	1	134	0	0	42.46	675
581	26.60	28.35	1.75	QUARTZ-CELSIAN-ROCK	2.9	0.11	0.207	0.008	3.24	25	25	3100	0	0	10.15	2074
582	28.35	29.14	0.79	MUSCOVITE-QUARTZ-CELSIAN-SCHIST	2.8	0.10	0.303	0.015	1.85	67	84	14000	0	9	7.23	4737
583	29.14	31.52	2.38	GRAPHITIC MUSCOVITE-SCHIST AND DOLOMITE	2.7	0.07	0.385	0.017	3.19	52	75	5700	0	0	1.62	1981
584	31.52	35.18	3.66	"	2.8	1.32	0.397	0.208	4.57	33	50	571	0	1	0.69	62
585	35.18	37.31	2.13	"	2.9	5.23	0.253	0.462	3.78	20	20	533	0	5	0.37	326
586	37.31	38.17	0.86	CALCAREOUS MUSCOVITE-SCHIST	2.8	3.54	0.369	0.307	4.07	31	32	780	0	2	0.38	39
587	38.17	42.79	4.62	CALCAREOUS CHLORITE-SCHIST	2.9	6.06	1.008	0.142	8.54	39	33	154	0	0	0.05	31
588	42.79	45.23	2.44	MUSCOVITE-DOLOMITE-CHLORITE-SCHIST	2.8	5.98	0.888	0.241	6.66	31	40	115	0	2	0.19	28
589	45.23	47.61	2.38	DOLOMITIC MUSCOVITE-SCHIST	2.8	1.23	0.401	0.138	3.22	23	37	413	0	1	0.52	575
590	47.61	48.49	0.88	SPHALERITIC AND PYRITIC DOLOMITE	2.9	8.74	0.265	0.731	5.33	20	28	8000	0	3	0.34	2318
591	48.49	53.45	4.96	METABASITE	2.8	6.09	1.031	0.133	9.00	41	52	180	0	0	0.06	45
592	53.45	54.89	1.44	DOLOMITIC MUSCOVITE-SCHIST	2.9	4.18	0.541	0.219	4.26	21	41	702	0	2	0.73	532
593	54.89	56.58	1.69	"	2.8	1.96	0.252	0.167	2.84	21	24	13800	0	3	0.48	3010
594	56.58	56.95	0.37	DOLOMITIC AND SPHALERITIC LIMESTONE	-	9.63	0.086	0.822	4.72	23	37	29200	0	8	0.10	6773
595	56.95	59.78	2.83	DOLOMITIC MUSCOVITE-SCHIST	2.9	1.49	0.384	0.129	3.37	32	51	2212	0	0	0.37	1456
596	59.78	63.00	3.22	GRAPHITIC MUSCOVITE-SCHIST	3.0	3.25	0.347	0.230	3.47	25	32	1879	0	3	0.32	811
597	63.00	66.09	3.09	"	3.0	4.84	0.280	0.223	3.52	25	35	1585	0	0	0.32	803
598	66.09	67.60	1.51	"	2.8	4.58	0.218	0.216	2.96	14	16	355	0	5	0.34	320
599	67.60	71.62	4.02	GRAPHITIC AND DOLOMITIC MUSCOVITE-SCHIST	3.0	3.39	0.360	0.185	4.11	24	44	282	0	0	0.96	242
600	71.62	73.60	1.98	QUARTZ-CELSIAN-DOLOMITE-ROCKS	3.2	2.45	0.169	0.496	4.56	20	10	1558	0	0	11.65	1050
601	73.60	74.58	0.98	QUARTZ-CELSIAN-ROCK	3.0	3.48	0.423	0.609	7.51	30	94	599	0	1	9.77	450
602	74.58	76.07	1.49	CELSIAN-QUARTZ-ROCK AND LIMESTONE	3.1	4.68	0.195	0.557	4.13	24	15	827	0	0	14.17	360
603	76.07	76.32	0.25	MASSIVE PYRRHOTINE	-	0.80	0.053	0.141	28.39	75	192	337	0	0	4.43	1159
604	76.32	78.37	2.05	QUARTZITE AND QUARTZ-CELSIAN-ROCK	3.0	4.66	0.072	0.659	5.84	9	14	2534	0	3	4.85	1272
605	78.37	81.80	3.43	MUSCOVITE-SCHIST MODERATELY GRAPHITIC	2.9	1.12	0.332	0.130	4.77	26	53	5700	0	7	1.19	2695
606	81.80	84.77	2.97	"	2.8	0.30	0.385	0.031	3.16	23	52	1738	0	5	0.66	1213
607	84.77	87.56	2.79	"	2.8	0.96	0.378	0.120	3.36	28	50	876	0	5	0.39	1198
608	87.56	90.53	2.97	"	-	2.32	0.364	0.180	4.14	23	38	626	0	4	0.18	261
609	90.53	92.54	2.01	GRAPHITIC MUSCOVITE-SCHIST	-	3.68	0.350	0.224	5.40	27	41	441	0	0	0.08	122
610	92.54	95.54	3.00	"	-	1.28	0.387	0.130	6.09	29	36	640	0	2	0.10	89
611	95.54	97.97	2.43	"	-	1.20	0.373	0.119	6.39	29	43	374	0	2	0.09	87
612	97.97	100.46	2.51	"	-	0.43	0.450	0.071	6.48	30	36	272	0	1	0.12	62

APPENDIX II      TABLE X      BOREHOLE 10  
 \*\*\*\*\*      \*\*\*\*\*      \*\*\*\*\*

SAMPLE CYD NO.	FROM M	TO M	INTER- SECTION M	GENERALISED LITHOLOGY	SP. GR.	CA %	TI %	MN %	FE %	NI PPM	CU PPM	ZN PPM	AG PPM	SR PPM	BA %	PB PPM
629	3.05	5.75	2.70	MUSCOVITE-SCHIST	-	0.04	0.424	0.028	3.51	30	61	368	1	0	1.22	7
630	5.75	8.14	2.39	GRAPHITIC MUSCOVITE-SCHIST	-	1.17	0.377	0.096	4.41	35	79	315	1	0	1.43	108
631	8.14	10.08	1.94	"	-	1.44	0.364	0.115	3.82	32	72	389	2	0	1.56	184
632	10.08	11.35	1.27	"	-	1.84	0.342	0.193	3.86	37	46	330	3	0	3.64	328
633	11.35	12.88	1.53	MUSCOVITE-QUARTZ-SCHIST	3.0	2.00	0.423	0.175	3.91	36	50	252	4	0	9.73	283
634	12.88	13.79	0.91	MUSCOVITE-SCHIST AND QUARTZ-CELSIAN-ROCK	3.4	1.80	0.561	0.135	3.69	37	55	256	4	0	8.93	110
635	13.79	15.74	1.95	CALCAREOUS BIOTITE-SCHIST	2.9	5.50	0.924	0.135	7.75	43	38	173	2	0	1.88	12
636	15.74	16.70	0.96	MUSCOVITE-QUARTZ-SCHIST	2.8	2.56	0.465	0.338	5.95	47	84	554	4	0	3.78	167
637	16.70	17.12	0.42	"	2.9	5.10	0.940	0.152	7.54	41	80	256	1	3	3.13	19
638	17.12	17.46	0.34	"	-	5.76	0.839	0.493	6.02	28	40	124	2	0	1.80	18
639	17.46	18.98	1.52	CALCAREOUS BIOTITE-SCHIST	2.9	5.89	0.900	0.129	7.40	38	40	174	0	0	2.03	17
640	18.98	19.66	0.68	MUSCOVITE-CHLORITE-SCHIST	2.9	1.85	0.595	0.163	7.32	38	82	5320	3	3	3.12	538
641	19.66	20.45	0.79	GRAPHITIC MUSCOVITE-SCHIST	2.8	0.11	0.421	0.010	3.52	23	40	650	4	1	1.56	2823
642	20.45	22.13	1.68	MUSCOVITE-QUARTZ-SCHIST	2.8	0.11	0.375	0.011	3.52	26	49	932	2	0	2.73	1354
643	22.13	24.10	1.97	CALCAREOUS BIOTITE-SCHIST	3.0	5.38	0.891	0.152	6.49	34	39	159	1	1	4.22	21
644	24.10	26.68	2.58	"	2.9	5.28	0.956	0.125	7.80	46	38	139	2	0	2.48	15
645	26.68	27.04	0.36	QUARTZ-CELSIAN-ROCK	2.8	2.30	0.550	0.113	3.28	32	40	538	5	0	19.21	340
646	27.04	27.36	0.32	MUSCOVITE-QUARTZ-SCHIST	-	0.22	0.425	0.012	3.11	27	49	703	4	0	6.63	471
647	27.36	29.52	2.16	GRAPHITIC-MUSCOVITE-SCHIST	2.8	0.88	0.387	0.128	3.54	25	42	1090	1	4	0.36	648
648	29.52	31.24	1.72	"	2.9	0.90	0.422	0.137	4.41	37	59	419	1	8	0.47	133
649	31.24	33.25	3.01	"	2.6	3.09	0.341	0.361	4.07	27	37	527	3	4	0.67	178
650	33.25	36.52	3.27	MUSCOVITE-CHLORITE-SCHIST	2.9	3.09	0.319	0.375	5.27	36	46	284	1	1	0.85	103
651	36.52	39.45	2.93	GRAPHITIC MUSCOVITE-SCHIST	2.9	1.19	0.386	0.169	4.66	32	57	217	2	5	0.53	29
652	39.45	41.70	2.25	"	2.8	1.06	0.400	0.094	4.22	31	43	166	2	2	0.30	30
653	41.70	43.45	1.75	"	2.8	1.59	0.418	0.111	5.20	36	46	115	1	3	0.28	26
654	43.45	43.64	0.19	QUARTZ-BIOTITE-SCHIST	-	0.17	0.443	0.035	7.20	42	52	167	0	0	0.18	21
655	43.64	47.97	4.33	QUARTZITE AND GRAPHITIC SCHIST	2.8	0.49	0.421	0.052	4.99	28	30	131	1	0	0.18	24
656	47.97	52.04	4.07	MICACEOUS QUARTZITE	2.7	0.96	0.374	0.086	5.06	21	16	131	0	8	0.18	19
657	52.04	56.77	4.73	GRAPHITIC MUSCOVITE-SCHIST	2.8	0.44	0.490	0.068	6.21	35	35	192	3	0	0.13	41
658	56.77	60.46	3.69	"	2.7	0.57	0.493	0.066	5.99	37	35	170	2	3	0.14	56
659	60.46	61.21	0.75	QUARTZITE	2.6	1.01	0.426	0.090	4.97	20	20	124	1	1	0.08	41
660	61.21	61.86	0.65	GRAPHITIC MUSCOVITE-SCHIST	2.7	0.33	0.482	0.059	6.09	42	40	177	1	0	0.13	48
661	61.86	63.09	1.23	QUARTZITE	2.6	0.33	0.398	0.046	4.79	24	35	89	0	1	0.08	35
662	63.09	63.95	0.86	GRAPHITIC MUSCOVITE-SCHIST	2.5	0.27	0.472	0.058	5.86	41	56	123	0	2	0.12	43
663	63.95	64.48	0.53	QUARTZITE	2.8	1.55	0.237	0.132	3.78	12	19	40	1	5	0.39	23
664	64.48	66.72	2.24	GRAPHITIC MUSCOVITE-SCHIST	2.7	0.54	0.479	0.079	5.75	30	28	158	1	2	0.11	43
665	66.72	68.83	2.11	QUARTZITE	2.6	0.60	0.443	0.078	5.23	32	37	152	2	0	0.09	43
666	68.83	69.31	0.48	LIMESTONE	2.6	8.23	0.208	0.646	5.38	12	5	516	1	3	0.06	47
667	69.31	72.10	2.79	GARNET-MICA-SCHIST	2.9	0.81	0.490	0.099	5.65	36	37	208	0	0	0.12	52
668	72.10	72.96	0.86	QUARTZITE	2.7	1.09	0.276	0.112	3.52	16	19	532	1	1	0.05	34
669	72.96	74.45	1.47	GARNET-MICA-SCHIST	2.7	0.35	0.485	0.100	6.15	31	28	276	2	6	0.14	49
670	74.45	76.26	1.83	QUARTZITE	2.6	0.84	0.382	0.133	4.59	23	31	993	1	4	0.14	50
671	76.26	76.69	0.43	"	2.6	1.60	0.238	0.196	2.54	12	18	2560	0	6	0.11	1325
672	76.69	77.30	0.61	GRAPHITIC MUSCOVITE-SCHIST	-	0.39	0.466	0.059	2.64	12	14	471	2	5	0.28	318
673	77.30	77.79	0.49	QUARTZITE	2.8	2.65	0.225	0.279	2.84	6	7	1093	0	0	0.10	6100
674	77.79	80.63	2.84	"	2.5	1.93	0.333	0.145	4.17	23	27	332	1	3	0.15	224
675	80.63	83.15	2.52	DOLOMITIC QUARTZITE	2.5	1.51	0.149	0.110	1.52	0	5	39	0	8	0.02	84
676	83.15	83.98	0.83	GRAPHITIC MUSCOVITE-SCHIST	2.7	1.99	0.451	0.163	4.13	31	40	70	2	4	0.11	198
677	83.98	85.36	1.38	QUARTZITE	2.7	2.54	0.289	0.197	3.62	17	23	54	1	6	0.06	50
678	85.36	87.30	1.94	GRAPHITIC MUSCOVITE-SCHIST	3.0	1.49	0.428	0.135	4.20	30	36	283	2	6	0.11	164
679	87.30	89.58	2.28	QUARTZITE	2.6	1.66	0.319	0.130	4.04	29	28	612	2	0	0.09	666
680	89.58	91.38	1.80	GRAPHITIC QUARTZ-MICA-SCHIST	2.9	0.70	0.442	0.073	6.28	37	46	346	0	4	0.07	51
681	91.38	95.94	4.56	QUARTZITE	2.6	0.86	0.316	0.064	3.88	22	36	967	1	1	0.07	70
682	95.94	98.06	2.12	GRAPHITIC MUSCOVITE-SCHIST	2.6	1.00	0.408	0.097	3.98	25	37	393	1	1	0.07	265
683	98.06	104.32	6.26	QUARTZITE	2.6	1.23	0.345	0.116	3.17	16	23	2034	0	3	0.07	579
684	104.32	108.26	3.94	GRAPHITIC MUSCOVITE-SCHIST	2.6	1.47	0.405	0.150	4.69	29	43	701	0	0	0.11	404
685	108.26	108.54	0.28	LIMESTONE	-	12.61	0.129	0.785	5.21	9	8	341	1	0	0.04	887
686	108.54	111.34	2.80	QUARTZITE	2.6	1.76	0.319	0.159	3.75	20	35	1718	2	3	0.09	1186
687	111.34	114.14	2.80	GRAPHITIC MUSCOVITE-SCHIST	2.5	1.08	0.393	0.105	4.68	29	37	1806	2	5	0.12	785
688	114.14	117.18	3.04	"	2.6	1.38	0.374	0.133	5.63	36	44	360	1	5	0.12	159
689	117.18	120.53	3.35	"	2.5	1.25	0.401	0.120	5.77	44	44	513	1	2	0.15	642
690	120.53	121.56	1.03	"	2.8	1.54	0.459	0.152	5.21	34	45	2121	2	2	0.07	527
691	121.56	125.75	4.19	GRAPHITIC QUARTZ-MUSCOVITE-SCHIST	2.7	0.99	0.424	0.104	4.78	30	44	525	2	4	0.06	161
692	125.75	126.49	0.74	QUARTZITE	2.5	0.80	0.198	0.069	2.32	14	27	360	0	0	0.03	269
693	126.49	128.36	1.87	GRAPHITIC QUARTZ-MUSCOVITE-SCHIST	2.8	0.69	0.512	0.079	4.13	22	29	340	2	2	0.09	98
694	128.36	130.04	1.68	MICACEOUS QUARTZITE	2.6	1.67	0.273	0.148	3.68	16	27	818	0	7	0.04	180
695	130.04	131.38	1.34	GRAPHITIC MUSCOVITE-SCHIST	2.7	0.30	0.451	0.064	7.34	43	38	260	0	4	0.12	64
696	131.38	134.85	3.47	GRAPHITIC QUARTZ-MUSCOVITE-SCHIST	2.8	2.02	0.352	0.170	4.31	22	35	1401	2	0	0.55	628
697	134.85	136.25	1.40	LIMESTONE	2.9	8.67	0.194	0.311	4.66	17	16	1581	2	7	0.13	294

APPENDIX II      TABLE XI      BOREHOLE 11  
 \*\*\*\*\*      \*\*\*\*\*      \*\*\*\*\*

SAMPLE CYD NO.	FROM M	TO M	INTER- SECTION M	GENERALISED LITHOLOGY	SP.GR.	CA %	TI %	MN %	FE %	NI PPM	CU PPM	ZN PPM	AG PPM	SB PPM	BA %	PB PPM
747	22.81	24.13	1.32	DOLOMITIC MICA-SCHIST	2.6	3.66	0.318	0.080	3.11	17	41	71	1	8	0.59	36
748	24.13	28.33	4.20	QUARTZ-CELSIAN-ROCK	2.7	1.25	0.208	0.037	1.30	5	46	5	5	0	11.01	16
749	28.33	30.08	1.75	LIMESTONE	2.8	4.95	0.286	0.126	3.64	19	46	24	4	1	3.22	19
750	30.08	35.53	5.45	CELSIAN-QUARTZ-ROCK	2.7	1.35	0.240	0.045	1.10	10	12	5	9	0	12.08	18
751	35.53	36.46	0.93	DOLOMITIC LIMESTONE	2.8	4.46	0.294	0.151	1.83	6	12	36	8	0	11.33	150
752	36.46	38.45	1.99	CELSIAN-QUARTZ-ROCK	2.7	2.06	0.205	0.074	1.43	6	21	519	8	0	10.89	1184
753	38.45	39.38	0.93	GRAPHITIC MUSCOVITE-SCHIST	2.6	3.92	0.430	0.124	3.88	31	47	32	3	0	3.48	14
754	39.38	41.30	1.92	QUARTZITE	2.6	1.90	0.224	0.051	2.14	4	22	14	0	3	0.28	14
755	41.30	46.44	5.14	GRAPHITIC MUSCOVITE-SCHIST	2.7	3.21	0.443	0.109	4.47	24	47	39	2	1	1.90	14
756	46.44	49.17	2.73	MICACEOUS QUARTZITE	2.9	2.53	0.204	0.059	1.69	6	30	37	2	0	3.75	11
757	49.17	50.64	1.47	GRAPHITIC QUARTZ-MUSCOVITE-SCHIST	2.7	3.74	0.359	0.103	3.89	19	42	141	1	1	1.19	11
758	50.64	54.80	4.16	CALCAREOUS CHLORITE-MICA-SCHIST	2.7	2.91	0.461	0.094	5.56	33	31	91	2	4	0.20	6
759	54.80	57.70	2.90	"	2.7	1.65	0.452	0.067	6.14	35	63	101	0	0	0.54	12
760	57.70	58.40	0.70	CALCAREOUS MUSCOVITE-QUARTZ-SCHIST	2.9	4.32	0.344	0.154	4.28	16	54	26	1	0	1.10	9
761	58.40	60.00	1.60	CALCAREOUS MICA-QUARTZ-SCHIST	2.8	1.21	0.470	0.061	5.15	31	64	78	1	2	1.32	9
762	60.00	62.85	2.85	QUARTZ-MICA-CHLORITE-SCHIST	2.6	3.08	0.403	0.114	5.43	33	38	115	1	3	0.68	11
763	62.85	65.10	2.25	CALCAREOUS QUARTZ-MICA-SCHIST	2.7	5.34	0.288	0.102	3.15	13	31	21	2	0	1.84	9
764	65.10	68.37	3.27	MUSCOVITE-QUARTZ-SCHIST	2.7	4.63	0.330	0.105	3.39	17	51	30	2	0	2.73	11
765	68.37	69.70	1.33	QUARTZ-MUSCOVITE-SCHIST	2.8	4.88	0.417	0.100	3.49	27	61	14	3	0	3.57	7
766	69.70	70.25	0.55	CALCAREOUS BIOTITE-QUARTZ-SCHIST	2.8	4.65	0.860	0.110	7.14	51	84	71	2	0	1.19	17
767	70.25	75.45	5.20	CALCAREOUS MICA-QUARTZ-SCHIST	2.7	4.20	0.351	0.078	4.62	41	70	57	0	0	0.51	9
768	75.45	75.91	0.46	CALCAREOUS QUARTZITE	3.0	4.81	0.246	0.087	3.91	63	211	22	1	2	0.28	6
769	75.91	82.50	6.59	QUARTZ-MICA-SCHIST	2.7	3.57	0.341	0.065	4.41	30	62	45	2	6	0.37	7
770	82.50	90.38	7.88	"	2.7	4.50	0.330	0.075	4.68	29	57	39	2	0	0.24	1
771	90.38	95.15	4.77	CHLORITE-MICA-QUARTZ-SCHIST	2.7	3.15	0.364	0.055	5.19	28	22	55	0	2	0.22	5
772	95.15	95.98	0.83	QUARTZITE	2.8	4.65	0.295	0.067	4.50	32	39	38	1	0	0.20	9
773	95.98	97.44	1.46	CHLORITE-MICA-SCHIST	2.7	2.49	0.388	0.052	5.72	37	23	56	0	3	0.42	6
774	97.44	98.06	0.62	QUARTZITE	2.8	5.11	0.274	0.075	4.22	17	14	30	2	2	0.13	6
775	98.06	103.68	5.62	CHLORITE-SCHIST AND QUARTZITE	2.7	3.29	0.380	0.059	4.91	25	29	45	0	0	0.33	9
776	103.68	110.60	6.92	"	2.8	3.37	0.376	0.069	5.13	28	39	146	2	8	0.68	26
777	110.60	111.33	0.73	MICA-QUARTZ-DOLOMITE-SCHIST	2.8	4.80	0.335	0.091	4.43	30	18	76	2	1	1.90	20
778	111.33	113.07	1.74	QUARTZITE	2.8	3.57	0.124	0.101	4.10	5	99	2706	2	3	0.50	2651
779	113.07	115.03	1.96	GRAPHITIC MUSCOVITE-SCHIST	2.8	2.47	0.289	0.139	2.86	22	56	3791	3	0	2.51	3665
780	115.03	117.13	2.10	QUARTZ-CELSIAN-ROCK	3.1	1.67	0.104	0.106	8.12	16	135	7156	15	6	6.89	3422
781	117.13	118.06	0.93	CELSIAN-DOLOMITE-ROCK	3.2	4.62	0.211	0.409	4.87	38	140	11180	24	10	12.12	9330
782	118.06	120.42	2.36	DOLOMITIC QUARTZITE	3.1	1.11	0.176	0.055	2.33	11	59	3146	4	1	2.23	2684
783	120.42	122.82	2.40	GRAPHITIC QUARTZ-MUSCOVITE-SCHIST	2.9	1.21	0.362	0.099	3.28	24	65	2091	2	0	2.12	1257
784	122.82	123.21	0.39	MICACEOUS QUARTZITE	2.8	1.96	0.183	0.155	2.91	14	57	2278	3	0	3.44	2036
785	123.21	126.37	3.16	QUARTZ-CELSIAN-ROCK	2.9	1.33	0.270	0.134	2.94	32	72	2078	9	0	10.53	1623
786	126.37	126.92	0.55	MICACEOUS QUARTZITE	2.8	3.12	0.207	0.134	2.79	14	48	2006	2	2	1.38	1618
787	126.92	129.11	2.19	GRAPHITIC QUARTZ-MUSCOVITE-SCHIST	2.7	3.27	0.334	0.212	3.91	25	58	585	3	0	0.88	628
788	129.11	129.90	0.79	MUSCOVITE-SCHIST AND LIMESTONE	3.0	3.00	0.307	0.229	2.63	22	48	2370	4	2	4.94	1175
789	129.90	131.12	1.22	CELSIAN-QUARTZ-ROCK	3.0	2.38	0.146	0.329	1.58	15	9	1543	13	4	21.00	822
790	131.12	132.60	1.48	GRAPHITIC MUSCOVITE-SCHIST	2.8	0.35	0.327	0.021	2.22	24	46	3083	2	1	2.44	1260
791	132.60	133.75	1.15	QUARTZ-CELSIAN-ROCK	3.0	1.61	0.199	0.132	2.05	15	44	3787	7	1	7.62	1037
792	133.75	136.36	2.61	"	2.9	3.05	0.117	0.229	2.21	8	22	157	7	0	8.55	104
793	136.36	137.17	0.81	DOLOMITIC QUARTZITE	2.7	1.55	0.160	0.095	2.77	11	121	167	2	0	2.68	163
794	137.17	138.18	1.01	GRAPHITIC MUSCOVITE-SCHIST	3.2	3.47	0.272	0.186	3.60	29	53	813	3	7	3.29	272
795	138.18	140.00	1.82	SERICITE-DOLOMITE-QUARTZ-SCHIST	3.2	3.33	0.313	0.133	3.20	30	81	53	6	0	7.51	24
796	140.00	140.90	0.90	QUARTZ-CELSIAN-ROCK	2.8	4.04	0.294	0.101	3.44	23	130	481	3	0	7.41	44
797	140.90	142.87	1.97	"	3.1	5.01	0.254	0.483	1.97	23	20	2124	14	0	15.80	1513
798	142.87	144.92	2.05	BARYTE-ROCK	4.2	1.81	0.089	0.151	2.02	8	75	11294	29	11	40.90	4092
799	144.92	145.67	0.75	GRAPHITIC MUSCOVITE-SCHIST	3.0	0.41	0.201	0.047	5.04	28	147	8470	5	10	1.77	4463
800	145.67	151.88	6.21	GRAPHITIC MUSCOVITE-QUARTZ-SCHIST	2.8	3.21	0.322	0.208	4.26	29	60	3735	1	9	0.48	1384
801	151.88	152.83	0.95	DOLOMITIC LIMESTONE AND QUARTZITE	2.9	7.21	0.182	0.374	4.70	29	55	4353	1	0	0.04	367
802	152.83	159.95	7.12	GRAPHITIC MUSCOVITE-QUARTZ-SCHIST	2.8	0.89	0.403	0.077	5.88	32	50	112	1	0	0.08	20
803	159.95	170.57	10.62	CHLORITIC AND GRAPHITIC MICA-SCHIST	2.8	0.67	0.434	0.083	6.45	36	52	176	1	0	0.06	33
804	170.57	174.90	4.33	MICA-QUARTZ-SCHIST	2.8	0.33	0.401	0.068	4.92	28	36	69	0	0	0.78	22

## APPENDIX III

the grid location of the outcrop and the polished thin section number. Other columns are as for Tables I to X.

### SUMMARY OF PETROGRAPHIC DATA

#### Introduction

Tables I to XI give petrographic data, in summary form, for polished thin sections from boreholes 1 to 11 (none were prepared for borehole 6) and for outcrop specimens (Table XI).

For Tables I to X the following notes apply:—

(a) In the first column "depth" refers to inclined depth measured from the borehole collar.

(b) The second column gives the number by which the polished thin sections are registered with the Applied Mineralogy Unit.

(c) The third column gives a rock name to each specimen. These are made as brief as possible, supplementary information being provided in the subsequent columns. Schists and amphibolites are taken as containing quartz, and this mineral is often omitted from names, e.g. "muscovite-schist" has muscovite dominant over quartz in the mode, but "quartz-muscovite-schist" has quartz dominant. Two-mica schists (muscovite and biotite present) are simply called "mica-schist". Most baryte-bearing rocks have baryte greatly in excess of other phases, and are simply called "baryte-rock". Celsian-bearing rocks present a problem since the terms arkose and meta-arkose imply a detrital origin, which is probably not the case with these rocks. Rock names only refer to the sulphide and oxide content where dominant. In general these minerals form less than 20%, and to refer to them would proliferate a confusing and unwieldy nomenclature.

(d) Columns four and five refer respectively to major and minor/accessory mineral constituents. They are generally in order of volumetric importance in column 4, but in column 5 this is not attempted. The abbreviations are as follows:—

Ab — albite	Hb — hornblende
Ap — apatite	Hm — hematite
Br — baryte	Hy — hyalophane
Bt — biotite	Im — ilmenite
Ca — calcite	Mc — marcasite
Ch — chlorite	Ms — muscovite
Cn — celsian	Mt — magnetite
Cp — chalcopyrite	Po — pyrrhotine
Ct — cymrite	Py — pyrite
Cv — covellite	Qz — quartz
Cy — clay (non-specific)	Ru — rutile
Do — dolomite	Se — sphene
Fem — Fe-oxides (non specific)	Sp — sphalerite
Fu — fuchsite	To — tourmaline
Ga — garnet (almandine)	Zc — zircon
Gl — galena	Zt — clinzoisite
Go — goethite	tr — trace amount
Gr — graphitic granules	only

Estimated volumes may be expressed as (>10%), (~3%), etc.

Relative volumes may be expressed as (Mt>G1≈Sp), etc.

(e) The sixth column gives brief comments intended to bring out textural and other features not implicit in the foregoing information.

(f) Some of the tables have footnotes giving the results of X-ray diffractometry, carried out by A.M. Shilston and D. Atkin.

In Table XI, for surface outcrop specimens, the field number (CYR 1 etc.) of the sample is given together with

APPENDIX III TABLE I BOREHOLE 1

Depth (m)	PTS No.	Rock Name	Mineral Constituents		Comments
			Major	Minor	
10.6	4080	Pyrite-celsian-baryte-band	Py Ch Br	Sp (~ 5%) Gl Do Ch	Coarse, granular matrix of pyrite and lesser sphalerite (total sulphide ~ 50%) with coarse celsian grains set in coarse, sub-poikilitic baryte and dolomite; minor fractures cemented by chlorite
13.2	4081	Baryte-rock	Br	Ch Bt(tr) Py (~ 4%) Sp Gl Cp	Coarse, mosaic textured rock from which quartz and carbonates are absent
14.6	4082	Baryte-rock	Br Py (~ 20%)	Do Ch(tr) Sp Gl	Coarse, mosaic textured rock from which quartz is notably absent
15.3	4083	Baryte-rock	Br Py (~ 10%)	Fu(tr) Ch(tr) Sp Gl	Coarse, mosaic textured rock from which quartz and carbonates are absent
16.8	4084	Baryte-rock	Br	Qs Do Fu Ch Ru(tr) Mt Py Po(tr) Cp(tr)	Coarse, mosaic textured rock in which banding produces increase in the opaque content from a general level of < 1% to ~ 10%; the opaque constituents are dominated by magnetite
17.2	4085	Baryte-rock	Br Py (~ 8%)	Qs Do Ch Fu Sp Gl Cp	Coarse, mosaic textured rock with discontinuous hair veinlets of chlorite, crossed by a brecciated zone in which fragments of baryte, baryte plus quartz, sulphides etc. are set in a finer matrix of dolomite, baryte, quartz and chlorite
18.6	4086	Baryte-rock	Br	Qs Do Fu Ch Py Gl Sp Cp	Coarse, mosaic textured rock with disseminated quartz, fuchsite and sulphides; dolomite also occurs in hair veinlets; the opaque content is ~ 10% (Py > Gl > Sp and Cp)
20.5	4087	Banded baryte-rock	Br Qs (~ 30%)	Do Ch Py Sp	Baryte-rich bands poor in quartz and opaques alternate with opaque-rich quartzose bands poor in baryte
22.4	4088	Banded baryte-rock	Br Qs Py	Cn Ms Ch Sp Gl Cp	Coarse, mosaic textured baryte rock crossed by quartz band flanked by sulphide enriched band which contains celsian
25.2	4089	Baryte-rock	Br Qs Do	Fu Mt Py (< Mt) Cp(tr)	Coarse baryte-rock with disseminated quartz and dolomite; dolomite also occurs in irregular patches
25.9	4090	Baryte-rock	Br	Qs Do Fu Ch Py(tr)	
28.9	4091	Banded dolomite	Do Qs	Cn Ru Ch Py	Banding is expressed by rise in the quartz and/or celsian content; celsian occurs as branching, platy porphyroblasts
29.9	4092	Graphitic muscovite-schist	Qs Ms Ca	Cr Py Sp (~ 4%) Gl Cp(tr)	Calcareous black schist with an appreciable sulphide content (especially sphalerite); no discrete barian phase observed

Bulk-XRD examination (AMS) from borehole 1 -

2.85m - Quartz with celsian and dolomite possible with minor calcite

4.20m - Quartz and pyrite with celsian and dolomite



APPENDIX III TABLE II BOREHOLE 2

Depth (m)	PTS No.	Rock Name	Mineral Constituents		Comments
			Major	Minor	
1.7	3892	Baryte-rock	Br	Qs Ms Bt(tr) Py Sp Cl Cp(tr)	Coarse mosaic texture. Sulphides disseminated and concentrated in certain bands. Baryte content > 95% by volume
4.3	3893	Baryte-rock	Br	Qs Fu	Coarse mosaic texture. Fuchsite flakes are thinly disseminated. Pyrite and magnetite in comparable amounts; total opaque $\approx$ 1%
6.5	3894	Quartzite	Qs	Py Ms Fes	Massive fine quartzite with very minor sulphide and alteration products as dissemination and occasional hair veinlets
6.8	3895	Celsian-quartz rock	Cn Qs Fy	Ru Ms Sp(tr)	Massive, medium grained rock with $\sim$ 20% pyrite as dissemination modified by opaque-rich bands. The muscovite has a faint yellow body colour
7.5	3896	Celsian-quartz rock	Cn Qs Fy	Ru Do Hm(tr)	Similar to the 6.8m specimen; but finer, not banded and sparingly dolomitic
8.2	3897	Baryte-rock	Br	Qs Py( 3%) Sp Cl	Coarse mosaic texture with > 3% disseminated sulphides
10.5	3900	Baryte-rock	Br	Qs Ch Ms Mt Py	Coarse mosaic texture with disseminated opaque (mt > py) Rare, minute spots of chlorite (? pseudomorphs) are present
10.5	3899	Baryte-rock	Br Qs( 10%)	Ch Mt Gl Py	Coarse mosaic texture with disseminated opaque (mt > gl > py); brown chloritic spots present
10.7	3898	Baryte-rock	Br	Qs Ch Do Ms Mt Fy Gl Cp(tr)	Coarse mosaic texture crossed by layer of baryte-bearing fine-grained quartzite; magnetite is the dominant opaque constituent
11.8	3901	Baryte-rock	Br Qs	Ms Do Ch Fu Ru(tr) Fy Mt Cp Po	Coarse, mosaic textured rock in which banding is expressed largely by the opaque constituents
13.3	3902	Baryte-rock	Br	Qs Fu Fes Fy Mt	Coarse mosaic texture
13.5	3903	Sulphide-celsian rock	Py Sp Qs Cn	Ru(tr) Ch Fes Cl	Strongly banded rock in which bands with all combinations of the principal constituents occur
13.8	3904	Massive pyrite lens	Fy	Qs Cl Ca Br	Massive pyrite with enclosed subhedral quartz grains and corroded blades of part-calcified baryte
14.1	3905	Sulphide-rich celsian-bearing quartz-rock	Qs Sp Ca Ch	Cn Py Gl Cp	Coarse quartz with angular coarse patches of sphalerite, calcite, and chlorite (pseudomorphs)
14.4	3907	Sulphide-rich celsian-bearing quartz-rock	Qs Ca Fy	Ch Cy Cn Ru Br Cp	Quartzite in which poikiloblastic calcite and pyrite patches occur; chlorite, a probable clay-mineral and minor feldspar (possibly barian) are present; baryte occurs in hair cross veinlets
14.6	3906	Sulphide-rich celsian-bearing quartz-rock	Qs Ca Fy	Ch Cn Br Cp(tr)	Similar to the preceding specimen, but here celsian and baryte co-exist; chlorite replacement of pyrite and replacement of baryte by chlorite and dolomite are seen
15.7	3908	Graphitic quartz muscovite-schist	Qs Ms	Fy Sp Gl(tr) Br Ru Ca Gr	Cremulate lamination with sulphides and baryte in conforming laminae, and introduced veinlets with pyrite and calcite

Bulk-XRD examination (AMS) of sample at 7.45m from borehole 2: celsian with lesser quartz

APPENDIX III TABLE III BOREHOLE 3

Depth (m)	PTS No.	Rock Name	Mineral Constituents		Comments
			Major	Minor	
3.6	3957	Dark grey dolomite	Do	Qz Ms Fem Sp Cl Po Mc	Represents grey, massive bands within black schist intersection; the mica and quartzose laminae reflect refolded banding parallel to that of the schist
19.6	3958	Dolomitic sulphide-rich breccia	Do Qz Cn Po Sp	Ch Ru Cp Gl	Dolomite, quartz and celsian occur in coarse fragments set in a quartz-sulphide matrix. Pyrite is largely replaced by coarsely crystalline pyrite. Pyrrhotine mantles colloform quartz patches, but appears not to replace them significantly
21.0	3959	Banded dolomite	Do	Ch Cn Po Py Cp Mc	Crude banding in granular, mosaic-textured dolomite
22.2	3960	Sulphide-rich breccia	Do Cn Py	Ch Ru Mc Cp Py	Fragments of dolomite and apple green celsian set in sulphide-rich matrix
23.3	3961	Celsian-bearing dolomite	Do	Cn Ru Po Sp Gl Cp	Crudely banded dolomite with cross-cutting plates of celsian
24.6	3962	Banded dolomite-sulphide rock	Do Cn Py	Sp Gl	Pyritic band in sharp, planar contact with dolomitic band
27.8	3963	Banded baryte-rock	Br Qz Py	Ca Ru Mt	Interbanding of baryte-rich opaque-poor rock with baryte-poor rock rich in opaques and quartz
31.7	3964	Banded baryte-rock	Br Qz	Ca Py Gl Sp (tr)	Banding expressed by changes in the baryte/quartz ratio, though baryte is generally dominant
32.7	3965	Banded calcite-rock	Ca Br Qz	Ch Py Gl	Slightly irregular banding is expressed by variations in the mineral assemblage, though calcite is generally dominant
33.1	3966	Brecciated quartzite	Qz Py	Ca Ms Ch Ru Br ?Cn Sp Cl Cp Mc	Quartzite fragments set in a pyritic matrix; irregular calcite patches occur

## Bulk-XRD examination (AMS), borehole 3 -

- 21.48m - Dolomite with trace amounts of clay (?chlorite and illite/mica)
- 23.15m - Dolomite with a little sphalerite and a trace of clay minerals
- 26.95m - Dolomite with lesser sphalerite and a trace of clay minerals
- 27.16m - Baryte with minor quartz
- 29.56m - Baryte with quartz and possibly a trace of calcite

APPENDIX III TABLE IV SCHEDULE 4

Depth (m)	PTS No.	Rock Name	Mineral Constituents		Comments
			Major	Minor	
11.7	3909	Banded calcareous schist	Do Qs Ms	Ch Py	Bands of dolomite alternate with bands of dolomite muscovite-schist; the pyrite occurs in cross-cutting veinlets
13.0	3910	Dolomitic schist	Qs Ms Do	Py	Pyrite occurs in cross-cutting veinlets which may be in part of pre-metamorphic origin
13.5	3911	Contorted dolomitic schist	Qs Ms Do	Py	Some suggestion that pyrite stringers may be of pre-metamorphic origin
14.3	3912 3913	Mineralised dolomitic rock	Qs Do Br Py	Sp Cl	Coarse, mosaic-textured rock in which evidence of strain deformation is seen
16.3	3914	Baryte-rock	Br	Qs Py	Coarse, mosaic texture
17.0	3915	Baryte-rock	Br Py (~5%)	Qs Sp Cl	Coarse, mosaic textured rock with disseminated sulphides
17.5	3916	Massive sulphide	Py Sp	Qs Cy Cl	Porous, ochre-coloured granular aggregates largely of pyrite and sphalerite
17.8	3917	Breccia	Qs Do	Br Sp Cl Cp Py	Quartz and baryte fragments set in sulphide-rich dolomite matrix
18.5	3918	Limestone	Ca Qs (±Ca) Py	Sp Cl Do	Banding expressed in wide variations in quartz and sulphide contents
18.8	3919	Dolomitic limestone	Ca Do	Qs Py Sp Cl	Textural irregularities suggest a limestone breccia modified by subsequent recrystallisation
19.2	3920	Mineralised breccia	Qs Do Py	Cn Sp Cl	Fragments of quartzite and dolomite set in a sulphide-rich matrix with minor celestine
19.7	3921	Dolomitic baryte-rock	Br Do Py	Qs Sp Cl	Banding expressed in changes of lithology; total baryte content less than 50%
20.0	3922 3923	Mineralised dolomitic rock	Qs Br Do	Py Sp Cl	Very variable lithology and texture with a large total sulphide content
20.4	3924	Sphaleritic breccia	Qs Do Sp	Py Cl	Coarse rock with breccia texture and variable texture
20.6	3925	Dolomite	Do Py (±Do)	Qs Sp Cl Cp(tr)	Fine, granular rock with sulphide disseminated and in stringers
21.2	3926	"Striped" limestone	Ca Qs Do	Py Sp Cl	Banding expressed in changes in the quartz/calcite ratio; total sulphide content is high
21.5	3927 3928	Limestone	Ca Py Do	Qs Sp Cl	Banding expressed in changes of lithology
21.8	3929	Quartzose limestone	Ca Qs Do	Py Sp Cl	Banding expressed in changes of lithology
22.5	4077	Celestine-quartz rock	Qs Cn Py Sp	Br	Medium-grained, homogeneous, granular rock crossed by hair veinlets of baryte
23.9	4078	Quartz-celestine rock	Qs Cn Py	Br Sp	Comparable to the 22.5 m specimen
24.9	4079	Celestine-quartz rock	Cn Qs Py	Do Sp Br	Similar to the 22.5 m specimen but is dolomitic and has a laminated fabric due to a weak alignment of celestine blades and a weak lithological banding

Note: In distinguishing the carbonate phases extensive use of Alizarin-Red staining was made

APPENDIX III TABLE V BOREHOLE 5

Depth (m)	PTS No.	Rock Name	Mineral Constituents		Comments
			Major	Minor	
4.0	4135	Celsian-quartz rock	Cn Qs (< Cn) Do Py	Ru Sp Gl	Banding expressed in contrasting mineral assemblages, though the texture is medium-grained granoblastic throughout
5.2	4136	Quartz-celsian rock	Qs Cn Py	Br Sp Cp(tr)	Banded rock in which baryte is a minor constituent occurring in cross-cutting hair veinlets
6.6	4137	Baryte-rock	Br	Qs Py Sp Cv(tr)	Coarse rock exhibiting pronounced tectonic flattening of baryte grains
8.0	4138	Quartz-celsian rock	Qs Do Cn	Ms Bt Ru Po Py Cp (tr)	Medium-grained, homogeneous rock
8.6	4139	(?) Hyalophane-quartz-rock	Qs Do Hy	Ms Ru Po Py Cp(tr)	Medium-grained, banded rock containing feldspar enriched in Ba and yielding an orthoclase or hyalophane XRD pattern
11.4	4140	Pebbly quartz-celsian rock	Qs Do Ms Py	Cn Ru Gr Cp Gl(tr)	Medium-grained sediment containing flattened, celsian-bearing pebbles; black grains seen in hand specimen are probably carbonaceous material
16.2	4141	Quartz-celsian rock	Qs Do Cn Ms Py	Br Ru Cp(tr)	Banded sediment crossed by hair veinlets of baryte
18.2	4142	Celsian-rock	Cn Py	Qs Do Ru	Coarse rock of which some 70% is celsian
23.2	4143	Baryte-rock	Br	Cn Qs Ap Ru Do Py Sp Gl	Coarse baryte mosaic with discrete porphyroblasts of celsian, and accessory apatite
24.2	4144	Celsian-dolomite-quartz rock	Cn Do Qs	Bt Br Ru Ms Py	Coarse parallel plates of celsian form some 50% set in a polymineralic matrix dominated by dolomite
27.4	4145	Quartz-celsian rock	Qs Cn Py	Ru Br Sp Gl(tr)	Celsian-bearing rock crossed by veinlet in which baryte and celsian appear to coexist
31.2	4146	Quartz-celsian rock	Qs Cn Py	Ms Ru	Banded rock

## Bulk XRD examination (AMS) from borehole 5 -

3.95m - Major quartz, dolomite and celsian

7.97m - Major quartz and celsian with lesser dolomite and mica

8.58m - Major quartz and dolomite with lesser orthoclase and a little mica. Powder analysis data suggest the feldspar may be the barian variety hyalophane

31.17m - Major quartz with lesser celsian and mica

## APPENDIX III TABLE VI BOREHOLE 7

Polished thin sections

Depth (m)	PTS No.	Name	Mineral Constituents		Comments
			Major	Minor	
9.1	4305	Banded mica-schist	Do Qs Ms	Bt Ch Zc Kp (tr) Ru(tr) Py(tr)	Banded metasediment in which the dominant lithology is dolomite-quartz-muscovite
27.4	4306	Quartz-celsian rock	Qs Cn	Do Bt Ru Py Sp(tr)	Medium-grained, mosaic-textured, banded rock with accessory pale "phlogopitic" biotite
32.6	4307	Celsian-quartz rock	Cn Qs Py	Do Ru Bt	Mosaic-textured quartz with abundant platy celsian crystals; medium-grained, banded rock
36.7	4308	Muscovite-schist	Ms Qs	YEr(tr) Py	Highly contorted schist with low-grade, cryptic anomalous Bz; pyrite occupies inter-granular space developed on the line of an incipient fracture
40.5	4309	Muscovite-schist	Qs Ms	Hy Ru Py Sp Gl	Banded schist in which quartzose layers contain grains of hyalophane; pyritic cross-veins developed on lines of incipient fracturing are common
55.8	4310	Pyritic segregation	Qs Py	Ms Cy Go Sp Gl	Seive-like sulphide segregation enclosing quartz, muscovite and late-formed clay/goethite material; is enclosed in foliated muscovite-schist
64.3	4311	Pyritic segregation	Do Py Sp	Qs Ms YEr Hy Ca Cp Gl(tr)	Seive-like sulphide segregation enclosing dolomite, quartz, muscovite and probable Ba-phases
71.6	4312	Mica-schist	Qs Ms Do	Bt YHy Ru Py Cp(tr)	Foliated schist in which muscovite is the dominant mica
76.8	4313	Quartz-celsian rock	Qs Cn Py Sp	Do Ru Ch(tr)	Laminated due to parallelism of platy celsian crystals; total sulphide c 20% (Sp <sup>2</sup> Py)
81.6	4314	Quartz-celsian rock	Qs Cn Sp	Do Er Ms Py Gl	Interbanding of a celsian-quartz lithology and a quartz-sphalerite lithology; crossed by dolomite-baryte veinlets
83.4	4315	Pyritic muscovite-schist	Qs Ms Do Py		Laminated dolomitic schist rich in pyrite, but with no visible barian phase
85.4	4316	Dolomite with quartz and celsian	Do Qs Py	Cn Ms Sp Cp(tr)	Irregular patchy structure with dolomite patches and patches of celsian-quartz lithology. Sulphides (~8%) are dispersed irregularly
87.1	4317	Quartz-celsian rock	Qs Cn	Ca Er Ru Ms(tr) Py Sp	Banded quartz-celsian rock displaced on cross-fractures carrying calcite veins with minor baryte
91.8	4318	Pyritic segregation	Py Qs Ms	Ca Cn Ch Cp Sp	Seive-like pyritic lens encloses quartz, calcite and celsian; set in contorted muscovite-schist
95.1	4319	Graphitic muscovite-schist	Qs Ms Gr	Ch Ca Ab Hy Ru(tr) Py Cp(tr)	Foliated schist notable for the presence of ovoid porphyroblasts of hyalophane
104.4	4320	Limestone band	Ca Qs Ms	Ru Fo	Grey limestone band in sequence of grey muscovite schist; medium-grained granoblastic texture
113.0	4321	Hyalophane-dolomite-schist	Do Qs Ms Hy	Gr Py Cp	Dolomite band rich in porphyroblasts of hyalophane
130.3	4322	Quartz-dolomite lens	Qs Do Ms	Bt Ch YZc Py	Foliated muscovite-schist rich in minute probable zircons; contains lens of quartz and dolomite patches irregularly intergrown (cf. PTS 4316)
150.4	4323	Amphibolite	Hb Qs Bt Ca	Se Ap Ch Py Cp(tr)	Laminated, coarse amphibolite
152.7	4324	Hornblende-mica-schist	Cn Ms Hb Ca Qs	Bt Zt Se Ru Py Cp(tr)	Calcareous rock containing fine, acicular crystals of probable clinozoisite
166.0	4325	Mica-schist	Ms Bt Ca Ch Qs	Se Zt Ru Py	Calcareous rock with acicular crystals of probable clinozoisite

APPENDIX III TABLE VII BOREHOLE 8

Depth (m)	PTS No.	Rock Name	Mineral Constituents		Comments
			Major	Minor	
8.3	4510	Dolomitic muscovite-schist	Qz Do Ms	Ch Gr Bt To Ba Po Py Cp(tr)	Anomalous barium probably occurs in muscovite; no discrete barium mineral was observed
10.4	4511	Dolomite rock	Do Ms	Qz Bt To Zc	No opaque minerals observed
13.0	4512	Muscovite-schist	Qz Ms	Do Gr Ru Po	Granulated schistosity
18.2	4513	Muscovite-schist	Qz Ms Do	Ru Py Po	Anomalous barium probably occurs in muscovite; pyrrhotine is disseminated, whereas pyrite forms a veinlet developed on incipient fractures of the rock
40.2	4674	Dolomite-rock	Do Qz Ms Sp	Bt Ch Po Py Cl	Foliated impure dolomite rock with sulphides ( 4% by volume) disseminated
68.3	4675	Quartzite	Qz	Ms Do Ab Ch Ru Py(tr)	The presence of albite grains suggests that this rock is a true detrital quartzite
105.8	4514	Muscovite-schist	Ms Qz Po	Do Ru Cp(tr)	Muscovite is in excess over quartz; pyrrhotine occurs as isolated, skeletal poikiloblasts
115.8	4515	Muscovite schist	Qz Ms	Do Gr Sp Po Cl Cp 7Ry	Anomalous barium probably occurs, in muscovite and some may occur in cryptic grains of hyalophane (optically resembling quartz)
129.5	4516	Graphitic muscovite-schist	Qz Ms Po	Ca Gr Ry Ch Py Cp(tr)	Crystals of Ba-feldspar occur with sheaves of muscovite heavily clouded with graphitic microgramules
134.9	4178	Graphitic muscovite-schist	Qz Ms	Gr Do Br(tr)	Contorted schist in which the muscovite contains about 6% Ba
135.5	4179	Graphitic muscovite-schist	Qz Ms	Gr Do Py Sp Po Cl	Contorted schist in which the muscovite contains about 8% Ba
142.6	4676	Quartz-dolomite- celesian rock	Do Qz Cn Py Sp	Ch Cy Cl Po(tr) Cp(tr)	Coarsely banded rock in which dolomite and quartzose bands alternate; the latter contain coarse celsian crystals and tend to be invaded by vein-like apophyses of dolomite; a radial-spheroidal chlorite phase is a prominent though minor constituent
143.6	4677	Quartz-celsian dolomite rock	Qz Cn Do Py	Ch Ru Sp Cp(tr)	Banded rock includes almost monomineralic layers of coarse celsian
148.2	4678	Mica-schist	Qz Do Ms	Bt Ch Ru Ry Py	Biotite-muscovite-schist with prominent chlorite

APPENDIX III TABLE VIII BOREHOLE 9

(a) Polished thin sections

Depth (m)	PTS No.	Name	Mineral Constituents		Comments
			Major	Minor	
4.9	4326	Mica-schist	Ms Bt Ch	Qz Do Ru Ab	Banded muscovite-biotite-dolomite-schist with chlorite replacing biotite
8.6	4327	Dolomite	Do	Qz Ms Bt Ru Ch	Medium-grained granoblastic dolomite with a laminated fabric due to drawn out quartz patches
14.4	4328	Dolomitic schist	Ms Qz	Do Ru Po Cp(tr) Pu(tr)	Disseminated sulphide grains are often drawn out in keeping with the contorted schistosity
17.6	4329	Muscovite-schist	Ms Qz Py	Ca Ru	Contains ~ 10% of disseminated pyrite
25.1	4679	Baryte-quartz rock	Br Qz Cy	Ru Ch Py Co	Coarse, banded rock in which primary mica is replaced by clay minerals, and goethite and chlorite are present
28.6	4330	Celsian-bearing schist	Ms Qz Cn	Gr Hy Se Py Sp Cp Gl	Bladed porphyroblasts of celsian are strongly zoned and intergrown with hyaloplase
29.8	4331	Muscovite-schist	Qz Ms Sp Py	Ch Cp Gl	Sphalerite-rich rock (~6% Sp) in which pyrite is altered to microcrystalline, concentrically banded patches
35.2	4680	Dolomite	Do Ms Qz	Ru Sp Gl	Massive, medium-grained dolomite with quartz-dolomite veinlets carrying accessory sulphides
35.4	4681	Quartz-muscovite-schist	Qz Ms Do	Bt Zc Po Cp Sp Py Gr	Crenulation cleavage emphasised by the distribution of intergranular films of graphite
38.2	4332	Calcareous schist	Qz Ca Ms	To Po	Laminated rock notable for the presence of small, green tourmaline porphyroblasts
41.4	4333	Calcareous schist	Ca Ch Qz	Bt Ms Ru Po	Chlorite is more abundant than the micas
43.1	4334	Muscovite-schist	Ms Ch Qz	Do Ru Po Cp(tr)	Dolomitic schist
43.4	4335	Chloritic schist	Qz Ch Do	Bt Ms Po Im Cp(tr) Sp(tr)	Poorly laminated rock containing minute crystals of ilmenite
47.7	4336	Sphaleritic dolomite	Do Qz Sp	Ms Po Py Gl	(Do > Qz > Ms); granoblastic dolomite in which drawn out quartz patches define a schistosity
56.0	4337	Sphaleritic dolomite	Do Qz Sp	Ms Po Gl	(Do > Qz > Ms); similar to PTS 4336
66.4	4338	Quartzose schist	Qz Ms Do	Sp Py Po Gr	Pyrite and pyrrhotine are segregated into different parts of the thin section
71.2	4339	Muscovite-schist	Ms Qz Do	Po Py(tr) Cp(tr) Gr Ca	
72.5	4340	Celsian-dolomite	Cn Do	Qz Py Sp Cp(tr)	Coarse, orientated mosaic of celsian porphyroblasts with sieve-textures in which quartz and sulphide grains are embedded, set in a matrix of coarse dolomite
73.5	4341	Banded quartz-celsian rock	Qz Cn Do Py Po	Ap Gl	Sulphide and carbonate rich rock whose mineralogy changes rapidly from band to band
75.6	4342	Celsian-quartz rock	Cn Qz Po	Do Ru Py Sp	Marked by the abundance of coarse, sieve-textured celsian porphyroblasts enclosing quartz and sulphide grains; dolomite occurs mostly in thin bands
76.0	4343	Pyrrhotine lens	Po	Qz Cn Do Cy Py Cp	Massive lens, becomes skeletal and intergrown with celsian-quartz rock at its margins
77.0	4344	Banded quartzite	Qz Do Sp	Py Sp Gl	Conformable bands rich in dolomite porphyroblasts or in sulphides
81.0	4345	Quartzite	Qz	Ms Do Py Sp Gl(tr)	

(b) XRD powder identification

42.8m - green spots in calcareous chlorite-schist (probably altered phenocrysts or lithic fragments were identified as 2M<sub>1</sub> muscovite/illite (D. Atkin, Ph 5950)

Depth (m)	PTE No.	Name	Mineral Constituents		Comments
			Major	Minor	
7.3	4517	Pyritic muscovite-schist	Qz Ms Do Py	Po Sp Gl Mc	Cremulated schistosity; colloform pyrite, and sketched and boxwork structures in pyrite and pyrrhotine are common
10.7	4518	Calcareous graphitic schist	Qz Ms Ca Py	Gr Po Cp Sp Gl	Calcareous schist with some 6% pyrite; some secondary colloform pyrite is included
13.3	4682	Celsian-quartz rock	Cn Qz Do Po	Ru Cy/Ch Py	Banded celsian-rich rock; secondary alteration has developed strongly coloured grey-green clay/chlorite material, bright emerald green in places
15.1	4683	Biotite-schist	Qz Bt Ch	Ca Ms Ap(tr) Po Mt Py(tr) Cp(tr) Hm(tr)	Dark schist in which minute grains of magnetite are a minor constituent
16.5	4519	Banded quartz-celsian rock	Qz Cn Py	Do Cy Ap Ru(tr) Po Cp(tr)	Coarse quartz-rock with coarse celsian, dolomite, pyritic segregations; alteration of colloform pyrite to coarse pyrite is common. The rock is porous due to groundwater leaching, and has a secondary clay constituent
17.2	4520	Dolomitic schist	Do Qz Ms	Bt Ru Po Py Cp(tr)	Biotite-bearing schist in which dolomite occurs as disseminated grains and discrete, ovoid porphyroblasts
19.2	4521	Pyrrhotine segregation	Po Ms Qz	Py Cp Ru	Muscovite-schist occurs as a fragment within a pyrrhotine segregation with much colloform pyrite and coarsely crystalline pyrite
21.7	4522	Muscovite-schist	Ms Qz	Ru Po Py	Quartz segregation set in muscovite-rock, monomineralic save for common rutile and accessory pyrrhotine; pyrite occurs as a cross-cutting veinlet
30.5	4523	Muscovite-schist	Ms Qz	Gr Po Py Cp	No carbonates occur in this or the preceding specimen
36.7	4524	Muscovite-schist	Qz Ms	Gr Do Bt Ru Po Py Cp Sp Gl	Cremulated schist
113.7	4525	Quartz-muscovite-celsian rock	Qz Ms Sp	Cn Py Cp	Carbonate-free, with minor Ba-feldspar



## Polished thin sections

Depth (m)	PTS No.	Name	Mineral Constituents		Comments
			Major	Minor	
4.1	4684	Chlorite-mica-schist	Qz Ms Ch	Bt Ca Ru Zt Ap Hb Po Py Cp(tr)	Calcareous schist rich in retrograde chlorite; minute crystals of probable clinozoisite are surrounded by pleochroic haloes in mica and chlorite
9.1	4685	Hornblende-garnet-schist	Qz Ch Ga Hb	Ms Bt Ca Zt Zc Py Hm(tr)	Coarsely segregated rock in which coarse quartz, almandine and hornblende crystals are set in chloritic schist; clinozoisite is a minor constituent
11.5	4686	Chloritic schist	Qz Ch Ga Hb	Ms Bt Ca Zt Zc Ap Py Mt	Homogeneous rock similar to PTS 4685; apatite and magnetite are accessory constituents
12.7	4687	Quartz-muscovite schist	Qz Ms Ca	Ch Bt Zt Zc Mt Po Cp Py	Magnetite and clinozoisite are present as minor constituent
19.0	4688	Quartz-muscovite-schist	Qz Ms Do Ch	Ca Bt Cy To Zc Py Cp(tr)	Dolomitic schist with accessory tourmaline; calcite occurs in pyritic hair veinlets
23.0	4689	Impure quartzite	Qz Do Ms	Bt Ab Ru Zc Ca Py Cp(tr)	Albite grains of apparent detrital origin are common; calcite occurs in hair fracture veinlets
25.5	4690	Quartz-celsian rock	Qz Cn Do	Ms Ch Ct	Replacement of quartz by celsian is indicated by the irregular dismembered character of the quartz crystals; platy cymrite is a minor constituent
26.8	4691	Quartz-celsian rock	Cn Qz Do	Ms Ch Ru Zc Py	Celsian here has a thin platy habit comparable to that of coexisting muscovite
32.3	4692	Celsian-quartz rock	Cn Qz	Do Ms Ru Zc Po Py	Celsian is much in excess over quartz
35.7	4693	Celsian-quartz-rock	Qz Do Cn	Ms Ch Gr Py	Celsian is confined to certain thin bands, and is often crowded with opaque microgranules
79.2	4694	Dolomitic quartzite	Qz Do	Ms Ch Ru To Ab 'Cy' Po Cp Py	Albite and tourmaline are accessory constituents; brown isotropic to microcrystalline fragments of glass-like material ('Cy') are common
84.5	4695	Muscovite-schist	Ms Qz	Ch Do Bt Ru Ap Py	Polymineralic bands alternate with bands of almost monomineralic muscovite
92.4	4696	Chlorite-muscovite-schist	Qz Ch Ms	Bt Ru Do Hy	Accessory hyalophane porphyroblasts occur in a rock dominated by retrograde chlorite
107.0	4697	Quartz-dolomite-celsian rock	Qz Do Cn	Ms Ch Br Ru Bt Po Py Sp Gl Cp	Celsian occurs as slender prisms or thin plates; baryte occurs in cross cutting hair veinlets
114.9	4698	Quartz-celsian rock	Qz Cn	Ms Do Ru Po Py	Celsian again occurs as slender platy crystals
117.7	4699	Dolomite-celsian rock	Cn Qz Do Po	Ms Ru Gl Sp Py	Sulphide-rich rock in which galena occurs in excess over sphalerite
125.6	4700	Celsian-quartz rock	Cn Qz	Ru Ms Do Ch Py Po Gl Sp Cp	The barium feldspar grains are crowded with opaque microgranules, not yet identified
127.3	4701	Muscovite-schist	Ms Qz Do	Ch To Ru(tr) Py	Tourmaline is a prominent accessory constituent; no barium mineral was identified optically
134.0	4702	Quartz-celsian rock	Qz Cn Py	Ch(tr)	Rock is remarkable for its lack of carbonate, mica and rutile
140.5	4703	Quartz-dolomite-celsian rock	Qz Do	Cn Ru Ch Ms Br Py Cp(tr)	Baryte occurs in a cross-cutting veinlet emplaced later than pyrite developed on incipient zones of cross-fracturing
142.1	4704	Pyritic quartzite	Qz Ca Py		No feldspar was observed in this mineralogically simple rock; quartz forms ~80% by volume

APPENDIX III TABLE XI

Summary of petrographic notes for outcrop specimens from the Ben Eagach area

Polished thin sections

Specimen no. Nat. Grid Ref (NN)	PTS No.	Rock Name	Mineral Constituents		Comments
			Major	Minor	
CZR 1555 8183 5438	2467	Quartz- muscovite- schist	Qz Ms Do	Ch Ab Zc Po Cp(tr)	Laminated rock with cremlate schistosity. Minor untwinned feldspar is probably albite
CZR 1559 8275 5641	2468 2468	Muscovite- schist	Ms Qz	Bt Do Ru Zc Ch Py Cp(tr)	Contains some 50% of muscovite
CZR 1589 9042 5872	2469	Garnet- muscovite- schist	Ms Qz Ga	Bt Do Ch Zc Py Cp(tr)	Almandine porphyroblasts up to 2 mm in diameter contain sigmoidal inclusion trails
CZR 3552A 8267 5504	2470	Quartz- celsian rock	Qz	Cn Ms Ru Zc Ch Py Go	Saccharoidal quartzite interbanded with laminated quartz- celsian rock
CZR 3552B 8267 5504	2471	Baryte- rock	Br	Qz Py Cp Sp Gl Fem	Coarse, granoblastic texture
CZR 3552C 8267 5504	2472	Quartz- celsian rock	Qz Cn Ca Py	Gl Sp Hm	Interlamination of celsian-rich and calcite-rich bands
CZR 3552E 8267 5504	2473	Quartz- celsian rock	Qz Cn	Do Ch Ru Go Py Gl Sp	Sulphide-rich bands are conspicuous
CZR 3558 8195 5490	2474	Baryte- rock	Br	Qz Py (~ 12%) Gl Sp	Massive, coarse, granoblastic rock
CZR 3573A 8073 5469	2475	Celsian- quartz rock	Cn Qz	Ru Bt Py	Alignment of the platy celsian crystals gives a laminated fabric. The biotite is a light coloured 'phlogopitic' variety
CZR 3573B 8073 5469	2476	Quartz- celsian rock	Qz Cn Py	Go Ru	This rock has a laminated fabric as in PTS 2475, and contains some 35% of pyzite
CZR 3573C 8073 5469	2477	Quartz- celsian rock	Qz Cn Py	Go Do Ru	A laminated fabric is not well developed, the celsian forming branching pseudopismatic porphyroblasts which appear dendritic in thin-section
CZR 3596 8378 5620	2478	Muscovite- schist	Ms Qz	Bt Ru Zc Py Mt(tr)	
CZR 3870A 8071 5471	2877	Sphaleritic quartzite	Qz Sp	Gl Py Cp Cv(tr) Fem	Granoblastic quartzite containing small lenses and bands of sphalerite-rich material
CZR 3871 8071 5471	2878	Quartz- celsian rock	Qz Cn	Py Sp Gl Go	As with other surface examples of quartz-celsian rock, no carbonate is present, possibly due to weathering solution

APPENDIX III TABLE XI (CONTINUED)

Specimen no. Nat. Grid Ref (NHN)	PTS No.	Rock Name	Mineral Constituents		Comments
			Major	Minor	
CER 3874 8071 5471	2879	Quartz-celsian rock	Qz Cn	Py Sp Cl Cp Cv Co Bornite(tr)	In the surface specimens chalcopyrite often shows marginal alteration to secondary Cu-sulphide
CER 3875 8071 5471	2880	Quartz-celsian rock	Qz Cn	Py Sp Cl Cp	
CER 3877 8071 5471	2881	Quartz-celsian rock	Qz Cn	Py Sp Cl Cp Co	Fine grained quartz-with-celsian fabric crossed by coarser sulphide-enriched bands
CER 3881A 8121 5465	2882	Quartz-celsian rock	Qz Cn	Py Cl	
CER 3882A 8121 5465	2883	Quartz-celsian rock	Qz Cn Ms	Py Hm/Co	Schistose fabric in this celsian-rich rock (Cn ~ 40% of the section)
CER 3884 8148 5453	2884	Quartz-baryte rock	Qz Br(~40%)	Ms Cn Py	This rock is notable for the coexistence of celsian with baryte
CER 3885A 8267 5504	2885	Fuchsite-quartzite	Qz	Fu Ca	The emerald-green Cr-mica is a prominent constituent of this rock
CER 3886 8267 5504	2886	Quartzite	Qz	Ms	The presence of muscovite imparts a crude schistosity
CER 3893 8627 5504	2887	Quartz-muscovite-schist	Qz Ms	Mt	Crenulated cleavage. Magnetite is the only ore-phase present
CER 3893A 8267 5505	2888	Biotite-schist	Bt	Qz Ms Ca Py Co	Coarse biotite forms some 50% by volume
CER 3909 B/1 8446 559	2889	Pyrite segregation	Py	Qz Cn Ms Cp	Coarse sulphide segregation in which pyrite grains are set in a matrix of quartz with celsian and muscovite
CER 3909 B/2 8446 5559	2890	Quartz-celsian rock	Qz Cn	Py Cp Co	Sub-parallel alignment of bladed celsian crystals imparts a banded fabric on the rock
CER 3909A 8446 5559	2891	Sulphide-rich quartzite	Qz	Py Sp Cp Co	Sulphide-rich, heavily weathered quartzite
CER 3920 8455 5562	2892	Quartz-celsian rock	Qz Cn Py	Ms	Heavily weathered pyritic rock
CER 3921 8528 5605	2893	Quartz-celsian rock	Qz Cn	Ms Py Mt Co	The presence of magnetite is unusual for this lithology
CER 3922 8531 5640	2894	Baryte-quartz rock	Br Qz	Py	Coarse-grained, banded, pyritic rock

APPENDIX III TABLE XI (CONTINUED)

Specimen no. Nat. Grid Ref (NN)	PTS No.	Rock Name	Mineral Constituents		Comments
			Major	Minor	
CZR 3923 8551 5637	2895	Quartzite	Qz	Py Sp Gl Cp Go Fem	Massive rock in which banding is expressed in the distribution of the sulphide grains
CZR 3932 8531 5640	2896	Quartzose limestone	Ca Qz	Py Sp Gl Fem	Coarse, light-grey rock in which banding is picked out by the distribution of ore grains
CZR 3933A 8556 5648	2897	Baryte-quartz rock	Br Qz	Py	
CZR 3933B 8556 5648	2898	Quartz-celsian rock	Qz Cn	Ch Py Go Fem	Iron-stained, schistose rock
CZR 3934A 8267 5504	2899	Quartz-celsian-calcite rock	Qz Cn Ca	Py Sp Gl	Banded, schistose rock
CZR 3934B 8267 5504	2900	Quartz-celsian-calcite rock	Qz Cn Ca	Py Sp Gl	As CZR 3934A
CZR 3935 8267 5503	2901	Banded quartzose rock	Qz ?Cn Ms	Ca Py Sp	Quartz + feldspar bands alternate with muscovite + calcite + sulphide bands
CZR 3936 8696 5677	2902	Quartzite	Qz	Py Go Fem	Even-grained quartzite with little impurity
CZR 3937 8696 5677	2903	Baryte-quartz rock	Br Qz	Py	Baryte forms some 60% by volume
CZR 3938 8696 5676	2904	Quartz-celsian rock	Qz Cn	Ms Py (~ 10%) Hm	
CZR 3939 8696 5676	2905	Muscovite-celsian quartzite	Qz Ms	Cn Py Gl Sp Go	Celsian and the sulphides are largely confined to certain bands
CZR 3940 8696 5675	2906	Celsian-quartzite	Qz	Ms Cn Py Sp	Fine-grained schistose rock, not notably banded
CZR 3941 8696 5675	2907	Baryte-rock	Br Qz	Py	Friable, weathered rock
CYR 1 8530 5639	4093	Quartz-celsian rock	Qz Cn	Py Sp Gl(tr)	Laminated fabric imparted by poikilitic celsian porphyroblasts
CYR 2 8530 5639	4094	Quartz celsian rock	Qz Cn Py	Ru Sp Cp	Poikiloblastic celsian crystals similar to those in CYR 1
CYR 3 8530 5638	4095	Quartz-celsian rock	Qz Cn Py	Bt Ru	Finer grained than CYR 2. The 'biotite' is a pale coloured variety
CYR 4 8530 5640	4096	Celsian-quartz rock	Cn Qz Py	Do Ru Cl. Br	Baryte is an accessory constituent. Pyrite forms 20% by volume
CYR 5 8119 5457	4097	Calcareous schist	Qz Ca	Ch Bt Ms Mt Py	Biotite-bearing schist rich in ovoid calcite porphyroblasts. Chlorite is conspicuous in this probable metabasite
CYR 6 8268 5506	4117	Muscovite-quartzite	Qz Ms	Br Go Fem Sp	Schistose rock in which baryte occurs with quartz and goethitic material as polymineralic patches with outwardly euhedral tabular forms resembling igneous phenocrysts when seen in hand specimen. Similar 'phenocrysts' seen at 28.6m in Borehole 9 proved to consist largely of celsian

## APPENDIX IV

### GEOCHEMICAL ANALYSES OF DEEP OVERBURDEN SAMPLES

Samples of the deep overburden were collected using a 'Minuteman' power auger in 1977-78 over the geophysical lines listed in column 2 of the table, relative to an origin at the collar of BH 5. Lines are quoted as positive in a westerly direction and the position (column 3) on each line as positive to the north and negative to the south of the baseline. Samples were collected from the depth of maximum auger penetration (column 4) which is assumed to be the base of the overburden profile. This may not be true in till containing large boulders but generally the results are consistent with the samples being collected from the lodgement till.

After air-drying and disaggregation, the samples were sieved through a 250  $\mu\text{m}$  aperture nylon mesh and the undersize fraction ground in an agate ball mill for homogenisation prior to analysis. Cu, Pb, Zn and Ag were determined by atomic absorption spectrophotometry and Mn, Fe and Ba by photographic emission spectrography. All elements are quoted in parts per million, except for Fe in percent. The percentage loss on ignition (LOI in column 12) was determined by heating to 450°C for 3 hours and is a measure of the organic content of the sample. The upper calibration limit for Ba is 100000 ppm or 10% Ba and values above this are quoted at the limit. Heavy mineral concentrates were prepared from the deep overburden material by coarse screening and panning; then analysed for Ce, Ba, Sb, Sn, Pb, Zn, Cu, Ca, Ni, Fe, Mn, Ti, Ag and As using an XRF method similar to that used for analysis of drainage panned concentrates (p.4). The analytical results are not presented here but are available on request from the Head of the Metalliferous Minerals and Applied Geochemistry Unit, Keyworth Office.

APPENDIX IV

SAMPLE NUMBER	LINE POSITION (NORTH)	DEPTH (M)	CU	PB	ZN	AC	MM	FE %	RA	LOI %	
1	6000	-180	2.00	55	570	1200	1	2886	3.80	4090	8.9
2	6000	-170	1.00	20	310	4000	1	691	3.87	5800	20.9
3	6000	-160	1.00	10	100	220	1	503	4.04	3754	2.4
4	6000	-150	1.25	40	350	2100	2	1817	7.74	2595	8.1
5	6000	-140	0.30	80	330	1200	0	7165	6.65	9184	4.1
6	6000	-130	0.20	5	40	140	0	210	1.23	100000	9.0
7	6000	-120	0.75	10	40	60	0	222	1.32	4188	10.5
8	6000	-110	0.50	70	260	600	0	2219	4.30	1726	2.7
9	6000	-90	1.40	50	230	500	0	392	5.54	1953	6.6
10	6000	-80	0.30	50	180	240	1	12351	8.41	1721	9.6
11	5940	-180	0.75	10	110	1150	0	511	4.06	2354	7.6
12	5940	-170	1.70	50	120	950	1	259	3.97	2000	2.1
13	5940	-160	2.60	80	430	3600	2	6886	6.90	8700	4.4
14	5940	-150	1.00	30	80	300	1	377	3.07	8103	2.3
15	5940	-140	1.50	50	210	830	1	2696	3.34	6819	7.8
16	5940	-130	2.00	50	140	3000	1	1997	7.19	3788	4.5
17	5940	-120	1.50	10	70	220	1	687	3.51	1834	15.6
18	5940	-110	2.20	45	230	700	1	313	3.28	3804	4.1
19	5940	-100	1.40	40	400	250	1	118	0.55	1116	8.1
20	5940	-90	3.80	45	150	840	1	402	4.10	1818	11.9
21	5940	-80	1.00	50	250	370	1	237	1.83	4021	8.3
22	5820	-240	1.50	20	200	320	2	1422	2.57	100000	11.7
23	5820	-250	2.60	75	480	2750	2	94	2.37	47548	2.3
24	5820	-230	1.20	40	460	800	2	1249	3.12	100000	3.1
25	5820	-220	1.40	15	120	210	3	145	1.94	100000	10.5
26	5820	-210	1.60	65	520	1500	2	183	3.09	100000	2.3
27	5820	-200	0.90	60	170	550	1	2015	4.04	4127	2.0
28	5820	-190	1.40	100	1200	1200	1	5539	4.73	6494	1.0
29	5820	-180	1.60	40	70	250	1	1419	5.56	7066	5.5
30	5820	-170	2.00	15	120	2050	1	1071	3.14	1933	12.9
31	5820	-160	4.80	90	1650	2800	2	4511	4.57	8662	5.1
32	5820	-150	5.00	25	300	2450	1	7748	3.00	6563	2.4
33	5820	-140	3.50	45	100	500	1	431	2.88	3654	5.5
34	5700	-220	1.40	35	80	130	1	551	3.76	1297	8.8
35	5700	-210	1.60	55	100	220	1	2067	5.13	3438	3.0
36	5700	-200	1.50	45	30	100	1	1586	4.60	2975	7.2
37	5700	-190	0.80	5	40	190	1	414	2.39	1081	3.3
38	5700	-180	1.10	45	110	190	1	352	1.45	2150	6.9
39	5700	-170	1.50	45	170	360	1	891	2.34	1894	9.6
40	5700	-160	4.00	60	150	2300	1	589	5.59	5813	2.9
41	5700	-150	3.50	50	60	900	1	745	4.32	4638	5.4
42	5700	-140	3.30	65	70	1450	1	368	2.28	2937	7.7
43	5700	-130	2.70	65	80	5300	1	183	2.76	1987	4.4
44	5700	-120	1.10	40	80	550	1	382	2.48	2160	0.0
45	5700	-110	1.50	50	130	1000	0	518	3.68	1174	0.0
46	5700	-100	1.10	60	200	790	1	519	2.92	1251	2.4
47	5700	-90	4.00	80	450	680	0	515	5.12	1396	0.0
48	5700	-80	3.00	40	320	440	0	433	2.71	1193	9.3
49	5640	-200	1.40	40	60	230	1	1479	4.89	1189	1.1
50	5640	-190	1.90	40	100	250	1	1171	4.24	1342	0.0
51	5640	-180	1.10	45	60	220	0	814	4.29	1129	2.9
52	5640	-170	1.40	45	40	200	0	316	3.03	984	8.3
53	5640	-160	2.30	50	30	480	1	536	3.73	960	1.5
54	5640	-140	1.50	40	140	1730	0	874	6.63	783	6.9
55	5640	-130	1.60	35	30	76000	0	893	13.15	286	28.8
56	5640	-120	2.40	40	70	2000	0	672	6.97	600	7.4
57	5640	-110	1.60	50	180	2310	0	524	6.01	629	2.9
58	5640	-100	1.50	25	100	1170	0	694	3.08	3091	18.7
59	5580	-80	2.70	20	60	580	0	1990	7.35	2028	11.5
60	5580	-90	2.40	30	60	620	0	374	4.50	1145	5.0
61	5580	-110	4.70	20	20	160	0	256	2.30	630	3.8
62	5580	-120	2.40	30	20	140	0	186	3.29	865	7.6
63	5580	-130	4.50	20	20	370	0	547	2.93	745	0.0
64	5580	-140	2.00	20	20	90	0	230	2.84	586	1.6
65	5580	-150	3.00	20	20	290	0	412	3.05	804	2.3
66	5580	-165	2.90	25	40	260	0	331	2.60	808	4.9
67	5580	-181	1.80	15	40	630	0	431	2.54	1079	33.3
68	5580	-190	1.50	50	40	340	0	2613	4.82	321	1.3
69	5580	-200	1.00	30	370	630	0	1578	6.33	6401	10.0
70	5520	-140	2.10	35	20	110	0	944	5.82	713	6.5
71	5520	-130	1.60	120	10	120	0	456	3.40	1570	4.6
72	5520	-120	2.20	35	20	300	0	641	3.22	1041	5.4
73	5520	-110	2.70	35	40	980	0	429	2.80	525	1.7
74	5520	-100	1.80	45	30	250	0	484	2.96	652	5.5
75	5520	-90	2.70	40	30	160	0	310	4.53	562	1.4
76	5520	-80	2.20	50	30	110	0	193	3.64	691	1.5
77	5520	-70	2.00	40	30	140	0	533	3.37	1190	2.2
78	5520	-60	2.10	35	30	120	0	626	3.50	745	5.6
79	5520	-50	1.00	25	50	580	0	789	3.63	1487	11.8
80	5520	-40	4.00	20	20	90	0	829	3.50	718	0.0
81	5520	-30	2.50	20	30	100	0	1002	3.80	705	8.1
82	5520	-20	2.40	30	20	70	0	863	4.12	606	6.4
84	5520	-10	2.70	40	20	60	0	3244	7.21	522	3.2
85	5520	0	1.80	45	30	90	0	354	3.56	692	6.0
86	5460	70	2.50	50	100	150	0	946	3.69	688	4.3
87	5460	80	3.50	15	40	70	0	381	1.98	506	26.4
88	5460	60	2.70	60	50	140	0	3269	6.06	341	1.5
89	5460	50	2.80	40	50	150	0	255	2.68	580	5.1
90	5460	40	2.10	15	30	50	0	385	2.53	393	12.7
91	5460	30	2.00	30	40	110	0	246	2.70	510	9.8
92	5460	20	2.20	40	40	130	0	417	4.61	489	4.3
93	5460	10	3.00	40	30	110	0	1483	5.13	507	5.6
94	5460	0	2.80	40	70	320	0	1943	4.84	718	0.0
95	5460	-10	2.80	40	70	1230	0	4232	5.70	3837	3.1
96	-450	180	3.25	50	130	400	0	769	6.59	5567	3.8
97	-450	170	2.50	40	280	550	0	5179	6.91	3601	0.0
98	-450	160	3.00	50	60	280	0	525	4.51	1730	0.0
99	-450	150	3.40	35	100	210	0	286	2.50	9747	0.0
100	-450	140	1.50	40	260	530	0	279	1.48	7046	0.0
101	-450	130	1.20	65	70	300	0	427	5.03	2873	3.3
102	-450	120	1.00	35	130	300	0	208	2.75	2210	0.9
103	-450	110	3.40	20	90	290	0	236	2.59	2443	1.1
104	-450	100	2.10	25	70	350	0	441	2.81	3107	4.2
105	-440	90	1.40	45	140	540	0	659	3.97	2210	1.1
106	-440	80	3.00	35	190	610	0	323	2.14	2638	2.8
108	-440	60	3.00	20	80	280	0	379	2.28	5614	2.0
109	-440	50	3.80	25	140	500	0	427	2.19	7651	1.5
110	-440	40	4.50	25	110	370	0	641	2.30	5872	2.0
111	-440	30	3.30	25	80	240	0	502	2.85	2246	1.2
112	-440	20	2.70	65	60	350	0	600	4.64	2278	1.1
113	-440	10	2.30	55	70	1640	0	505	3.06	2159	2.0
114	-440	0	2.00	30	100	200	0	455	2.86	1801	1.0
115	-440	-10	2.00	45	70	190	0	506	3.34	1470	0.0
116	-440	-20	2.00	20	60	630	0	612	3.77	1522	14.3
117	-440	-30	2.00	35	80	280	0	437	5.16	2874	5.8
118	-510	-30	0.70	40	110	170	0	364	3.66	1017	1.7
119	-510	-20	0.80	45	50	160	0	610	4.20	830	6.3
120	-510	-10	0.80	10	50	30	0	183	0.84	644	11.4
122	-430	40	2.80	40	80	180	0	215	2.71	2300	2.0
123	-410	0	3.00	40	80	290	0	606	3.11	2446	0.0
124	-410	10	4.00	35	90	230	0	679	2.91	2868	0.0
125	-410	20	2.00	25	70	930	0	270	1		

## APPENDIX V

**BENEFICIATION STUDIES ON BARYTE SAMPLES**  
(Essentially reproduced from Applied Mineralogy Unit Report no. 259 by D.A. Briggs, D.A.W. Bernard, D.J. Bland and J.A. Bain)

### Introduction

Following the examination of drill cores, a selection of samples from the baryte-rich horizons in Borehole 2 (see A I, T II; A III, T II) were subjected to preliminary mineral dressing trials to assess their amenability to upgrading and determine the principal factors to be taken into account in evaluating the rocks as mineral raw materials.

The barium silicate, celsian, recorded in varying concentrations in other parts of the deposit was largely absent in the samples treated. These represented two continuous sections of the core depths of 1.05–5.75 m and 7.68–13.33 m respectively. For convenience, the samples were labelled as follows:

Sample No. CYD	1	2	3	6
Depth m	1.05	1.85	3.56	7.68
	to	to	to	to
	1.85	3.56	5.75	8.47
Sample No. CYD	7	8	9	10
Depth m	8.47	9.73	10.93	12.10
	to	to	to	to
	9.73	10.93	12.10	13.33

As the principal use of the baryte recovered from the deposit is likely to be as a weighting agent in drilling muds employed in rotary drilling for oil and gas wells, particular attention was paid to the density of the products recovered in processing. Although there appears to be no particular restriction on the presence of other mineral phases, the products should obviously be high in baryte content. A bulk density in excess of 4.20 g/ml is stipulated; iron content should be relatively low.

For other uses, particularly for the chemical, glass and ceramics industries, purity is of particular concern but for application as a white mineral filter the colour of the baryte is of paramount importance. It is of interest to note that fluorite, a deleterious constituent frequently found in association with baryte, is absent in these samples.

The specific gravity of the baryte itself was found to be 4.38; it contains a little strontium in the mineral lattice, equivalent to about 1% mol. SrSO<sub>4</sub>. In the pure state it is colourless (white when ground to a powder).

### Rock composition and physical properties

The rock is generally banded in texture with areas of massive granular baryte (often coarser grained) alternating with baryte layers which contain clusters or stringers of opaque metallic oxides and sulphides.

The associated minerals are essentially quartz, particularly in samples 7–10 where quartz is the principal impurity. The opaque mineral here is mainly magnetite, although traces of sulphide (mostly pyrite) also occur. In

samples 1–3, carbonate appears as an important accessory and sulphides comprise the principal opaque constituent. The former is dolomite (ankeritic?) and the latter consists mainly of pyrite although this is accompanied in varying degrees by sphalerite, galena and chalcopyrite.

Sample 6 contains accessory celsian and also bears occasional flakes of white, or greenish-white mica.

In thin section, the baryte, particularly where it occurs in concentrated bands, is seen to be rather coarser-grained than the other constituents and grain sizes up to 1.5 mm in diameter can be recorded. On crushing, the baryte might therefore, be expected to concentrate preferentially in the coarser sizes, although the good cleavage displayed by the mineral might also lead to the production of excessive fines.

### Density determination

The density of individual pieces of core was determined simply by weighing in air and water. The range for each sample is shown in Table I, together with the average for each core section so treated. The latter is relatively close to the bulk specific gravity determined from a representative portion of the sample after crushing prior to the separation treatment (see below). The specific gravities of all crushed and ground material were determined with an air comparison pycnometer which not only produces a result rapidly but does so wholly in the dry state.

The bulk specific gravities are related to baryte content but only in a general way as the differing values of quartz (2.65) and dolomite (2.9) must be taken into account. The presence of subsidiary magnetite and pyrite (5.0 – 5.2 specific gravity) also affect the overall values in a minor way. The higher bulk SG of sample 6 is partly a function of the presence of celsian (SG of 3.35) in the gangue.

Sample 1, with the lowest SG value, contains the greatest amount of diluent material; barium analysis by X-ray fluorescence examination of the ground material suggests the presence of about 75% baryte. Barium analysis of the other samples suggest baryte contents of 85–90% by weight.

### Liberation characteristics

As a first stage in investigating the release of diluent minerals from the baryte rocks, several core pieces in each sample were jaw-crushed <4 mm diameter and the products screened through the BS sieve series 8 mesh to 240 mesh (2 mm to 63 μm aperture). An additional sieve, with an aperture of 32 μm, was added at the fine end as a check on the production of finely-powdered material. The resulting particle size distribution is shown in Table II.

The density of each size fraction was determined by pycnometry and the results recorded in the middle section of Table II. These show a bimodal distribution, with higher values, reflecting higher baryte content, at 0.5–0.25 mm and again at 32 μm. In the coarser sizes, diluent minerals still form aggregates with baryte. When liberated, they tend to report in the finer sizes except for the very fine fraction (<32 μm) where the superior cleavage of baryte yields

**Table I Specific gravity measurements**

Sample No CYD	1	2	3	6	7	8	9	10
SG of individual core fragments	3.72–4.38	3.72–4.42	3.74–4.46	4.10–4.47	3.98–4.45	3.96–4.45	3.91–4.66	3.88–4.38
Average SG	4.01	4.15	4.21	4.27	4.16	4.24	4.16	4.14
Bulk SG of ground head sample	4.07	4.17	4.20	4.27	4.12	4.17	4.11	4.11

APPENDIX V

TABLE II

Liberation Characteristics  
Separation of gangue from jaw-crushed samples (<4 mm particle size)

SIZE FRACTION Sieve aperture (mm or μ)	WT. % OF WHOLE ROCK										SPECIFIC GRAVITY of whole fraction (upper figure) of heavy separate (lower figure)										METHYLENE IODIDE FLOAT (wt.%)									
	SAMPLE NO.										SAMPLE NO.										SAMPLE NO.									
	1	2	3	6	7	8	9	10	1	2	3	6	7	8	9	10	1	2	3	6	7	8	9	10						
-4.0 + 2.0 mm	31.1	27.9	26.3	26.1	25.6	28.3	33.0	31.5	4.03	4.11	4.16	4.24	4.08	4.15	4.08	4.11	No free gangue													
-2.0 + 1.0 mm	12.5	15.3	13.2	10.6	13.3	13.2	13.7	14.1	4.06	4.19	4.19	4.20	4.07	4.15	4.08	4.08	No free gangue													
-1.0 + 0.5 mm	9.9	11.6	11.3	8.8	12.0	13.2	10.9	10.8	4.12	4.20	4.20	4.24	4.11	4.20	4.10	4.07	3.5	2.0	2.7	0.5	3.1	1.0	1.8	1.7						
-0.5 + 0.25 mm	12.6	11.8	12.3	17.4	14.1	13.8	11.3	10.9	4.17	4.31	4.31	4.31	4.21	4.29	4.18	4.15	5.8	2.9	4.9	1.1	10.2	5.8	7.3	8.4						
-250 + 125 μm	14.7	11.2	12.3	16.1	12.4	11.3	10.5	10.5	4.21	4.26	4.25	4.37	4.11	4.20	4.11	4.09	14.5	6.4	7.8	4.5	13.6	8.8	11.1	12.2						
-125 + 63 μm	7.8	7.8	8.4	7.2	7.4	6.3	6.1	5.0	4.27	4.37	4.34	4.40	4.35	4.34	4.28	4.24	21.1	12.5	8.7	7.7	10.2	6.9	6.8	11.4						
-63 + 32 μm	7.4	7.9	7.7	7.3	7.4	7.4	7.7	9.3	4.11	4.21	4.23	4.32	4.05	4.15	4.09	4.08	22.1	1.5	3.1	1.9	1.3	2.1	2.9	2.0						
-32 μm	4.0	6.5	8.5	6.5	7.8	6.5	6.8	7.9	4.34	4.37	4.42	4.43	4.42	4.41	4.37	4.41														
	100.0	100.0	100.0	100.0	100.0	100.0	100.0	100.0	3.85	4.11	4.12	4.17	4.08	4.11	4.10	4.00														
									4.23	4.39	4.43	4.41	4.41	4.38	4.38	4.33														
									4.01	4.22	4.28	4.23	4.24	4.21	4.17	4.20														
									4.30	4.30	4.35	4.34	4.15	4.37	4.31	4.34														
									4.14	4.18	4.28	4.25	4.31	4.23	4.26	4.26														

NOTE: Centre column of results provides two values of SG for the fractions between 1.0 mm and 32 μm. The upper value refers to the fraction prior to separation, the lower value to the methylene iodide sink product after removal of the float material recorded in the right hand column of the table.

APPENDIX V

TABLE III

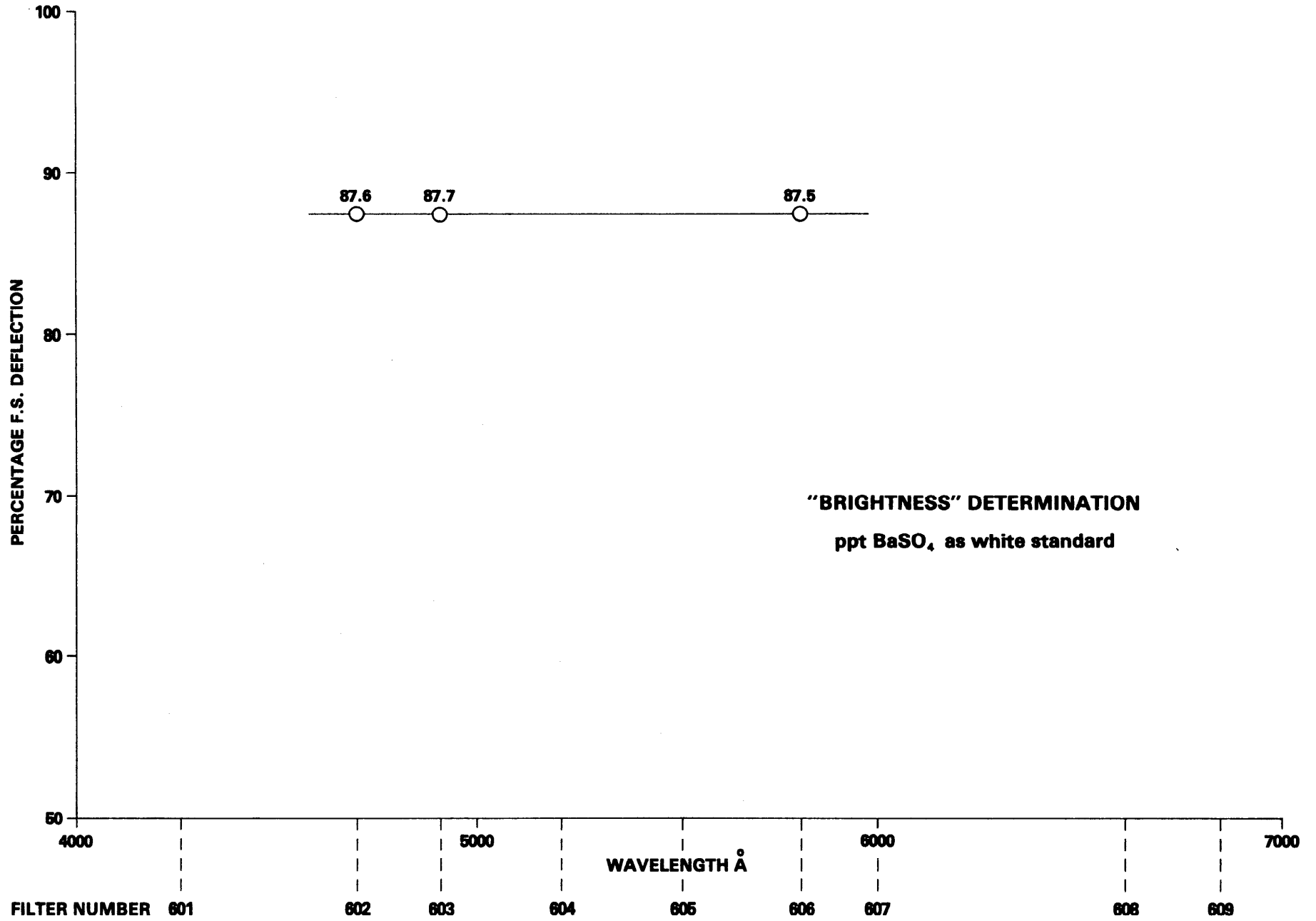
Treatment of bulk samples crushed to pass a 60 mesh (250 μm aperture) sieve

	WT. % OF HEAD SAMPLE										SPECIFIC GRAVITY (g/ml)										BARYTE CONTENT (wt.%)									
	SAMPLE NO.										SAMPLE NO.										SAMPLE NO.									
	1	2	3	6	7	8	9	10	1	2	3	6	7	8	9	10	1	2	3	6	7	8	9	10						
-250 μm + 125 μm FRACTION																														
MAGNETIC SEPARATE	7.7	8.1	4.6	2.7	5.5	6.1	8.0	6.6									94	96	95	96*	96	96	96	96						
LIGHT SEPARATE	12.3	5.3	5.5	3.6	7.7	5.3	7.4	6.5	4.41	4.42	4.39	4.41	4.39	4.40	4.37	4.34	(83)	92	87	85*	83	90	85	87						
HEAVY SEPARATE	61.4	59.6	68.6	74.5	65.6	66.2	61.3	58.6									87	93	94	96*	95	94	95	94						
TOTAL	81.4	73.0	78.7	80.8	78.8	77.6	76.7	71.7																						
-125 μm + 32 μm FRACTION																														
LIGHT SEPARATE	1.6	0.3	0.2	0.4	0.2	0.1	0.2	0.8	3.87	4.15	4.00	4.12	3.96	4.13	3.92	4.06														
HEAVY SEPARATE	5.2	7.9	3.4	4.1	5.4	6.4	5.2	5.0																						
TOTAL	6.8	8.2	3.6	4.5	5.6	6.5	5.4	5.8																						
-32 μm FRACTION																														
	11.8	18.8	17.7	14.7	15.6	15.9	17.9	22.5	4.12	4.28	4.32	4.36	4.31	4.29	4.29	4.30														

LIGHT SEPARATE = Material with specific gravity < 3.3  
HEAVY SEPARATE = " " " " " " > 3.3

\*Slightly excessive (no account taken of celestian content)





Appendix V Fig. 1. Brightness of -250 + 125 $\mu$ m baryte concentrate from sample 8 determined as % reflectivity of white light (EEL Spectrophotometer)

greater production of very small particles. These features accord with the textural characteristics noted in hand specimen.

Microscopic examination confirmed that diluent minerals were locked in particles  $>1.00$  mm in diameter and the two fractions concerned were not examined further.

With the exception of the  $-32\ \mu\text{m}$  material, the size fractions were separated in a heavy liquid to remove a lighter fraction. Methylene iodide ( $\text{SG}=3.3$ ) was chosen rather than the more usual bromoform ( $\text{SG}=2.9$ ) because of the presence of dolomite. The proportionate recovery of float material (free quartz and carbonate) is recorded in Table II. The resulting figures generally range about 1–3% for 1.0–0.5 mm, 3–8% for 0.5–0.25 mm and 8–13% for 250–125  $\mu\text{m}$  materials, thereafter levelling out. Values for sample 1 are higher because of the greater quantity of diluent minerals in the core. Those for sample 6 are lower because of the incomplete separation of celsian. It will be seen, however, that for practical purposes, full liberation of gangue is achieved only at particle sizes  $<125\ \mu\text{m}$ .

The density of the baryte separates was subsequently determined by pycnometry and the results are given in Table II. Fractions  $<0.25$  mm yield SG values close to that of baryte itself and, influenced by the increased concentration of oxide and sulphide minerals, often exceeding it. Below 63  $\mu\text{m}$  the separation of fine particles in methylene iodide becomes less efficient (at least without the use of centrifugal force to improve settling) and the specific gravity values decrease slightly.

#### *Production of baryte concentrates*

The efficiency of baryte separation from the rock as a whole was assessed by treatment of a new "head sample" prepared by crushing the core to pass a 250  $\mu\text{m}$  aperture sieve so as to achieve maximum liberation of gangue at the coarsest practical mesh size. The product was further screened at 125  $\mu\text{m}$  and 32  $\mu\text{m}$  to provide three size fractions (Table III).

The additional crushing to which the samples had been subjected increased the amount of fines – as shown by the  $-32\ \mu\text{m}$  fraction in Table III. The coarsest fraction, however, retained the bulk of the material (71%–82% of the original rock) and processing was directed mainly at this material.

A preliminary magnetic separation removed the magnetite and also some of the dolomite and sulphide impurities. The baryte was then recovered from the non-magnetic fraction by gravity concentration – retaining the methylene iodide sink/float procedure as the simplest laboratory procedure and giving the highest possible yield.

The resulting "heavy separate" produced from the 250–125  $\mu\text{m}$  material, as shown in Table III, represented a recovery of about two-thirds of the whole rock and yielded specific gravities in the range 4.37 to 4.42, well above the minimum specification for a drilling mud weighting agent. Analysis by X-ray fluorescence indicated baryte contents of 94% to 96%.

A heavy liquid separation of the 125–32  $\mu\text{m}$  fraction proved much less successful (see results for SG of the baryte concentrate in Table III) but the finest  $-32\ \mu\text{m}$  fraction was already sufficiently rich in baryte to provide the required density without upgrading and would therefore allow substantial additional recoveries. As shown in Table III, the fine material passing the 32  $\mu\text{m}$  aperture sieve contains 87% to 95% baryte by analysis.

#### *Conclusions*

Provided the rock is crushed to liberate gangue minerals, in effect  $<250\ \mu\text{m}$ , the necessary high-grade product can be recovered by gravity concentration, a preliminary magnetic separation proving an effective, if not necessary, aid in removing accessory iron-bearing impurities (see also below).

A recovery of up to two-thirds of the rock as a whole can be achieved solely by confining the concentration to the more-easily treated coarser particle sizes. Specific gravities of 4.37 to 4.41 can thus be obtained. In addition, the substantial fines produced by the crushing operation appear to consist largely of baryte itself and can be accepted without further treatment.

In practice, the pronounced banded texture displayed by the rocks in hand specimen might be exploited by introducing a heavy-media separation as a first-stage "rougher" concentration, in order to remove the baryte-rich material from a coarse lump-size product prior to the main crushing operation described here.

Although the baryte concentrates produced from the 250–125  $\mu\text{m}$  fractions assayed 94–96%  $\text{BaSO}_4$ , important differences could be detected in the composition and physical nature of the impurities.

In samples 1–3, sulphides remain in the heavy separate as a significant impurity and would have to be removed independently, e.g. by an additional froth flotation treatment, to prepare high purity baryte. The sulphides also adversely affect the potentially white colour of the baryte product but towards the top of the borehole the latter also shows increasing secondary iron oxide staining. If necessary this could be removed by a chemical leach or "bleaching" treatment but the discolouration decreases with depth and is virtually absent below 8.5 m. Samples 7–10, from this section of the borehole, are also notable for the presence of magnetite, rather than sulphides, as the principal opaque accessory and magnetic separation serves to eliminate the oxide. Less than 1% of pyrite remains in the baryte concentrate.

The white nature of the heavy separate from the 250–125  $\mu\text{m}$  fraction of sample 8 was assessed quantitatively by measuring the % reflectivity of white light photometrically against a white powder standard (precipitated barium sulphate). The data recorded from a pressed disc of the finely powdered concentrate, at three separate wavelengths in the visible spectrum, are shown in Fig. 1. Reflectivity at a wavelength of 457 nm, the usual reference standard for assessing white mineral fillers, proved to be 87.6%, a markedly high figure. The horizontal aspect of the reflectance "curve" displayed in Fig. 1 confirms that the white nature of the baryte concentrate shows no colour tint.

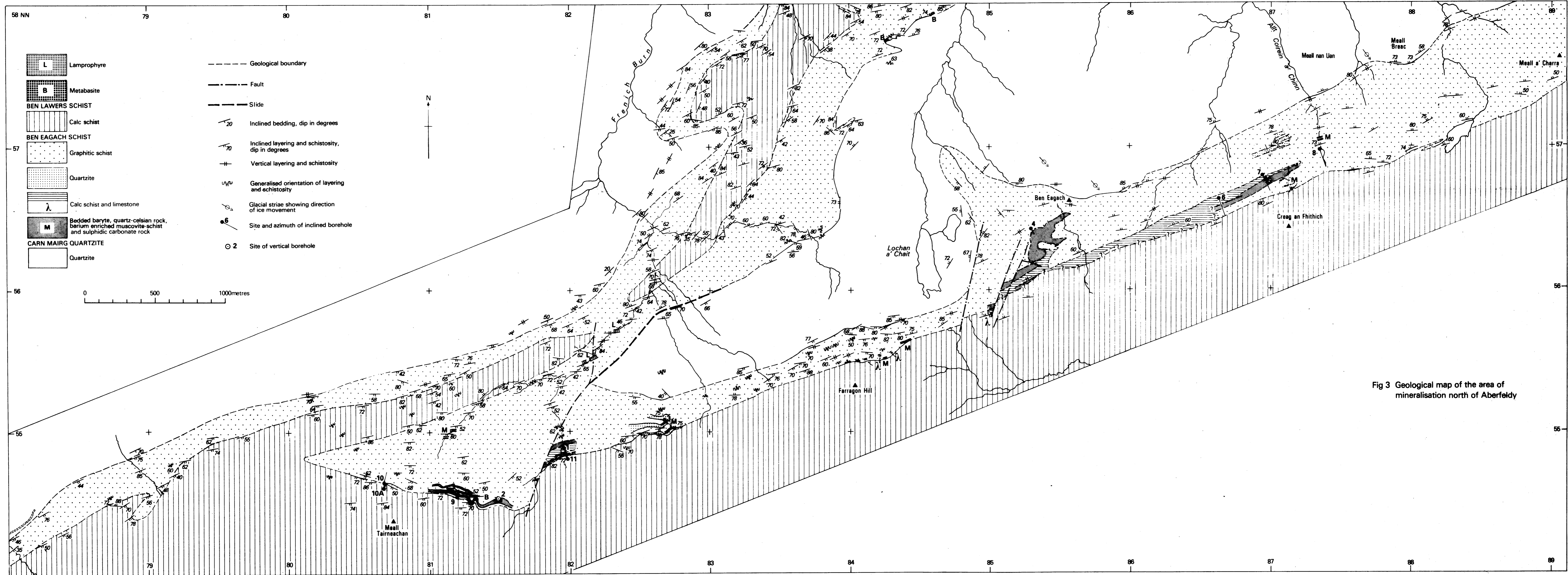


Fig 3 Geological map of the area of mineralisation north of Aberfeldy

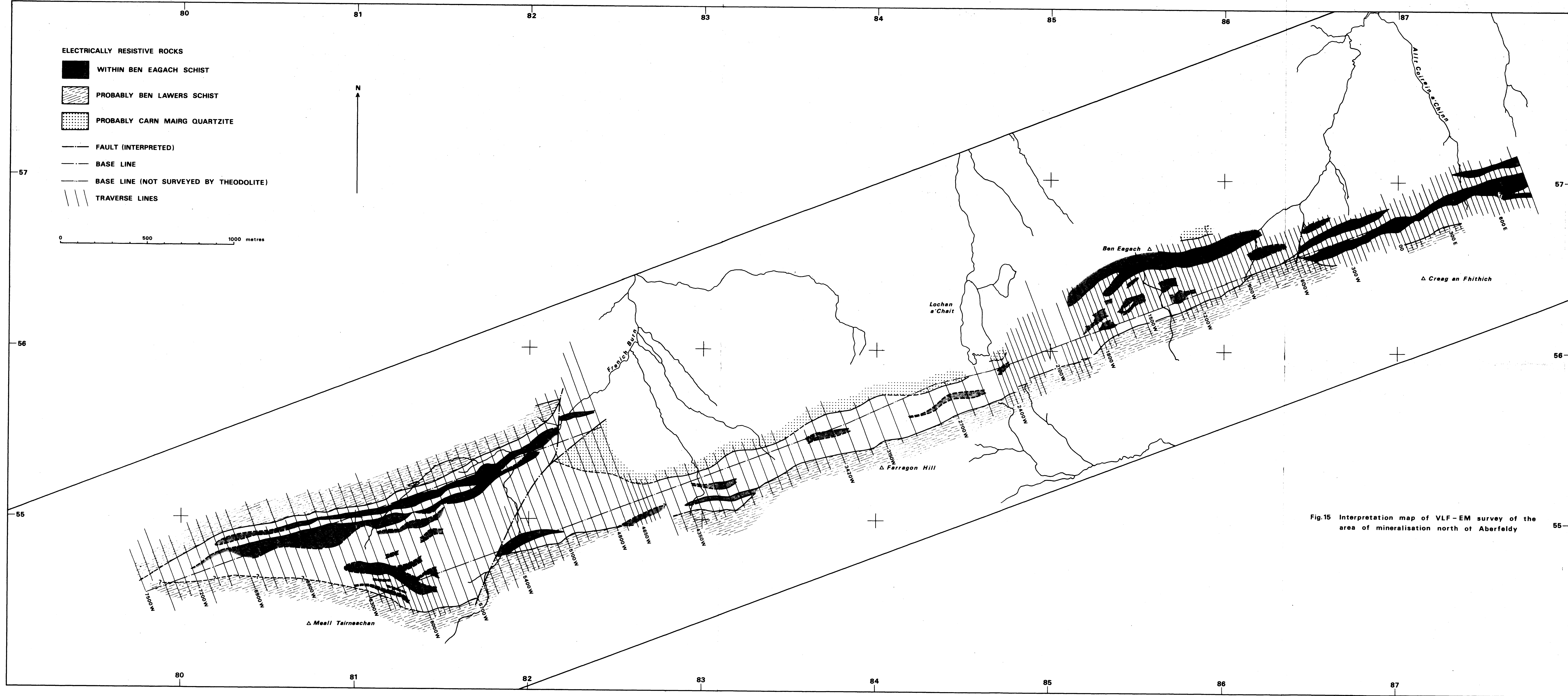


Fig.15 Interpretation map of VLF-EM survey of the area of mineralisation north of Aberfeldy

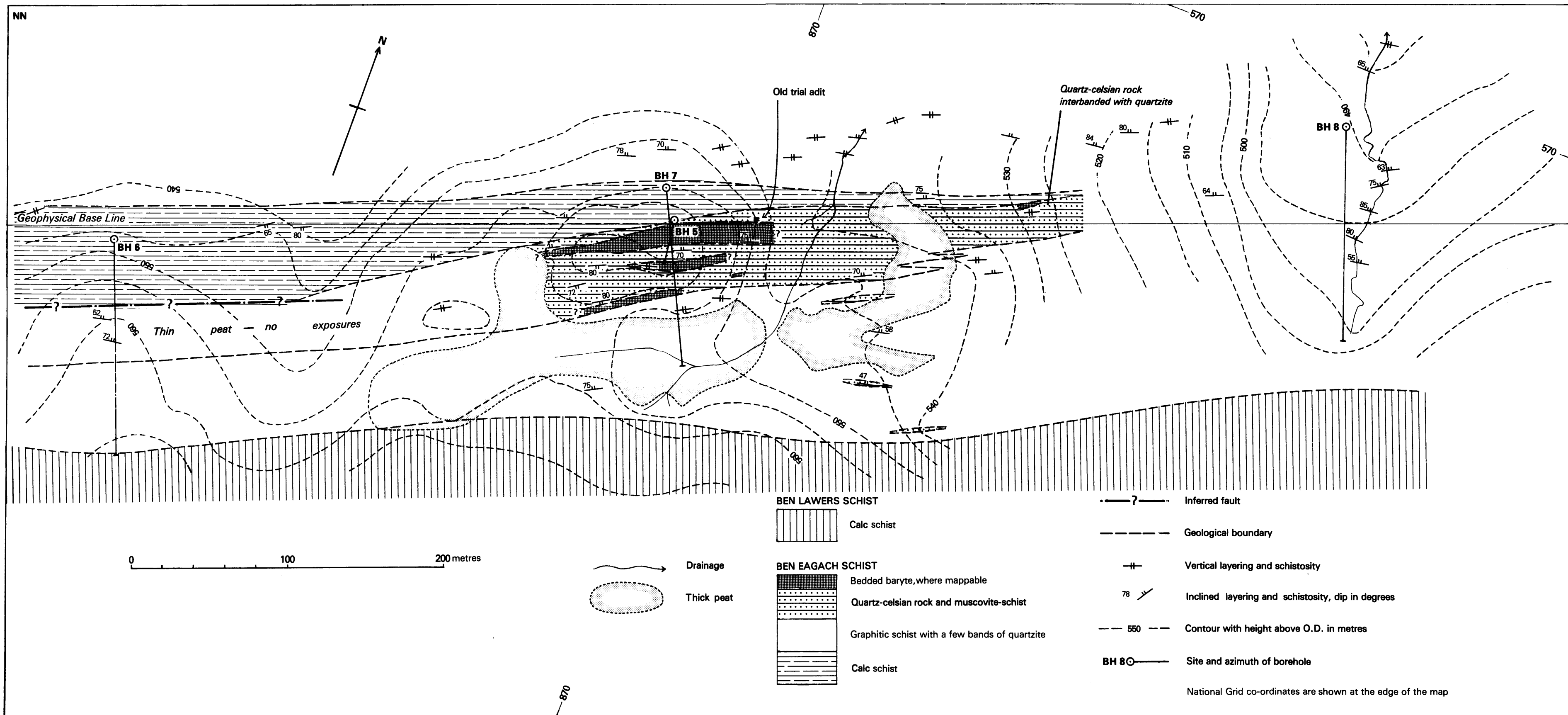
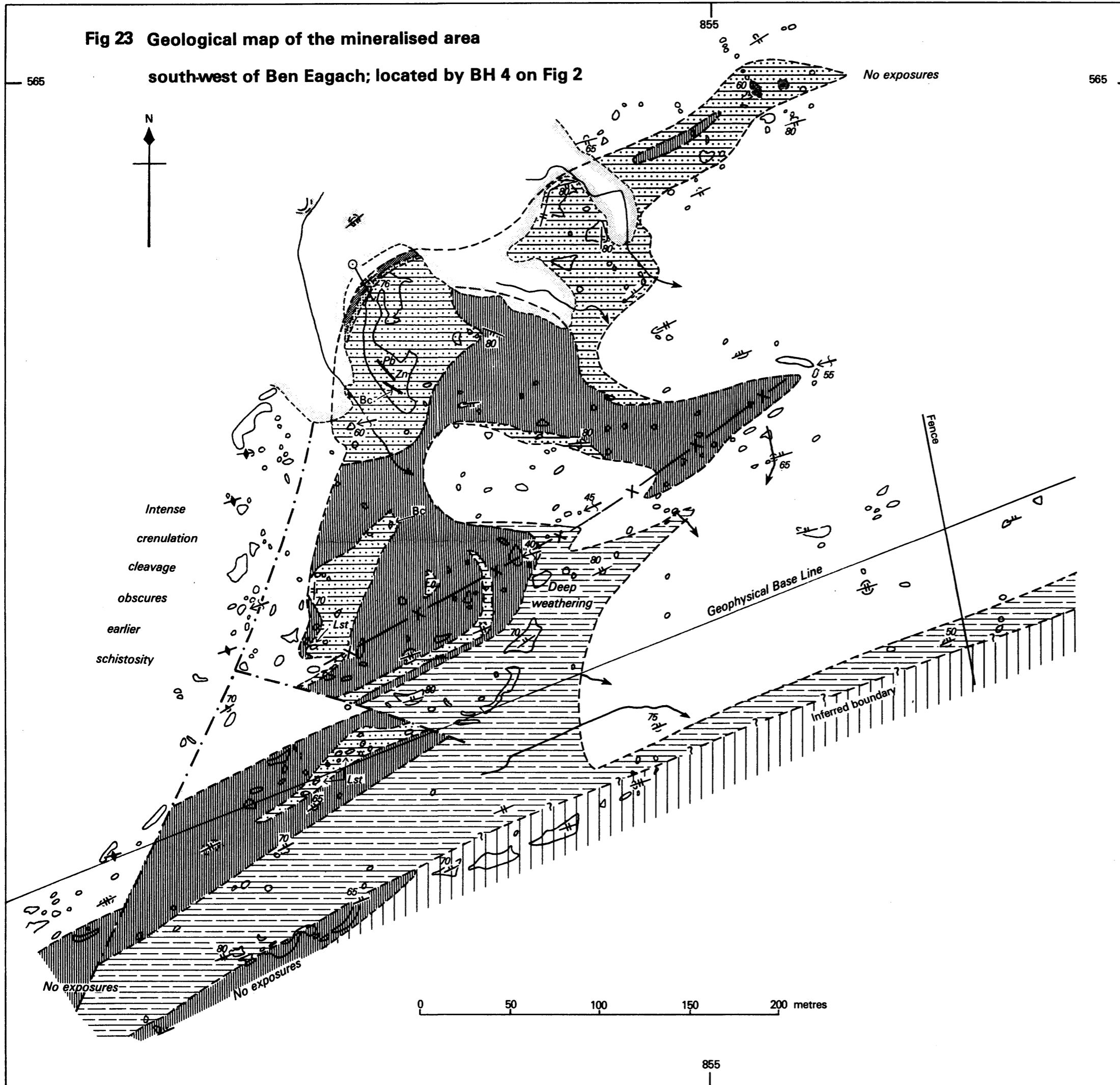


Fig 17 Geology of the Creag an Fhithich area

**Fig 23 Geological map of the mineralised area**


south-west of Ben Eagach; located by BH 4 on Fig 2



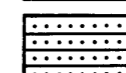
**BEN LAWERS SCHIST**

 Calc schist


**BEN EAGACH SCHIST**

 Graphitic schist with a few bands of quartzite

 Baryte-rock

 Quartz-celsian rock

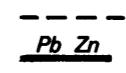
 Muscovite-schist

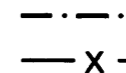
 Sulphide-bearing dolomitic limestone

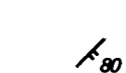
 Calc schist

 Peat

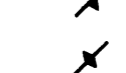
 Rock exposure

 Geological boundary


 Vein carrying galena and sphalerite

 Fault

 Axial trace of synform

 Inclined layering and schistosity, dip in degrees

 Vertical layering and schistosity

 Inclined crenulation cleavage

 Vertical crenulation cleavage

 Plunge of minor fold, in degrees

 Drainage

 Site and azimuth of borehole 4

 Limestone pods

 Breccia

Associated with synform

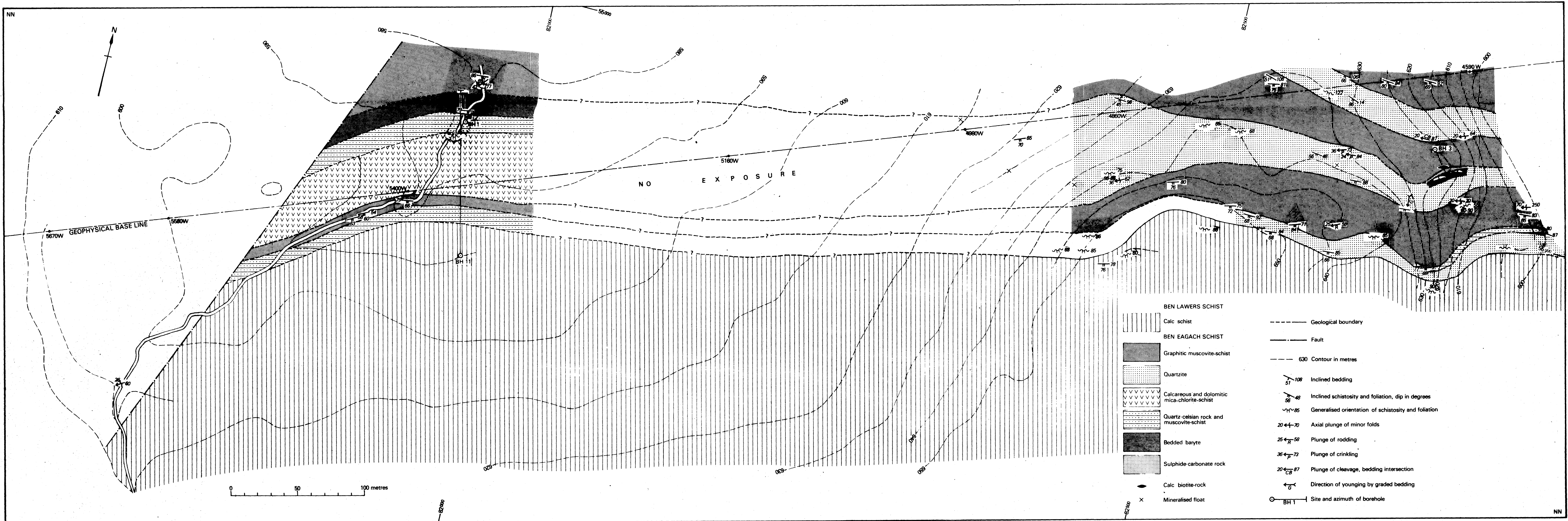
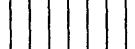




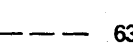

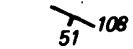
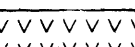

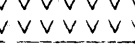


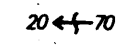
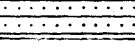
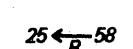

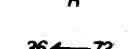



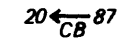
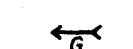


Fig 24 Geology of the area between Creagan Loch and Frenich Burn

- |   |   |   |  |
|---|---|---|--|
|    | BEN LAWERS SCHIST                             |    | Geological boundary                                  |
|    | Calc schist                                   |    | Fault  |
|   | BEN EAGACH SCHIST                             |   | 630 Contour in metres                                |
|  | Graphitic muscovite-schist                    |  | Inclined bedding                                     |
|  | Quartzite                                     |  | Inclined schistosity and foliation, dip in degrees   |
|  | Calcareous and dolomitic mica-chlorite-schist |  | Generalised orientation of schistosity and foliation |
|  | Quartz-celsian rock and muscovite-schist      |  | Axial plunge of minor folds                          |
|  | Bedded baryte                                 |  | Plunge of rodding                                    |
|  | Sulphide-carbonate rock                       |  | Plunge of crinkling                                  |
|  | Calc biotite-rock                             |  | Plunge of cleavage, bedding intersection             |
|  | Mineralised float                             |  | Direction of younging by graded bedding              |
|   |   |  | Site and azimuth of borehole                         |

0 50 100 metres

NN

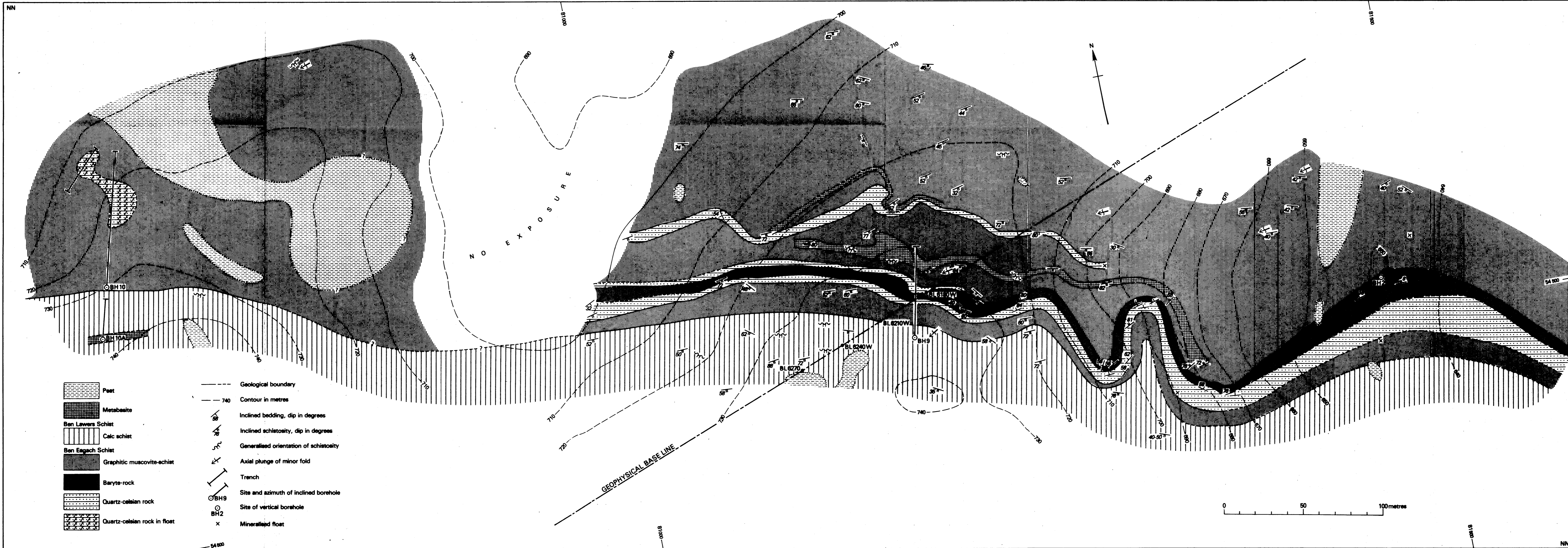


Fig 29 Geology of the area between Creag an Chanaich and Meall Tairneachan